Oxidative Medicine and Cellular Longevity

Pathological Consequences of Drug Abuse: Implication of Redox Imbalance

Lead Guest Editor: Stefania Schiavone
Guest Editors: Margherita Neri and Brian Harvey

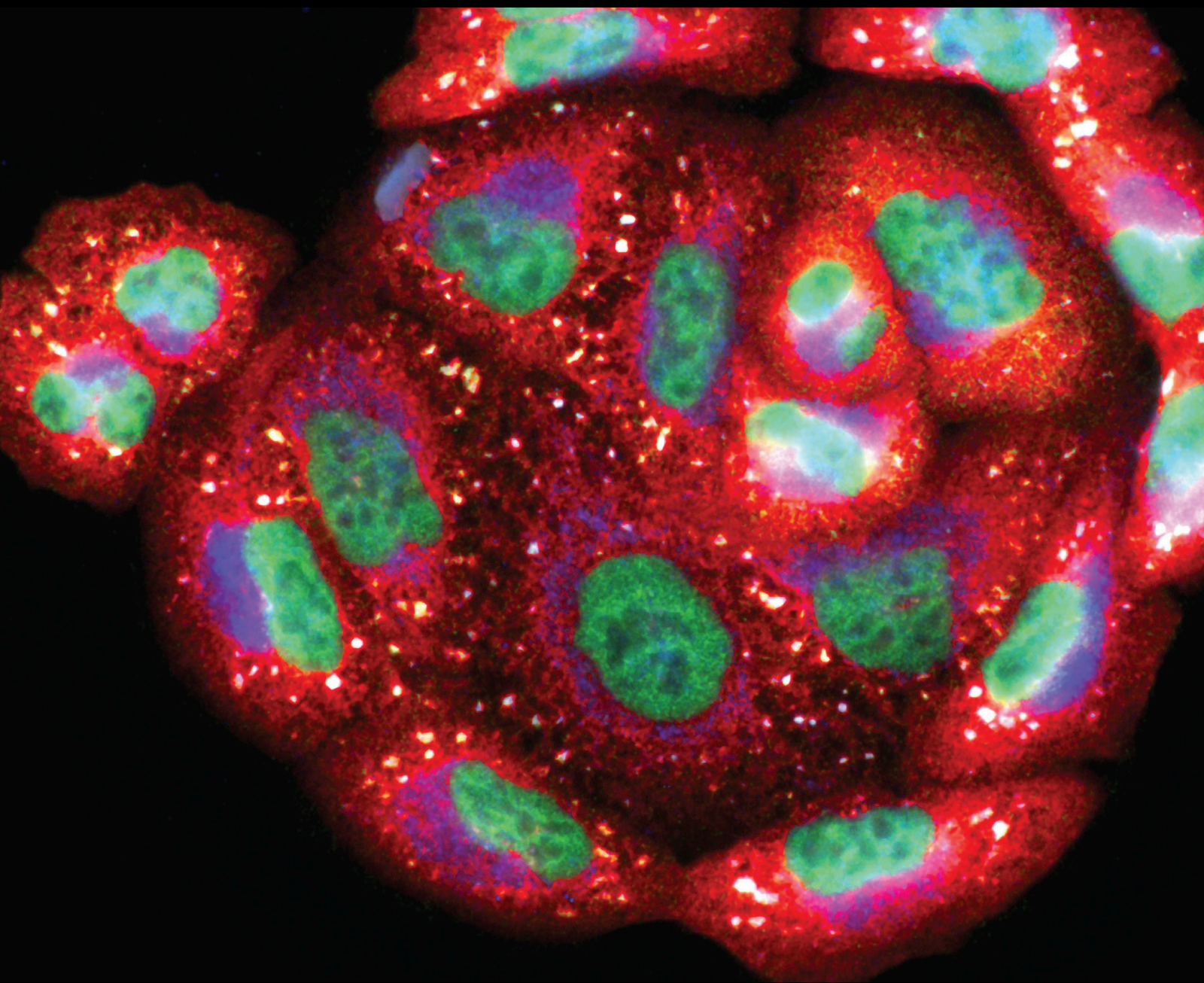

Pathological Consequences of Drug Abuse: Implication of Redox Imbalance

Oxidative Medicine and Cellular Longevity

Pathological Consequences of Drug Abuse: Implication of Redox Imbalance

Lead Guest Editor: Stefania Schiavone
Guest Editors: Margherita Neri and Brian Harvey

Contents

Hindawi
Oxidative Medicine and Cellular Longevity
Volume 2019, Article ID 4780852, 3 pages
https://doi.org/10.1155/2019/4780852

Editorial

Pathological Consequences of Drug Abuse: Implication of Redox Imbalance

Stefania Schiavone[1], **Margherita Neri**[2] **and Brian H. Harvey**[3]

[1]*Department of Clinical and Experimental Medicine, University of Foggia, Foggia, Italy*
[2]*Department of Morphology, Surgery and Experimental Medicine, University of Ferrara, Ferrara, Italy*
[3]*Department of Pharmacology, Center of Excellence for Pharmaceutical Sciences, North West University, Potchefstroom, South Africa*

Correspondence should be addressed to Stefania Schiavone; stefania.schiavone@unifg.it

Received 8 July 2019; Accepted 11 July 2019; Published 22 September 2019

The onset, progression, and outcome of numerous pathological conditions, affecting different organs and systems, have been widely reported to be significantly impacted by the abuse of psychoactive compounds. In the last decades, preclinical and clinical reports have contributed to a lively scientific debate on the possible pathogenic role that redox imbalance, defined as a disequilibrium between reactive oxygen species (ROS) generating and degrading systems, plays in this scenario [1]. Moreover, increasing interest has focused on the possibility that enhanced ROS production or decreased antioxidant defenses in different body compartments, such as the blood, central nervous system (CNS), cardiovascular, gastrointestinal, and respiratory apparatuses may represent reliable biomarkers that will enable the detection of both the early phases of drug abuse-associated complications and the response to pharmacological treatments. Indeed, in a recent review where the authors attempted to assemble a biomarker panel for mood and psychotic disorders, it was clear that disordered redox forms an integral component of the mood-psychosis continuum [2]. Since prolonged substance abuse invariably leads to the development of a mood and/or psychotic disorder, it is understandable that targeting redox pathways may offer beneficial alternatives to traditional treatment interventions in such conditions [3].

In this special issue, a team of international experts presents their preclinical and clinical findings related to the impact of redox imbalance on pathological conditions associated with the abuse of psychoactive compounds, describing different underlying mechanisms and also highlighting the possibility of translating their results into the development of more targeted pharmacological interventions.

The pathological consequences of ethanol (EtOH) consumption have been widely reported, also that it is considered one of the oldest and most intoxicating psychoactive compounds still being used and abused by humans. Among the different mechanisms proposed to explain the toxicity of this substance, its potential to induce the production of ROS in several body tissues and compartments has been confirmed and extended by several lines of preclinical and clinical evidence [4].

In this context, D. Pamplona-Santos and coauthors performed a study on the effects of serious and episodic EtOH drinking patterns, comparable to weekend utilization. The acute consumption of EtOH promotes an imbalance in CNS metabolic functions, resulting in neurodegeneration and cerebral dysfunctions. In this study, the authors investigated the effects of physical training on a treadmill versus the deleterious effects of EtOH on hippocampal functions related to memory and learning. They demonstrate that physical exercise contributes to the reestablishment of the redox status by elevating GSH levels in the blood and hippocampus, and that exercise is a significant nonpharmacological intervention for the prevention of cognitive dysfunctions caused by EtOH exposure following a binge drinking pattern of consumption.

Importantly, epidemiologic studies have highlighted enhanced EtOH consumption among specific subpopulations,

such as women [5] and/or adolescents [6]. With respect to this issue, by using a preclinical approach for their research, L. M. P. Fernandes et al. investigated the impact of moderate EtOH consumption in female rats on oxidative damage-related biomarkers in the liver, brain (motor cortex), and blood, as well as on behavior. These authors reported that repeated EtOH binge drinking in female rats during adolescence was able to induce lipid peroxidation in the brain and liver, where steatosis and structural disruption of the parenchyma were also detected, although no evidence of systemic oxidative damage was found. Moreover, EtOH-induced damage in the brain and liver was accompanied by significant locomotor dysfunction, viz. motor incoordination, even following a single episode of binge-like EtOH exposure. However, bradykinesia and decreased spontaneous exploration required more prolonged EtOH consumption. The authors conclude that their paper questions the adequacy of lipid peroxidation as a reliable biomarker of the detrimental effects of EtOH abuse, at least in the female gender and during the adolescent period, considering the significant vulnerability of the brain and liver to oxidative damage, even in the absence of a systemic ROS increase.

Psychedelic substances have been the object of increasing interest with respect to the possible mental and physical pathological consequences related to their consumption. One of the most widely abused and addictive compound belonging to this class is methamphetamine (METH), which has been reported to induce episodic and/or permanent neuropsychiatric conditions. Moreover, prolonged abuse of this substance is associated with neurotoxicity as well as damages to other peripheral organs. Nevertheless, despite the significant efforts of the scientific community to better understand the complexity of the molecular mechanisms underpinning METH toxicity, several aspects of this process remain to be elucidated. In this context, the review by F. Limanaqi and coauthors discussed the epigenetic effects caused by METH. The manuscript reports the most important molecular events, starting at the presynaptic dopamine terminals to reach the nucleus of postsynaptic neurons. They describe how specific neurotransmitters and signaling cascades produce persistent genetic modifications that enable the shift of neuronal phenotypes to induce alterations in behavior. In the postsynaptic neurons, epigenetic effects induced persistent changes, including sensitization and desensitization, priming, and shift of neuronal phenotype.

As noted earlier, METH induces the production of a number of ROS that leads to lipid peroxidation, protein misfolding, and nuclear damage in the CNS that are detrimental to axon terminals and cell bodies. The overproduction of oxidized proteins, lipids, and nucleic acids requires cellular clearing systems for detoxification and elimination. Cell clearing pathways such as ubiquitin proteasome (UP) and autophagy (ATG) are two such powerful defense mechanisms [7]. However, their integrity and function are challenged by METH administration. Fortunately, the cell clearing organelle, "autophagoproteasome" (APP), possesses both ATG and UP components. Moreover, this organelle is purported to be activated by the mammalian target of rapamycin (mTOR), thus offering a potential pharmacological target for circumventing the actions of METH toxicity. In their paper, G. Lazzeri et al. dissect the ultrastructural morphometry of both UP and ATG components in different cell compartments and, apart from strengthening the concept that mTOR inhibition and ATG protect against METH toxicity, they provide further detail as to the significance of specific ATG-related structures. While the paper contributes towards a better understanding of the neuromolecular processes governing METH toxicity, their findings also speak towards novel insight into cell clearing pathways to counteract several kinds of oxidative damages, as well as hint at new pharmacological strategies for treating METH-associated toxicity.

The pathological impact of ketamine, a N-methyl-D-aspartate (NMDA) receptor antagonist, on mental and physical health has been largely demonstrated by preclinical and clinical evidence. Ketamine is widely recognized in the treatment of resistant depression, although its penchant to induce psychedelic side effects and possible addiction limits its general use. This has prompted the search for alternative treatments or approaches that may abrogate ketamine's psychedelic effects. Among the different molecular mechanisms proposed to explain the detrimental effects of this psychedelic compound, oxidative stress has been reported to play a crucial role [8], which hints at the possible use of antioxidants as an adjunctive treatment when using ketamine. With respect to this topic, S. de Carvalho Cartágenes et al. investigated the effects on oxidative status and behavior after immediate withdrawal of intermittent ketamine administration in adolescent female rats. Although studies exploring gender differences in ketamine responses are limited, they demonstrate that females are much more sensitive than males to the effects of this drug [9]. The data reported by the authors showed that immediate ketamine withdrawal in the adolescence period promotes systemic and hippocampal oxidative stress, and this was accompanied by alterations in emotional behavior.

In recent years, opioid use has approached epidemic proportion, especially in some countries of Europe and North America. An increasing number of evidence has reported a pathological link between opioid addiction and redox dysregulation in both the CNS and periphery [10]. With respect to opioid compounds generally used as substitutes in the maintenance treatment for heroin addiction, such as buprenorphine and methadone, limited lines of evidence are available concerning their possible impact on the redox status. In this context, the clinical approach presented by C. Leventelis and coworkers described increased levels of redox biomarkers and reduced antioxidant defense in blood samples obtained from buprenorphine-treated patients compared to healthy subjects. The same was also observed in subjects receiving methadone, whose impact was even more significant than that of buprenorphine. These findings are important as they suggest that opioids, such as buprenorphine and methadone, that are used to treat opioid addiction, also impact a redox regulatory process in a similar manner as do the more addictive opioid drugs for which they are being used as an intervention strategy against addiction. The authors conclude that their work highlights the

possibility of a concomitant administration of antioxidant compounds with the maintenance therapy for heroin addiction. From the presented findings, reflection is needed in the attempt to further elucidate the link between opioid addiction and redox dysregulation, especially regarding the effects of heroin itself and the possibility that buprenorphine and methadone also independently impact on the cellular redox systems. The latter actions displayed by buprenorphine and methadone could underplay their own addictive potential.

In conclusion, this special issue has confirmed and extended the pathological role of disordered redox systems in a variety of pathological conditions, including EtOH, METH, and opioid abuse, as well as the psychedelic substance, ketamine. These findings have been provocative to understanding how apparently different types of neuro- and psychopathology induced by a broad array of psychotropic substances ultimately impact cellular redox systems. Identifying the source of redox disturbance, e.g., ubiquitin proteasome (UP) and autophagy (ATG), as well as a putative pharmacological target, e.g., mTOR, may provide answers how to best treat a certain disorder presenting as a pro-oxidative state. While oxidative stress being prevalent in so many distinct illnesses questions the usefulness of redox parameters as a disease-specific biomarker [2], it does not lessen the importance of targeting these systems to enable a better therapeutic outcome through the use of adjunctive antioxidants in treating conditions varying from mood and psychotic disorders to addiction. However, to better enable this approach requires a thorough understanding of the redox processes involved, in which this special issue has sought to reveal.

Conflicts of Interest

The authors declare no conflict of interest with respect to the topic of this editorial.

Stefania Schiavone
Margherita Neri
Brian H. Harvey

References

[1] S. Schiavone, M. Colaianna, and L. Trabace, "Drugs of abuse and oxidative stress in the brain: from animal models to human evidence," *Mini-Reviews in Organic Chemistry*, vol. 10, no. 4, pp. 335–342, 2013.

[2] S. J. Brand, M. Moller, and B. H. Harvey, "A review of biomarkers in mood and psychotic disorders: a dissection of clinical vs. preclinical correlates," *Current Neuropharmacology*, vol. 13, no. 3, pp. 324–368, 2015.

[3] T. Swanepoel, M. Moller, and B. H. Harvey, "N-Acetyl cysteine reverses bio-behavioural changes induced by prenatal inflammation, adolescent methamphetamine exposure and combined challenges," *Psychopharmacology*, vol. 235, no. 1, pp. 351–368, 2018.

[4] M. Comporti, C. Signorini, S. Leoncini et al., "Ethanol-induced oxidative stress: basic knowledge," *Genes & Nutrition*, vol. 5, no. 2, pp. 101–109, 2010.

[5] T. Slade, C. Chapman, W. Swift, K. Keyes, Z. Tonks, and M. Teesson, "Birth cohort trends in the global epidemiology of alcohol use and alcohol-related harms in men and women: systematic review and metaregression," *BMJ Open*, vol. 6, no. 10, article e011827, 2016.

[6] L. P. Spear, "Adolescent alcohol exposure: are there separable vulnerable periods within adolescence?," *Physiology & Behavior*, vol. 148, pp. 122–130, 2015.

[7] M. Lin, P. Chandramani-Shivalingappa, H. Jin et al., "Methamphetamine-induced neurotoxicity linked to ubiquitin-proteasome system dysfunction and autophagy-related changes that can be modulated by protein kinase C delta in dopaminergic neuronal cells," *Neuroscience*, vol. 210, pp. 308–332, 2012.

[8] L. de Oliveira, C. M. Spiazzi, T. Bortolin et al., "Different sub-anesthetic doses of ketamine increase oxidative stress in the brain of rats," *Progress in Neuro-Psychopharmacology and Biological Psychiatry*, vol. 33, no. 6, pp. 1003–1008, 2009.

[9] W. Y. Chen, M. C. Huang, and S. K. Lin, "Gender differences in subjective discontinuation symptoms associated with ketamine use," *Substance Abuse Treatment, Prevention, and Policy*, vol. 9, no. 1, p. 39, 2014.

[10] M. Zahmatkesh, M. Kadkhodaee, A. Salarian, B. Seifi, and S. Adeli, "Impact of opioids on oxidative status and related signaling pathways: an integrated view," *Journal of Opioid Management*, vol. 13, no. 4, p. 241, 2017.

Hindawi
Oxidative Medicine and Cellular Longevity
Volume 2019, Article ID 2415243, 12 pages
https://doi.org/10.1155/2019/2415243

Research Article

Aerobic Physical Exercise as a Neuroprotector Strategy for Ethanol Binge-Drinking Effects in the Hippocampus and Systemic Redox Status in Rats

Dinair Pamplona-Santos,[1] Kátia Lamarão-Vieira,[1] Priscila C. Nascimento,[1] Leonardo Oliveira Bittencourt,[1] Márcio G. Corrêa,[1] Savio M. dos Santos,[2] Sabrina C. Cartágenes,[3] Luanna Melo Pereira Fernandes,[3] Marta C. Monteiro,[2] Cristiane S. F. Maia,[3] and Rafael Rodrigues Lima[1]

[1]*Laboratory of Functional and Structural Biology, Institute of Biological Sciences, Federal University of Pará (UFPA), Belém, PA, Brazil*
[2]*Laboratory of In Vitro Tests, Immunology and Microbiology, Institute of Health Sciences, Federal University of Pará (UFPA), Belém, PA, Brazil*
[3]*Laboratory Pharmacology of Inflammation and Behavior, Institute of Health Sciences, Federal University of Pará (UFPA), Belém, PA, Brazil*

Correspondence should be addressed to Rafael Rodrigues Lima; rafalima@ufpa.br

Received 7 December 2018; Revised 6 May 2019; Accepted 27 May 2019; Published 4 July 2019

Guest Editor: Margherita Neri

The heavy and episodic EtOH drinking pattern, equivalent to weekend consumption, characterizes the binge-drinking pattern and promotes a misbalance of encephalic metabolic functions, concurring to neurodegeneration and cerebral dysfunction. And for being a legal drug, it has global public health and social relevance. In this way, we aimed to investigate the effects of physical training, in a treadmill, on the deleterious effects of EtOH on hippocampal functions, related to memory and learning. For this, we used 40 Wistar rats, divided into four groups: Control group, Trained group (trained animals with doses of distilled water), EtOH group (nontrained animals with doses of 3 g/kg/day of EtOH, 20% *w*/*v*), and Trained+EtOH group (trained animals exposed to EtOH). The physical exercise was performed by running on a treadmill for 5 days a week for 4 weeks, and all doses of EtOH were administered through intragastric gavage in four repeated cycles of EtOH in binge. After the experimental period, the animals were submitted to the object recognition task and Morris water maze test, and after being euthanized, the blood and hippocampus were collected for Trolox Equivalent Antioxidant Capacity (TEAC), Reduced Glutathione Content (GSH), and Nitrite and Lipid Peroxidation (LPO) level measurements. Our results showed that EtOH caused marked oxidative stress and mnemonic damage, and the physical exercise promoted neuroprotective effects, among them, the modulation of oxidative biochemistry in plasma (by restoring GSH levels) and in the hippocampus (by reducing LPO levels and increasing antioxidant parameters) and cognitive function improvement. Therefore, physical exercise can be an important prophylactic and therapeutic tool in order to ameliorate and even prevent the deleterious effects of EtOH on cognitive functions.

1. Introduction

Ethanol (EtOH) is a psychotropic drug that generates behavioral changes and may lead to addiction, i.e., dependency. It is a licit substance, with easy access and even encouraged by society, but excessive consumption is associated with psychosocial and medical disorders, being considered as a serious public health issue, both in terms of morbidity and mortality [1].

Furthermore, EtOH has been associated with short- and long-term neuropsychological effects, and the increased prevalence of the binge-drinking pattern during adolescence,

when the brain is still in development and maturation, constitutes an important global health problem since it predisposes individuals to dependence and comorbidities [2–4]. This is quite evident in the hippocampus, where the consumption of EtOH in the intermittent model promotes the reduction of neurogenesis, hippocampal volume, synaptic communication, and neurotrophins associated with neuroplasticity as a brain-derived neurotrophic factor (BDNF) [2, 5–8], which is therefore strongly associated with cognitive impairments.

Considering this problem, several strong strategies for neuroprotection have been studied in experimental animal models and humans. Physical exercise seems to be associated with reduction of neuroinflammation [9–11], improvement of cognitive functions [12–14], increase in BDNF levels [15–17], hippocampal neurogenesis modulation [10, 13, 16], cerebral oxidative stress modulation [18, 19] and induction of several positive morphological changes [10, 15, 17]. However, the beneficial effects of the association between physical exercise and EtOH consumption are not completely understood, still requiring elucidation of the main mechanism by which physical training may help alcoholic drinkers, especially over cognitive functions associated with hippocampal formation.

In this perspective, the objective of this study was to investigate the effects of aerobic physical exercise of moderate intensity on the possible neuroprotection and/or minimization of the alcoholic intoxication damage in the hippocampus of rats.

2. Materials and Methods

2.1. Ethical Statement and Experimental Group Formation. This research was submitted to the Ethics Committee on Experimental Animal Research (CEPAE) from the Federal University of Pará (UFPA) and authorized under the protocol CEPAE–UFPA 227-14l, following all NIH guidelines for the use and care of experimental animals [20]. Forty male Wistar rats (*Rattus norvegicus*), weighing between 60 and 80 g and 30 days old, were provided from the UFPA animal house and placed in a collective with 4 animals each. During the experimental period, the animals were housed in a climate-controlled (25°C) room with a dark-light cycle of 12 h, respectively (lights on at 7 a.m.), and water and food *ad libitum*.

The experimental animals were divided into four groups: Group 1, composed of sedentary animals treated only with distilled water by intragastric gavage (Control group); Group 2, trained animals treated only with distilled water by gavage (Trained group); Group 3, sedentary animals treated with EtOH by intragastric gavage (EtOH group); and Group 4, trained animals treated with EtOH by intragastric gavage (Trained+EtOH group). Figure 1 summarizes all methodological steps of this study.

2.2. Physical Training Protocol. The physical training protocol was performed in a treadmill (Insight, Brazil) adapted for rodents, during four consecutive weeks for 30 minutes each training session [21–23]. The running sessions were executed between 8 a.m. and 12 a.m. in a motorized treadmill adapted for rodents, measuring a width of 10 cm and a length of 50 cm and with bays separated by acrylic walls.

2.3. Protocol of EtOH Exposure. Through intragastric gavage, we administered distilled water or ethanolic solution, at a dose of 3 g/kg (20% *w*/*v*), being weekly adjusted after weighting the animals [24, 25]. At the fifth day of training in each week, during three consecutive days in the week, we performed the water or EtOH administration only after the last training session of the day. In this way, the animals went through twelve EtOH exposures throughout the experimental period. Figure 2 summarizes the training and EtOH exposure protocols.

2.4. Behavioral Assessment. The tests were performed 24 hours after the last administration of EtOH or distilled water, and 10 animals per group were randomly selected and conducted to the assay room, where the sound and illumination were controlled in order to avoid any stressful environment.

2.4.1. Object Recognition Test. This task investigates the emotionality and memory capacity of the animals. The apparatus for this assay consists of a square wooden arena ($100 \times 100 \times 30$ cm), with a recording camera on the roof, in which the videos recorded are further analyzed by ANY-maze software (Stoelting Co., UK). The task consists of four phases: habituation (30 minutes in the arena), training and two test phases, in which two objects are placed in extreme corners of the arena. In the training phase, the animals are presented to two objects that they will become familiar with for 3 minutes, while in the test phase, one of the objects is replaced by a different one from that which was already familiar to the animals. In this way, the investigation time spent by the animals on each object in the training phase (T1) was recorded, as well as the time spent exploring the newest object in the test phase (T2) by the camera mentioned before. The exploration of an object was defined as the head of the animal facing the object at a distance equal to or less than 4 cm [26]. The analyses were performed considering the total exploration time spent on the two objects in the training phase, and the recognition index was defined by the difference in the time of exploration between the new object and the familiar object divided by the total time spent exploring between the same objects in the test phases: $(T2 - T1)/(T2 + T1)$.

2.4.2. Morris Water Maze Test. The spatial memory was verified by the Morris water maze [27]. The apparatus consists of a circular water tank (diameter of 150 cm), with an acrylic platform underwater and a recording camera positioned on the roof. The tank was dived into four quadrants (Q1-Q4) by imaginary lines, and it was filled with water ±25°C up to 45 cm and colored with a blue nontoxic and water-soluble dye to turn it dark (to contrast with the animal color in the recordings), and on Q4, we positioned the acrylic platform with a diameter of 10 cm and a height of 43 cm. It used a version of reference spatial memory, in which the experimental protocol consists of four training sessions and two test

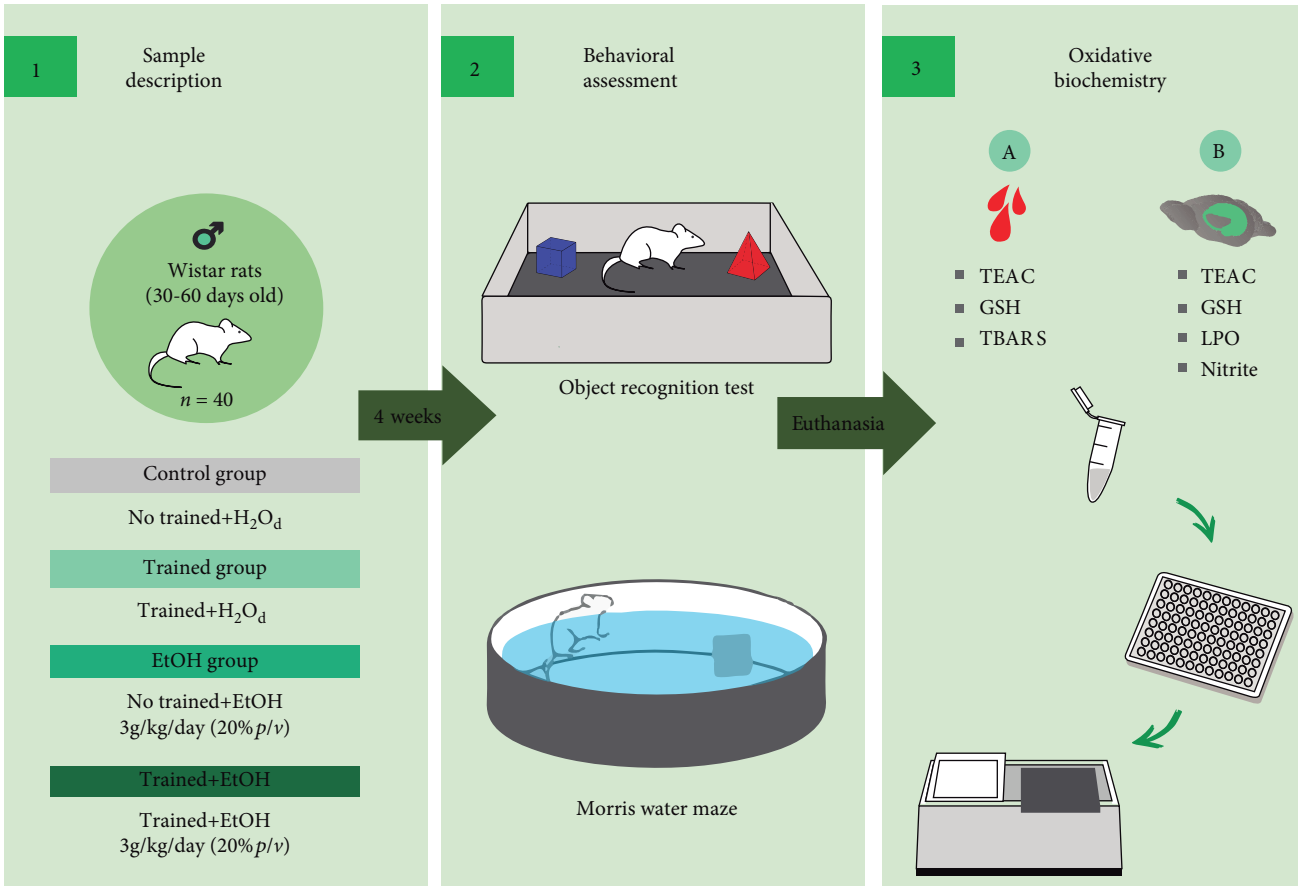

Figure 1: Sample description and experimental design. (1) Sample characteristics and the division of the experimental groups of the treadmill physical training and ethanol (EtOH) or distilled water (H_2O_d) administration; (2) after four weeks (28 days), accomplishment of the behavioral assays: object recognition test and Morris water maze; (3A) after euthanasia, blood plasma collection for oxidative balance analyses through Trolox Equivalent Antioxidant Capacity (TEAC), Reduced Glutathione [14], and Thiobarbituric Acid Reactive Substances (TBARS); (3B) also, hippocampus collection for oxidative balance analyses through TEAC, GSH, Lipid Peroxidation (LPO), and nitrite levels (Nitrite).

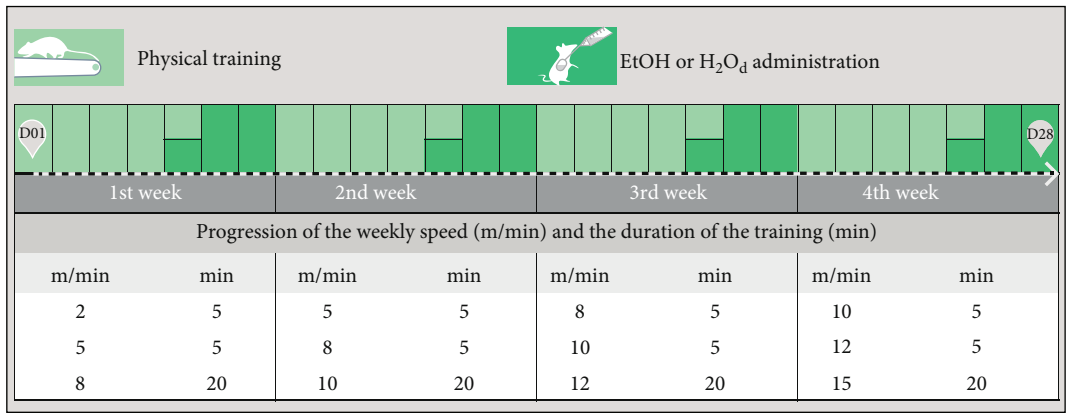

Progression of the weekly speed (m/min) and the duration of the training (min)

m/min	min	m/min	min	m/min	min	m/min	min
2	5	5	5	8	5	10	5
5	5	8	5	10	5	12	5
8	20	10	20	12	20	15	20

Figure 2: Experimental schedule of the treadmill physical training protocol and ethanol (EtOH) or distilled water (H_2O_d) administration by intragastric gavage since day 1 (D01) until day 28 (D28). The physical training protocol was adapted from Arida et al. [21].

sessions, as previously described by Prediger [28]. The first test session (short-term memory) was executed 1 hour after the training, and 24 hours after, the test to evaluate long-term memory was proceeded with the same methodology [28, 29].

2.5. Blood and Hippocampal Oxidative Biochemistry Analyses. Ten animals were randomly selected and used for evaluation of the oxidative biochemistry state in the blood and hippocampus. The animals were deeply anesthetized

through intraperitoneal injection of ketamine hydrochloride (90 mg/kg) and xylazine hydrochloride (10 mg/kg), and then, the blood collection was executed by intracardiac puncture in tubes containing EDTA. The blood samples were centrifuged for 10 minutes at 1400 rpm, and the plasma was collected and stored at -80°C. The hippocampi were collected after total loss of retinal and paw reflexes by craniotomy and brain dissection. The hippocampi were washed in PBS and immediately frozen in liquid nitrogen and stored at -80°C until further analyses. For biochemical analyses, firstly, the hippocampus samples were thawed, suspended in Tris Buffer Solution (HCl 20 mM, pH 7.4) at 4°C, and homogenized by ultrasonic degradation, and after, the homogenate was centrifuged at 3000 rpm for 10 minutes (at 4°C), in which the supernatant was collected for the analyses described below.

2.5.1. Trolox Equivalent Antioxidant Capacity (TEAC). This method was described by Rufino et al. [30] and consists of [31] the 2,2-azino-bis(3-ethylbenzothiazoline)-6-sulfonic acid (ABTS; 7 mM) incubation with potassium persulfate (2.45 mM) at room temperature for 16 hours to produce the radical $ABTS^{+}$. The work solution was prepared from the $ABTS^{+}$ radical in PBS (pH 7.2) until absorbance of 0.7 ± 0.02 at 734 nm. Subsequently, an aliquot of 35 μL from the samples or trolox standard was added to 2970 μL of ABTS solution, and the absorbance was read after 5 minutes. The absorbances were read in triplicate and we established a standard curve in order to calculate the proportional TEAC [32]. The results were expressed as percentage of control.

2.5.2. Glutathione Peroxidase (GPx) and Glutathione Reductase (GR) Assay. The assay of GPx was based on the method described by Flohe and Gunzler [33]. One unity of enzyme is defined as the quantity of enzyme that catalyzes the oxidation of 1 μmol of NADPH per minute. The enzymatic activity was determined using the extinction coefficient of 6.2 M^{-1} cm^{-1}. The blanks were made in the absence of enzymatic extract and in the absence of GSSG. The GR activity was executed following the oxidation of 0.1-0.25 mM of NADPH by 1-5 mM GSSG in 1 mL of potassium phosphate buffer (50 mM, pH 7.2), with 0.5 mM of EDTA, containing 50 μL of protein extract [34]. The oxidation of NADPH was monitored at 340 nm. We also used the methodology described by Smith et al. [35] that uses 5,5′-dithiobis(2-nitrobenzoic acid) (DTNB; 0.47 mmol). The results were expressed as a percentage of control.

2.5.3. Lipid Peroxidation (LPO) Determination by Thiobarbituric Acid Reactive Substances. This procedure is a method that evaluates LPO and acts as an indicator of oxidative stress. It is based on the reaction of MDA and other substances with thiobarbituric acid (TBA), performed according to the proposed method in da Silveira et al. [36]. In each assay tube, 10 nM of TBA (Sigma-Aldrich) and 0.5 mL of sample were added. After, the tubes were heated at 94°C for 60 minutes to form the complex MDA-TBA, which is dyed pink. After this procedure, the samples were refrigerated in tap water and the butyl alcohol was added to the samples in order to obtain maximum extraction of MDA in the organic phase. Finally, the tubes were centrifuged, and the supernatant was collected and read at 535 nm. The results were expressed as a percentage of control.

2.5.4. Estimation of Nitrite Level Assay. For nitrite level estimation, we used Griess' protocol [37] that consists of centrifuging the samples at 21000g during 20 minutes at 4°C and using the supernatant to proceed the assay. The samples were incubated at room temperature during 20 minutes with 100 μL of Griess reagent (0.1% naphthyl-ethylenediamine and 1% sulfonamide in 5% phosphoric acid—1 : 1). The absorbances were read at 550 nm by a spectrometer, and we established a standard curve by the absorbance of known concentrations of nitrite. The results were plotted and expressed as a percentage of control.

2.5.5. Statistical Analyses. After data collection, the distribution was tested by the Shapiro-Wilk method for verification of normality. Statistical comparisons between groups were performed using one-way ANOVA and Tukey post hoc test, except for the weight curve that was evaluated with two-way ANOVA followed the Tukey post hoc test. The p values < 0.05 were considered statistically significant. The GraphPad Prism 7.0 (San Diego, CA, USA) software was used to perform statistical analyses.

3. Results

3.1. The Repeated Cycles of EtOH in a Binge-Like Pattern and Treadmill Physical Exercise Did Not Affect the Animals' Weight Gain. Repeated cycles of physical training on the treadmill and EtOH binge drinking for four weeks did not interfere with the animals' weight ($p = 0.937$). At the end of the experiments, the animals did not show mean body weight difference (Control group: 194.9 ± 9.5; Trained group: 179.5 ± 4.6; EtOH group: 177.86 ± 5.59; Trained+EtOH group: 180.93 ± 5.85) as observed in Figure 3.

3.2. The Aerobic Physical Exercise Modulated the Oxidative Biochemistry of Rats' Plasma by Reestablishing Glutathione Levels after 4 Weeks of EtOH Exposure in a Binge-Like Manner. After repeated cycles of physical exercise on the treadmill and EtOH binge-like exposure for four weeks, EtOH did not induce changes in TEAC levels (EtOH group: 93.35 ± 1.05%; Trained+ EtOH group: 102.9 ± 0.65), when compared to plasma from control and trained-only animals (Control group: 100 ± 1.57%; Trained group: 95.77 ± 3.01%; $p = 0.076$; Figure 4(a)).

However, we observed a significant decrease in GSH plasma levels in rats exposed to EtOH (EtOH group: 65.37 ± 7.13%) compared to the other groups (Control group: 100 ± 8.38%; Trained group: 97.93 ± 6.85%; Trained+EtOH group: 104 ± 3.87%; $p = 0.005$; Figure 4(b)), emphasizing that physical exercise avoided the changes induced by EtOH. No significant difference was observed in TBARS levels among the experimental groups (Control group: 100 ± 19.86%; Trained group: 82.26 ± 20.7%; EtOH group: 75.55 ± 3.77%; Trained+EtOH group: 83.74 ± 15.16%; $p = 0.965$; Figure 4(c)).

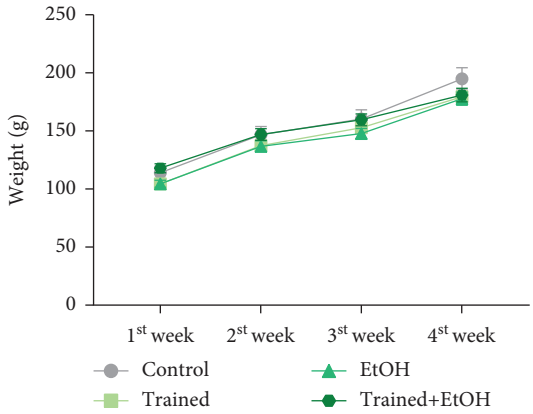

Figure 3: Effects of four cycles of treadmill physical training and exposure to binge-like ethanol, for 28 days, on body weight gain (g) of Wistar rats. Results are expressed as mean ± standard error of the mean. Two-way ANOVA and Tukey's post hoc test, $p > 0.05$.

3.3. The Aerobic Physical Training Modulated the Oxidative Biochemistry Balance in the Hippocampus of Rats Exposed to Four Cycles of Binge Drinking. As observed in Figure 5, the exposure to EtOH in a binge-like pattern also misbalanced the oxidative biochemistry in the hippocampus of rats. The EtOH reduced TEAC levels (EtOH group: 78.88 ± 3.67%; Figure 5(a)) in comparison to the control group (100 ± 3.41%; $p = 0.016$). We observed that the physical exercise could avoid this misbalance provoked by EtOH (Trained +EtOH group: 89.38 ± 7.09%; $p = 0.385$; Figure 5(a)).

Exposure to EtOH also modified oxidative parameters related to GSH levels (EtOH group: 73.58 ± 7.54%) when compared to the control group (100 ± 2.87%; $p = 0.009$) that was not observed in the trained animals (Trained group: 93.95 ± 1.44%; Trained+EtOH group: 93.24 ± 4.7%; $p > 0.05$; Figure 5(b)).

Furthermore, an increase of LPO was observed in the hippocampus of animals exposed to EtOH (EtOH group: 150 ± 11.09%) in comparison to the other group, highlighting the reestablishment of the LPO levels to normal levels due to physical exercise (Control group:100 ± 6.33%; Trained group:105.4 ± 9.44%; Trained +EtOH group:105 ± 7.03%; $p = 0.003$; Figure 5(c)).

Besides that, the EtOH group presented higher nitrite concentrations (EtOH group: 155 ± 8.24%) in comparison to the other groups without EtOH exposure (Control group: 100 ± 9.04%; Trained group: 100 ± 11.55%; $p < 0.05$). However, there was no statistical difference in comparison to the Trained+EtOH group (147.5 ± 7.08%; $p = 0.958$; Figure 5(d)).

3.4. Physical Exercise Minimized Memory Deficits of Rats Exposed to Repeated Cycles of EtOH in a Binge-Like Pattern. Repeated cycles of EtOH binge-like consumption for four weeks induced injury to working memory, long-term spatial memory, and learning ability in rats, as observed in the object recognition and MWM tests. In the object recognition test, trained animals that were exposed to EtOH showed better recognition index (Trained+EtOH group: 0.56 ± 0.1) when compared to those which were only exposed to EtOH (EtOH group: −0.15 ± 0.19; $p = 0.005$; Figure 6), revealing the benefits of physical exercise on short-term memory of animals exposed to EtOH.

When learning and memory were assessed by the Morris water maze (Figure 7), our data showed that the physical exercise avoided the deleterious effects of EtOH. This fact was observed in the first test (Control group: 15.89 ± 1.06; Trained group: 15.38 ± 1.14; EtOH group: 11.22 ± 0.74; Trained+EtOH group: 15 ± 0.42; $p = 0.002$) and on the time spent in the target quadrant during the test (Control group: 15.83 ± 0.54, Trained group: 16.38 ± 1.01, Trained group: 11.5 ± 0.42, Trained+EtOH group: 17.2 ± 1.53, $p = 0.002$) (Figure 7(a)). Regarding the number of entries in the target quadrant (Figure 7(b)), there was no difference in the first test among the groups (Control group: 4.66 ± 0.16; Trained group: 4 ± 0.42; EtOH group: 4.77 ± 0.22; Trained+EtOH: 4.44 ± 0.17; $p = 0.182$), while in the second test, the EtOH group showed difference in comparison to the Trained and Trained+EtOH groups (Trained group: 3.37 ± 0.26; EtOH group: 4.6 ± 0.26; Trained+EtOH group: 3.33 ± 0.33; $p < 0.05$), but not in comparison to the control group (Control group: 3.88 ± 0.3; $p = 0.319$).

4. Discussion

Considering the health impacts that EtOH consumption may cause and the constant need to investigate new therapeutic tools that ameliorate its damage, this work brings important data about how physical exercise positively affects cognitive functions that are deeply affected by EtOH consumption, even in a binge-drinking pattern. This study revealed that physical exercise is associated with GSH level restoration in the blood of rats exposed to EtOH. Moreover, this nonpharmacological therapeutic tool is also associated with TEAC and GSH level restoration in the hippocampus of rats exposed to EtOH and also the reduction of LPO levels into the basal state, comparable to nonexposed animals. And following this perspective of EtOH binge-drinking pattern impacts, we are showing that physical exercise substantially improves cognitive hippocampal functions, such as memory and learning.

Binge drinking or episodic heavy drinking is the practice of consuming large amounts of alcohol in a single session and causing a blood alcohol concentration (BAC) equal to or greater than 0.8 g/L. This dosage is equivalent to five or more doses for men, or four or more doses for women in a two-hour period [38]. The model of alcoholic intoxication in the binge-drinking pattern used in this work reproduces the pattern of encephalic oxidative damage seen in humans who drink in binge [39–42]. However, the degree of severity of brain damage may depend on some variables, such as exposure time, sex, and age.

The exposure to EtOH is associated with several neurological disorders, which may include prenatal exposure, featuring fetal alcohol syndrome, and effects in postnatal individuals, like poor motor performance and cognitive decline [2, 39, 43, 44]. This last one is commonly associated with visuospatial capacities, executive functions, and episodic

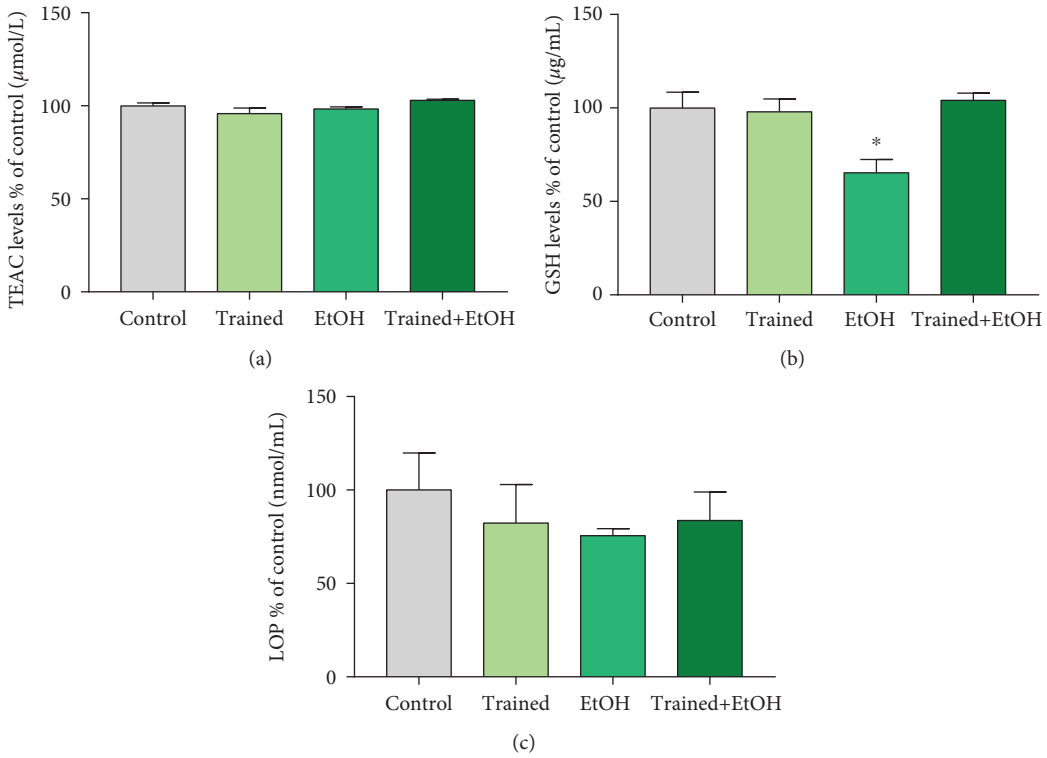

Figure 4: Effects of four cycles of treadmill physical exercise and exposure to binge-like ethanol, for 28 days, on oxidative balance in the blood plasma of Wistar rats. (a) TEAC levels, (b) GSH levels, and (c) Lipid Peroxidation (LPO). Results are expressed as mean ± standard error of the mean of control percentage. One-way ANOVA and Tukey's post hoc test, $p < 0.05$. *Statistical difference in relation to the other groups.

memory [45, 46]. Following this cognitive component, the hippocampus plays a pivotal function in this process, since, anatomically, it is related to other structures that are deeply associated with memory processes [47]. Also, the hippocampus is an integrator center of projections from the perirhinal, parahippocampal, and entorhinal cortices [48], which are included in communication pathways for spatial memory (part of declarative memories) [49–51]. And although the literature presents controversial findings of the hippocampal role in the object recognition task, some studies have pointed that this organ is mainly associated with visual memory and affects the recognition memory; therefore, it also reinforces the hippocampus as an associative structure [52–58] that is required for an efficient cognitive process. In this way, for our behavioral assessment, we elected both these paradigms to investigate hippocampal failure after EtOH exposure: spatial memory and recognition memory.

The object recognition test is based on the presentation of the rodents to familiar and new objects. Instinctively, they spend most of their time exploring the new object. This preference is used as an indication of memory in relation to the familiar object [59]. Our results in this test were markedly significant, since rats exposed to EtOH had marked memory deficits compared to controls and trained exposures. The Morris water maze test, especially indicated for measuring spatial learning and hippocampal-dependent mnemonic processes [27–29, 60], demonstrated that the rats exposed to EtOH had long-term spatial memory deficit.

This study showed that alcoholic intoxication in a binge pattern for three consecutive days per week (during four weeks), generated oxidative stress in the hippocampus but not in the blood. Hippocampal stress, on the other hand, promoted short-term and long-term memory impairment. In addition, for the first time, it has been shown that forced physical exercise, on a treadmill, concomitantly with EtOH intoxication, minimized the deleterious oxidative and behavioral effects generated by exposure to EtOH in young adult rats.

Several studies have highlighted the strong association between oxidative stress and cognitive decline, specially evaluating anti- and prooxidative agents in the blood of patients with compromised cognitive functions [61–64]. And interestingly, those studies have pointed that reduced levels of glutathione peroxidase or glutathione in the blood may be a strong biomarker for cognitive decline [61, 63, 64]. In this perspective, we hypothesize that the reduction of GSH levels found in the blood of rats exposed to EtOH may exert a strong association with the hippocampal deficit found in this study. Despite repeated cycles of intoxication in binge, the serum concentration of TBARS was not significant among the groups, discarding the possibility of physical exercise playing a harmful role in the oxidative dynamics. Still, in a recent work [40], the authors observed that adolescent female Wistar rats, treated with EtOH in a binge pattern, presented cumulative effects on oxidative damage in the motor cortex and liver, which were also not detectable peripherally; it that seems that gender and age variables did not interfere in this scenario.

We did not notice significant changes in the body weight of our rats among the groups and throughout the

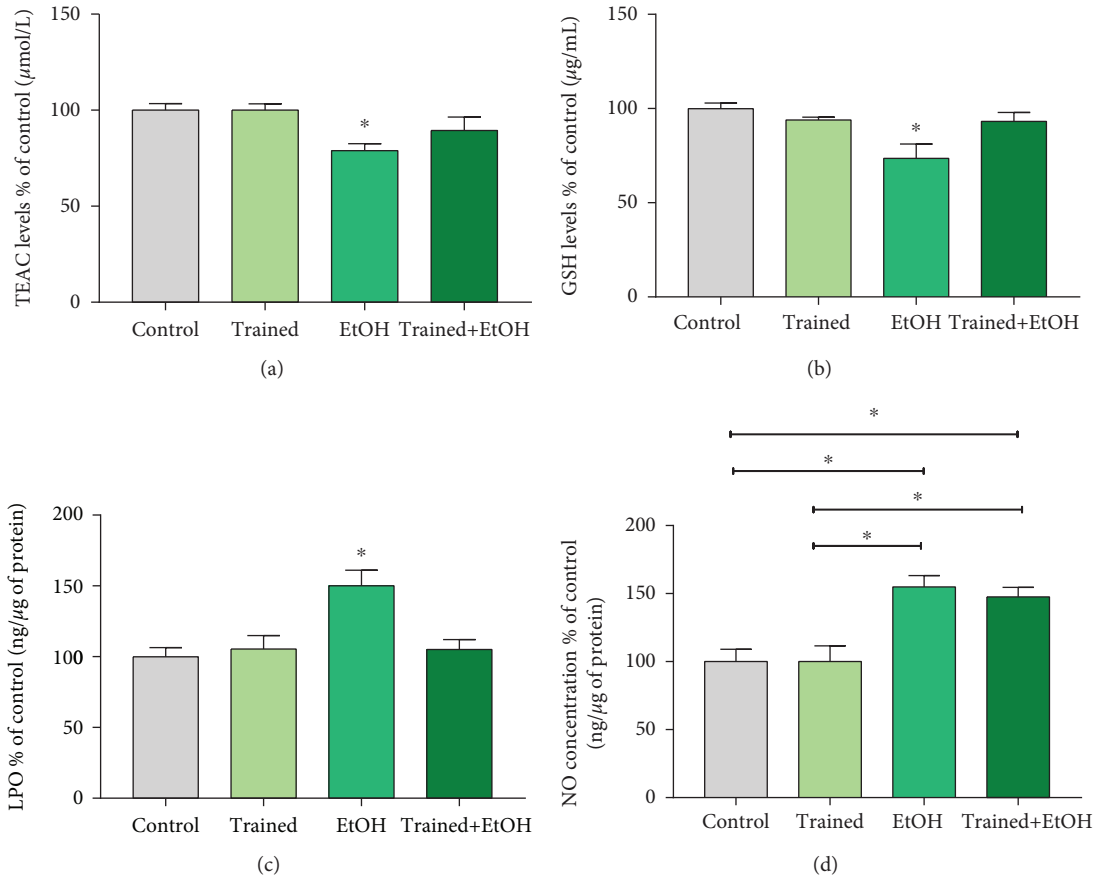

Figure 5: Effects of four cycles of the treadmill physical exercise and exposure to binge-like ethanol, for 28 days, on oxidative balance in the hippocampus of Wistar rats. (a) TEAC levels, (b) GSH levels, (c) percentages of Lipid Peroxidation (LPO) in relation to the control group, and (d) percentages of nitrite per milligram of protein in relation to the control group. Results are expressed as mean ± standard error of the mean. One-way ANOVA and Tukey's post hoc test, $p < 0.05$. *Statistical difference in relation to the other groups or between the groups indicated.

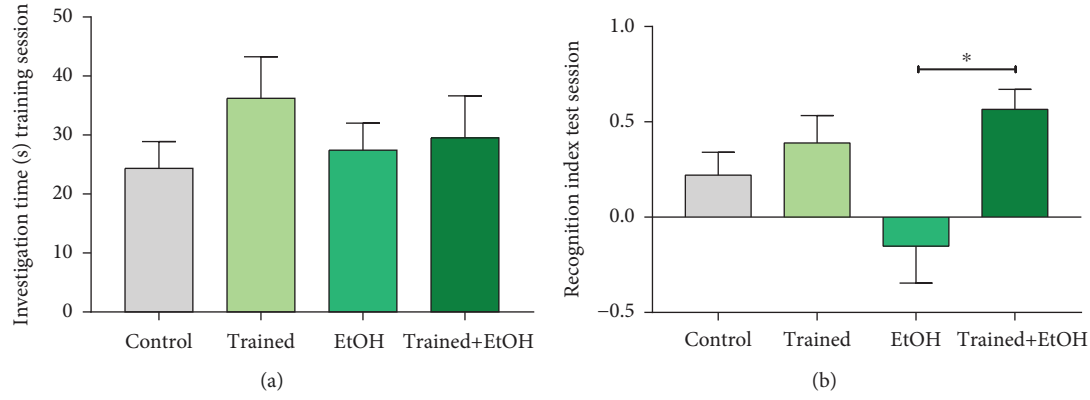

Figure 6: Effects of four cycles of the treadmill physical exercise and exposure to binge-like ethanol, for 28 days, on working memory of Wistar rats. Results are expressed as mean ± standard error of the mean of (a) investigation time (s) in the training session and (b) recognition index in the test session. One-way ANOVA and Tukey's post hoc test, $p < 0.05$. *Statistical difference in relation to the other groups or between the groups indicated.

experiment. Previous work reported that EtOH induced a decrease in body weight. This decrease seems to be dose-dependent, and the higher the EtOH dose, the lower the weight of rats [39, 65]. This decrease was significant from the dose of 1.2 g of EtOH per kilogram of body weight over four weeks [65]. Our sample's weight remained stable for the same exposure period at the dose of 0.8 g/kg. Physical exercise also did not interfere with weight loss or gain in our experimental design.

When in the blood, EtOH molecules are transported quickly to all tissues that have cells with high concentrations of water like the brain, liver, heart, and kidneys [66]. The

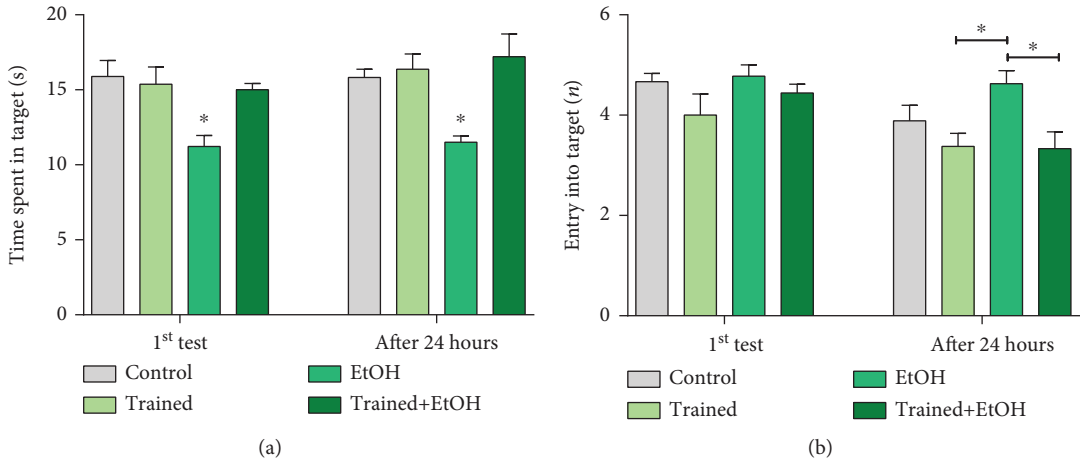

Figure 7: Effects of four cycles of the treadmill physical exercise and exposure to binge-like ethanol, (EtOH) for 28 days, on spatial long-term memory and learning capacity of Wistar rats. Results are expressed as mean ± standard error of the mean of (a) time spent in the target (s) and (b) number of entries into the target. Both measurements were performed in the first test and the test after twenty-four hours. One-way ANOVA and Tukey's post hoc test, $p < 0.05$. *Statistical difference in relation to the other groups or between the groups indicated.

vulnerability of the CNS to the effects of EtOH and exposure during brain development may cause irreversible abnormalities of brain structures and functions [3, 4]. The evaluation of LPO in the CNS system has a relevant importance considering that the brain is particularly vulnerable to free radicals, due to the high oxygen consumption and high content in easily oxidizable substrates, in contrast to the low activity of antioxidant enzymes.

The CNS has a high cellular metabolism, which demands high consumption of oxygen and naturally results in ROS production, which requires an efficient antioxidant system acting [67]. EtOH consumption promotes oxidative imbalance causing LPO, DNA, and protein oxidation, which is enough to promote mitochondrial dysfunction and subsequent neuronal damage. On the other hand, ROS is associated with neuroinflammation that also contributes to the alteration of organelles; however, detoxification, repair, and adaptation are expected responses during an inflammatory state, which, in a deficit situation, may drive to oxidation of the cellular components mentioned above [67, 68], which may increase cell death resulting in cognitive impairments such as memory and learning [69] also observed in this study.

Therefore, the toxicity of EtOH during its metabolism leads to a marked oxidative stress, including in the CNS, due to a reduction of antioxidant enzymes and marked production of oxidizing molecules, such as H_2O_2, hydroxyl radicals ($OH^{\cdot}$), and singlet oxygen during the process to the mitochondrial transport chain phosphorylation [70, 71]. Recently, our group showed that EtOH exposure is able to promote oxidative changes and functional changes in the cerebellum of rats, which can be minimized by physical exercise due to the neuroprotection and decrease in total antioxidant capacity (TEAC) and an increase in levels of Lipid Peroxidation (MDA) in the cerebellum [23]. In addition, we also showed that EtOH exposure led to oxidative stress with increased MDA levels, possibly reflecting on the CNS, which led to a profile of psychiatric disorders or cognitive impairment and impact motor performance [2, 71]. In this regard, we also showed that this EtOH consumption induces marked oxidative stress in the liver and motor cortex leading to changes in motor function; however, it did not alter the levels of prooxidant and antioxidant factors in the blood similar to the results demonstrated in this study [72]. In this study, our experimental data showed that MDA levels were not altered in the periphery, indicating that in clinical practice, MDA levels in the blood could not be used as peripheral markers of ethanol toxicity. These findings may be explained by the fact that reduced antioxidant defenses against oxidative damage may particularly affect the organs most susceptible to this type of damage, such as the brain. Brain cells are more vulnerable to oxidative damage due to reduced levels of antioxidant enzymes and a high level of oxidative metabolism in this tissue [73]. Thus, in this tissue, ROS can lead to oxidative damage in cellular components, impairing cellular energy and signaling pathways (redox signaling) that can cause acute and chronic CNS dysfunctions [74].

In contrast to EtOH, the beneficial effects of exercise on brain functions are well documented, including by our group, who recently showed that moderate-intensity aerobic exercise improved antioxidant levels and reduced oxidative stress in regions associated with motor functions, as the motor cortex, cerebellum, and striatum [23, 69]. In addition, physical exercise may modulate mitochondrial functions, elevating autophagy and expression of neurotrophic factors such as BDNF (brain-derived neurotrophic factor), FGF (fibroblast growth factor), and VEGF (vascular endothelial growth factor) by the development and maintenance of the nervous system [15, 75–78]. Thus, increased levels of BDNF and other transcription factors, such as the transcription factor cAMP response element-binding protein (CREB), can help to sustain the structural and functional integrity of the hippocampus and neurogenesis and synaptic processes such as long-term potentiation (LTP) [75].

Accordingly, in damage caused by EtOH in the CNS, several studies showed that exercise can increase the availability of neurotrophins, leading to a sufficient supply of trophic

molecules, so that both mature cells and those newly generated in the brain become more resistant to the damage caused by alcohol [15, 76–78]. In addition, physical exercise alters levels of neurotransmitters in the hippocampus, such as acetylcholine by stimulating cholinergic fibers that lead to increased vasodilation, and thus elevate blood flow in the hippocampus during exercise [79]. Thus, these effects caused by physical exercise have an essential role in the performance of hippocampus-dependent learning and memory tasks and stimulate the process of redox regulation, thus controlling the oxidative stress caused by alcohol [75]. These findings may explain our data that show the beneficial effects of exercise on behavioral impairments and changes in redox status induced by EtOH, such as increased LPO and reduced levels of GSH and TEAC in the hippocampus. Thus, the results suggest that EtOH induces oxidative stress that exerts pathological effects on the hippocampus and on cognitive functions, and this process can be regulated and thus controlled by physical exercise.

In this regard, the protocol of physical exercise used [21] was absolutely innocuous in relation to oxidative dynamics, since our biochemical analyses in the plasma show that the levels of the marker of LPO were not significant when we compared the trained group with the control one and the decrease of the levels of GSH was seen only in the untrained intoxicated group. In recent work [80], the authors also used a forced exercise protocol on a treadmill and showed that exercise increased the level of cortisone and correlated with increased ischemic brain damage, although they did not evaluate oxidative damage in the blood tissue. This effect, unlike ours, can be explained by the difference between the exercise protocols. Daily, we kept the animals for at least 10 minutes at lower speeds and the remaining 20 minutes at the highest velocity of the weekly program (see Figure 1). Treadmill exercise protocols that standardize a gradual increase in velocity allow the maintenance of the balance between pro- and antioxidants as confirmed by our results.

We must consider the paradox in relation to the effects of physical exercise practice, as it causes an increase in oxygen consumption and, consequently, the generation of reactive oxygen species (ROS). However, the increased synthesis of antioxidant enzymes that are also induced by physical exercise constitutes a metabolic adaptation capable of protecting cells and tissues from the oxidative stress imposed by physical exercise itself [14, 81], as previously mentioned. The elevation of LPO in the hippocampus of rats exposed to EtOH and the elevation of TEAC in Trained+EtOH rats translate this metabolic adaptation and allow us to suggest that the cognitive improvement we observed was due to this oxidative biochemistry status reestablishment.

In this way, we strongly believe that one of the mechanisms by which EtOH exerts its deleterious effects on CNS, especially on cognitive functions, is by oxidative stress. But more interestingly is that the moderate and gradual intensity of physical exercise restores the normal rates of antioxidant and prooxidant agents in the blood and/or in the hippocampus.

5. Conclusions

We demonstrated that physical exercise is a strong nonpharmacological therapeutic tool for the prevention of cognitive dysfunction caused by EtOH exposure in binge-drinking pattern consumption. The physical exercise exerts a role in reestablishing the redox status by elevating GSH levels in the blood and hippocampus of rats exposed to EtOH; besides, it increases TEAC levels and reduces LPO levels, both in the hippocampus, which is associated with the improvement of cognitive functions of the exposed animals. One of the main contributions of the present study was to show, by a preclinical model, that the damage promoted in the hippocampus of rats due to excessive EtOH consumption can be minimized by moderate and gradual intensity of aerobic physical exercise. In this way, by unraveling the protective mechanisms, the identification of important therapeutic targets become the main strategy for neuroprotection with nonpharmacological alternatives, such as physical exercise.

Data Availability

The data used to support the findings of this study are available from the corresponding author upon request.

Conflicts of Interest

The authors declare no conflict of interest.

Authors' Contributions

Dinair Pamplona-Santos and Kátia Lamarão-Vieira contributed equally to this work.

Acknowledgments

This work was supported by the Brazilian National Council for Scientific and Technological Development (CNPq) and Pró-Reitoria de Pesquisa e Pós-Graduação da UFPA (PROPESP, UFPA, Brazil). Rafael R. Lima is an investigator from CNPq (Edital MCTI/CNPq/Universal 14/2014). This paper had financial support from CNPq–Brazilian Minister of Science, Technology and Innovation, through MCTI/CNPq/Universal 14/2014. This study was financed in part by the Coordenação de Aperfeiçoamento de Pessoal de Nível Superior–Brasil (CAPES)—Finance Code 001.

References

[1] WHO, *Global status report on alcohol and health 2018*, World Health Organization, 2018.

[2] A. C. Oliveira, M. C. S. Pereira, L. N. . S. Santana et al., "Chronic ethanol exposure during adolescence through early adulthood in female rats induces emotional and memory deficits associated with morphological and molecular alterations in hippocampus," *Journal of Psychopharmacology*, vol. 29, no. 6, pp. 712–724, 2015.

[3] L. Cantacorps, H. González-Pardo, J. L. Arias, O. Valverde, and N. M. Conejo, "Altered brain functional connectivity and behaviour in a mouse model of maternal alcohol binge-

drinking," *Progress in Neuro-Psychopharmacology and Biological Psychiatry*, vol. 84, Part A, pp. 237–249, 2018.

[4] C. Guerri and M. Pascual, "Mechanisms involved in the neurotoxic, cognitive, and neurobehavioral effects of alcohol consumption during adolescence," *Alcohol*, vol. 44, no. 1, pp. 15–26, 2010.

[5] S. A. Morris, D. W. Eaves, A. R. Smith, and K. Nixon, "Alcohol inhibition of neurogenesis: a mechanism of hippocampal neurodegeneration in an adolescent alcohol abuse model," *Hippocampus*, vol. 20, no. 5, pp. 596–607, 2010.

[6] D. M. Lovinger and M. Roberto, "Synaptic effects induced by alcohol," in *Behavioral Neurobiology of Alcohol Addiction*, W. Sommer and R. Spanagel, Eds., vol. 13 of Current Topics in Behavioral Neurosciences, pp. 31–86, Springer, Berlin, Heidelberg, 2013.

[7] C. R. Geil, D. M. Hayes, J. A. McClain et al., "Alcohol and adult hippocampal neurogenesis: promiscuous drug, wanton effects," *Progress in Neuro-Psychopharmacology and Biological Psychiatry*, vol. 54, pp. 103–113, 2014.

[8] F. T. Crews, R. P. Vetreno, M. A. Broadwater, and D. L. Robinson, "Adolescent alcohol exposure persistently impacts adult neurobiology and behavior," *Pharmacological Reviews*, vol. 68, no. 4, pp. 1074–1109, 2016.

[9] S. Gomes da Silva, P. S. R. Simões, R. A. Mortara et al., "Exercise-induced hippocampal anti-inflammatory response in aged rats," *Journal of Neuroinflammation*, vol. 10, no. 1, p. 827, 2013.

[10] C. M. Hueston, J. F. Cryan, and Y. M. Nolan, "Adolescent social isolation stress unmasks the combined effects of adolescent exercise and adult inflammation on hippocampal neurogenesis and behavior," *Neuroscience*, vol. 365, pp. 226–236, 2017.

[11] C. Bernardi, A. C. Tramontina, P. Nardin et al., "Treadmill exercise induces hippocampal astroglial alterations in rats," *Neural Plasticity*, vol. 2013, Article ID 709732, 10 pages, 2013.

[12] M. Tahamtan, M. Allahtavakoli, M. Abbasnejad et al., "Exercise preconditioning improves behavioral functions following transient cerebral ischemia induced by 4-vessel occlusion (4-VO) in rats," *Archives of Iranian Medicine*, vol. 16, no. 12, pp. 697–704, 2013.

[13] M. A. Farzi, S. Sadigh-Eteghad, K. Ebrahimi, and M. Talebi, "Exercise improves recognition memory and acetylcholinesterase activity in the beta amyloid-induced rat model of Alzheimer's disease," *Annals of Neurosciences*, vol. 25, no. 3, pp. 121–125, 2018.

[14] X. Shen, A. Li, Y. Zhang et al., "The effect of different intensities of treadmill exercise on cognitive function deficit following a severe controlled cortical impact in rats," *International Journal of Molecular Sciences*, vol. 14, no. 11, pp. 21598–21612, 2013.

[15] N. C. Berchtold, G. Chinn, M. Chou, J. P. Kesslak, and C. W. Cotman, "Exercise primes a molecular memory for brain-derived neurotrophic factor protein induction in the rat hippocampus," *Neuroscience*, vol. 133, no. 3, pp. 853–861, 2005.

[16] M. D. Brandt, A. Maass, G. Kempermann, and A. Storch, "Physical exercise increases Notch activity, proliferation and cell cycle exit of type-3 progenitor cells in adult hippocampal neurogenesis," *European Journal of Neuroscience*, vol. 32, no. 8, pp. 1256–1264, 2010.

[17] Z. Ke, S. P. Yip, L. Li, X. X. Zheng, and K. Y. Tong, "The effects of voluntary, involuntary, and forced exercises on brain-derived neurotrophic factor and motor function recovery: a rat brain ischemia model," *PLoS One*, vol. 6, no. 2, article e16643, 2011.

[18] A. R. Patten, S. Y. Yau, C. J. Fontaine, A. Meconi, R. C. Wortman, and B. R. Christie, "The benefits of exercise on structural and functional plasticity in the rodent hippocampus of different disease models," *Brain Plasticity*, vol. 1, no. 1, pp. 97–127, 2015.

[19] Y. W. Di Wang, W. Chen, M. Ma, Y. Hua, and J. Kang, "Aerobic exercise alleviates hippocampus injury in chronic stressed depression rats," *European Journal of Experimental Biology*, vol. 8, no. 4, p. 26, 2018.

[20] Council, NR, *Guide for the Care and Use of Laboratory Animals: Eighth Edition*, The National Academies Press, Washington, DC, 2011.

[21] R. M. Arida, F. A. Scorza, A. F. Silva de Lacerda, S. Gomes da Silva, and E. A. Cavalheiro, "Physical training in developing rats does not influence the kindling development in the adult life," *Physiology & Behavior*, vol. 90, no. 4, pp. 629–633, 2007.

[22] R. M. Arida, F. A. Scorza, S. G. da Silva, R. M. Cysneiros, and E. A. Cavalheiro, "Exercise paradigms to study brain injury recovery in rodents," *American Journal of Physical Medicine & Rehabilitation*, vol. 90, no. 6, pp. 452–465, 2011.

[23] K. Lamarão-Vieira, D. Pamplona-Santos, P. C. Nascimento et al., "Physical exercise attenuates oxidative stress and morphofunctional cerebellar damages induced by the ethanol binge drinking paradigm from adolescence to adulthood in rats," *Oxidative Medicine and Cellular Longevity*, vol. 2019, Article ID 6802424, 14 pages, 2019.

[24] K. Lauing, R. Himes, M. Rachwalski, P. Strotman, and J. J. Callaci, "Binge alcohol treatment of adolescent rats followed by alcohol abstinence is associated with site-specific differences in bone loss and incomplete recovery of bone mass and strength," *Alcohol*, vol. 42, no. 8, pp. 649–656, 2008.

[25] C. Lindtner, T. Scherer, E. Zielinski et al., "Binge drinking induces whole-body insulin resistance by impairing hypothalamic insulin action," *Science Translational Medicine*, vol. 5, no. 170, article 170ra14, 2013.

[26] A. Ennaceur and J. Delacour, "A new one-trial test for neurobiological studies of memory in rats. 1: behavioral data," *Behavioural Brain Research*, vol. 31, no. 1, pp. 47–59, 1988.

[27] R. G. M. Morris, P. Garrud, J. N. P. Rawlins, and J. O'Keefe, "Place navigation impaired in rats with hippocampal lesions," *Nature*, vol. 297, no. 5868, pp. 681–683, 1982.

[28] S. Prediger, "The relevance of didactic categories for analysing obstacles in conceptual change: revisiting the case of multiplication of fractions," *Learning and Instruction*, vol. 18, no. 1, pp. 3–17, 2008.

[29] L. O. Bittencourt, A. Dionizio, P. C. Nascimento et al., "Proteomic approach underlying the hippocampal neurodegeneration caused by low doses of methylmercury after long-term exposure in adult rats," *Metallomics*, vol. 11, no. 2, pp. 390–403, 2019.

[30] M. S. M. Rufino, R. E. Alves, and E. S. Brito, *Metodologia científica: determinação da atividade antioxidante total em frutas pela captura do radical livre ABTS°+. [2007]*, Embrapa Agroindústria Tropical. Comunicado técnico, 2007.

[31] G. H. N. Miranda, B. A. Q. Gomes, L. O. Bittencourt et al., "Chronic exposure to sodium fluoride triggers oxidative biochemistry misbalance in mice: effects on peripheral blood

circulation," *Oxidative Medicine and Cellular Longevity*, vol. 2018, Article ID 8379123, 8 pages, 2018.

[32] R. Re, N. Pellegrini, A. Proteggente, A. Pannala, M. Yang, and C. Rice-Evans, "Antioxidant activity applying an improved ABTS radical cation decolorization assay," *Free Radical Biology & Medicine*, vol. 26, no. 9-10, pp. 1231–1237, 1999.

[33] L. Flohé and W. A. Günzler, "[12] Assays of glutathione peroxidase," *Methods in Enzymology*, vol. 105, pp. 114–120, 1984.

[34] G. R. Ramos-Vasconcelos, L. A. Cardoso, and M. Hermes-Lima, "Seasonal modulation of free radical metabolism in estivating land snails Helix aspersa," *Comparative Biochemistry and Physiology Part C: Toxicology & Pharmacology*, vol. 140, no. 2, pp. 165–174, 2005.

[35] P. K. Smith, R. I. Krohn, G. T. Hermanson et al., "Measurement of protein using bicinchoninic acid," *Analytical Biochemistry*, vol. 150, no. 1, pp. 76–85, 1985.

[36] C. C. S. d. M. da Silveira, L. M. P. Fernandes, M. L. Silva et al., "Neurobehavioral and antioxidant effects of ethanolic extract of yellow propolis," *Oxidative Medicine and Cellular Longevity*, vol. 2016, Article ID 2906953, 14 pages, 2016.

[37] H. I. Kohn and M. Liversedge, "On a new aerobic metabolite whose production by brain is inhibited by apomorphine, emetine, ergotamine, epinephrine, and menadione," *Journal of Pharmacology and Experimental Therapeutics*, vol. 82, no. 3, p. 292, 1944.

[38] Institute on Alcohol, A and N Alcoholism, "NIAAA council approves definition of binge drinking," vol. 3, 2004.

[39] F. B. Teixeira, L. N. . S. Santana, F. R. Bezerra et al., "Chronic ethanol exposure during adolescence in rats induces motor impairments and cerebral cortex damage associated with oxidative stress," *PLoS One*, vol. 9, no. 6, article e101074, 2014.

[40] L. M. P. Fernandes, S. C. Cartágenes, M. A. Barros et al., "Repeated cycles of binge-like ethanol exposure induce immediate and delayed neurobehavioral changes and hippocampal dysfunction in adolescent female rats," *Behavioural Brain Research*, vol. 350, pp. 99–108, 2018.

[41] M. E. Maynard and J. L. Leasure, "Exercise enhances hippocampal recovery following binge ethanol exposure," *PLoS One*, vol. 8, no. 9, article e76644, 2013.

[42] Z. Ji, L. Yuan, X. Lu, H. Ding, J. Luo, and Z. J. Ke, "Binge alcohol exposure causes neurobehavioral deficits and GSK3β activation in the hippocampus of adolescent rats," *Scientific Reports*, vol. 8, no. 1, article 3088, 2018.

[43] A. Ornoy and Z. Ergaz, "Alcohol abuse in pregnant women: effects on the fetus and newborn, mode of action and maternal treatment," *International Journal of Environmental Research and Public Health*, vol. 7, no. 2, pp. 364–379, 2010.

[44] D. B. Matthews, M. R. Watson, K. James, A. Kastner, A. Schneider, and G. Mittleman, "The impact of low to moderate chronic intermittent ethanol exposure on behavioral endpoints in aged, adult, and adolescent rats," *Alcohol*, vol. 78, pp. 33–42, 2019.

[45] F. Bernardin, A. Maheut-Bosser, and F. Paille, "Cognitive impairments in alcohol-dependent subjects," *Frontiers in Psychiatry*, vol. 5, p. 78, 2014.

[46] A. P. Le Berre, R. Fama, and E. V. Sullivan, "Executive functions, memory, and social cognitive deficits and recovery in chronic alcoholism: a critical review to inform future research," *Alcoholism: Clinical and Experimental Research*, vol. 41, no. 8, pp. 1432–1443, 2017.

[47] L. R. Squire, "Memory and the hippocampus: a synthesis from findings with rats, monkeys, and humans," *Psychological Review*, vol. 99, no. 2, pp. 195–231, 1992.

[48] P. Lavenex and D. G. Amaral, "Hippocampal-neocortical interaction: a hierarchy of associativity," *Hippocampus*, vol. 10, no. 4, pp. 420–430, 2000.

[49] H. Eichenbaum, "The hippocampus and mechanisms of declarative memory," *Behavioural Brain Research*, vol. 103, no. 2, pp. 123–133, 1999.

[50] H. Eichenbaum, "A cortical-hippocampal system for declarative memory," *Nature Reviews. Neuroscience*, vol. 1, no. 1, pp. 41–50, 2000.

[51] H. Eichenbaum, "The hippocampus and declarative memory: cognitive mechanisms and neural codes," *Behavioural Brain Research*, vol. 127, no. 1-2, pp. 199–207, 2001.

[52] R. E. Clark, S. M. Zola, and L. R. Squire, "Impaired recognition memory in rats after damage to the hippocampus," *The Journal of Neuroscience*, vol. 20, no. 23, pp. 8853–8860, 2000.

[53] G. T. Prusky, R. M. Douglas, L. Nelson, A. Shabanpoor, and R. J. Sutherland, "Visual memory task for rats reveals an essential role for hippocampus and perirhinal cortex," *Proceedings of the National Academy of Sciences of the United States of America*, vol. 101, no. 14, pp. 5064–5068, 2004.

[54] N. J. Broadbent, L. R. Squire, and R. E. Clark, "Spatial memory, recognition memory, and the hippocampus," *Proceedings of the National Academy of Sciences of the United States of America*, vol. 101, no. 40, pp. 14515–14520, 2004.

[55] G. R. I. Barker and E. C. Warburton, "Object-in-place associative recognition memory depends on glutamate receptor neurotransmission within two defined hippocampal-cortical circuits: a critical role for AMPA and NMDA receptors in the hippocampus, perirhinal, and prefrontal cortices," *Cerebral cortex*, vol. 25, no. 2, pp. 472–481, 2015.

[56] G. R. I. Barker and E. C. Warburton, "When is the hippocampus involved in recognition memory?," *The Journal of Neuroscience*, vol. 31, no. 29, pp. 10721–10731, 2011.

[57] M. Leger, A. Quiedeville, V. Bouet et al., "Object recognition test in mice," *Nature Protocols*, vol. 8, no. 12, pp. 2531–2537, 2013.

[58] E. M. Stanley, M. A. Wilson, and J. R. Fadel, "Hippocampal neurotransmitter efflux during one-trial novel object recognition in rats," *Neuroscience Letters*, vol. 511, no. 1, pp. 38–42, 2012.

[59] K. Rutten, O. A. H. Reneerkens, H. Hamers et al., "Automated scoring of novel object recognition in rats," *Journal of Neuroscience Methods*, vol. 171, no. 1, pp. 72–77, 2008.

[60] S. Sharma, S. Rakoczy, and H. Brown-Borg, "Assessment of spatial memory in mice," *Life Sciences*, vol. 87, no. 17-18, pp. 521–536, 2010.

[61] C. Berr, B. Balansard, J. Arnaud, A. M. Roussel, A. Alpérovitch, and EVA Study Group, "Cognitive decline is associated with systemic oxidative stress: the EVA study," *Journal of the American Geriatrics Society*, vol. 48, no. 10, pp. 1285–1291, 2000.

[62] M. Schrag, C. Mueller, M. Zabel et al., "Oxidative stress in blood in Alzheimer's disease and mild cognitive impairment: a meta-analysis," *Neurobiology of Disease*, vol. 59, pp. 100–110, 2013.

[63] F. Revel, T. Gilbert, S. Roche et al., "Influence of oxidative stress biomarkers on cognitive decline," *Journal of Alzheimer's Disease*, vol. 45, no. 2, pp. 553–560, 2015.

[64] I. Hajjar, S. S. Hayek, F. C. Goldstein, G. Martin, D. P. Jones, and A. Quyyumi, "Oxidative stress predicts cognitive decline with aging in healthy adults: an observational study," *Journal of Neuroinflammation*, vol. 15, no. 1, p. 17, 2018.

[65] S. K. Das, K. R. Hiran, S. Mukherjee, and D. M. Vasudevan, "Oxidative stress is the primary event: effects of ethanol consumption in brain," *Indian Journal of Clinical Biochemistry*, vol. 22, no. 1, pp. 99–104, 2007.

[66] S. Zakhari, "Overview: how is alcohol metabolized by the body?," *Alcohol Research & Health*, vol. 29, no. 4, pp. 245–254, 2006.

[67] M. Patel, "Targeting oxidative stress in central nervous system disorders," *Trends in Pharmacological Sciences*, vol. 37, no. 9, pp. 768–778, 2016.

[68] M. Baierle, S. N. Nascimento, A. M. Moro et al., "Relationship between inflammation and oxidative stress and cognitive decline in the institutionalized elderly," *Oxidative Medicine and Cellular Longevity*, vol. 2015, Article ID 804198, 12 pages, 2015.

[69] R. P. Vetreno and F. T. Crews, "Binge ethanol exposure during adolescence leads to a persistent loss of neurogenesis in the dorsal and ventral hippocampus that is associated with impaired adult cognitive functioning," *Frontiers in Neuroscience*, vol. 9, p. 35, 2015.

[70] A. P. Kudin, D. Malinska, and W. S. Kunz, "Sites of generation of reactive oxygen species in homogenates of brain tissue determined with the use of respiratory substrates and inhibitors," *Biochimica et Biophysica Acta*, vol. 1777, no. 7-8, pp. 689–695, 2008.

[71] I. J. A. Belém-Filho, P. C. Ribera, A. L. Nascimento et al., "Low doses of methylmercury intoxication solely or associated to ethanol binge drinking induce psychiatric-like disorders in adolescent female rats," *Environmental Toxicology and Pharmacology*, vol. 60, pp. 184–194, 2018.

[72] L. M. P. Fernandes, K. S. Lopes, L. N. S. Santana et al., "Repeated cycles of binge-like ethanol intake in adolescent female rats induce motor function impairment and oxidative damage in motor cortex and liver, but not in blood," *Oxidative Medicine and Cellular Longevity*, vol. 2018, Article ID 3467531, 14 pages, 2018.

[73] I. Olmez and H. Ozyurt, "Reactive oxygen species and ischemic cerebrovascular disease," *Neurochemistry International*, vol. 60, no. 2, pp. 208–212, 2012.

[74] M. Shichiri, "The role of lipid peroxidation in neurological disorders," *Journal of Clinical Biochemistry and Nutrition*, vol. 54, no. 3, pp. 151–160, 2014.

[75] T. Hashemi Nosrat Abadi, L. Vaghef, S. Babri, M. Mahmood-Alilo, and M. Beirami, "Effects of different exercise protocols on ethanol-induced spatial memory impairment in adult male rats," *Alcohol*, vol. 47, no. 4, pp. 309–316, 2013.

[76] F. Gomez-Pinilla, L. Dao, and V. So, "Physical exercise induces FGF-2 and its mRNA in the hippocampus," *Brain Research*, vol. 764, no. 1-2, pp. 1–8, 1997.

[77] F. Gomez-Pinilla, V. So, and J. P. Kesslak, "Spatial learning and physical activity contribute to the induction of fibroblast growth factor: neural substrates for increased cognition associated with exercise," *Neuroscience*, vol. 85, no. 1, pp. 53–61, 1998.

[78] F. Gomez-Pinilla, S. Vaynman, and Z. Ying, "Brain-derived neurotrophic factor functions as a metabotrophin to mediate the effects of exercise on cognition," *The European Journal of Neuroscience*, vol. 28, no. 11, pp. 2278–2287, 2008.

[79] K. Nakajima, S. Uchida, A. Suzuki, H. Hotta, and Y. Aikawa, "The effect of walking on regional blood flow and acetylcholine in the hippocampus in conscious rats," *Autonomic Neuroscience*, vol. 103, no. 1-2, pp. 83–92, 2003.

[80] M. Svensson, P. Rosvall, A. Boza-Serrano, E. Andersson, J. Lexell, and T. Deierborg, "Forced treadmill exercise can induce stress and increase neuronal damage in a mouse model of global cerebral ischemia," *Neurobiology of Stress*, vol. 5, pp. 8–18, 2016.

[81] C. D. Schneider, J. Barp, J. L. Ribeiro, A. Belló-Klein, and A. R. Oliveira, "Oxidative stress after three different intensities of running," *Canadian Journal of Applied Physiology*, vol. 30, no. 6, pp. 723–734, 2005.

Hindawi
Oxidative Medicine and Cellular Longevity
Volume 2019, Article ID 9417048, 9 pages
https://doi.org/10.1155/2019/9417048

Research Article

Buprenorphine and Methadone as Opioid Maintenance Treatments for Heroin-Addicted Patients Induce Oxidative Stress in Blood

Christonikos Leventelis,[1,2] Nikolaos Goutzourelas,[1] Aikaterini Kortsinidou,[1] Ypatios Spanidis,[1] Georgia Toulia,[3] Antzouletta Kampitsi,[2,4] Christina Tsitsimpikou,[5] Dimitrios Stagos,[1] Aristidis S. Veskoukis,[1] and Demetrios Kouretas[1]

[1]*Department of Biochemistry and Biotechnology, University of Thessaly, 41500 Larissa, Greece*
[2]*Organization Against Drugs, 10433 Athens, Greece*
[3]*Department of Nursing, University of West Attica, 12243 Athens, Greece*
[4]*General Anticancer Hospital "Agios Savvas", 11522 Athens, Greece*
[5]*General Chemical State Laboratory of Greece, 11521 Athens, Greece*

Correspondence should be addressed to Demetrios Kouretas; dkouret@uth.gr

Received 7 December 2018; Revised 11 March 2019; Accepted 17 March 2019; Published 9 April 2019

Guest Editor: Stefania Schiavone

Buprenorphine and methadone are two substances widely used in the substitution treatment of patients who are addicted to opioids. Although it is known that they partly act efficiently towards this direction, there is no evidence regarding their effects on the redox status of patients, a mechanism that could potentially improve their action. Therefore, the aim of the present investigation was to examine the impact of buprenorphine and methadone, which are administered as substitutes to heroin-dependent patients on specific redox biomarkers in the blood. From the results obtained, both the buprenorphine ($n = 21$) and the methadone ($n = 21$) groups exhibited oxidative stress and compromised antioxidant defence. This was evident by the decreased glutathione (GSH) concentration and catalase activity in erythrocytes and the increased concentrations of thiobarbituric acid reactive substances (TBARS) and protein carbonyls in the plasma, while there was no significant alteration of plasma total antioxidant capacity (TAC) compared to the healthy individuals ($n = 29$). Furthermore, methadone revealed more severe oxidant action compared to buprenorphine. Based on relevant studies, the tested substitutes mitigate the detrimental effects of heroin on patient redox status; still it appears that they need to be boosted. Therefore, concomitant antioxidant administration could potentially enhance their beneficial action, and most probably, buprenorphine that did not induce oxidative stress in such a severe mode as methadone, on the regulation of blood redox status.

1. Introduction

Drug addiction is a serious health problem that modern society has to face. It is indicative that mortality rates due to the increasing prevalence of opioid use have risen approaching an epidemic scale in some countries [1]. According to recent epidemiological data, there is an upward trend in Europe with regard to the number of overdose deaths, and intriguingly, opioids are responsible for the 81% of them [2]. In addition, it has been reported that in the European Union, opioids are the main substances of use (i.e., 38% of all cases), whereas heroin comprises the 79% of them. There is also a serious issue of this kind in North America since there has been observed enhanced morbidity and mortality associated with the abuse of prescription opioids, heroin, and lately, the use of high-potency synthetic opioids, especially fentanyl derivatives [2].

Opioids in general have twofold inhibitory action. They act both at the presynaptic nerve terminal by inhibiting neurotransmitter release and at the postsynaptic neuron.

Specifically, they primarily block μ (mu) receptors, thus, preventing the secretion of γ-aminobutyric acid (GABA) that acts on dopaminergic neurons by inhibiting dopamine release. The inhibitory action of opioids on GABA results in increased dopamine release by dopaminergic neurons in the ventral tegmental area (VTA), which is associated with the reward system through projecting to the nucleus accumbens [3]. The latter are considered the neural mediators for food intake, sexual behavior, motivation for reward, stress-related behavior, and substance dependence [4, 5]. Some of the well-described (side) effects of opioid use are analgesia, respiratory depression, euphoria, and psychological dependence [6]. The augmentation of dopamine release appears to be responsible for addiction in opioids. Interestingly, the increase of dopamine induced by stimuli associated with pleasure that are an outcome of opioid substance use leads to memorizing signals announcing the reward. Therefore, when the dopamine system is overstimulated, the desire to repeat this experience may be at the expense of other important targets [7, 8].

There are several studies in the literature demonstrating a connection between addiction in opioids and oxidative stress in neuron cells. Noteworthy, repeated use of large opioid doses causes permanent damage to the dopamine mechanism. This is due to elevated dopamine release, hence, causing its autooxidation that generates 3,4-dihydroxyphenylacetic acid (DOPAC), a metabolite of dopamine and H_2O_2 [9–11]. Hydrogen peroxide can subsequently react with metal ions (Fe^{++} and Cu^{+}) and during the Fenton reaction generates $OH^{\cdot}$ radical, which is probably the most reactive free radical in the cellular environment potentially inducing oxidative stress [12–18]. Furthermore, it has been shown that the increased dopamine release through its oxidation leads to the production of quinone radicals lowering the GSH : GSSG ratio and, therefore, the available reductive equivalents [17, 19–21]. The reactive species induced by opioid use activate the Jun N-terminal kinase/stress-activated protein kinase pathway (JNP/SAPK) causing neuron cell apoptosis [22, 23]. Due to potentially high levels of dopamine oxidation, it has been hypothesized that dopaminergic neuron endings more likely maintain dopamine levels in synaptic vesicles than neutralize the dopamine oxidation resulting in neurotoxic effects [10, 24].

Buprenorphine and methadone treatment is a common practice for rehab of individuals that use addictive substances. It involves the prescription of these drugs as substitutes to the opioids that a patient is dependent on [25–28]. Buprenorphine seems to be more effective than methadone because it causes less analgesia since it is not a full agonist of μ receptors [29]. It has been also demonstrated that methadone reduces opioid tolerance and alters redox status, thus alleviating the side effects of opioids [30]. To this end, there are numerous substitution programs worldwide administering buprenorphine and methadone and it has been reported that they increase the probability of recovery for the addictive individuals [31].

To our knowledge, there is scarce evidence that methadone and buprenorphine act through redox-related mechanisms [32, 33]. However, the literature lacks observational studies regarding their effects on the redox status of individuals that are addictive to opioid substances. It is known that drug addictions have a negative impact on the systemic antioxidant defences. Therefore, the goal of the present investigation was to examine the effects of methadone and buprenorphine, when used as substitute treatments, on the redox status of patients suffering from heroin addiction.

2. Materials and Methods

2.1. Participants. Seventy-one subjects participated in the present investigation. They were randomly divided into two groups, namely, the observation group ($n = 42$), which includes patients being under opioid maintenance treatment (OMT) in the therapeutic units of Attica Organization Against Drugs in Greece, and the control group ($n = 29$) comprising healthy individuals without prior contact with substances able to induce addiction. The OMT group was further divided in the MMT (methadone maintenance treatment) ($n = 21$) and the BMT (buprenorphine maintenance treatment) ($n = 21$) groups. The participating patients were fully informed about the purpose and objectives of the study. All necessary information and safeguards were provided to ensure the confidentiality of data, and each patient signed a consensus form before the study began. According to our inclusion criteria, all subjects were over 20 years of age and were long-term heroin or other opioid drug users and suffering from physical and mental dependence due to using. Participants with severe psychopathology and other serious medical problems, such as infection by human immunodeficiency virus (HIV) or hepatitis B virus (HBC), were excluded from the study. Patients with relapse to other addictive substances were not also included. In order to avoid this, all participants underwent weekly urine tests during the three-month period of the substitution treatment (i.e., methadone or buprenorphine) to rule out the use of other substances (i.e., opioids, methamphetamine, methadone, benzodiazepines, cannabis, tetrahydrocannabinol, amphetamine, and buprenorphine by one-step multidrug test kits). All subjects were found negative for substance abuse. The subjects' demographic data of the participants in the OMT programs including age, gender, area of residence, years attending Organization Against Drugs (OKANA, Athens, Greece) programs, age started using, and duration of using addictive substances before the OMT were obtained. All applied experimental procedures were in line with the European Union Guidelines laid down in the 1964 Declaration of Helsinki and approved by the Institutional Review Board of the University of Thessaly (Larissa, Greece) and the Organization Against Drugs (Athens, Greece).

2.2. Drug Administration. Commercial methadone hydrochloride solution (10 mg/ml) and buprenorphine/buprenorphine-naloxone pills (2-8 mg) were used for regular doses. The mean daily dose of methadone was 60 mg. According to the relevant literature, methadone doses of 40-50 mg or 80-100 mg per day are effective as opioid maintenance treatments for heroin-addicted patients [34, 35]. However, given

that, to our knowledge, there are no studies reporting an optimal methadone daily dose, and additionally, the inter-individual differences of patients constitute a crucial factor for drug efficiency; a medium dose (i.e., 60 mg) was chosen to be administered. With respect to buprenorphine, the mean daily dose was 16 mg. On the basis of the available data, this dosage regimen is the most commonly used in order buprenorphine to exert its action [35]. The substitutes were administered to the patients for three months that, according to previous studies, this is a proper time period for exerting their action without any side effects, although no relevant publications exist regarding their effects on blood redox status. It is worth mentioning that the patients used only heroin before the three-month period of the experimental procedure, whereas, as stated above, they received no other substances during it.

2.3. Blood Collection and Handling. Blood samples were drawn from a forearm vein of seated individuals and stored in ethylenediaminetetraacetic acid (EDTA; Becton-Dickinson, Franklin Lakes, NJ, USA) tubes. The samples were immediately centrifuged (1,370 g, 10 min, 4°C), and the supernatant (i.e., plasma) was collected for the measurement of the concentrations of protein carbonyls (PC) as a biomarker of protein oxidation, thiobarbituric acid reactive substances (TBARS) as a biomarker of lipid peroxidation, and total antioxidant capacity (TAC) as a crude biomarker for assessing blood antioxidant potency [36]. Subsequently, distilled water (dH_2O, 1 : 1 (v/v)) was added to the packed erythrocytes; they were inverted vigorously and centrifuged (4,020 g, 15 min, 4°C). The supernatant (i.e., the erythrocyte lysate) was collected and used for measuring the activity of catalase (CAT) as a fundamental antioxidant enzyme. A small amount of erythrocyte lysate (i.e., 500 μl) was treated with 5% trichloroacetic acid (TCA, Sigma-Aldrich, Munich, Germany) (1 : 1 (v/v)), vortexed, and centrifuged (28,000 g, 5 min, 4°C). The supernatant was then removed, and the same procedure was repeated once more. The clear supernatant was transferred in plastic tubes and used for the measurement of reduced glutathione (GSH) concentration as the most potent intrinsic antioxidant molecule [36]. Plasma and erythrocyte lysates were stored at -80°C until further analysis.

2.4. Protocols for the Measurement of Redox Biomarkers. The concentration of PC was determined on the basis of the method of Patsoukis et al. [37] as described by Veskoukis et al. [38]. In this assay, 50 μl of 20% TCA was added to 50 μl of plasma; the mixture was incubated for 15 min in an ice bath and centrifuged (15,000 g, 5 min, 4°C). The supernatant was removed, and 500 μl of 10 mM 2,4-dinitrophenylhydrazine (DNPH; Sigma-Aldrich, Munich, Germany) (in 2.5 N HCl) for the samples and 500 μl of 2.5 N HCl for the blank were added to the pellet. The samples were incubated in the dark at room temperature (RT) for 1 h with intermittent vortexing every 15 min and were centrifuged (15,000 g, 5 min, 4°C). The supernatant was removed, and 1 ml of 10% TCA was added; the samples were vortexed and centrifuged (15,000 g, 5 min, 4°C). The supernatant was then discarded, and 1 ml of ethanol-ethyl acetate mixture (1 : 1 (v/v)) was added; the samples were vortexed and centrifuged (15,000 g, 5 min, 4°C). This washing step was repeated twice. The supernatant was discarded again, and 1 ml of 5 M urea (pH = 2.3) was added; the samples were vortexed and incubated at 37°C for 15 min. They were then centrifuged (15,000 g, 3 min, 4°C), and the absorbance was monitored at 375 nm using a spectrophotometer (Hitachi U-1900; serial no. 2023-029; Hitachi, Tokyo, Japan). The determination of PC concentration was based on the millimolar extinction coefficient of DNPH (22 l/mmol/cm).

The assay for the determination of TBARS concentration was based on the method described by Keles et al. [39]. According to it, 100 μl of plasma (or dH_2O for the blank) was mixed with 500 μl of 35% TCA (Merck KGaA, Darmstadt, Germany) and 500 μl of Tris-HCl (Sigma-Aldrich, St. Louis, MO, USA; 200 mM, pH = 7.4) and incubated at RT for 10 min. One milliliter of 2 M sodium sulfate (Na_2SO_4) and 55 mM of thiobarbituric acid solution were added, and the samples were incubated in a waterbath at 95°C for 45 min. The samples were cooled on ice and vortexed following the addition of 1 ml of 70% TCA. Then, they were centrifuged (15,000 g, 3 min, 25°C) and the absorbance of the supernatant was monitored at 530 nm. The calculation of the TBARS concentration was based on the molar extinction coefficient of malondialdehyde [40].

TAC measurement was based on the method described by Janaszewska and Bartosz [41]. Briefly, 20 μl of plasma (or dH_2O for the blank) was added to 480 μl of sodium potassium phosphate buffer (10 mM, pH = 7.4) and 500 μl of 0.1 mM 1,1-diphenyl-1-picrylhydrazyl radical ($DPPH^{\cdot}$) and the samples were incubated in the dark at RT for 60 min. The samples were then centrifuged (20,000 g, 3 min, 25°C), and the absorbance was monitored at 520 nm. TAC determination was based on the mmol of $DPPH^{\cdot}$ reduced by the antioxidants present in the plasma [40].

CAT activity was determined on the basis of the method of Aebi [42] as described by Veskoukis et al. [38]. In particular, 4 μl of erythrocyte lysate (diluted 1 : 10) was added to 2,991 μl of sodium potassium phosphate buffer (67 mM, pH = 7.4) and the samples were incubated at 37°C for 10 min. Then, 5 μl of 30% H_2O_2 solution was added and the change in absorbance was immediately read at 240 nm for 130 sec. The calculation of CAT activity was based on the molar extinction coefficient of H_2O_2.

GSH concentration was measured based on the method of Reddy et al. [43] as described by Veskoukis et al. [38]. For this assay, 20 μl of erythrocyte lysate (or dH_2O for the blank) previously treated with 5% TCA was mixed with 660 μl of sodium-potassium phosphate buffer (67 mM, pH = 8) and 330 μl of 1 mM 5,5-dithiobis-2 nitrobenzoate (DTNB; Sigma-Aldrich, Munich, Germany). The samples were incubated in the dark at RT for 45 min, and the absorbance was monitored at 412 nm. The GSH concentration was calculated on the basis of a standard curve using commercially available standards.

Total protein in plasma samples was measured using Bradford reagent. Hemoglobin concentration in erythrocyte lysates was determined with a commercially available kit

(Drabkin) according to the manufacturer's instructions. Each assay was performed in triplicate at two different occasions.

2.5. Statistical Analysis. Data regarding redox biomarkers were analyzed by one-way ANOVA followed by Dunnett's test for multiple pairwise comparisons. Correlation analysis between redox biomarkers and demographic data was carried out using Pearson's correlation coefficient. The statistical significance was set at $p < 0.05$. For all statistical analyses, SPSS software version 21.0 (SPSS Inc., Chicago, IL, USA) was used. Data are presented as the mean ± standard error of the mean (SEM).

3. Results

3.1. Demographic Data. With respect to the control group, the mean age was 36.3 ± 3.2 years old and 68.9% of the participants were men. The demographic data of the participants in the OMT programs are depicted in Table 1. In brief, the mean age was 40.5 ± 1.3 years old, 68.9% of the participants were men, they mostly lived in urban areas (i.e., 92.9%), the mean time of attending OKANA programs was 0.98 ± 0.17 years, and they mainly started using addictive substances at the age of 11-20 (i.e., 66.7%) for 11-20 years (i.e., 45.2%). Furthermore, Spearman's correlations between the demographic data and the redox biomarkers exerted no statistical significance.

3.2. Redox Biomarkers. Regarding GSH concentration and catalase activity, they were both found significantly decreased in the group of patients as a whole compared to the control by 54% and 16%, respectively (Figure 1). According to the results on the basis of each administered substance, GSH concentration was reduced in both the BMT and MMT groups compared to the control by 51% and 58%, respectively (Figure 2). No significant difference between the BMT and MMT groups was observed. Furthermore, CAT activity decreased in both the BMT and MMT groups compared to the control by 10% and 22%, respectively. There was also a significant difference in CAT activity between the MMT and BMT groups (Figure 2). With respect to PC and TBARS concentrations, a significant increase was observed in the levels of both biomarkers in the group of patients as a whole compared to the control by 34% and 112%, respectively (Figure 3). On the basis of each administered substance, PC concentration was increased in both the BMT and MMT groups by 34% and 51%, respectively (Figure 4). TBARS concentration was increased in both the BMT and MMT groups compared to the control by 120% and 105%, respectively. No significant differences between the BMT and MMT groups in either PC or TBARS levels were noticed. Finally, there were no alterations in TAC levels between the tested groups of participants (Figures 5 and 6).

Table 1: Demographic data of the participants in the OMT programs ($n = 42$).

Age (yrs)	40.5 ± 1.3
Gender (%)	Men **(73.8)**
	Women **(26.2)**
Area of residence (%)	Urban **(92.9)**
	Rural **(7.1)**
Years attending OKANA programs	0.98 ± 0.17
Age started using addictive substances (%)	11-20 **(66.7)**
	21-30 **(26.2)**
	31-40 **(7.1)**
Years using addictive substances (%)	0-10 **(21.4)**
	11-20 **(45.2)**
	21-30 **(21.4)**
	31-40 **(11.9)**

4. Discussion

The main findings of the present investigation indicate that buprenorphine and methadone, two opioid substitutes administered to heroin users in order to get into the rehab period, induce oxidative stress compared to healthy individuals. It becomes apparent, hence that although they impair the unpleasant and often inhumane side effects of heroin, they still disrupt redox balance in the blood of patients.

It is worth mentioning that methadone is a full agonist of the μ-opioid receptor, whereas buprenorphine is a partial agonist of the μ-opioid receptor and a κ-receptor antagonist [44, 45]. Both agents are used in substitution treatment to reduce opioid damage, which is referred to as MMT (methadone maintenance treatment) and BMT (buprenorphine maintenance treatment), respectively [46, 47]. Several studies have asserted the relation of opioid cytotoxic effects with the disruption of redox balance and have stressed the protective role of GSH. Specifically, increased production of reactive oxygen species (ROS) has been associated with heroin-induced intracellular dopamine and DOPAC [16], whereas dopamine infusion in GSH-depleted SK-N-SH neuroblastoma cells increased apoptosis, nuclear DNA fragmentation, and cell membrane lesions [48]. In line with the above studies, it has also been demonstrated that a reduction of extracellular GSH was observed when astrocytes were cultured in a dopamine-rich solution indicating that dopamine is an oxidant agent especially in the absence of GSH [20], while methamphetamine-treated rats exhibited reduced GSH concentration in the striatum [21].

The negative impact of both opioids used in the present investigation (i.e., buprenorphine and methadone) on blood antioxidant status is depicted by the results in GSH concentration and CAT activation. Specifically, they were both found reduced at the patient group compared to the healthy individuals implying that their antioxidant defence was compromised. In addition, methadone seems to have a more severe effect as indicated by the significantly lower values of catalase compared to buprenorphine. These results are supported by previous findings [49–52]. Specifically, methadone appears to have a greater impact on lowering antioxidant defence since patients under MMT have shown a depletion of GSH and CAT levels [50, 52]. Nevertheless, studies comparing heroin users and methadone-treated patients have reported that the MMT group exhibits improvement in redox biomarkers [30, 53, 54]. On the same grounds, TAC

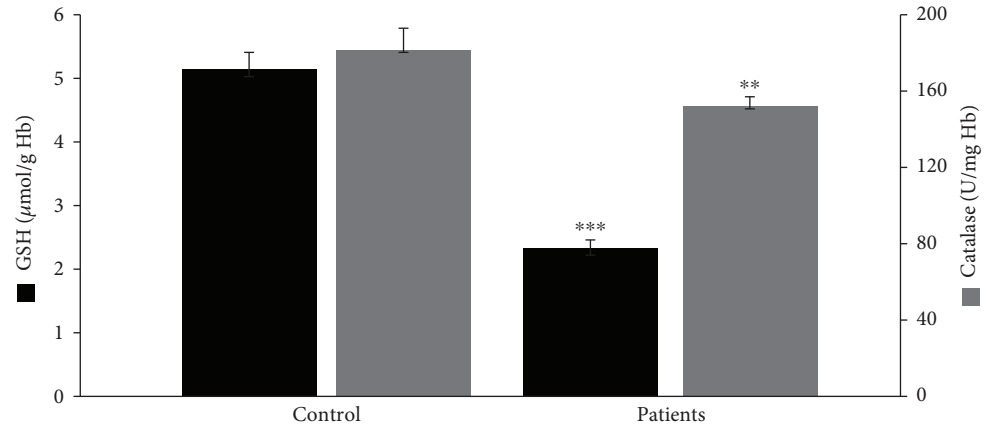

Figure 1: GSH concentration and catalase activity in the control group ($n = 29$) and the OMT patients as a whole ($n = 42$). **,***Significantly different compared to the control group ($p < 0.05$ and $p < 0.001$, respectively).

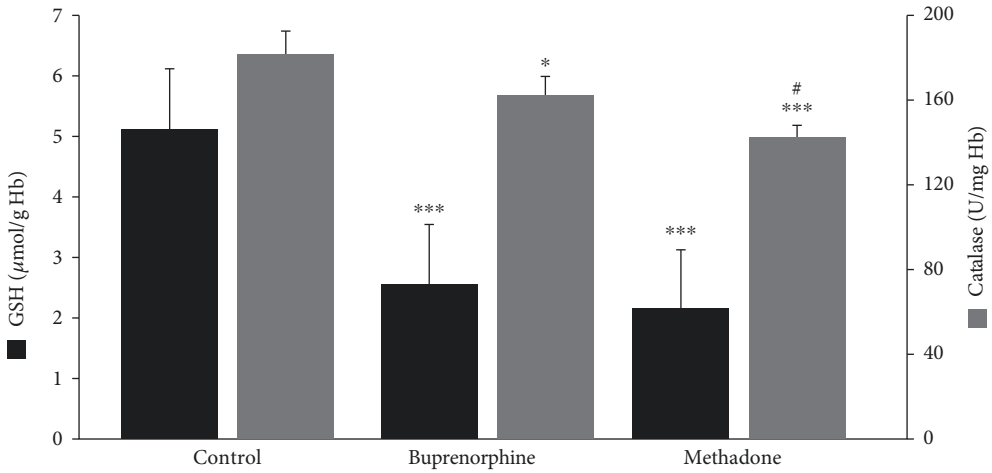

Figure 2: GSH concentration and catalase activity in the control ($n = 29$), the BMT (buprenorphine) ($n = 21$), and the MMT (methadone) ($n = 21$) groups. *,***Significantly different compared to the control group ($p < 0.05$ and $p < 0.001$, respectively). #Significantly different compared to the buprenorphine group ($p < 0.05$).

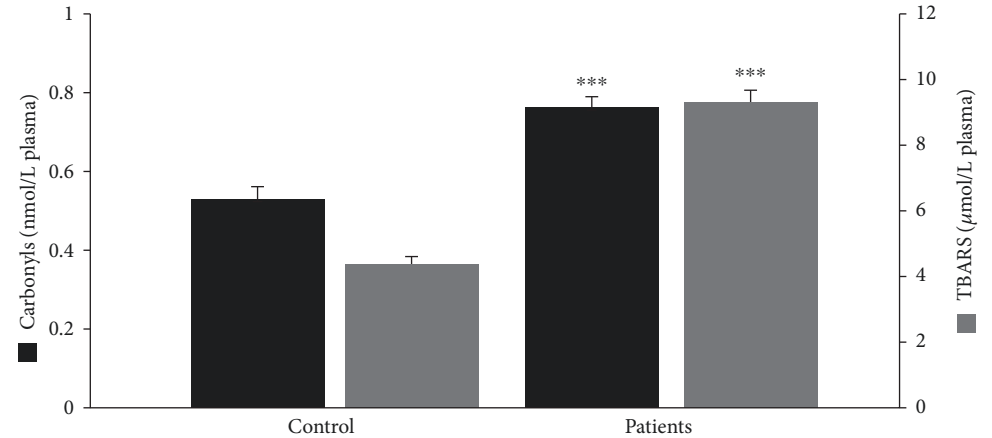

Figure 3: Protein carbonyl and TBARS concentrations in the control group ($n = 29$) and the OMT patients as a whole ($n = 42$). *** Significantly different compared to the control group ($p < 0.001$).

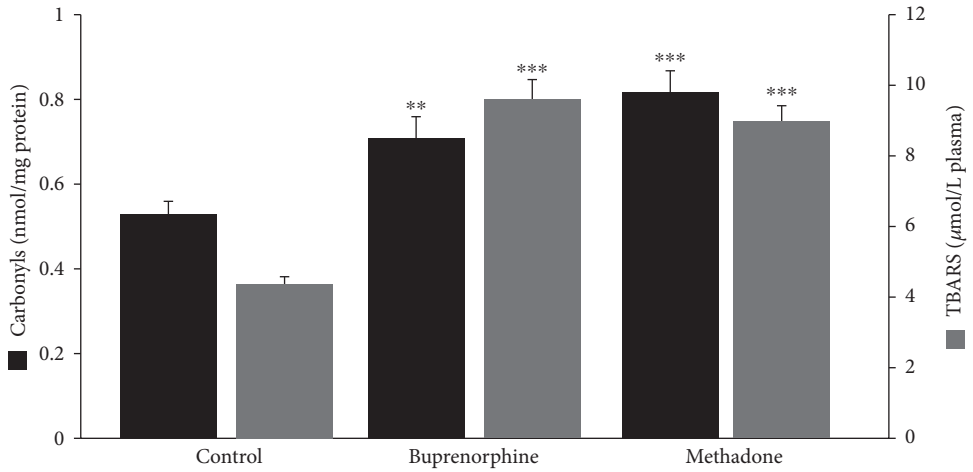

Figure 4: Protein carbonyl and TBARS concentrations in the control ($n = 29$), the BMT (buprenorphine) ($n = 21$), and the MMT (methadone) ($n = 21$) groups. **,***Significantly different compared to the control group ($p < 0.01$ and $p < 0.001$, respectively).

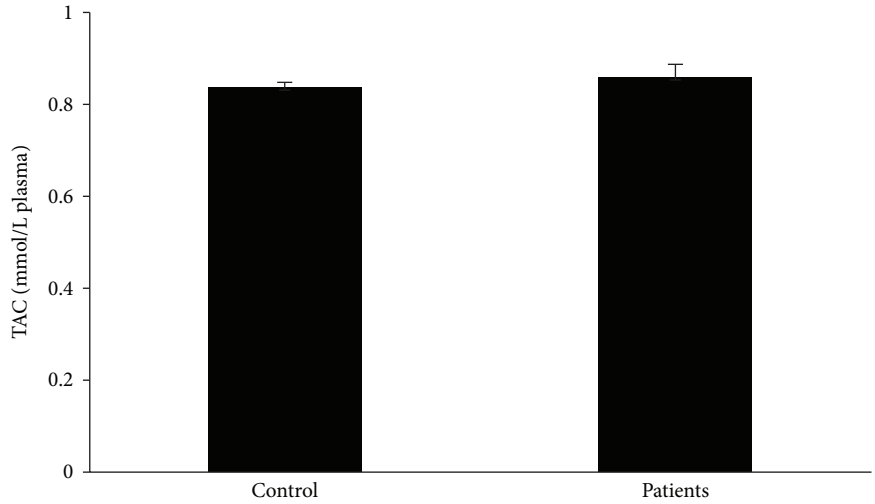

Figure 5: TAC levels in the control group ($n = 29$) and the OMT patients as a whole ($n = 42$).

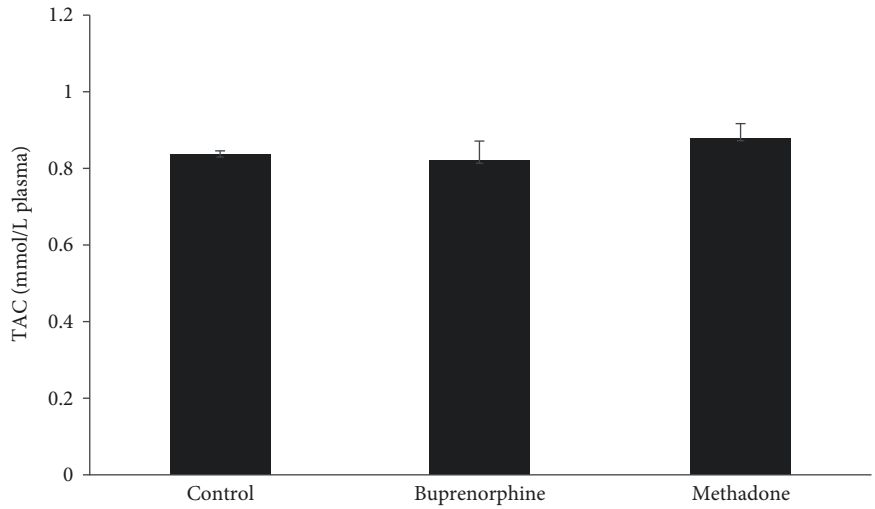

Figure 6: TAC levels in the control ($n = 29$), the BMT (buprenorphine), ($n = 21$) and the MMT (methadone) ($n = 21$) groups.

is decreased after opioid administration, especially heroin [9, 55–57], but it seems that substitutes have a positive effect [9, 58] increasing the antioxidant capacity of the organism. These findings are optimistic because they support the notion that although substitute treatment induces oxidative stress, this occurs in much less extent in comparison to heroin, thus reinforcing its use at rehab programs. In addition, reduction of heroin damage by substitute treatment enhances total antioxidant activity [58]. With respect to the biomarkers illustrating the oxidative modification of biomolecules, both PC and TBARS concentrations were elevated in the MMT and BMT groups. Several studies are in line with our findings indicating that methadone and buprenorphine induce oxidative stress [55, 59]. Indeed, malondialdehyde (MDA) levels were found elevated in opioid addicts [60] and in heroin users compared to methadone-administered individuals [9, 32]. Similarly, an increase in TBARS concentration has been observed in mice following heroin administration [56], whereas no significant difference after the administration of buprenorphine in comparison to the healthy animals was observed in rats [51].

It is known that, although buprenorphine and methadone induce oxidative stress as is the case in the present study too, they do it in lower extent in comparison to opioids, such as heroin that an individual can potentially be dependent on. Comparing the two agonists, buprenorphine appears to have a less severe impact on oxidative stress keeping a higher burden of intrinsic antioxidants, a fact that is in conformity with previous results reporting that buprenorphine inhibits oxidative stress [61]. To this direction, it has been proposed that internalizing opioids (methadone, fentanyl, sufentanil) activate phospholipase D2 (PLD2) and lead to enhanced ROS generation, while noninternalizing agonists (i.e., buprenorphine) do not [62]. PLD2 activation is contributed to the endocytosis of the μ-receptor and the development of opioid tolerance [63, 64]. PLD2 is considered to play an important role not only in the membrane trafficking of the μ receptor but also in the functional selectivity of opioids at it. Furthermore, the increase of free radical generation by PLD2-activating opioids is also implicated in other signaling pathways induced by growth factors playing an important role in cell proliferation and differentiation [60]. The mechanism by which ROS mediate cell proliferation appears to be associated with the activation of extracellular signal-regulated kinase 5 and p38 MAPK, which are redox-sensitive [65]. Furthermore, the product of PLD, phosphatidic acid, has been found to lead through its interaction with the mammalian target of rapamycin (mTOR) in the release and activation of cytokines [66, 67]. Notably, it has been demonstrated that exogenous administration of antioxidants can act protectively against free radical generation induced by opioids used for maintenance treatment [32, 56].

5. Conclusion

The present investigation asserts that buprenorphine and methadone, two widely used substitutes for opioid maintenance treatment, induce oxidative stress and compromise blood antioxidant defence mechanisms. It is noteworthy that according to the findings of other relevant studies, they (especially buprenorphine) attenuate the severe oxidative impact of heroin and other opioids that cause addiction. Thus, with respect to improving the antioxidant burden of patients dependent on opioids, it appears that buprenorphine and methadone act towards the desirable direction. However, as it has been previously reported, concomitant antioxidant administration could potentially enhance their beneficial action by regulating blood redox status.

Data Availability

The data used to support the findings of this study are available from the corresponding author upon request.

Conflicts of Interest

The authors declare no conflict of interest.

Acknowledgments

This article was supported by the Department of Biochemistry and Biotechnology, University of Thessaly, Greece.

References

[1] J. Jones, C. Mateus, P. Malcolm, K. Brady, and S. Back, "Efficacy of ketamine in the treatment of substance use disorders: a systematic review," *Frontiers in Psychiatry*, vol. 9, p. 277, 2018.

[2] European Monitoring Centre for Drugs and Drug Addiction (EMCADA), *European Drug Report 2018: Trends and Developments*, Publications Office of the European Union, Luxembourg, 2018.

[3] L. D. Langlois and F. S. Nugent, "Opiates and plasticity in the ventral tegmental area," *ACS Chemical Neuroscience*, vol. 8, no. 9, pp. 1830–1838, 2017.

[4] C. A. Owesson-White, J. Ariansen, G. D. Stuber et al., "Neural encoding of cocaine-seeking behavior is coincident with phasic dopamine release in the accumbens core and shell," *European Journal of Neuroscience*, vol. 30, no. 6, pp. 1117–1127, 2009.

[5] J. A. Kauer, "Learning mechanisms in addiction: synaptic plasticity in the ventral tegmental area as a result of exposure to drugs of abuse," *Annual Review of Physiology*, vol. 66, no. 1, pp. 447–475, 2004.

[6] R. Ting-A-Kee and D. van der Kooy, "The neurobiology of opiate motivation," *Cold Spring Harbor Perspectives in Medicine*, vol. 2, no. 10, 2012.

[7] J. Cami and M. Farre, "Drug addiction," *The New England Journal of Medicine*, vol. 349, no. 10, pp. 975–986, 2003.

[8] D. N. Volkow, G. J. Wang, S. J. Fowler, and D. Tomasi, "Addiction circuitry in the human brain," *Annual Review of Pharmacology and Toxicology*, vol. 52, no. 1, pp. 321–336, 2012.

[9] Z. Pereska, B. Dejanova, C. Bozinovska, and L. Petkovska, "Prooxidative/antioxidative homeostasis in heroin addiction and detoxification," *Bratislavske Lekarske Listy*, vol. 108, no. 9, pp. 393–398, 2007.

[10] T. G. Hastings, D. A. Lewis, and M. J. Zigmond, "Role of oxidation in the neurotoxic effects of intrastriatal dopamine injections," *Proceedings of the National Academy of Sciences of the United States of America*, vol. 93, no. 5, pp. 1956–1961, 1996.

[11] C. W. Olanow and W. G. Tatton, "Etiology and pathogenesis of Parkinson's disease," *Annual Review of Neuroscience*, vol. 22, no. 1, pp. 123–144, 1999.

[12] C. Mylonas and D. Kouretas, "Lipid peroxidation and tissue damage," *In Vivo*, vol. 13, no. 3, pp. 295–309, 1999.

[13] V. Chiurchiù and M. MacCarrone, "Chronic inflammatory disorders and their redox control: from molecular mechanisms to therapeutic opportunities," *Antioxidants and Redox Signaling*, vol. 15, no. 9, pp. 2605–2641, 2011.

[14] B. Halliwell and J. M. C. Gutteridge, *Free Radicals in Biology and Chemistry*, Oxford Science Publications, New York, NY, USA, 6th edition, 2015.

[15] A. S. Veskoukis, A. M. Tsatsakis, and D. Kouretas, "Dietary oxidative stress and antioxidant defense with an emphasis on plant extract administration," *Cell Stress & Chaperones*, vol. 17, no. 1, pp. 11–21, 2012.

[16] M. T. Oliveira, A. C. Rego, M. T. Morgadinho, T. R. A. Macedo, and C. R. Oliveira, "Toxic effects of opioid and stimulant drugs on undifferentiated PC12 cells," *Annals of the New York Academy of Sciences*, vol. 965, no. 1, pp. 487–496, 2002.

[17] J. Hirrlinger, J. B. Schulz, and R. Dringen, "Effects of dopamine on the glutathione metabolism of cultured astroglial cells: implications for Parkinson's disease," *Journal of Neurochemistry*, vol. 82, no. 3, pp. 458–467, 2002.

[18] R. Von Bernhardi and J. Eugenín, "Alzheimer's disease: redox dysregulation as a common denominator for diverse pathogenic mechanisms," *Antioxidants and Redox Signaling*, vol. 16, no. 9, pp. 974–1031, 2012.

[19] J. B. Schulz, J. Lindenau, J. Seyfried, and J. Dichgans, "Glutathione, oxidative stress and neurodegeneration," *European Journal of Biochemistry*, vol. 267, no. 16, pp. 4904–4911, 2000.

[20] A. D. Rabinovic and T. Hastings, "Role of endogenous glutathione in the oxidation of dopamine," *Journal of Neurochemistry*, vol. 71, no. 5, pp. 2071–2078, 1998.

[21] A. Moszczynska, S. Turenne, and S. J. Kish, "Rat striatal levels of the antioxidant glutathione are decreased following binge administration of methamphetamine," *Neuroscience Letters*, vol. 255, no. 1, pp. 49–52, 1998.

[22] J. L. Cadet, S. Jayanthi, and X. Deng, "Speed kills: cellular and molecular bases of methamphetamine-induced nerve terminal degeneration and neuronal apoptosis," *The FASEB Journal*, vol. 17, no. 13, pp. 1775–1788, 2003.

[23] H. Pu, X. Wang, L. Su et al., "Heroin activates ATF3 and CytC via c-Jun N-terminal kinase pathways to mediate neuronal apoptosis," *Medical Science Monitor Basic Research*, vol. 21, pp. 53–62, 2015.

[24] M. T. Oliveira, A. C. Rego, T. R. A. Macedo, and C. R. Oliveira, "Drugs of abuse induce apoptotic features in PC12 cells," *Annals of the New York Academy of Sciences*, vol. 1010, no. 1, pp. 667–670, 2003.

[25] E. Wu, N. El Bassel, L. Gilbert, M. Chang, and G. Sanders, "Effects of receiving additional off-site services on abstinence from illicit drug use among men on methadone: a longitudinal study," *Evaluation and Program Planning*, vol. 33, no. 4, pp. 403–409, 2009.

[26] A. Ponizovsky, A. Grinshpoon, A. Margolis, R. Cohen, and P. Rosca, "Well-being, psychosocial factors, and side-effects among heroin-dependent inpatients after detoxification using buprenorphine versus clonidine," *Addictive Behaviors*, vol. 31, no. 11, pp. 2002–2013, 2006.

[27] H. Wittchen, S. Apelt, M. Soyka, M. Gastpar, and M. Backmund, "Feasibility and outcome of substitution treatment of heroin-dependent patients in specialized substitution centers and primary care facilities in Germany: a naturalistic study in 2694 patients," *Drug and Alcohol Dependence*, vol. 95, no. 3, pp. 245–257, 2008.

[28] M. Geitona, V. Carayanni, and P. Petratos, "Economic evaluation of opioid substitution treatment in Greece," *Heroin Addiction and Related Clinical Problems*, vol. 14, no. 3, pp. 77–88, 2012.

[29] P. J. Whelan and K. Remski, "Buprenorphine vs methadone treatment: a review of evidence in both developed and developing worlds," *Journal of Neurosciences in Rural Practice*, vol. 3, no. 1, pp. 45–50, 2012.

[30] P. Mannelli, A. Patkar, S. Rozen, W. Matson, R. Krishnan, and R. Kaddurah-Daouk, "Opioid use affects antioxidant activity and purine metabolism: preliminary results," *Human Psychopharmacology*, vol. 24, no. 8, pp. 666–675, 2009.

[31] B. J. Yarborough, S. P. Stumbo, D. McCarty, J. Mertens, C. Weisner, and C. A. Green, "Methadone, buprenorphine and preferences for opioid agonist treatment: a qualitative analysis," *Drug and Alcohol Dependence*, vol. 160, pp. 112–118, 2016.

[32] A. Salarian, M. Kadkhodaee, M. Zahmatkesh et al., "Opioid use disorder induces oxidative stress and inflammation: the attenuating effect of methadone maintenance treatment," *Iranian Journal of Psychiatry*, vol. 13, no. 1, pp. 46–54, 2018.

[33] J. Cote and L. Montgomery, "Sublingual buprenorphine as an analgesic in chronic pain: a systematic review," *Pain Medicine*, vol. 15, no. 7, pp. 1171–1178, 2014.

[34] E. C. Strain, G. E. Bigelow, I. A. Liebson, and M. L. Stitzer, "Moderate- vs high-dose methadone in the treatment of opioid dependence," *JAMA*, vol. 281, no. 11, pp. 1000–1005, 1999.

[35] A. J. Saxon, Y. I. Hser, G. Woody, and W. Ling, "Medication-assisted treatment for opioid addiction: methadone and buprenorphine," *Journal of Food and Drug Analysis*, vol. 21, no. 4, pp. S69–S72, 2013.

[36] A. S. Veskoukis, E. Kerasioti, A. Priftis et al., "A battery of translational biomarkers for the assessment of the *in vitro* and *in vivo* antioxidant action of plant polyphenolic compounds: the biomarker issue," *Current Opinion in Toxicology*.

[37] N. Patsoukis, G. Zervoudakis, N. T. Panagopoulos, C. D. Georgiou, F. Angelatou, and N. A. Matsokis, "Thiol redox state (TRS) and oxidative stress in the mouse hippocampus after pentylenetetrazol-induced epileptic seizure," *Neuroscience Letters*, vol. 357, no. 2, pp. 83–86, 2004.

[38] A. S. Veskoukis, A. Kyparos, V. Paschalis, and M. G. Nikolaidis, "Spectrophotometric assays for measuring redox biomarkers in blood," *Biomarkers*, vol. 21, no. 3, pp. 208–217, 2016.

[39] M. S. Keles, S. Taysi, N. Sen, H. Aksoy, and F. Akçay, "Effect of corticosteroid therapy on serum and CSF malondialdehyde and antioxidant proteins in multiple sclerosis," *The Canadian Journal of Neurological Sciences*, vol. 28, no. 2, pp. 141–143, 2001.

[40] A. S. Veskoukis, M. G. Nikolaidis, A. Kyparos et al., "Effects of xanthine oxidase inhibition on oxidative stress and swimming performance in rats," *Applied Physiology, Nutrition, and Metabolism*, vol. 33, no. 6, pp. 1140–1154, 2008.

[41] A. Janaszewska and G. Bartosz, "Assay of total antioxidant capacity: comparison of four methods as applied to human

blood plasma," *Scandinavian Journal of Clinical and Laboratory Investigation*, vol. 62, no. 3, pp. 231–236, 2002.

[42] H. Aebi, "[13] Catalase *in vitro*," *Methods in Enzymology*, vol. 105, pp. 121–126, 1984.

[43] Y. N. Reddy, S. V. Murthy, D. R. Krishna, and M. C. Prabhakar, "Role of free radicals and antioxidants in tuberculosis patients," *The Indian Journal of Tuberculosis*, vol. 51, pp. 213–221, 2004.

[44] A. Ferrari, C. P. R. Coccia, A. Bertolini, and E. Sternieri, "Methadone—metabolism, pharmacokinetics and interactions," *Pharmacological Research*, vol. 50, no. 6, pp. 551–559, 2004.

[45] E. C. Strain, "Pharmacology of buprenorphine," in *The Treatment of Opioid Dependence*, E. C. Strain and M. L. Stitzer, Eds., pp. 213–229, Johns Hopkins Press, Baltimore, MD, USA, 2006.

[46] M. Kahan, A. Srivastava, A. Ordean, and S. Cirone, "Buprenorphine: new treatment of opioid addiction in primary care," *Canadian family physician Medecin de famille canadien*, vol. 57, no. 3, pp. 281–289, 2011.

[47] J. Seifert, C. Metzner, W. Paetzold et al., "Mood and affect during detoxification of opiate addicts: a comparison of buprenorphine versus methadone," *Addiction Biology*, vol. 10, no. 2, pp. 157–164, 2005.

[48] A. H. Stokes, D. Y. Lewis, L. H. Lash et al., "Dopamine toxicity in neuroblastoma cells: role of glutathione depletion by L-BSO and apoptosis," *Brain Research*, vol. 858, no. 1, pp. 1–8, 2000.

[49] M. Hemshekhar, V. Anaparti, C. Hitchon, and N. Mookherjee, "Buprenorphine alters inflammatory and oxidative stress molecular markers in arthritis," *Mediators of Inflammation*, vol. 2017, Article ID 2515408, 10 pages, 2017.

[50] M. G. Di Bello, E. Masini, C. Ioannides et al., "Erratum to: histamine release from rat mast cells induced by the metabolic activation of drugs of abuse into free radicals," *Inflammation Research*, vol. 62, no. 2, p. 247, 2013.

[51] S. Samarghandian, M. Azimi-Nezhad, R. Afshari, T. Farkhondeh, and F. Karimnezhad, "Effects of buprenorphine on balance of oxidant/antioxidant system in the different ages of male rat liver," *Journal of Biochemical and Molecular Toxicology*, vol. 29, no. 6, pp. 249–253, 2015.

[52] C. Aranas, A. Cutando, M. J. Ferrera et al., "Parameters of oxidative stress in saliva from diabetic and parenteral drug addict patients," *Journal of Oral Pathology and Medicine*, vol. 35, no. 9, pp. 554–559, 2006.

[53] J. Díaz-Flores Estévez, F. Díaz-Flores Estévez, C. Hernández Calzadilla, E. Rodríguez Rodríguez, C. Díaz Romero, and L. Serra-Majem, "Application of linear discriminant analysis to the biochemical and haematological differentiation of opiate addicts from healthy subjects: a case–control study," *European Journal of Clinical Nutrition*, vol. 58, no. 3, pp. 449–455, 2004.

[54] M. A. Rodriguez-Delgado, J. F. Diaz-Flores Estevez, F. Diaz-Flores Estevez, C. Hernandez Calzadilla, and C. Diaz Romero, "Fast determination of retinol and α-tocopherol in plasma by LC," *Journal of Pharmaceutical and Biomedical Analysis*, vol. 28, no. 5, pp. 991–997, 2002.

[55] B. Xu, Z. Wang, G. Gang et al., "Heroin-administered mice involved in oxidative stress and exogenous antioxidant-alleviated withdrawal syndrome," *Basic Clinical Pharmacology Toxicology*, vol. 99, no. 2, pp. 153–161, 2006.

[56] J. Pan, Q. Zhang, Y. Zhang, Z. Ouyang, Q. Zheng, and R. Zheng, "Oxidative stress in heroin administered mice and natural antioxidants protection," *Life Sciences*, vol. 77, no. 2, pp. 183–193, 2005.

[57] A. Ghazavi, G. Mosayebi, H. Solhi, M. Rafiei, and S. M. Moazzeni, "Serum markers of inflammation and oxidative stress in chronic opium (Taryak) smokers," *Immunology Letters*, vol. 153, no. 1-2, pp. 22–26, 2013.

[58] M. Akbari, R. Afshari, M. Sharifi, S. I. Hashemy, S. Majidinia, and N. K. Tousi, "Evaluation of the effect of diacetyl morphine on salivary factors and their changes after methadone therapy," *The Journal of Contemporary Dental Practice*, vol. 15, no. 6, pp. 730–734, 2014.

[59] B. Soykut, A. Eken, O. Erdem et al., "Oxidative stress enzyme status and frequency of micronuclei in heroin addicts in Turkey," *Toxicology Mechanisms and Methods*, vol. 23, no. 9, pp. 684–688, 2013.

[60] K. Najafi, S. Ahmadi, M. Rahpeyma et al., "Study of serum malondialdehyde level in opioid and methamphetamine dependent patients," *Acta Medica Iranica*, vol. 55, no. 10, pp. 616–620, 2017.

[61] L. Xu and W. W. Huang, "Effect of buprenorphine transdermal patch combined with patientcontrolled intravenous analgesia on the serum pain-related biochemical indexes in elderly patients with intertrochanteric fracture," *Journal of Hainan Medical University*, vol. 23, no. 17, pp. 67–70, 2017.

[62] T. Koch, A. Seifert, D. F. Wu et al., "μ-Opioid receptor-stimulated synthesis of reactive oxygen species is mediated via phospholipase D2," *Journal of Neurochemistry*, vol. 110, no. 4, pp. 1288–1296, 2009.

[63] T. Koch, A. Widera, K. Bartzsch et al., "Receptor endocytosis counteracts the development of opioid tolerance," *Molecular Pharmacology*, vol. 67, no. 1, pp. 280–287, 2005.

[64] T. Koch, D. F. Wu, L. Q. Yang, L. O. Brandenburg, and V. Hollt, "Role of phospholipase D2 in the agonist-induced and constitutive endocytosis of G-protein coupled receptors," *Journal of Neurochemistry*, vol. 97, no. 2, pp. 365–372, 2006.

[65] S. Okamoto, D. Krainc, K. Sherman, and S. Lipton, "Antiapoptotic role of the p38 mitogen-activated protein kinase–myocyte enhancer factor 2 transcription factor pathway during neuronal differentiation," *Proceedings of the National Academy of Sciences of the United States of America*, vol. 97, no. 13, pp. 7561–7566, 2000.

[66] Y. Fang, M. Viella-Bach, R. Bachmann, A. Flanigan, and J. Chen, "Phosphatidic acid-mediated mitogenic activation of mTOR signaling," *Science*, vol. 294, no. 5548, pp. 1942–1945, 2001.

[67] H. Lim, Y. Choi, W. Park, T. Lee, S. Ryu, and S. Kim, "Phosphatidic acid regulates systemic inflammatory responses by modulating the Akt-mammalian target of rapamycin-p70 S6 kinase 1 pathway," *Journal of Biological Chemistry*, vol. 278, no. 46, pp. 45117–45127, 2003.

Hindawi
Oxidative Medicine and Cellular Longevity
Volume 2019, Article ID 5452727, 10 pages
https://doi.org/10.1155/2019/5452727

Research Article

"Special K" Drug on Adolescent Rats: Oxidative Damage and Neurobehavioral Impairments

Sabrina de Carvalho Cartágenes,[1] Luanna Melo Pereira Fernandes,[1] Taiana Cristina Vilhena Sarmento Carvalheiro,[1] Thais Miranda de Sousa,[1] Antônio Rafael Quadros Gomes,[2] Marta Chagas Monteiro,[2] Ricardo Sousa de Oliveira Paraense,[3] Maria Elena Crespo-López,[3] Rafael Rodrigues Lima,[4] Enéas Andrade Fontes-Júnior,[1] Rui Daniel Prediger,[5] and Cristiane Socorro Ferraz Maia[1]

[1]*Laboratory of Pharmacology of Inflammation and Behavior, Pharmacy Faculty, Institute of Health Sciences, Federal University of Pará, Belém, Pará, Brazil*
[2]*Laboratory of Microbiology and Immunology of Teaching and Research, Pharmacy Faculty, Institute of Health Science, Federal University of Pará, Belém, Pará, Brazil*
[3]*Laboratory of Molecular Pharmacology, Institute of Biological Sciences, Federal University of Pará, Belém, Pará, Brazil*
[4]*Laboratory of Functional and Structural Biology, Institute of Biological Sciences, Federal University of Pará, Belém, Pará, Brazil*
[5]*Department of Pharmacology, Center of Biological Sciences, Federal University of Santa Catarina, Florianópolis, Santa Catarina, Brazil*

Correspondence should be addressed to Cristiane Socorro Ferraz Maia; crismaia@ufpa.br

Received 17 April 2018; Revised 19 December 2018; Accepted 31 December 2018; Published 14 March 2019

Guest Editor: Margherita Neri

Ketamine is used in clinical practice as an anesthetic that pharmacologically modulates neurotransmission in postsynaptic receptors, such as NMDA receptors. However, widespread recreational use of ketamine in "party drug" worldwide since the 1990s quickly spread to the Asian orient region. Thus, this study aimed at investigating the behavioral and oxidative effects after immediate withdrawal of intermittent administration of ketamine in adolescent female rats. For this, twenty female Wistar rats were randomly divided into two groups: control and ketamine group ($n = 10$/group). Animals received ketamine (10 mg/kg/day) or saline intraperitoneally for three consecutive days. Three hours after the last administration, animals were submitted to open field, elevated plus-maze, forced swim tests, and inhibitory avoidance paradigm. Twenty-four hours after behavioral tests, the blood and hippocampus were collected for the biochemical analyses. Superoxide dismutase, catalase, nitrite, and lipid peroxidation (LPO) were measured in the blood samples. Nitrite and LPO were measured in the hippocampus. The present findings demonstrate that the early hours of ketamine withdrawal induced oxidative biochemistry unbalance in the blood samples, with elevated levels of nitrite and LPO. In addition, we showed for the first time that ketamine withdrawal induced depressive- and anxiety-like profile, as well as short-term memory impairment in adolescent rodents. The neurobehavioral deficits were accompanied by the hippocampal nitrite and LPO-elevated levels.

1. Introduction

Adolescence consists of the transition from childhood to adulthood [1]. The age group from 10 to 19 years old comprises the adolescence period in humans [2], which corresponds to 28 to 42 days postnatal in rodents [3]. During this period, individuals suffer physical, psychosocial, and cognitive transformations related to adolescent brain matu-

ration [4]. These changes provide a biological basis for adolescent-specific behaviors during this period with repercussions in adult life [1].

Actually, important structural and functional changes in synaptic plasticity and neural connectivity occur during the development and maturation of the Central Nervous System (CNS). The brain refines its connections, generating greater communication between the CNS regions, enabling better interaction and increased complexity in specific functions [5]. Thus, the adolescent brain is vulnerable to the harmful effects of drug abuse [1, 6]. Therefore, exposure to psychotropic drugs during the critical stages of development in adolescents may disturb the processes of maturation and plasticity, leading to behavioral and cognitive deficits [5].

Among adolescents, the use of prevalent substance abuse known as "club drugs" (drugs at nightclubs, raves, and bars) occurs. These substances have several psychotropic effects and are associated with a variety of levels of neurotoxicity, dependence, and adverse effects. Among these drugs, ketamine can be highlighted [7].

Ketamine is a neuroleptic anesthetic agent in clinical use since the 1960s. Chemically, it presents itself as a [2-O-chlorophenyl-2-(methylamino) cyclohexanone] [8], consisting of a phencyclidine derivative. When introduced in clinical practice, it was regarded as an ideal and complete anesthetic drug, since it provides all the required components of surgical anesthesia (i.e., pain relief, immobility, amnesia, and loss of consciousness) [9]. Pharmacologically, ketamine modulates neurotransmission at postsynaptic receptors such as N-methyl-D-aspartate (NMDA) glutamate receptors and gamma-aminobutyric acid (GABA) receptors. As an uncompetitive antagonist, ketamine blocks NMDA receptor and induces a dissociative anesthesia [10].

Recreational use of ketamine was first reported in 1967 among subjects with access to the drug, particularly medical professionals [11]. The ketamine misuse spread beyond this group to the community-at-large, firstly in the United States followed by other countries in the world, associated with the "rave" dance subculture of the 1980-1990s. On the streets, ketamine is known as "angel dust," Special K, Cat Valium, "K," or "Kit Kat" [11, 12].

Low doses of ketamine induces distortion of time and space, hallucinations, and mild dissociative effects. At large doses, ketamine induces a more severe dissociation commonly referred to as a "K-hole," wherein the user experiences intense detachment to the point that their perceptions appear completely divorced from their previous reality [13]. In rodents, acute subanesthetic doses of ketamine produce a schizophrenia-like symptomatology, including hyperlocomotion, enhanced stereotyped behaviors, cognitive and sensorimotor gating deficits, and impaired social interactions [14–16].

It is important to emphasize that drug abuse generates toxic effects in different organs, which depends on the administration pathway used by the addict [17, 18]. The affected organs by drug addiction consists of the brain, heart, liver, and kidneys, generally through oxidative stress processes that may derive from direct or indirect effects of the chemical compound, as well as during the drug withdrawal [18]. In fact, studies in humans have reported that ketamine induces neurotoxicity through oxidative stress mechanisms [13]. In rodents, ketamine causes a compensatory overexpression of NMDA receptors and increased the Ca^{2+} levels [19], resulting in Ca^{2+} accumulation that leads to mitochondrial excitotoxic injury and production of reactive oxygen species (ROS) [19, 20].

The neurobehavioral alterations generated by the recreational use of ketamine indicate gender differences in the substance-related epidemiology, social factors, biological responses, and progression to dependence [21, 22]. For example, the consumption of some licit substances, such as alcohol, in women progresses faster than in men. Besides, women present more serious problems and greater health-related consequences with the use of licit and illicit substances, due to the dopaminergic system in the limbic regions that, in part, mediate the sexual difference in drug abuse [21, 23]. Additionally, the stimulus and relapse by the search for drugs in abstinent individuals is different between men and women, in which women are more likely to initiate misuse and relapse after withdrawal than men [21, 24].

In fact, studies exploring different human responses of sex to ketamine are scarce [21]. An animal study designed by Winters et al. [25], which compared the different analgesic effects of ketamine in male and female rats, indicated that females were much more sensitive to the drug effects than males [21, 26, 27]. Moreover, females are more sensitive to neurotoxicity of ketamine and cerebral neural loss than males [28] and are more susceptible to ketamine withdrawal symptoms and adverse effects, especially in cognitive deficits [21, 29].

Thus, in the present study, we investigated the oxidative effects and neurobehavioral alterations after intermittent administration of ketamine in adolescent female rats.

2. Materials and Methods

2.1. Animals and Ethical Aspects. Twenty female Wistar rats (25 days old, weight 60-100 g) were provided from the Federal University of Pará (UFPA) and maintained in collective cages (five animals per cage). Animals were housed (12 h light/dark cycle, lights on 7:00 a.m.) with food and water *ad libitum*. This study followed the *NIH Guide for the Care and Use of Laboratory Animals*, and it was approved by the Committee for Ethics in Experimental Research with Animals of the Federal University of Pará (license number BIO 224-14).

2.2. Study Design. Animals were randomly divided into two groups (10 animals/group). At 35^{th} days old, animals received saline (control) or ketamine 10 mg/kg/day intraperitoneally (i.p) [30] for three consecutive days. Rats in the ketamine group presented with cataleptic immobility within 1 min after administration of 10 mg/kg ketamine i.p. Dextroketamine hydrochloride (Cristália, Brazil) was diluted in saline prior to administration at a volume/body weight ratio of 0.1 mL/100 g [31].

Gass et al. [32] used ketamine (5, 10 e 25 mg/kg) to investigate the modulatory effect of acute ketamine administration

on functional connectivity in the hippocampus and prefrontal cortex system of the rat and proved that ketamine produced a dose-dependent increase in the functional connectivity. Based on these references and our preliminary experiments, we selected the dosages of ketamine 10 mg/kg/day. Besides, to mimic the pattern of social behavior among adolescents, we performed the 3 ON-4 OFF paradigm that has been validated by our group on the study related to drug addiction during adolescence.

2.3. Behavioral Assays. Animals were acclimated for 1 h in the test room with attenuation of noise levels and low illumination (12 lux). To obtain the behavioral effects of ketamine on the immediate withdrawal, three hours after the last administration of saline or ketamine (37th days old), the animals were submitted to the open field (OF), elevated plus-maze (EPM), forced swimming (FS), and step-down inhibitory avoidance task. All behavioral assays were videotaped and analyzed by ANY-maze software (San Diego, CA), except for the rearing parameter of open field (OF) that was used as a manual counter and inhibitory avoidance task. In addition, blindness of the study was preserved.

2.3.1. Open-Field Test. In the OF test, animals were individually placed in the center of a black square arena ($100 \times 100 \times 40$ cm) and were permitted with spontaneous ambulation for five minutes. To evaluate the horizontal and vertical locomotor activity, the total distance traveled (in meters) and number of rearing were measured [33].

2.3.2. Elevated Plus-Maze (EPM). After OF test, animals were submitted to EPM. The maze consists of two open (no walls, $50 \times 10 \times 1$ cm) and two enclosed ($50 \times 10 \times 40$ cm) arms, arranged perpendicularly, and elevated 50 cm above the floor. Each animal was placed on the center of the equipment, facing the closed arm. Animals were able to explore the apparatus for 5 minutes. The parameters measured were the percentage of open arm entries (% OAE), the percentage of open arm time (% OAT) [34], and the frequency of enclosed arm entries (EAE) [35]. The % OAE and % OAT were calculated according to the formula $[(\text{open/total}) \times 100]$. Entry into an arm was defined when the animal places all four paws onto the arm.

2.3.3. Forced Swimming (FS) Test. After EPM, animals were gently placed individually in a vertical Plexiglas cylinder (high 50 cm by 30 cm diameter) filled with 40 cm water column at a temperature of $23 \pm 1^{\circ}$C. The test lasted for 5 min, which the first two minutes consisted of habituation of animals, and the last three minutes measured the immobility time, according to the criteria of Porsolt [36]. Immobility time (i.e., animal floated passively, with only small movements to keep the nose above the surface) and climbs (upward-directed movements) were measured during the three final minutes of the test.

2.3.4. Inhibitory Avoidance Task. After FS test, animals were conducted to the habituation session (180 s) of inhibitory avoidance test. The apparatus consists of an acrylic box ($50\,\text{cm} \times 25\,\text{cm} \times 25\,\text{cm}$), with a floor comprising parallel copper bars (1 mm diameter) connected to an electrical stimulator and a secure platform (7 cm wide × 2.5 cm high). After 24 hours (training session), animals were resubmitted to the secure platform of the apparatus, and immediately after stepping down on the grid, they received a 0.4 mA, 1.0 s scrambled foot shock. During test sessions (1.5 h after training session), animals were placed on the secure platform and the step-down latency (maximum 180 s) was used as measure of retention (short-term memory) [37].

2.4. Oxidative Biochemistry Assays. To avoid interference of behavioral assays on oxidative stress analysis [38], 24 h after the last behavioral task, animals were sacrificed by cervical dislocation for collection of blood contents by intraventricular cardiac puncture preceded by thoracotomy. Concomitantly, the brain was removed from the cranial box and washed with saline at 4°C. Then, the hippocampus was dissected, frozen in liquid nitrogen, and stored in a freezer -80°C until analysis. For analysis, the samples were thawed and resuspended in 20 mM Tris-hydrochloride (Tris-HCl) buffer, pH 7.4, at 4°C for sonic disintegration. The results were expressed as percentages of the control groups.

2.4.1. Oxidative Biochemistry in the Blood

(1) Determination of Serum Malondialdehyde (MDA). Determination of malondialdehyde (MDA) is a method that evaluates the lipid peroxidation and acts as an indicator of cell damage. The technical procedure was performed according to the protocol proposed by Kohn and Liversedge [39], adapted by Percario et al. [40]. The method is based on the reaction of MDA, among other substances, with thiobarbituric acid (TBA 10 nM; Sigma-Aldrich T5500), in pH 2.5 and high temperature ($94^{\circ}\text{C} \times 60$ min). The formation of the complex MDA-TBA generates a pink color that was measured by the spectrophotometric method (535 nm) and concentrations expressed in nmol/mL. 1,1,3,3-Tetraethoxypropane (Sigma-Aldrich; T9889) was used for the implementation of the standard curve.

(2) Determination of Serum Nitric Oxide (NO). The determination of nitric oxide (NO) was based according to the method described by Granger et al. [41]. In this assay, nitrate (NO_3-) present in the serum samples was reduced to nitrite using nitrate reductase, and the nitrite concentration was determined by the Griess method. Briefly, 100 μL of the serum supernatant was incubated with an equal volume of Griess reagent for 10 minutes at room temperature. The absorbance was then measured on a plate scanner (SpectraMax 250, Molecular Devices, Menlo Park, CA, USA) at 550 nm. Nitrite (NO_2-) was determined using a standard curve generated using sodium nitrate ($NaNO_2$). Nitrite production was expressed in μM.

(3) Measurement of Catalase (CAT) Activity. Catalase (CAT) activity was determined following the method

described by Bleuter [42], measuring the rate of enzymatic decomposition of hydrogen peroxide (H_2O_2) (10 mM) to H_2O and O_2. The decay of H_2O_2 was measured using ultraviolet spectrophotometry at 240 nm, and enzyme activity was expressed in CAT units, where one unit is the amount of enzyme needed to hydrolyze one μmol of H_2O_2/min/mg protein.

(4) Measurement of Superoxide Dismutase (SOD) Activity. Superoxide dismutase (SOD) activity was performed according to the procedure recommended by McCord and Fridovich [43]. This method evaluated the ability of SOD to catalyze the conversion of O_2- to H_2O_2 and O_2. SOD activity was measured using ultraviolet (UV) spectrophotometry at a wavelength of 550 nm and was expressed in nmol/mL.

2.4.2. Oxidative Biochemistry in the Tissue Samples

(1) Concentration of the Hippocampal Nitrite Levels. The nitrite levels were determined based on a reaction with Griess reagent (0.1% naphthylethylenediamine and 1% sulfanilamide in 5% phosphoric acid; 1 : 1). An aliquot of tissue homogenate was centrifuged at 21,000 g for 10 min at 4°C, and supernatant was used to analyze the nitrite levels. Fifty microliters of supernatant or standard sodium nitrite solution was added to 50 microliters of Griess reagent and incubated for 20 minutes at room temperature. The absorbance was measured at 550 nm wavelength and compared with the standard curve.

(2) The Hippocampal Lipid Peroxidation Levels. Lipid peroxidation was determined based on the measurement of the MDA and 4-hydroxyalkenals (4-HA) levels. An aliquot of homogenate was centrifuged at 2,500 g for 30 min at 4°C, and supernatant was used for reaction with N-methyl-phenyl indole (NMFI) and methanesulfonic acid at 45°C, during 40 min, yielding a stable chromophore measured at 570 nm wavelength and compared with the standard curve of MDA.

(3) Determination of Protein Content. Total protein content in the supernatants was assayed using the Bradford [44] methodology. An aliquot of homogenate was incubated with Bradford reagent (5% ethanol; 8.5% phosphoric acid; 0.25% Coomassie Brilliant Blue G-250) for 5 min at room temperature. The absorbance was measured at 570 nm and compared to standard solutions of bovine serum albumin. The results were used for the correction of the MDA and nitrite levels.

2.5. Statistical Analysis. The data on the inhibitory avoidance task are shown as median (interquartile range) of step-down latencies. Comparisons of both training and test session step-down latencies between the groups were performed with Mann-Whitney. The remaining data are expressed as mean ± standard error of the mean (SEM) ($n = 10$ animals per group for behavioral assays and $n = 5$ animals per group for oxidative stress parameters). Statistical comparisons between the groups were performed using Student's t-test. Probability values less than 0.05 ($p < 0.05$) were considered as statistically significant. Statistical analysis was performed using the GraphPad Prism 6.0 (GraphPad, San Diego, CA, USA) and Statistica 12.5 software (SigmaPlot, CA, USA).

3. Results

3.1. Ketamine Intermittent Administration in Adolescent Female Rats Does Not Alter Ambulation in the OF but Promotes Anxiogenic-like Behavior in the EPM Test. Administration of ketamine in the dose of 10 mg/kg for 3 consecutive days in female rat adolescents does not interfere in the animal ambulation (distance total traveled ($p = 0.6977$) and rearing number ($p = 0.6011$)) in the OF test (Figures 1(a) and 1(b)).

In the EPM test, ketamine decreased the % OAE ($p = 0.0002$; Figure 1(c)), as well as the % OAT parameter ($p = 0.0313$; Figure 1(d)), which suggests an anxiogenic-like effect. The EAE parameter was not altered in the animals treated with ketamine ($p = 0.7730$) (Figure 1(e)), which shows that the animals did not present motor behavior impairment, which corroborates with the findings in the OF test.

3.2. Ketamine Intermittent Administration in Adolescent Female Rats Promotes Depressive-like Behavior in the Forced Swimming Test. The administration intermittent of ketamine for a period of 3 consecutive days led to a significant increase in the immobility time ($p = 0.0059$), 3 h after last injection. Moreover, ketamine intoxication showed reduction in the climbing number ($p = 0.0037$), which suggests a depressive-like effect (Figures 2(a) and 2(b)).

3.3. Ketamine Intermittent Administration in Adolescent Female Rats Induces Cognitive Impairment. The behavioral effects of ketamine on the immediate withdrawal in adolescent on the short-term memory are illustrated in Figure 3. Wilcoxon's test indicated that 3 h after the last administration of ketamine (at the dose of 10 mg/kg/day), animals reduced the step-down latency from the secure platform in the test session ($p = 0.0017$). Such result suggests that the ketamine impair short-term memory in adolescent rats (Figure 3).

3.4. Ketamine Intermittent Administration in Adolescent Female Rats Increases the Nitrites and Lipid Peroxidation Levels in the Blood and Hippocampus. Ketamine administration increased the nitrites ($p = 0.0041$) and lipid peroxidation ($p = 0.0063$) levels in the blood samples (Figures 4(a) and 4(b)). However, the intermittent use of the drug did not change the serum levels of the antioxidants SOD ($p = 0.0556$) and CAT ($p = 0.0661$) enzymes (Figures 4(c) and 4(d)).

In the hippocampus, the oxidative stress effects of ketamine on the immediate withdrawal in adolescent rats also increased the MDA ($p = 0.0350$; Figure 5(a)) and nitrite

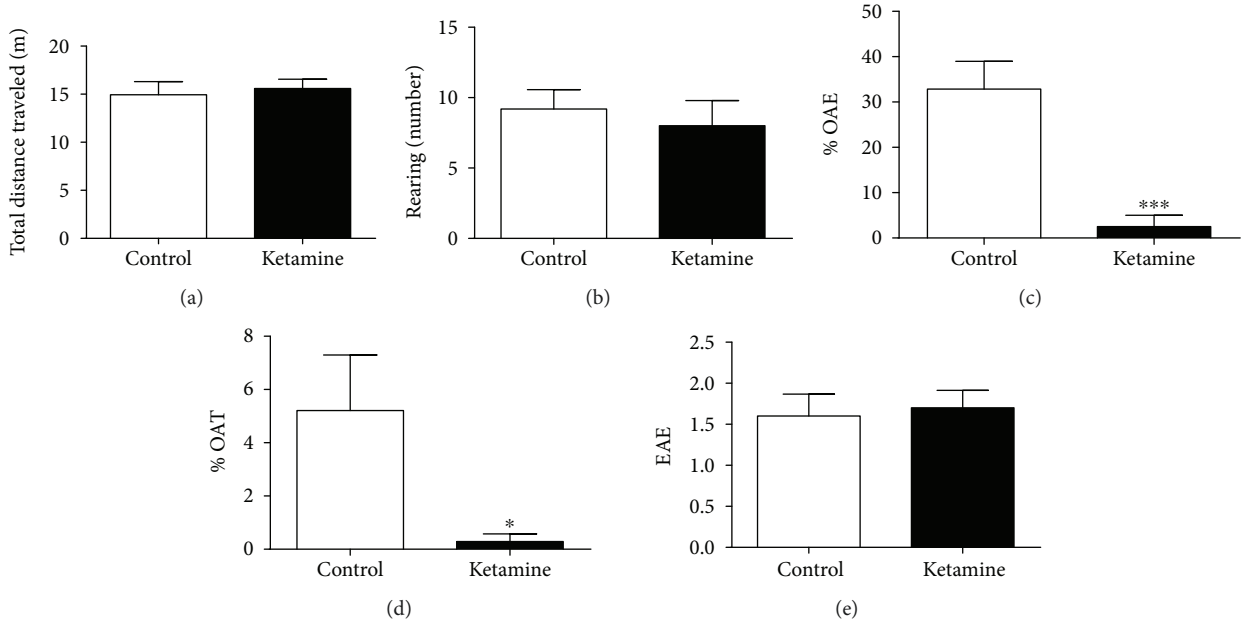

Figure 1: Effects of ketamine on the immediate withdrawal in adolescent female rats of 35th day until 37th day of life in the behavioral parameters: (a) traveled distance (meters) and (b) rearing number in the open-field (OF) test; (c) open arm entries (control percentage), (d) open arm time (control percentage), and (e) frequency of enclosed arm entries (number) in the elevated plus-maze. The results are expressed as the mean ± SEM ($n = 10$ animals per group). $^{*}p < 0.05$ compared to the control group; $^{***}p < 0.001$ compared to the control group (Student's t-test).

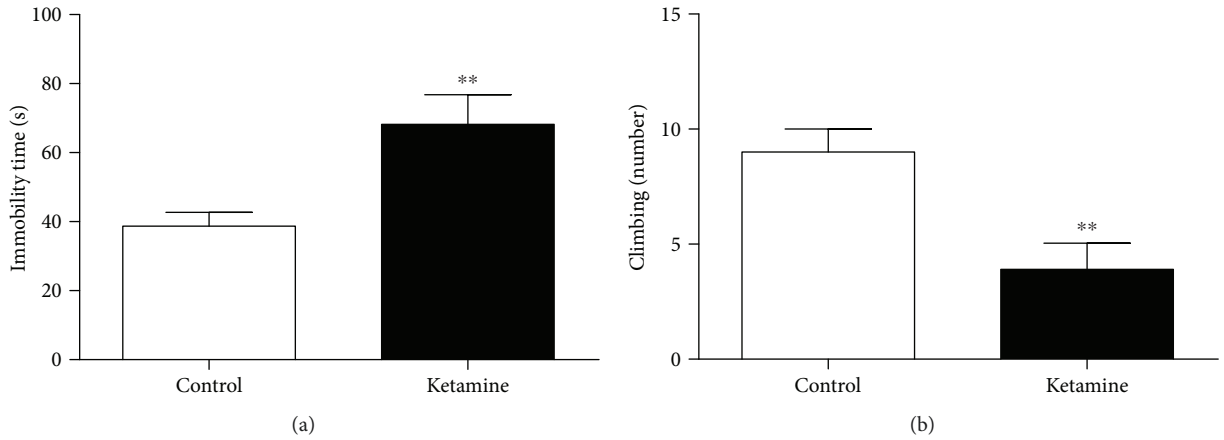

Figure 2: Effects of ketamine on the immediate withdrawal in adolescent female rats of 35th day until 37th day of life in the behavioral parameters: (a) immobility time (latency) and (b) climbing number. The results are expressed as the mean ± SEM ($n = 10$ animals per group). $^{**}p < 0.01$ compared to the control group (Student's t-test).

levels ($p = 0.0110$; Figure 5(b)), which suggest cell death and oxidative unbalance.

4. Discussion

This study demonstrates, for the first time, that ketamine intermittent administration in female rats on the adolescence period induced anxiety- and depression-like responses, as well as memory impairment, accompanied by hippocampal and systemic oxidative damage.

Ketamine essentially blocks NMDA receptors [45]. Glutamate is an essential neurotransmitter for the brain development and aging, as well as in the learning and memory process [46]. However, the blockade of glutamatergic receptors by ketamine promotes the accumulation of glutamate in the synaptic cleft [47], consequently, hyperstimulation of the glutamatergic pathway, which is extremely detrimental to the brain [48, 49].

Studies demonstrate that in the developing brain, especially in the period of early adolescent (prepubescent animals, PND 21-to-34) and midadolescent (periadolescent, PND 34–46) [50], NMDA-receptor antagonists have direct neurotoxic effects, affecting synaptogenesis or the brain growth during spurt period [51, 52]. Furthermore, excitotoxic cell death by excessive release of glutamate overestimates NMDA excitatory receptors to promote a different

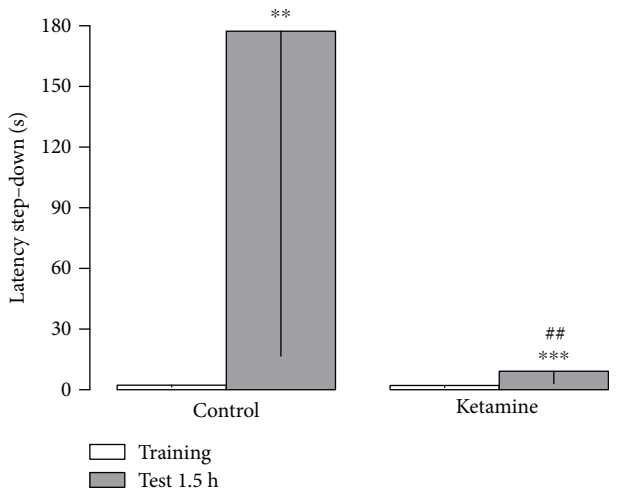

Figure 3: Effects of ketamine on the immediate withdrawal in adolescent female rats of 35th day until 37th day of life on short-term memory (1.5 hr). The results are expressed as the mean ± SEM. Data are shown as median (interquartile ranges) of latencies to step-down in the training and test sessions ($n = 10$ animals per group). $^{**}p < 0.01$ compared to the training session of the same group; $^{***}p < 0.001$ compared to the training session of the same group; $^{\#\#}p < 0.01$ compared to the test stage of the control-treated group (Mann-Whitney).

mechanism of apoptosis [53]. Besides, ketamine displays cell death in the developing brain by a mechanism involving a compensatory upregulation of NMDA receptor subunits, which in turn results in toxic accumulation of intracellular calcium, increased oxidative stress, and activation of the inflammatory pathways, becoming neurons more vulnerable [51, 52, 54].

Actually, the brain is especially sensitive to oxidative damage due to its extensive ability to consume large amounts of oxygen and the production of free radicals. In view of this, the process of oxidative stress is directly related to the onset of various brain diseases, including neurodegenerative disorders [55, 56] and psychiatric disorders [56, 57].

In the present study, the effects of ketamine in the immediate withdrawal promoted the increase in the MDA and NO_2- systemic levels, without altering the antioxidant factors as the enzyme catalase and SOD. Excessive reactive species can cause oxidation of lipids releasing MDA; this is the final product of lipid peroxidation of polyunsaturated fatty acids. These lipids are susceptible to oxidative attack typically by ROS, thus, MDA is a biomarker for this type of damage and indicative of excessive release EROs [51]. The enzymatic antioxidant defense systems that suppress such ROS is understood as hydroxyl radicals (OH), superoxide anions (O_2-), hydrogen peroxide (H_2O_2), superoxide dismutase (SOD), glutathione peroxidase (GPX), catalase (CAT), and thioredoxin peroxiredoxin (TRX-Prdx). These antioxidant enzymes can serve as redox biomarkers in different human diseases, because these antioxidant enzymes indicate the start of the redox state through oxidation/reduction processes. Although for SOD and CAT to be important antioxidants, it is not possible to observe difference in these antioxidants [58].

Increases of MDA and NO changes in the hippocampus demonstrate that this pathway is directly affected by intermittent ketamine administration, generating cell damage. According Patki et al. [59], the hippocampus seems to represent a common brain area that potentially mediates anxiety/-depression-like behaviors and cognitive dysfunction induced by social defeat, in this way, drugs that promote hippocampal damage induce anxiety, depression, and memory deficits.

Anxiety is an aversive emotional state, in which the feeling of fear is disproportionate to the nature of the threat [56]. Against threatening situations, the feeling of the emotion constitutes subjective feature of anxiety that is accompanied by emotional stress and involves behavioral, expressive and physiological features, avoidance of the source of the danger, and assuming defensive postures [56, 60].

According Kuloglu et al. [61], there is a recently established link between certain anxiety behavior and oxidative stress, demonstrating that other systems, such as oxidative metabolism, can affect the regulation of anxiety. Thus, oxidative balance in the brain or plasma is important in anxious behavior. It is a valid highlight that the hippocampus exercises a pivotal role in anxiety and emotional-motivated behaviors [62]; thus, damage at this region after drug exposure induced by increasing of free radicals leads to oxidative damage in tissue, corroborating with our data.

Beyond the anxiogenic-like effects, the ketamine showed depressant-like activity in the FS test. Animals intermittently exposed to ketamine and subsequently evaluated after a final dose, present a significant increase in immobility time, as well as reduction of escalation. Studies indicate that ROS induced neuronal damage and has an important role in the pathophysiology of depression. Depression is characterized by the activation of the inflammatory response system with increased production of procytokines. Proinflammatory cytokines and cytokine-induced ROS may increase lipid peroxidation [63]. Reduced volumetric area, density, and glial cell number have been observed in the PFC and the hippocampus of patients with depression [64]. One of the most plausible causes for these neuronal alterations is elevated oxidative stress due to increased production of free radicals [65]. In fact, the hippocampus presents a significant role on mnemonic (dorsal part) as well as emotional behavior (ventral sub-region) [66]. Thus, we hypothesize that the changes found in FS can be explained by the oxidative imbalance in the blood and hippocampus of adolescent rats.

In addition to emotional profile, short-term memory was evaluated by the step-down inhibitory avoidance task. Our results demonstrated that female rat ketamine intermittent administration on the adolescence promoted impairment in short-term inhibitory avoidance memory. The hippocampus plays a pivotal role in fear aversive memory consolidation and retrieval [67] and conditioned fear memory paradigms [68]. We believe that ketamine-induced hippocampal oxidative damage could explain, at least in part, the mnemonic impairments observed in this study.

Actually, our results demonstrated that hippocampal-dependent behavior as anxiety and depression was modified

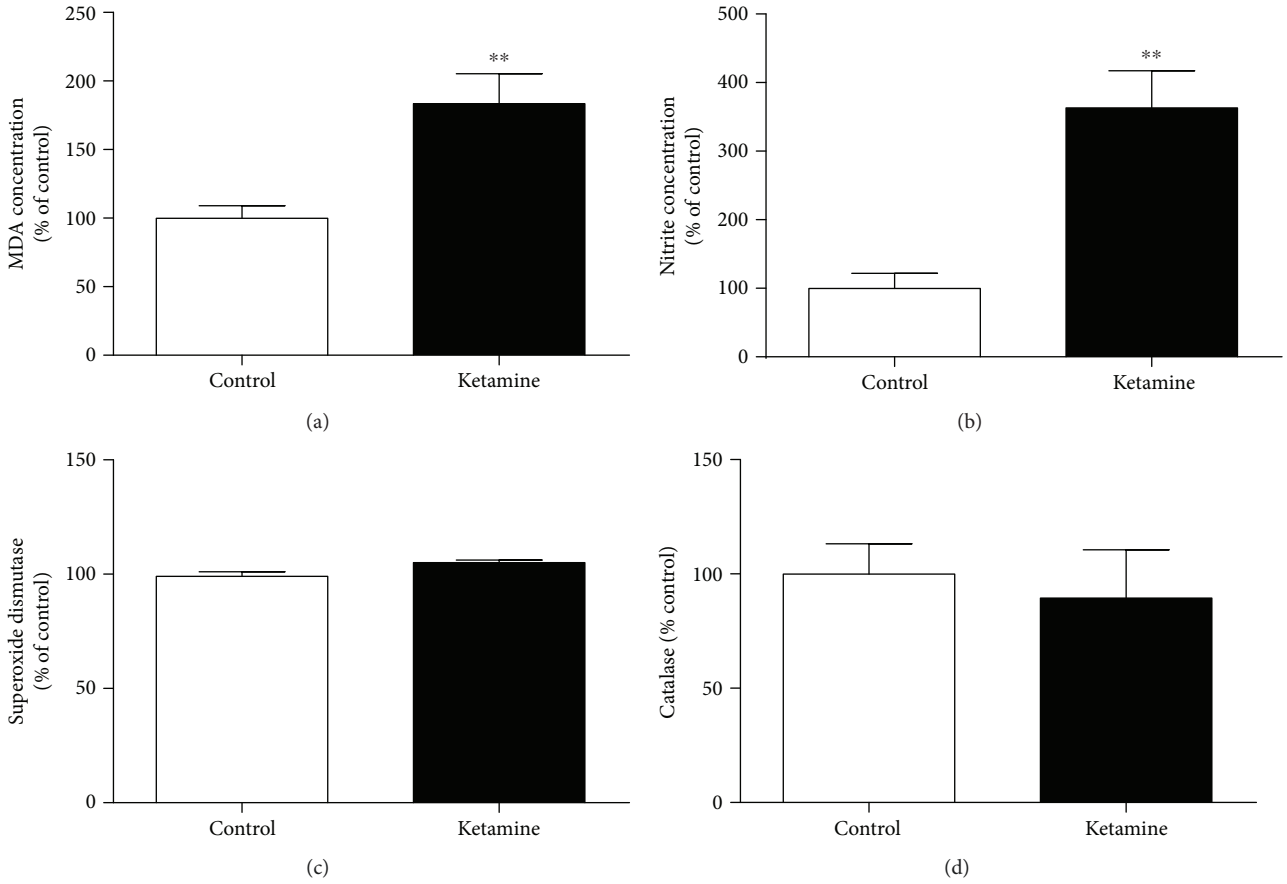

Figure 4: Effects of ketamine on the immediate withdrawal in adolescent female rats of 35th day until 37th day of life on oxidative stress on the blood samples. (a) Lipid peroxidation (malondialdehyde (MDA) concentration); (b) nitrite concentration; (c) superoxide dismutase; (d) catalase. The results are expressed as the mean ± SEM ($n = 5$ animals per group). $^{**}p < 0.01$ compared with the control group (Student's t-test).

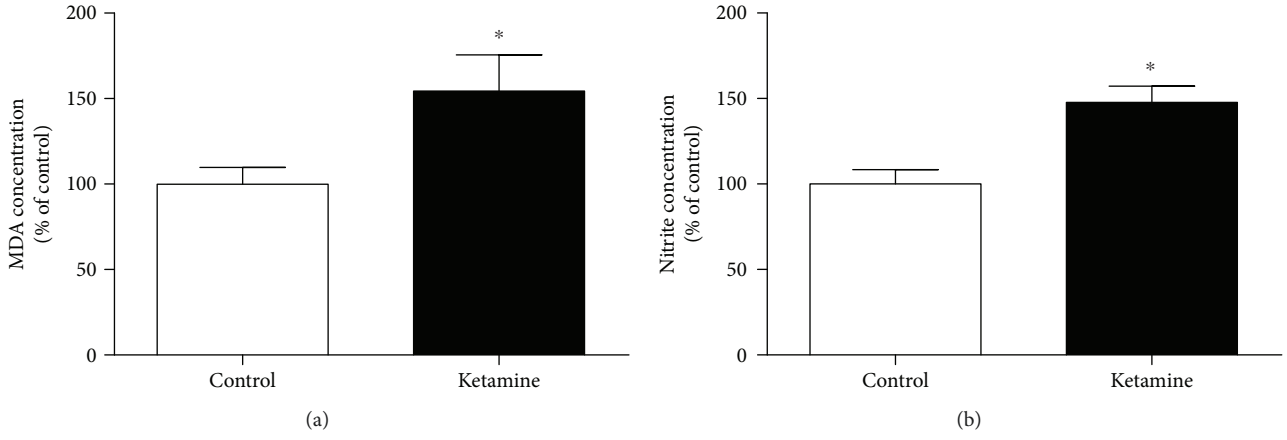

Figure 5: Effects of ketamine on the immediate withdrawal in adolescent female rats of 35th day until 37th day of life on oxidative stress on the hippocampus. (a) Lipid peroxidation (malondialdehyde (MDA) concentration); (b) nitrite concentration. The results are expressed as mean ± SEM ($n = 5$ animals per group). $^{*}p < 0.05$ compared with the control group (Student's t-test).

by ketamine misuse in the adolescence. However, the locomotor activity, three hours after the last intermittent administration of ketamine, was preserved. It is noteworthy that spontaneous locomotor activity (horizontal and vertical) is primarily dependent of basal ganglia, cerebellum, and cerebral motor cortex (for review see Takakusaki [69]), which were not evaluated here. Thus, we suggest that our ketamine paradigm damage did not affect the motor-related brain

areas sufficiently, which reflects on spontaneous motor behavior, even in the present systemic oxidative stress state.

The importance of this study relies on the major neurobehavioral changes associated with oxidative damage following ketamine misuse in the immediate withdrawal during adolescence. In fact, ketamine withdrawal symptoms characterized by anxiety, shaking, sweating, palpitations, and craving seem to be key problems in frequent ketamine users and have been proposed by many case studies. However, evidence of ketamine withdrawal in rodents at recreational or subanesthetic doses as well as during adolescence is scarce.

5. Conclusions

Overall, our data suggest that the effects of ketamine in the immediate withdrawal in the adolescence period promotes systemic and hippocampal oxidative stress, accompanied by emotional behavior alterations, i.e., anxiogenic and depressive profile, as well as mnemonic impairment, i.e., short-term memory, in the immediate withdrawal period. The present study consists of preliminary researchers focused on ketamine-misuse harmful effects. Thus, other works are necessary to investigate in detail other possible mechanisms that may contribute to oxidative stress in the behavioral alterations observed. In addition, the harmful effects of ketamine misuse during adolescence on brain structures are already unknown.

Data Availability

The quantitative and qualitative data used to support the findings of this study are included within the article.

Conflicts of Interest

There was no conflict of interests between the other authors during the accomplishment of this work.

Acknowledgments

This work is supported by Coordenação de Aperfeiçoamento de Pessoal de Nível Superior (CAPES) and Programa Integrado de Bolsas de Iniciação Científica (PIBIC) of the Universidade Federal do Pará (UFPA) from Brazil government. Cartágenes received research support from CAPES.

References

[1] F. Crews, J. He, and C. Hodge, "Adolescent cortical development: a critical period of vulnerability for addiction," *Pharmacology Biochemistry and Behavior*, vol. 86, no. 2, pp. 189–199, 2007.

[2] Organização Mundial da Saúde, "Vivendo a adolescência: Fase da vida? Faixa etária? Construção social? Afinal, o que é adolescência?," 2013, August 2016, http://www.adolescencia.org.br/site-pt-br/adolescencia.

[3] L. P. Spear, "The adolescent brain and age-related behavioral manifestations," *Neuroscience & Biobehavioral Reviews*, vol. 24, no. 4, pp. 417–463, 2000.

[4] H. Roehrs, M. A. Maftum, and I. P. S. Zagonel, "Adolescência na percepção de professores do ensino fundamental," *Revista da Escola de Enfermagem da USP*, vol. 44, no. 2, pp. 421–428, 2010.

[5] C. Guerri and M. Pascual, "Mechanisms involved in the neurotoxic, cognitive, and neurobehavioral effects of alcohol consumption during adolescence," *Alcohol*, vol. 44, no. 1, pp. 15–26, 2010.

[6] Y. W. Qiu, X. F. Lv, G. H. Jiang et al., "Potential gray matter unpruned in adolescents and young adults dependent on dextromethorphan-containing cough syrups: evidence from cortical and subcortical study," *Brain Imaging and Behavior*, vol. 11, no. 5, pp. 1470–1478, 2017.

[7] D. F. Guerreiro, A. L. Carmo, J. A. da Silva, R. Navarro, and C. Góis, "Club drugs: Um Novo Perfil de Abuso de Substâncias em Adolescentes e Jovens Adultos," *Acta Médica Portuguesa*, vol. 24, no. 5, pp. 739–756, 2011.

[8] D. L. Reich and G. Silvay, "Ketamine: an update on the first twenty-five years of clinical experience," *Canadian Journal of Anaesthesia*, vol. 36, no. 2, pp. 186–197, 1989.

[9] M. Annetta, D. Iemma, C. Garisto, C. Tafani, and R. Proietti, "Ketamine: new indications for an old drug," *Current Drug Targets*, vol. 6, no. 7, pp. 789–794, 2005.

[10] S. Tan, W. P. Lam, M. S. M. Wai, W. H. A. Yu, and D. T. Yew, "Chronic ketamine administration modulates midbrain dopamine system in mice," *PLoS ONE*, vol. 7, no. 8, article e43947, 2012.

[11] S. S. Kalsi, D. M. Wood, and P. I. Dargan, "The epidemiology and patterns of acute and chronic toxicity associated with recreational ketamine use," *Emerging Health Threats Journal*, vol. 4, no. 1, article 7107, 2011.

[12] P. Dillon, J. Copeland, and K. Jansen, "Patterns of use and harms associated with non-medical ketamine use," *Drug and Alcohol Dependence*, vol. 69, no. 1, pp. 23–28, 2003.

[13] C. J. A. Morgan, H. V. Curran, and the Independent Scientific Committee on Drugs (ISCD), "Ketamine use: a review," *Addiction*, vol. 107, no. 1, pp. 27–38, 2012.

[14] G. Keilhoff, A. Becker, G. Grecksch, G. Wolf, and H. G. Bernstein, "Repeated application of ketamine to rats induces changes in the hippocampal expression of parvalbumin, neuronal nitric oxide synthase and cFOS similar to those found in human schizophrenia," *Neuroscience*, vol. 126, no. 3, pp. 591–598, 2004.

[15] M. Pietraszek, "Significance of dysfunctional glutamatergic transmission for the development of psychotic symptoms," *Polish Journal of Pharmacology*, vol. 55, no. 2, pp. 133–154, 2003.

[16] R. A. Bressan and L. S. Pilowsky, "Hipótese glutamatérgica da esquizofrenia," *Revista Brasileira de Psiquiatria*, vol. 25, no. 3, pp. 177–183, 2003.

[17] T. Cunha-Oliveira, A. C. Rego, S. M. Cardoso et al., "Mitochondrial dysfunction and caspase activation in rat cortical neurons treated with cocaine or amphetamine," *Brain Research*, vol. 1089, no. 1, pp. 44–54, 2006.

[18] T. Cunha-Oliveira, A. Rego, and C. Oliveira, "Oxidative stress and drugs of abuse: an update," *Mini-Reviews in Organic Chemistry*, vol. 10, no. 4, pp. 321–334, 2013.

[19] Y. Li, X. Li, J. Zhao et al., "Midazolam attenuates autophagy and apoptosis caused by ketamine by decreasing reactive oxygen species in the hippocampus of fetal rats," *Neuroscience*, vol. 388, pp. 460–471, 2018.

[20] F. Liu, T. A. Patterson, N. Sadovova et al., "Ketamine-induced neuronal damage and altered N-methyl-D-aspartate receptor function in rat primary forebrain culture," *Toxicological Sciences*, vol. 131, no. 2, pp. 548–557, 2013.

[21] W. Y. Chen, M. C. Huang, and S. K. Lin, "Gender differences in subjective discontinuation symptoms associated with ketamine use," *Substance Abuse Treatment, Prevention, and Policy*, vol. 9, no. 1, p. 39, 2014.

[22] E. Tuchman, "Women and addiction: the importance of gender issues in substance abuse research," *Journal of Addictive Diseases*, vol. 29, no. 2, pp. 127–138, 2010.

[23] J. J. Anker and M. E. Carroll, "Females are more vulnerable to drug abuse than males: evidence from preclinical studies and the role of ovarian hormones," *Current Topics in Behavioral Neurosciences*, vol. 8, pp. 73–96, 2011.

[24] L. Fattore, P. Fadda, and W. Fratta, "Sex differences in the self-administration of cannabinoids and other drugs of abuse," *Psychoneuroendocrinology*, vol. 34, Supplement 1, pp. S227–S236, 2009.

[25] K. A. Bradley, S. Badrinath, K. Bush, J. Boyd-Wickizer, and B. Anawalt, "Medical risks for women who drink alcohol," *Journal of General Internal Medicine*, vol. 13, no. 9, pp. 627–639, 1998.

[26] W. D. Winters, A. J. Hance, G. C. Cadd, and M. L. Lakin, "Seasonal and sex influences on ketamine-induced analgesia and catalepsy in the rat; a possible role for melatonin," *Neuropharmacology*, vol. 25, no. 10, pp. 1095–1101, 1986.

[27] J. Lees, J. E. C. Hallak, J. F. W. Deakin, and S. M. Dursun, "Gender differences and the effects of ketamine in healthy volunteers," *Journal of Psychopharmacology*, vol. 18, no. 3, pp. 337–339, 2016.

[28] V. Jevtovic-Todorovic, D. F. Wozniak, N. D. Benshoff, and J. W. Olney, "A comparative evaluation of the neurotoxic properties of ketamine and nitrous oxide," *Brain Research*, vol. 895, no. 1-2, pp. 264–267, 2001.

[29] M. Sofuoglu, E. E. DeVito, A. J. Waters, and K. M. Carroll, "Cognitive enhancement as a treatment for drug addictions," *Neuropharmacology*, vol. 64, pp. 452–463, 2013.

[30] L. Huang, Y. Liu, W. Jin, X. Ji, and Z. Dong, "Ketamine potentiates hippocampal neurodegeneration and persistent learning and memory impairment through the PKCγ–ERK signaling pathway in the developing brain," *Brain Research*, vol. 1476, pp. 164–171, 2012.

[31] T. Kos, A. Nikiforuk, D. Rafa, and P. Popik, "The effects of NMDA receptor antagonists on attentional set-shifting task performance in mice," *Psychopharmacology*, vol. 214, no. 4, pp. 911–921, 2011.

[32] N. Gass, A. J. Schwarz, A. Sartorius et al., "Sub-anesthetic ketamine modulates intrinsic BOLD connectivity within the hippocampal-prefrontal circuit in the rat," *Neuropsychopharmacology*, vol. 39, no. 4, pp. 895–906, 2014.

[33] S. K. Singh, U. K. Misra, J. Kalita, H. K. Bora, and R. C. Murthy, "Nitrous oxide related behavioral and histopathological changes may be related to oxidative stress," *NeuroToxicology*, vol. 48, pp. 44–49, 2015.

[34] S. Pellow, P. Chopin, S. E. File, and M. Briley, "Validation of open: closed arm entries in an elevated plus-maze as a measure of anxiety in the rat," *Journal of Neuroscience Methods*, vol. 14, no. 3, pp. 149–167, 1985.

[35] S. E. File, "The interplay of learning and anxiety in the elevated plus-maze," *Behavioural Brain Research*, vol. 58, no. 1-2, pp. 199–202, 1993.

[36] R. D. Porsolt, G. Anton, N. Blavet, and M. Jalfre, "Behavioural despair in rats: a new model sensitive to antidepressant treatments," *European Journal of Pharmacology*, vol. 47, no. 4, pp. 379–391, 1978.

[37] K. Ghisoni, A. S. Aguiar Jr, P. A. de Oliveira et al., "Neopterin acts as an endogenous cognitive enhancer," *Brain, Behavior, and Immunity*, vol. 56, pp. 156–164, 2016.

[38] C. M. Schöler, C. V. Marques, G. S. da Silva, T. G. Heck, L. P. de Oliveira Junior, and P. I. Homem de Bittencourt, "Modulation of rat monocyte/macrophage innate functions by increasing intensities of swimming exercise is associated with heat shock protein status," *Molecular and Cellular Biochemistry*, vol. 421, no. 1-2, pp. 111–125, 2016.

[39] H. I. Kohn and M. Liversedge, "On a new aerobic metabolite whose production by brain is inhibited by apomorphine, emetine, ergotamine, epinephrine, and menadione," *Journal of Pharmacology and Experimental Therapeutics*, vol. 82, pp. 292–300, 1944.

[40] S. Percario, A. C. C. Vital, and F. Jablonka, "Dosagem do malondialdeido," *Newslab*, vol. 2, pp. 46–50, 1994.

[41] D. L. Granger, N. M. Anstey, W. C. Miller, and J. B. Weinberg, "[6] Measuring nitric oxide production in human clinical studies," in *Nitric Oxide Part C: Biological and Antioxidant Activities*, L. Packe, Ed., vol. 301 of Methods in Enzymology, pp. 49–61, Elsevier, 1999.

[42] E. Beutler, "The preparation of red cells for assay," in *Red Cell Metabolism: A manual of biochemical methods*, E. Bleuter, Ed., pp. 8–18, Grune Straton, New York, 1975.

[43] M. C. JM and I. Fridovich, "Superoxide dismutase. An enzymic function for erythrocuprein (hemocuprein)," *The Journal of Biological Chemistry*, vol. 244, no. 22, pp. 6049–6055, 1969.

[44] M. M. Bradford, "A rapid and sensitive method for the quantitation of microgram quantities of protein utilizing the principle of protein-dye binding," *Analytical Biochemistry*, vol. 72, no. 1-2, pp. 248–254, 1976.

[45] P. Zanos and T. D. Gould, "Mechanisms of ketamine action as an antidepressant," *Molecular Psychiatry*, vol. 23, no. 4, pp. 801–811, 2018.

[46] G. Segovia, A. Porras, A. del Arco, and F. Mora, "Glutamatergic neurotransmission in aging: a critical perspective," *Mechanisms of Ageing and Development*, vol. 122, no. 1, pp. 1–29, 2001.

[47] S. Maeng and C. A. Zarate Jr, "The role of glutamate in mood disorders: results from the ketamine in major depression study and the presumed cellular mechanism underlying its antidepressant effects," *Current Psychiatry Reports*, vol. 9, no. 6, pp. 467–474, 2007.

[48] H. W. Dong, L. W. Swanson, L. Chen, M. S. Fanselow, and A. W. Toga, "Genomic-anatomic evidence for distinct functional domains in hippocampal field CA1," *Proceedings of the National Academy of Sciences of the United States of America*, vol. 106, no. 28, pp. 11794–11799, 2009.

[49] A. V. Tzingounis and J. I. Wadiche, "Glutamate transporters: confining runaway excitation by shaping synaptic transmission," *Nature Reviews Neuroscience*, vol. 8, no. 12, pp. 935–947, 2007.

[50] E. Tirelli, G. Laviola, and W. Adriani, "Ontogenesis of behavioral sensitization and conditioned place preference induced by psychostimulants in laboratory rodents," *Neuroscience & Biobehavioral Reviews*, vol. 27, no. 1-2, pp. 163–178, 2003.

[51] J. Liu, A. Wang, L. Li, Y. Huang, P. Xue, and A. Hao, "Oxidative stress mediates hippocampal neuron death in rats after lithium–pilocarpine-induced status epilepticus," *Seizure*, vol. 19, no. 3, pp. 165–172, 2010.

[52] S. Shibuta, T. Morita, J. Kosaka, T. Kamibayashi, and Y. Fujino, "Only extra-high dose of ketamine affects l-glutamate-induced intracellular Ca^{2+} elevation and neurotoxicity," *Neuroscience Research*, vol. 98, pp. 9–16, 2015.

[53] T. M. du Bois and X.-F. Huang, "Early brain development disruption from NMDA receptor hypofunction: relevance to schizophrenia," *Brain Research Reviews*, vol. 53, no. 2, pp. 260–270, 2007.

[54] C. Wang, N. Sadovova, C. Hotchkiss et al., "Blockade of N-methyl-D-aspartate receptors by ketamine produces loss of postnatal day 3 monkey frontal cortical neurons in culture," *Toxicological Sciences*, vol. 91, no. 1, pp. 192–201, 2006.

[55] F. Ng, M. Berk, O. Dean, and A. I. Bush, "Oxidative stress in psychiatric disorders: evidence base and therapeutic implications," *The International Journal of Neuropsychopharmacology*, vol. 11, no. 6, pp. 851–876, 2008.

[56] J. Bouayed, H. Rammal, and R. Soulimani, "Oxidative stress and anxiety: relationship and cellular pathways," *Oxidative Medicine and Cellular Longevity*, vol. 2, no. 2, 67 pages, 2009.

[57] S. Salim, "Oxidative stress and psychological disorders," *Current Neuropharmacology*, vol. 12, no. 2, pp. 140–147, 2014.

[58] H. Y. Yang and T. H. Lee, "Antioxidant enzymes as redox-based biomarkers: a brief review," *BMB Reports*, vol. 48, no. 4, pp. 200–208, 2015.

[59] G. Patki, N. Solanki, F. Atrooz, F. Allam, and S. Salim, "Depression, anxiety-like behavior and memory impairment are associated with increased oxidative stress and inflammation in a rat model of social stress," *Brain Research*, vol. 1539, pp. 73–86, 2013.

[60] S. Leman, G. A. Le, and C. Belzung, "Liens anxiété-mémoire: Études expérimentales," in *Anxiété, anxiolytiques et troubles cognitifs*, M. Ferreri, Ed., pp. 71–79, Elsevier, 2004.

[61] M. Kuloglu, M. Atmaca, E. Tezcan, B. Ustundag, and S. Bulut, "Antioxidant enzyme and malondialdehyde levels in patients with panic disorder," *Neuropsychobiology*, vol. 46, no. 4, pp. 186–189, 2003.

[62] L. R. Jacinto, J. S. Reis, N. S. Dias, J. J. Cerqueira, J. H. Correia, and N. Sousa, "Stress affects theta activity in limbic networks and impairs novelty-induced exploration and familiarization," *Frontiers in Behavioral Neuroscience*, vol. 7, p. 127, 2013.

[63] I. Eren, M. Nazıroğlu, A. Demirdaş et al., "Venlafaxine modulates depression-induced oxidative stress in brain and medulla of rat," *Neurochemical Research*, vol. 32, no. 3, pp. 497–505, 2007.

[64] T. Maria Michel, D. Pulschen, and J. Thome, "The role of oxidative stress in depressive disorders," *Current Pharmaceutical Design*, vol. 18, no. 36, pp. 5890–5899, 2012.

[65] T. M. Michel, S. Frangou, D. Thiemeyer et al., "Evidence for oxidative stress in the frontal cortex in patients with recurrent depressive disorder - a post-mortem study," *Psychiatry Research*, vol. 151, no. 1-2, pp. 145–150, 2007.

[66] A. Tanti and C. Belzung, "Neurogenesis along the septo-temporal axis of the hippocampus: are depression and the action of antidepressants region-specific?," *Neuroscience*, vol. 252, pp. 234–252, 2013.

[67] I. Izquierdo, L. M. Bevilaqua, J. I. Rossato et al., "The molecular cascades of long-term potentiation underlie memory consolidation of one-trial avoidance in the CA1 region of the dorsal hippocampus, but not in the basolateral amygdala or the neocortex," *Neurotoxicity Research*, vol. 14, no. 2-3, pp. 273–294, 2008.

[68] M. Cammarota, L. R. Bevilaqua, J. I. Rossato, R. H. Lima, J. H. Medina, and I. Izquierdo, "Parallel memory processing by the CA1 region of the dorsal hippocampus and the basolateral amygdala," *Proceedings of the National Academy of Sciences of the United States*, vol. 105, no. 30, pp. 10279–10284, 2008.

[69] K. Takakusaki, "Functional neuroanatomy for posture and gait control," *Journal of Movement Disorders*, vol. 10, no. 1, pp. 1–17, 2017.

Hindawi
Oxidative Medicine and Cellular Longevity
Volume 2018, Article ID 6124745, 22 pages
https://doi.org/10.1155/2018/6124745

Research Article

mTOR Modulates Methamphetamine-Induced Toxicity through Cell Clearing Systems

Gloria Lazzeri[1], **Francesca Biagioni**[2], **Federica Fulceri**[3], **Carla L. Busceti**[2], **Maria C. Scavuzzo**[1], **Chiara Ippolito**[3], **Alessandra Salvetti**[3], **Paola Lenzi**[1], **and Francesco Fornai**[1,2]

[1]*Department of Translational Research and New Technologies in Medicine and Surgery, Human Anatomy, University of Pisa, Via Roma 55, Pisa 56126, Italy*
[2]*I.R.C.C.S Neuromed, Via Atinense 18, Pozzilli 86077, Italy*
[3]*Department of Clinical and Experimental Medicine, University of Pisa, Via Roma 55, Pisa 56126, Italy*

Correspondence should be addressed to Francesco Fornai; francesco.fornai@med.unipi.it

Received 26 April 2018; Accepted 31 August 2018; Published 29 October 2018

Academic Editor: Brian Harvey

Methamphetamine (METH) is abused worldwide, and it represents a threat for public health. METH exposure induces a variety of detrimental effects. In fact, METH produces a number of oxidative species, which lead to lipid peroxidation, protein misfolding, and nuclear damage. Cell clearing pathways such as ubiquitin-proteasome (UP) and autophagy (ATG) are involved in METH-induced oxidative damage. Although these pathways were traditionally considered to operate as separate metabolic systems, recent studies demonstrate their interconnection at the functional and biochemical level. Very recently, the convergence between UP and ATG was evidenced within a single organelle named autophagoproteasome (APP), which is suppressed by mTOR activation. In the present research study, the occurrence of APP during METH toxicity was analyzed. In fact, coimmunoprecipitation indicates a binding between LC3 and P20S particles, which also recruit p62 and alpha-synuclein. The amount of METH-induced toxicity correlates with APP levels. Specific markers for ATG and UP, such as LC3 and P20S in the cytosol, and within METH-induced vacuoles, were measured at different doses and time intervals following METH administration either alone or combined with mTOR modulators. Western blotting, coimmunoprecipitation, light microscopy, confocal microscopy, plain transmission electron microscopy, and immunogold staining were used to document the effects of mTOR modulation on METH toxicity and the merging of UP with ATG markers within APPs. METH-induced cell death is prevented by mTOR inhibition, while it is worsened by mTOR activation, which correlates with the amount of autophagoproteasomes. The present data, which apply to METH toxicity, are also relevant to provide a novel insight into cell clearing pathways to counteract several kinds of oxidative damage.

1. Introduction

Methamphetamine (METH) is a highly addictive and neurotoxic drug, which causes a variety of neuropsychiatric alterations mainly affecting the dopamine (DA) mesostriatal and mesolimbic systems in the brain [1, 2]. Exposure to repeated doses of METH produces striatal DA depletion and loss of mesostriatal DA terminals [3–12].

In the cell body of the substantia nigra *pars compacta* (SNpc), METH produces alterations in the cytoplasm which also occur in DA-PC12 cells and extend to the cytoplasm and nucleus of striatal GABA neurons [6, 13–16]. These alterations configure as multilamellar whorl staining for ubiquitin, parkin, and alpha-synuclein [6, 15, 17]. Recent studies indicate that high METH doses may reduce the number of nigral cell bodies [8, 18]. METH toxicity against DA cell bodies and axons relates to an increase of DA release and oxidative species [19]. In fact, METH alters the vesicular storage of DA [20–22], it inhibits physiological DA metabolism, which is naturally operated by MAO-A [23, 24], and it reverts and/or inhibits the activity of the plasma membrane DA transporter (DAT), thus leading to a loss of DAT-binding sites [1, 25, 26]. All these effects contribute to rise of dramatically free DA levels within the cytosol of DA-

containing cells. Since DA is no longer metabolized by MAO-A, it undergoes self-oxidation and spontaneous conversion to DA quinones, which in turn generate highly reactive oxidative species [27, 28]. In this way, a redox imbalance is generated by METH, which is detrimental for the integrity of both axon terminals and cell bodies where oxidized proteins, lipids, and nucleic acids are generated [29, 30]. A key molecular mechanism of protein oxidation consists in binding to cysteinyl residues to generate disulphuric bridges, which alter protein conformation [28, 31]. In this way, misfolded proteins such as alpha-synuclein [6, 14], ubiquitin [6, 32], prion protein [33], and parkin [6, 34] are generated. Again, METH inhibits complex II of the mitochondrial respiratory chain, which further elevates oxidative species and increases the number of altered mitochondria [35–39]. METH also oxidizes lipids to produce highly reactive by-products such as 4-hydroxynonenal [34, 40, 41]. All these oxidized substrates represent a target for cell clearing systems, which promote their removal. Thus, autophagy (ATG) and ubiquitin-proteasome (UP) represent a powerful defense to counteract redox imbalance generated by such a drug of abuse, and they are both challenged by METH administration. In detail, UP activity is inhibited by METH [13, 15, 16, 34], while UP inhibitors produce subcellular alterations which overlap with those produced by METH [6, 14, 42]. In line with this, METH toxicity is enhanced by concomitant exposure to UP inhibitors [15, 43]. ATG is quickly engaged during METH in PC12 cells [22, 44] and *in vivo*, in the SNpc and striatum [6, 15, 45]. Similarly to UP inhibitors, ATG blockers worsen METH toxicity [37]. Despite a massive engagement of ATG, which should sort neuroprotection, its activity is impaired by METH itself since the high amount of substrates (misfolded proteins and damaged mitochondria) engulfs this clearing system [16, 37, 46]. Therefore, despite being ATG overexpressed following METH [22, 44], it is not considered to be effective due to a lack of its progression [37, 46]. Such a combined defect in cell clearing systems produced by METH paves the way to deleterious effects induced by oxidative species, which are abundantly produced by such a drug of abuse.

Recently, a cell clearing organelle, which possesses both ATG and UP components, was described. This organelle appears as a multilamellar vacuole, which carries both UP and ATG key antigens [47]. This organelle corresponds to the "autophagoproteasome" (APP) as being defined in the Glossary published in the consensus manuscript "Guidelines for the Use and Interpretation of Assays for Monitoring Autophagy (3rd Edition)" by Klionsky et al. [48]. In the recent manuscript, it was demonstrated that APP is strongly activated by mTOR inhibition [47]. In fact, when the mTOR inhibitor rapamycin is administered, roughly all UP-positive puncta detected by P20S immunostaining at confocal microscopy move towards LC3-positive vacuoles, thus producing a massive switch from cytosolic to compartmentalized proteasome [47]. Despite a strong involvement of UP and ATG per se during METH toxicity, no study so far investigated what happens to this merging organelle. In the present manuscript, we dissect the ultrastructural morphometry of both UP and ATG components in different cell compartments, alone and in combination to merge within the autophagoproteasome (APP), under the effects of various METH doses at different time intervals. A variety of techniques were used to investigate these effects encompassing plain light microscopy, confocal microscopy, transmission electron microscopy, Western blotting, and coimmunoprecipitation. In detail, we aimed to assess whether (i) the autophagoproteasome was operating in the DA-containing PC12 cell line, (ii) the autophagoproteasome was modified following METH exposure, (iii) the amount of this organelle was associated with the modulation of METH toxicity, and (iv) whether these phenomena depend on mTOR activity as tested during either mTOR inhibition or activation.

2. Materials and Methods

2.1. Cell Cultures. In the current study, we chose the rat pheochromocytoma PC12 cell line, since these cells are able to synthetize and release DA and they express DA receptors on their external membrane. This is key in the case of METH, which exerts its mechanisms of action mainly by affecting molecular targets, which regulate DA transmission. In fact, the presence of DA and DA receptors, as well as DA uptake mechanisms, renders PC12 cell lines closer to DA terminals compared with their ancestors (i.e., chromaffin cells of the adrenal medulla). This concept is reinforced by the presence of the isoform of monoamine oxidase (MAO) type A, which characterizes also DA neurons, contrasting with the established prevalence of MAO type B within chromaffin cells of the adrenal medulla. Therefore, PC12 cells represent a model to predict the neurotoxicity of METH on central DA neurons with significant implications for the treatment of neuropsychiatric and neurodegenerative disorders [49].

The PC12 cell line was obtained from a cell bank (IRCCS San Martino Institute, Genova). The cells were grown in RPMI 1640 medium (Sigma-Aldrich, St. Louis, MO, USA) supplemented with heat inactivated 10% horse serum (HS, Sigma) and 5% fetal bovine serum (FBS, Sigma), penicillin (50 IU/ml)/streptomycin (50 mg/ml, Sigma), under standard culture conditions in a humidified atmosphere containing 5% CO_2 at 37°C. Experiments took place during the log phase of cell growth. At this time, cells were seeded into cell culture plates and they were incubated at 37°C in 5% CO_2 for further 24 hours. In particular, for transmission electron microscopy (TEM) and coimmunoprecipitation experiments, 1×10^6 PC12 cells were seeded in culture dishes in a final volume of 5 ml. For Western blotting, 5×10^5 cells were seeded in six-well plates in a final volume of 2 ml/well. Finally, for confocal microscopy experiments, 5×10^4 cells were grown on polylysine slides placed in 24-well plates at a final volume of 1 ml/well.

In order to study METH-induced toxicity, PC12 cells were treated with different doses of METH (1 nM, 10 nM, 100 nM, 1 μM, and 10 μM) for 72 hours. In a second set of experiments, PC12 cells were treated with 1 μM or 10 μM of METH for different time exposures (12, 24, and 72 hours). A study from Melega et al. [50] reports data deriving from an i.v. intake of 1000 mg/day METH in humans, approximately corresponding to 10 mg/kg, which can produce neurotoxicity (i.e., loss of DA terminals and neurons) in mice. However,

since the present study was designed to assess the ultrastructural effects of METH on specific subcellular organelles, apart from neurotoxicity, we chose METH doses from 1 μM to 10 μM based on the previous studies [6, 15, 37]. In our hands, at doses between 10 and 100 μM of METH in PC12 cell lines, only a few cells survive, and this is further exacerbated by METH doses above 100 μM [6, 43]. This is also due to intrinsic vulnerability of PC12 cells to DA-increasing agents, which explains such a discrepancy with DA neurons [49]. In fact, PC12 cells possess inherent features, which render these cells particularly sensitive to high doses of DA. These include (i) the presence of VMAT-1, which is less specific for the vesicular uptake of catecholamines when compared with its homolog VMAT-2 expressed in the brain, and (ii) low levels of the DAT, thus reduced cytosolic reuptake of DA. Thus, these cells have a limited ability to adapt the neurotransmitter synthesis and vesicle trafficking/release to the synaptic needs, which contrasts with the flexibility of DA neurons to respond appropriately to a releasing stimulus.

Further experiments were carried out to evaluate the effects produced on METH toxicity and APP components by the modulation of mTOR activity. In these experiments, cells were exposed to 100 nM rapamycin and 50 mM asparagine, alone or in combination with 10 μM METH, for 72 hours. When it was combined with METH, rapamycin was added 2 h before METH, while asparagine was administered 30 min before METH. The doses of asparagine and rapamycin were selected based on the previous papers [32, 47]. However, to validate these doses in these experimental conditions, the inhibition or activation of mTOR activity for each compound was tested by measuring the downstream product pS6.

METH and asparagine were dissolved directly in the culture medium. Dilutions of rapamycin were obtained by a stock solution (1 mM of rapamycin dissolved in the culture medium containing 10% DMSO).

2.2. Transmission Electron Microscopy. PC12 cells were centrifuged at 1000 *g* for 5 min. After removal of the supernatant, the pellet was rinsed in PBS before being fixed. The fixing procedure was carried out with a solution containing 2.0% paraformaldehyde and 0.1% glutaraldehyde in 0.1 M PBS (pH 7.4) for 90 min at 4°C. This aldehyde concentration minimally covers antigen epitopes, while fairly preserving tissue architecture. After removal of the fixing solution, specimens were postfixed in 1% OsO_4 for 1 h at 4°C; they were dehydrated in ethanol and finally embedded in epoxy resin.

For ultrastructural morphometry, grids containing nonserial ultrathin sections (40–50 nm thick) were examined at TEM, at a magnification of 8000x. Several grids were analyzed in order to count a total number of 50–100 cells for each experimental group. In particular, when counting cell death, 50 cells per group were sampled, while 50 cells per group were sampled to carry out ultrastructural morphometry and immunogold counts; when counting APP, 100 cells per group were used. Each count was repeated at least 3 times by three blind observers.

Plain TEM was implemented by a postembedding immunocytochemistry procedure for antibodies against LC3 and P20S, which were used as markers of ATG and UP pathways, respectively. Antibody specificity was assessed by a number of studies which were partially reported in Table 1 (extramural evidence), and they were routinely used for at least 10 years in our lab (intramural evidence) [51–76].

Table 1: Sources and references for antibodies reported in the present study.

Antibodies	References
LC3 (Abcam)	[47, 51–54]
LC3 (Sigma)	[55–57]
Proteasome 20S (Abcam)	[47, 58–61]
Alpha-synuclein (BD Biosciences)	[62–66]
SQSTM1-p62 (Abcam)	[67–71]
Phospho-p70 S6 kinase (Thr421/Ser424) (Cell Signaling Technologies)	[72–76]

It is worth mentioning that LC3 and P20S antigens were chosen as markers of ATG vacuoles (LC3 alone) or APP vacuoles (LC3 combined with P20S) accordingly to the manuscript "Guidelines for the Use and Interpretation of Assays for Monitoring Autophagy (3rd Edition)" [48].

Sometimes, in order to validate the count for ATG vacuoles, beclin 1 was used instead of or in combination with LC3 for detecting early time points. No significant difference between LC3- and beclin 1-based counts was detected; thus, results fully express the amount of LC3. At the end of the plain TEM or immunocytochemistry procedure, ultrathin sections were stained with uranyl acetate and lead citrate, and they were finally examined using a JEOL JEM-100SX transmission electron microscope (JEOL, Tokyo, Japan).

2.2.1. Postembedding Immunocytochemistry. Fixing and postfixing solutions and the use of epoxy resin were validated in our previous studies for immunogold-based ultrastructural morphometry [47]. In fact, a combination of aldehydes, OsO_4, and epoxy resin allows a minimal epitope covering, while preserving cell ultrastructure [47, 77, 78]. In particular, OsO_4 binds to cell membranes, thus enhancing the contrast of cytosolic compartments, and it prevents the formation of membrane's artifacts, which may mimic vacuoles. Moreover, epoxy resin is advantageous over acrylic resin in preserving cell morphology.

Postembedding procedure was carried out on ultrathin sections collected on nickel grids, which were incubated on droplets of aqueous sodium metaperiodate ($NaIO_4$), for 30 min, at room temperature in order to remove OsO_4. $NaIO_4$ is an oxidizing agent allowing a closer contact between antibodies and antigens by removing OsO_4 [77]. This step improves the visualization of immunogold particles specifically located within a sharp context of cell integrity, and it allows the counting of molecules within specific cell compartments. Then, grids were washed in PBS and incubated in a blocking solution containing 10% goat serum and 0.2% saponin for 20 min, at room temperature. Grids were then incubated with the primary antibody solution containing both rabbit anti-LC3 (Abcam, Cambridge, UK, diluted 1 : 50) and mouse anti-P20S (Abcam, Cambridge,

UK, diluted 1 : 50), with 0.2% saponin and 1% goat serum in a humidified chamber overnight, at 4°C. After washing in PBS, grids were incubated with the secondary antibodies conjugated with gold particles (10 nm mean diameter, for gold particle anti-rabbit; 20 nm mean diameter, for gold particle anti-mouse, BB International), diluted 1 : 30 in PBS containing 0.2% saponin and 1% goat serum for 1 h, at room temperature. Control sections were incubated with the secondary antibody only. After washing in PBS, grids were incubated on droplets of 1% glutaraldehyde for 3 min; additional extensive washing of grids on droplets of distilled water was carried out to remove extensive salt traces and prevent precipitation of uranyl acetate.

2.2.2. Ultrastructural Morphometry. In order to distinguish vacuoles (ATG from APP) and to count immunogold particles (ranging from 10 nm to 20 nm), observations were performed directly at TEM at a magnification of 8000x [79] since this represents the minimal magnification at which immunogold particles and all cell organelles can be concomitantly identified.

We started to count from a grid square corner in order to scan the whole cell pellet within that grid square, which was randomly identified. Assessments of vacuoles and measurement of immunogold particles were carried out according to Lenzi et al. [47].

Briefly, we counted the number of unstained vacuoles per cell as vacuoles with single, double, or multiple membranes possessing the same electron density of the surrounding cytoplasm or partly containing some electron dense structure. In each cell, we counted the total number of immunogold anti-LC3 and/or anti-P20S particles placed either in the cytoplasm or within vacuoles and we expressed the number of immunogold particles as the mean per cell. Finally, we counted the number of APPs per cell as a single, double, and multiple membrane vacuoles, in which immunogold particles of LC3 (10 nm) and P20S (20 nm) were colocalized.

2.3. Light Microscopy. For light microscopy, PC12 cells were harvested and centrifuged at 800g for 5 min to obtain a pellet, which was further resuspended in 0.5 ml of the culture medium in order to obtain a dense cell suspension. This was layered on glass slide spinning at 15,000g for 10 min by cytospin (Cytospin 4, Thermo Fisher).

2.3.1. Haematoxylin and Eosin Staining and Cell Count. Cells were fixed with 4% paraformaldehyde in PBS for 15 min and plunged in PBS and then in haematoxylin solution (Sigma) for 20 min. Haematoxylin staining was stopped by washing in distilled water and followed by plunging cells in the eosin solution (Sigma) for a few min. After repeated washing to remove the excess of dye, cells were dehydrated in increasing alcohol solutions, clarified in xylene, and finally covered with the DPX mounting medium (Sigma). Cell count was performed at light microscopy at 40x magnification. Briefly, for each experimental group, the number of stained cells detectable after each specific treatment was counted and expressed as a percentage of the control group. These values represent the means of six independent cell counts.

Moreover, we counted the number of giant cells occasionally observed after 10 μM METH. We considered as giant cells those owning a diameter higher than 14–15 μm. The amount of giant cells out of the total number of cells counted on the glass slide was expressed as a percentage, for each experimental group. The values represent the means of six independent cell counts.

2.3.2. Trypan Blue. For trypan blue staining, PC12 cells were seeded at a density of 1×10^4 cells/well and they were preincubated for 24 h. After METH treatments, PC12 cells were collected and centrifuged at 800g for 5 min. The cell pellet was suspended in the culture medium, and 25 μl of cell suspension was added to a solution of 1% trypan blue (62.5 μl) and PBS (37.5 μl). Cells were then incubated for 10 min, at room temperature. Soon after, 10 μl aliquot of this solution was counted at light microscopy using a Bürker glass chamber. Viable and nonviable cells were counted, and cell death was expressed as percentage of trypan blue frankly positive cells out of the total cells. The values represent the means of three independent cell counts.

2.4. Confocal Microscopy. PC12 cells were washed in PBS and fixed with paraformaldehyde 4% for 5 min at room temperature. Antigen retrieval was carried out in 100 mM Tris-HCl, 5% urea at 95°C, for 10 min. After washing in PBS, cells were permeabilized in 0.2% Triton X-100, for 10 min. They were blocked in PBS containing 0.1% Tween-20, supplemented with 1% bovine serum albumin (BSA) and 23 mg/ml of glycine, for 30 min. Afterwards, cells were incubated overnight at 4°C in 1% BSA in PBS-T containing 1 : 50 anti-LC3 antibody (Abcam) and 1 : 30 anti-P20S (Abcam). Finally, cells were incubated for 1 h with fluorophore-conjugated secondary antibodies (1 : 200; goat anti-rabbit Alexa 488 and goat anti-mouse Alexa 594, Molecular Probes, Life Technologies) in 1% BSA in PBS-T at room temperature. Then, cells were washed in PBS, and they were mounted in ProLong Diamond Antifade Mountant (Molecular Probes, Life Technologies). The analysis was performed using a Leica TCSSP5 confocal laser scanning microscope (Leica Microsystems, Mannheim, Germany) using a sequential scanning procedure. Confocal images were collected every 400 nm intervals through the z -axis of each section by means of 63x oil lenses. Z-stacks of serial optical planes were analyzed using the Multicolor Package software (Leica Microsystems). Negative controls were carried out by omitting primary antibodies.

2.5. Coimmunoprecipitation Assay. PC12 cells were homogenized at 4°C in an ice-cold lysis buffer. One microliter of homogenates was used for protein determinations. 30 μg of proteins from whole cell lysates was loaded to perform Western blotting before coimmunoprecipitation. β-Actin was used as a loading control for protein levels from the whole cell lysates, on which immunoprecipitation of LC3 was then performed.

Proteins (800 μg) were incubated at 4°C overnight with primary rabbit anti-LC3 antibody (2 μg for each sample; Sigma-Aldrich, Milan, Italy). The antibody/antigen complex was pulled out of the sample using protein A-Sepharose

beads. This process isolated the protein of interest from the rest of the sample. Proteins were separated on sodium dodecyl sulphate-polyacrylamide gel (12%) and transferred on immuno-PVDF membrane (Bio-Rad, Milan, Italy) for 1 h. Filter was blocked for 1 h in Tween-20 Tris-buffered saline (TTBS) (100 mM Tris-HCl, 0.9% NaCl, 1% Tween 20, pH 7.4) containing 5% nonfat dry milk. Blot was incubated at 4°C overnight with mouse monoclonal primary antibody anti-P20S (1 : 100, Abcam), mouse monoclonal anti-alpha-synuclein (1 : 1000, BD Biosciences), and rabbit monoclonal anti-SQSTM1 (anti-p62, 1 : 1000, Abcam, Milan, Italy); it was washed 3 times with the TTBS buffer and then incubated for 1 h with secondary peroxidase-coupled antibody (anti-mouse, 1 : 7000; anti-rabbit, 1 : 7000; Calbiochem, Milan, Italy). Then, blot was stripped with a solution of distilled water and 3.5% acetic acid in the presence of 1% NaCl 5 M. Blot was kept in this solution for 20 min, and then, it was washed in TTBS (8 washes for 5 min). Finally, to verify the correct immunoprecipitation, blot was incubated with primary rabbit anti-LC3 antibody (1 : 6000, Sigma-Aldrich), for 1 h, at room temperature. Filter was washed 3 times with the TTBS buffer and then incubated for 1 h with secondary peroxidase-coupled antibody (anti-rabbit, 1 : 7000; Calbiochem, Milan, Italy). Immunostaining was revealed by enhanced chemiluminescence (GE Healthcare, Milan, Italy). The total amount of proteins measured through optical density was normalized for total β-actin, which was measured in whole cell lysates, since β-actin is not present in LC3 immunoprecipitates. Thus, readers should consider that such a normalization could not refer to the immunoprecipitated blotted proteins, but rather to the total amount of proteins in the very same cells used to carry out the immunoprecipitate.

2.6. Western Blotting. PC12 cells were lysed in a buffer (100 mM Tris-HCl, pH 7.5, 5 M NaCl, 0.5 m EDTA, 10% SDS, 1% NP40, IGEPAL), containing protease and phosphatase inhibitor, and centrifuged at 15,000g for 20 min at 4°C. The supernatant was collected, and protein concentration was determined using a protein assay kit (Sigma). Samples containing 40 μg of total proteins were solubilized and electrophoresed on a 12% sodium dodecyl sulphate-(SDS-) polyacrylamide gel. Following electrophoresis, proteins were transferred to the nitrocellulose membrane (Bio-Rad Laboratories, MI, Italy). The membrane was immersed in a blocking solution (3% nonfat dried milk in 20 mM Tris and 137 mM NaCl at pH 7.6 containing 0.05% Tween-20) for 2 h on a plate shaker. Subsequently, the membrane was incubated with mouse anti-pS6 primary antibody (1 : 2000; Millipore, Burlington, MA, USA) overnight at 4°C on the plate shaker. Blot was probed with horseradish peroxidase-labeled secondary antibodies, and the bands were visualized with enhanced chemiluminescence reagents (Bio-Rad Laboratories). Image analysis was carried out by ChemiDoc System (Bio-Rad Laboratories).

2.7. Statistics. For ultrastructural morphometry data were given as an absolute number concerning the following measurements: (i) unstained vacuoles, (ii) LC3-positive vacuoles, (iii) P20S-positive vacuoles, (iv) LC3 + P20S-positive vacuoles (APP), and (v) immunogold particles (including LC3 and P20S). Ratios were used to express (i) the number of LC3 immunogold particles within vacuoles out of the number of cytoplasmic LC3 immunogold particles and (ii) the number of P20S immunogold particles within vacuoles out of the number of cytoplasmic P20S immunogold particles. All data were reported as the means ± SEM per cell from 50 cells per group in all counts but the LC3 + P20S which was expressed as the means ± SEM from 100 cells per group.

Data on the amount of cell death were expressed as the percentage of the mean ± SEM dead cells out of the total cell number in each grid being analyzed (i.e., 5 total grids, each containing at least 10 cells, for a total of 50 cells for each experimental group).

For confocal microscopy, the amount of P20S + LC3 puncta was counted. Values were expressed as the mean number of puncta ± SEM per cell counted in each slide in two separate experiments (each one carried out in duplicate).

For Western blot optical density was expressed as the means ± SEM calculated in six separate experiments.

All statistical analyses were carried out by using one-way analysis of variance, ANOVA, followed by Sheffè's post hoc analysis. Null hypothesis (H0) was rejected for $p \leq 0.05$.

3. Results and Discussion

3.1. Dose and Time Dependencies of METH-Induced Unstained Vacuoles. Confirming previous data, METH administration for 72 h filled catecholamine cells with vacuoles, as reported in representative micrographs (Figure 1(a)) and counted in the graph of Figure 1(b). As measured in Figure 1(b), unstained vacuoles increase dose-dependently within a wide range of METH doses (from 1 nM up to 1 μM). At the dose of 1 μM, the number of METH-induced unstained vacuoles reached the peak. Whereas, for the highest dose of METH (10 μM), the number of unstained vacuoles dropped down to levels measured following low METH doses (1 nM and 10 nM). This suggests that at 10 μM METH dose, toxicity occludes the development of novel intracellular structures, even in spared cells. Therefore, the doses of METH 1 μM and 10 μM were chosen for the time dependence study. As reported in representative micrographs of Figure 1(c), a time-dependent increase of unstained vacuoles was produced by METH at the 1 μM dose from 12 h up to 72 h. These effects were evidenced by staining with arrows the unstained vacuoles in each experimental condition to relate representative pictures to counts reported in the graph in Figure 1(d). As expected, even the dose of 10 μM METH at 72 h time-dependently increases the number of unstained vacuoles (Figure 1(f)). This was evident in representative micrographs of Figure 1(e); we investigated the effects of such a METH dose at earlier time intervals (representative pictures of Figure 1(e)). These effects were evidenced by staining with arrows the unstained vacuoles at each time interval to relate representative pictures to counts reported in the graph in Figure 1(f). The number of unstained vacuoles is consistent with the time course and dose dependency of multilamellar

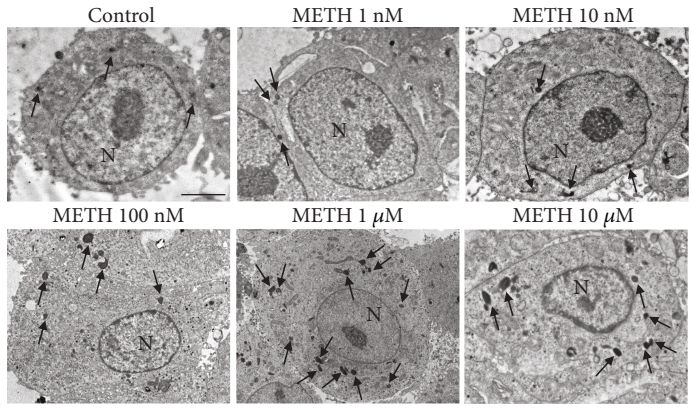

(a)

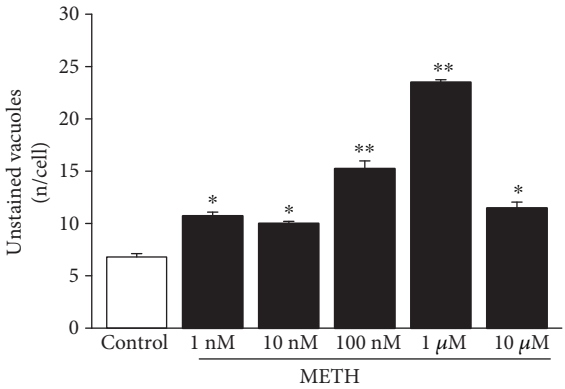

(b)

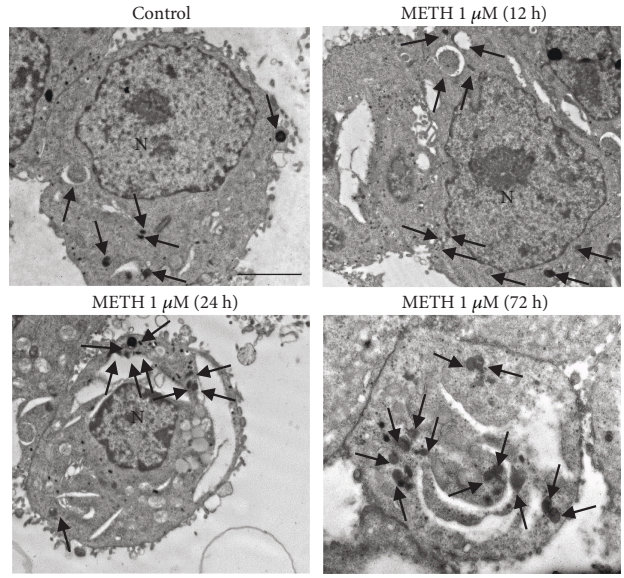

(c)

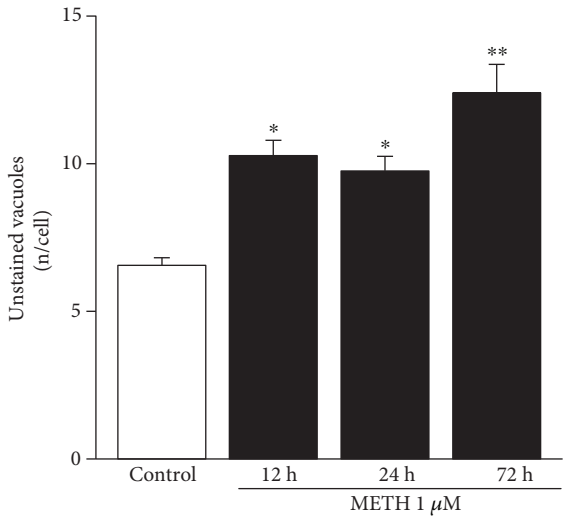

(d)

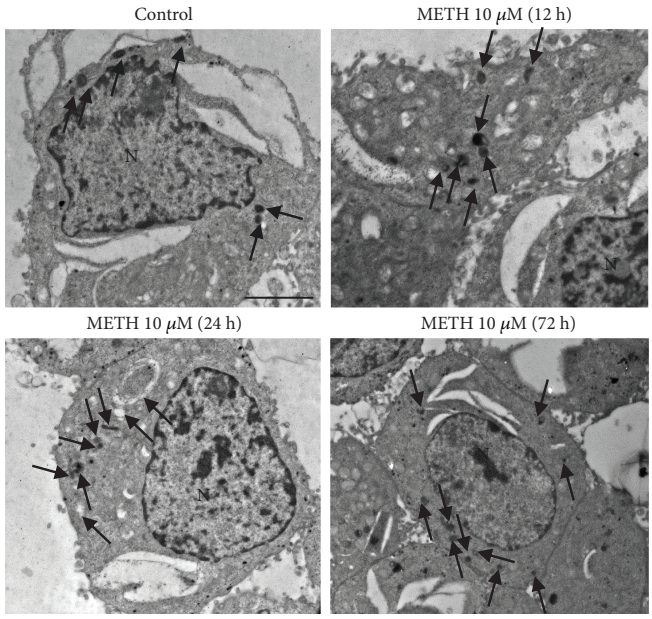

(e)

Figure 1: Continued.

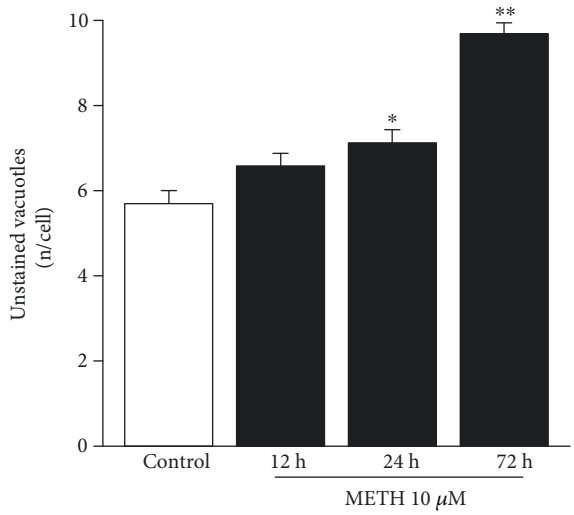

(f)

Figure 1: METH increases the amount of unstained vacuoles dose- and time-dependently. (a) Dose-dependent representative pictures of unstained vacuoles (arrows) of control and METH at 72 h treated cells at different doses. (b) Dose-dependent graph of unstained vacuoles per cell at 72 h. (c) Time-dependent representative pictures of unstained vacuoles (arrows) of control and 1 μM METH-treated cells. (d) Time-dependent graph of unstained vacuoles per cell of control and 1 μM METH-treated cells. (e) Time-dependent representative pictures of unstained vacuoles (arrows) of control and 10 μM METH-treated cells. (f) Time-dependent graph of unstained vacuoles per cell of control and 10 μM METH-treated cells. Values are given as the mean number of unstained vacuoles, which were counted in 50 cells per group. Error bars represent the standard error of the mean. $^{*}p \leq 0.05$ vs. control; $^{**}p \leq 0.05$ vs. other groups. N = nucleus. Scale bar = 1 μm.

bodies produced by METH, which we previously described under a different name (whorls) in this cell line [6].

3.2. Dose and Time Dependencies of METH-Induced Cell Death. When assessing the effects produced by a 10 μM dose of METH, there was a dramatic increase (roughly by half) in the amount of cell loss compared with controls and occasionally, giant cells appeared, which were never observed in controls (representative H&E staining of Figures 2(a) and 2(b); graph of Figure 2(c)). The counts for surviving cells carried out at H&E staining revealed a dose- and time-dependent decrease in cell survival (graphs of Figures 2(d) and 2(e), respectively). This was dramatic at 72 h following 10 μM METH. These same results were reproduced by trypan blue-positive counts for dying cells, which confirmed a dose- and time-dependent increase in dying cells (graphs of Figures 2(f) and 2(g), respectively). A similar phenomenon (cell death in the same range of doses and times induced by METH administration) was detected at TEM (representative TEM micrographs of Figures 2(g) and 2(h), respectively). The count of dying cells (either necrotic or apoptotic) at TEM for METH and controls (Figures 2(h) and 2(i), respectively) was overlapping with that reported for trypan blue staining. Remarkably dying cells were higher than controls also following the dose of 1 μM (at 72 h, Figures 2(j) and 2(k)). The pronounced toxicity induced by 10 μM METH is likely to impair cell metabolism even in spared cells, which when analyzed at 72 h own much less vacuoles compared with other doses.

3.3. METH Alters Dose and Time Dependency of the Amount and Placement of LC3 Particles. In order to identify ATG and UP components within METH-treated cells, we carried out ultrastructural morphometry by using 10 nm immunogold particles to reveal LC3, while 20 nm immunogold particles were used to stain P20S. Following METH administration, an increase in LC3-stained vacuoles was detected starting at the dose of 100 nM METH, while no increase compared with controls was counted in a lower range of doses (between 1 nM and 10 nM, Figure 3(a)). This was quite unexpected since the count of unstained vacuoles provided in Figure 1(b) indicates a significant increase (almost two-fold) compared with controls even at the dose of 1 nM METH. This is a key point, since unstained vacuoles are considered to correspond to pure ATG vacuoles. Thus, one would expect an overlapping between unstained and LC3-positive vacuoles. Such a discrepancy leaves the issue open on which the nature of METH-induced unstained vacuoles might be. In fact, these vacuoles were induced by METH administration since they increased two-fold compared with controls at the dose of 1 nM and 10 nM METH.

A lack of LC3 staining in these vacuoles for low METH doses suggests that these may not correspond to authentic ATG vacuoles, although they increase two-fold with respect to controls. Although the nature of these unstained vacuoles remains to be defined, the possibility exists that LC3 particles moving within ATG vacuoles remain undetected for these low METH doses. However, as shown in the graph of Figure 3(b), total LC3 particles in the cell for 1 nM and 10 nM METH do not increase either. This indicates a lack of ATG induction for low METH doses. Another possibility

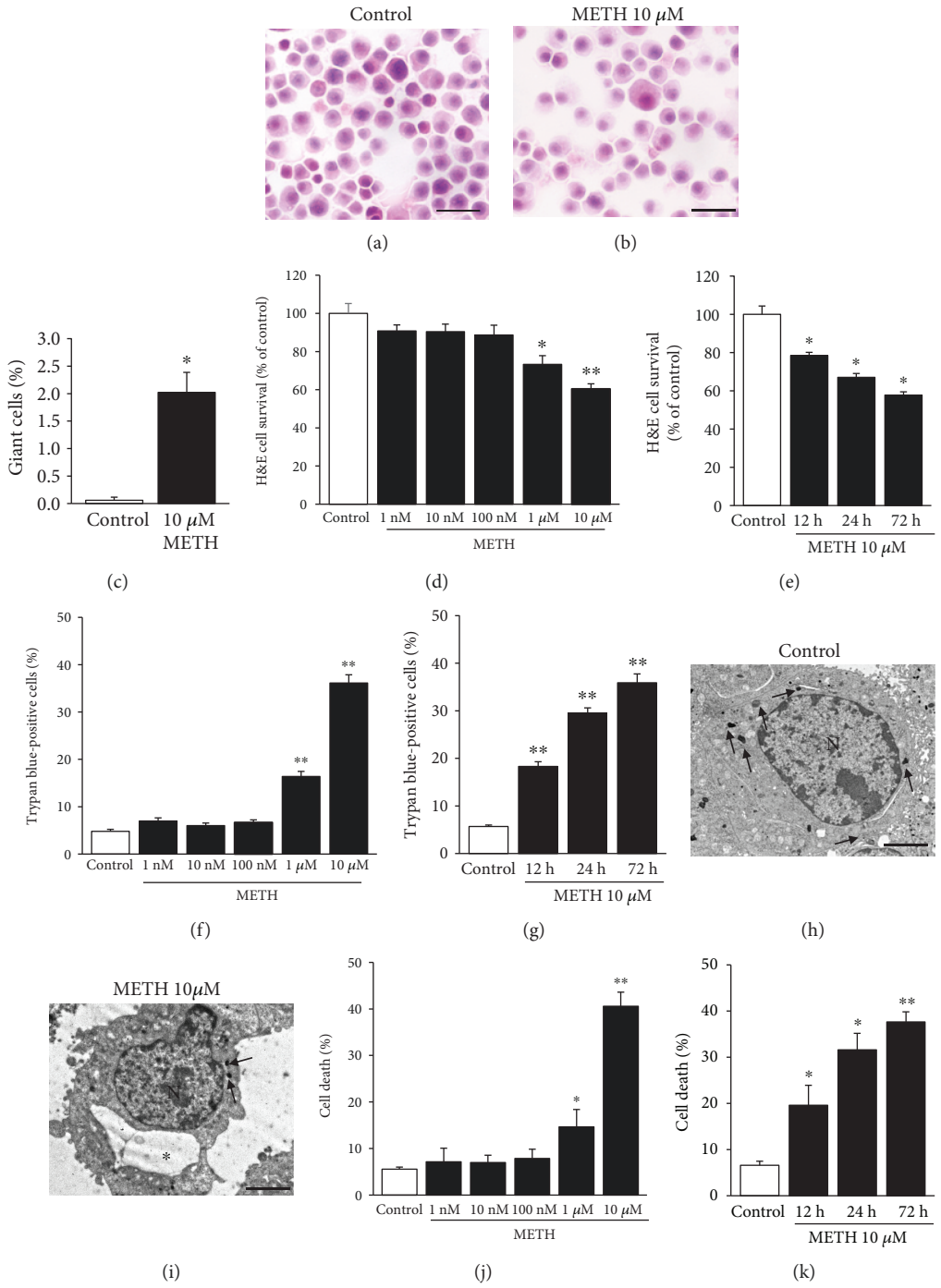

Figure 2: METH induces cell death time- and dose-dependently with a maximal effect at the 1 μM and 10 μM doses. (a) Representative H&E-stained picture from controls. (b) Representative H&E-stained picture following 10 μM METH at 72 h. (c) Graph reporting the percentage of giant cells counted in H&E-stained total cells from controls and METH at 72 h. (d) Dose-dependent graph of H&E-stained cells from control and METH at 72 h. (e) Time-dependent graph of H&E-stained cells from control and 10 μM METH-treated cells. (f) Dose-dependent graph of trypan blue-stained cells from control and METH at 72 h. (g) Time-dependent graph of trypan blue-stained cells from control and 10 μM METH-treated cells. (h) Representative micrograph from a control cell. (h) Representative micrograph from a control cell. (i) Representative micrograph from a METH cell at 72 h. (j) Dose-dependent graph of cell death from control and METH at 72 h. (m) Time-dependent graph of cell death from control and 10 μM METH-treated cells. For the graphs in (c)–(g), values are given as the percentage of cell counted in two triplicates ($n = 6$). For the graphs in (j) and (k), values are given as the percentage of cell counted on 5 grids. Error bars represent the standard error of the mean. $^{*}p \leq 0.05$ vs. control, $^{**}p \leq 0.05$ vs. other groups. Arrows point to vacuoles; asterisk (*) indicates a large vacuole. N = nucleus. Scale bar = 23.4 μm (a, b) and 2 μm (h, i).

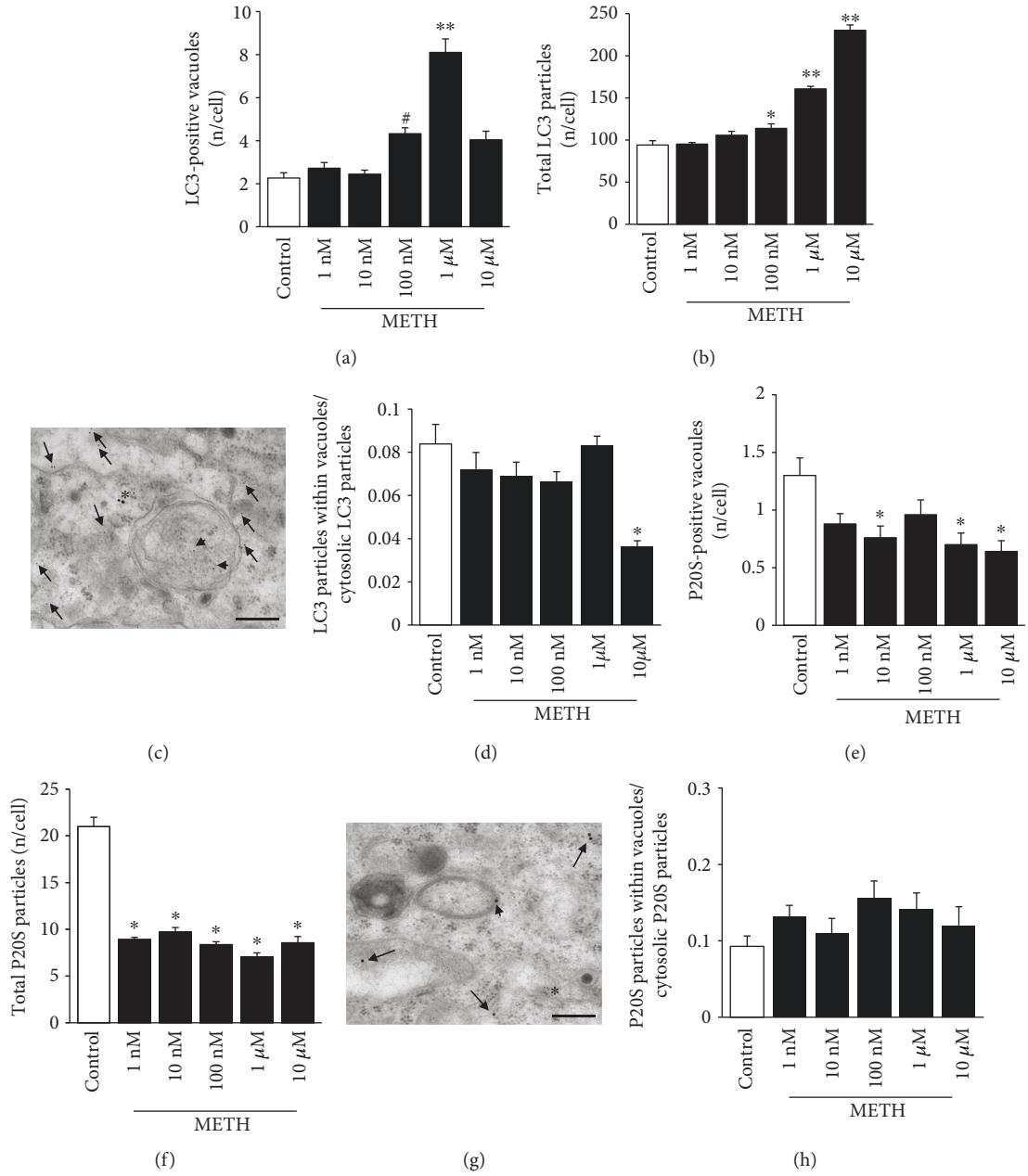

Figure 3: METH alters the amount and placement of LC3 and P20S particles dose-dependently, with P20S being more sensitive than LC3. (a) Dose-dependent graph of the number of LC3-positive vacuoles per cell from controls and METH at 72 h. (b) Dose-dependent graph of total LC3 particles per cell from controls and METH at 72 h. (c) Representative micrograph of LC3-positive vacuole from 10 μM METH at 72 h. (d) Dose-dependent graph of the ratio between the numbers of LC3 particles within vacuoles with respect to cytosolic LC3 particles from controls and METH at 72 h. (e) Dose-dependent graph of the number of P20S-positive vacuoles per cell from controls and METH at 72 h. (f) Dose-dependent graph of total P20S particles per cell from controls and METH at 72 h. (g) Representative micrograph of P20S-positive vacuoles from 10 μM METH at 72 h. (h) Dose-dependent graph of the ratio between the numbers of P20S particles within vacuoles with respect to cytosolic P20S particles from controls and METH at 72 h. Values are given as the mean number of LC3 or P20S particles and vacuoles counted in 50 cells per group. Error bars represent the standard error of the mean. $^{*}p \leq 0.05$ vs. control; $^{**}p \leq 0.05$ vs. other groups; $^{\#}p \leq 0.05$ vs. control and 1 nM and 10 nM METH. Arrows point to free cytosolic LC3 (10 nm) or P20S (20 nm); arrowheads point to LC3 (10 nm) or P20S (20 nm) within vacuoles; asterisk (*) indicates P20S in the cytosol (c) and LC3 in the cytosol (g). Scale bar = 200 nm.

deals with the dynamics of ATG vacuoles, which could maturate before LC3 is increased. This hypothesis remains unlikely, since other markers, such as beclin 1, which stains ATG vacuoles earlier than LC3, do not provide any staining either. Moreover, LC3 staining is a gold standard to define autophagosomes, and 72 h should be enough to complete the process. Instead, even at this time interval for low (1 nM and 10 nM) METH doses, LC3 particles do not increase in any cell compartments including the cytosol. This suggests that 1 nM and 10 nM METH do not really increase

ATG. Therefore, unstained vacuoles, which minimally occur in control cells and selectively increase following very low METH doses, are likely to belong to other pathways (such as the exosomal compartment). This hypothesis is currently under investigation in the lab. Vacuolar compartments other than ATG may be recruited for low METH doses. It is likely that DA turnover promoted by METH increases vesicle recycling, which may account for these unstained vacuoles. On the other hand, the lowest effects of METH on membrane trafficking may affect other compartments such as retromers or exosomes, which are more bound to cell release than ATG activation.

The increase in vacuoles measured for doses above 10 nM corresponds to LC3-positive (ATG) vacuoles. Data on the amount of LC3-positive vacuoles (shown in representative Figure 3(c)) parallels data on LC3 particles reported in the graph of Figure 3(b). In fact, they increase significantly only at the dose of 100 nM, while they do not differ from controls at low METH doses (1 nM and 10 nM METH). Thus, METH increases LC3 particles (Figure 3(b)) and LC3-positive vacuoles (Figure 3(a)) only at doses higher than 10 nM, although no compartmentalization of LC3 within vacuoles is produced by any dose of METH (graph of Figure 3(d)). In contrast, the trend indicates a dispersion rather than a polarization of LC3 particles from cell vacuoles towards the cytosol. This is indicated by the finding that the ratio of vacuolar *vs.* cytosolic LC3 particles following METH decreases dose-dependently (Figure 3(d)), which indicates a METH-induced loss of LC3 compartmentalization. Such an uncoupling between LC3 and ATG vacuoles is a novel finding in METH toxicity. In fact, so far, METH was thought to impair ATG machinery by engulfing ATG vacuoles, which become stagnant and filled with LC3. The present data show that, under METH, ATG vacuoles are impaired already in their maturation. In fact, for low METH doses, LC3 is not increased, while for higher METH doses, LC3 increases more in the cytosol than within vacuoles. It looks like that in these conditions (METH doses up to 1 μM), the drive which polarizes LC3 towards the ATG machinery is weakened. At 10 μM METH, there is a further drop in the ratio between vacuolar and cytosolic LC3 particles, which is likely to be due to a concomitant loss of cell ability to build organelles for toxic METH doses. This latter finding is confirmed by the fact that 10 μM METH strongly increases free LC3 particles compared with the dose of 1 μM, but the number of LC3-positive ATG vacuoles at 10 μM is roughly a half of that counted at 1 μM.

These observations, despite being unexpected, provide also novel methodological insights into ATG. In fact, when using confocal microscopy following high METH doses, there is a strong increase in LC3 immunofluorescence, which is routinely interpreted as produced by stagnant vacuoles. However, ultrastructural morphometry demonstrates that an increase in LC3 immunostaining is indeed driven by free cytosolic noncompartmentalized LC3 rather than by vacuolar LC3.

We may summarize these latter data by stating that, under METH administration, there is a loss of compartmentalization of LC3 particles within vacuoles, despite an increased amount of both LC3 particles and vacuoles per se, which represents a novel insight in ATG and METH toxicity.

This leads to reconsider the significance of densely fluorescent LC3 spots detected at confocal microscopy following METH [16, 80]. The stoichiometric counts at TEM demonstrate that a greater contribution is provided by free cytosolic LC3. This is representatively evidenced in micrograph of Figure 3(c), and it is remarked by the ratio between compartmentalized LC3 particles in ATG vacuoles and free cytosolic LC3 particles (graph of Figure 3(d)). This demonstrates a lack of METH-induced LC3 compartmentalization with a trend towards "METH-induced LC3 dispersion." This is frankly evident for a neurotoxic dose of METH (10 μM) where a loss of fine subcellular compartments take place. As discussed for Figure 1(b), this is likely to reflect a degeneration of the subcellular trim of spared cells, which organize protein trafficking, where the ability to create various cell compartments is reduced.

3.4. METH Alters the Amount and Placement of P20S Particles. When counting P20S-positive vacuoles, these were consistently decreased compared with controls for all METH doses (Figures 3(e) and 3(g)). These findings were reproduced when counting P20S immunogold particles, which were markedly decreased following all METH doses (ranging between 1 nM and 10 μM, Figure 3(f)). Remarkably, this was replicated even for the highest dose of 10 μM METH, which was shown to suppress compartmentalization of LC3 within vacuoles (Figure 3(d)). It is likely that such a discrepancy is related to a different sensitivity of P20S compared with LC3 to the effects of METH. Again, no polarization of P20S towards vacuoles was induced by METH, which left the ratio unmodified between P20S particles within vacuoles and cytosolic P20S particles compared with controls (Figure 3(h)), although the trend was different compared with LC3.

It is surprising that the effects induced by METH on the number of the ATG marker LC3 follow a different dose-response curve compared with the effects induced on the number of the UP marker P20S. In fact, in the range of 1 nM to 10 nM doses, no alterations were produced by METH in the number of LC3 immunogold particles (Figure 3(b)), while at the dose of 1 nM of METH, the reduction of P20S immunogold particles was already maximal (roughly, a half of controls, Figure 3(f)). This suggests that the biochemical pathways involved (regulating either ATG or UP) possess a different dose-response curve being the UP maximally affected already at the lowest dose of METH. Thus, the P20S protein component is markedly sensitive to doses of METH, which are likely to be in the picomolar range.

As previously discussed, the lowest dose of METH (1 nM) doubled the number of unstained vacuoles without affecting neither LC3 particles nor LC3 vacuoles. In contrast, this very same dose reduced roughly to a half both P20S particles and P20S-positive vacuoles. It is worth noting that this METH dose is sufficient to double the DA release in PC12 cells [6]. Thus, it is likely that an increased amount of free DA may already impair the P20S proteasome. This is consistent with our previous study showing that, at the dose of 1 nM of

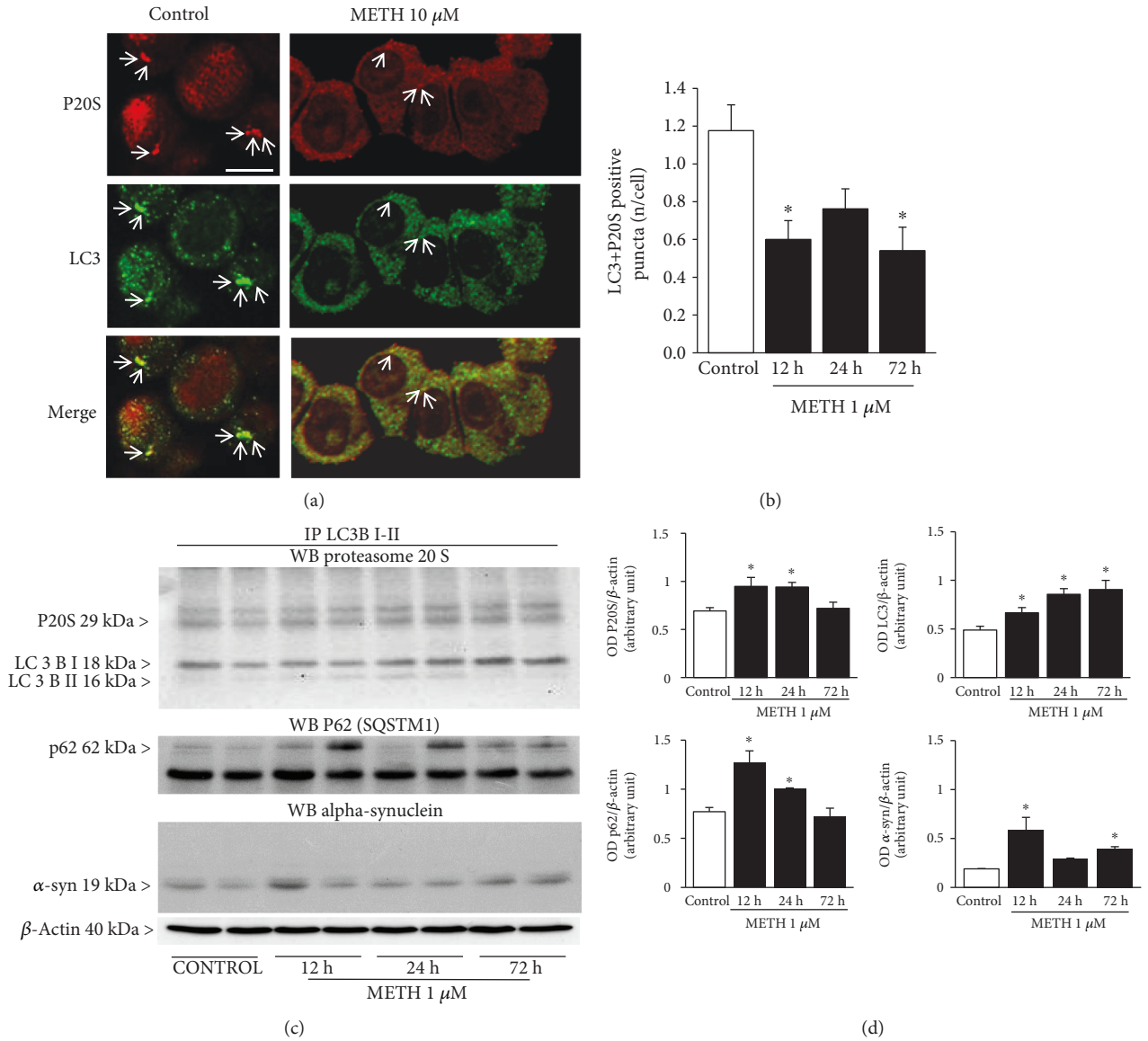

Figure 4: METH reduces the occurrence of the autophagoproteasome (APP) which hosts LC3, P20S, p62, and alpha-synuclein. (a) Representative immunofluorescence from controls and METH at 72 h. (b) Time-dependent graph of the number of LC3 + P20S-positive puncta per cell from control and METH at 1 μM. (c) P20S, p62, and alpha-synuclein Western blotting on LC3BI-II immunoprecipitates. (d) Densitometric analysis. Values are given as the optical density detected in four separate replicates ($n = 4$). Values are given as the mean number of LC3 + P20S puncta counted in 4 slides. Error bars represent the standard error of the mean. $^*p \leq 0.05$ vs. control. Arrows point to P20S (red fluorescence) or LC3 (green fluorescence) or merge P20S and LC3 (orange fluorescence). Scale bar = 6.6 μm.

METH, P20S is already suppressed [43]. While this corresponds to a two-fold decrease in P20S-positive vacuoles (Figure 3(e)), the number of unstained METH-induced vacuoles increases by 2-fold ([6, 43]; present study in Figure 1(b)). Remarkably, UP inhibition enhances neurotransmitter release [81, 82]; in fact, proteasome inhibitors produce striatal DA release [83]. This is due to an effect of proteasome activity in the recycling of short-lived proteins from and towards the plasma membrane including DA receptors [84], which is compatible with the retromer hypothesis for unstained vacuoles expressed above [85]. It is demonstrated that increased DA stimulation disassembles the proteasome structure, and it is related to sensitization [84]. Thus, a vicious circle may establish in which METH-induced DA release alters the proteasome structure, which in turn enhances DA release. This issue opens novel avenues to study the role of protein clearing systems in determining METH-induced sensitization. Thus, the increase in DA release occurring after 1 nM METH may be due to altered proteasome levels shown in this study. This is in line with imaging of P20S following METH compared with controls at confocal microscopy. In METH-treated cells, perimembranous rings of fluorescence appear instead of the diffuse fluorescent P20S staining occurring in controls (Figure 4(a)).

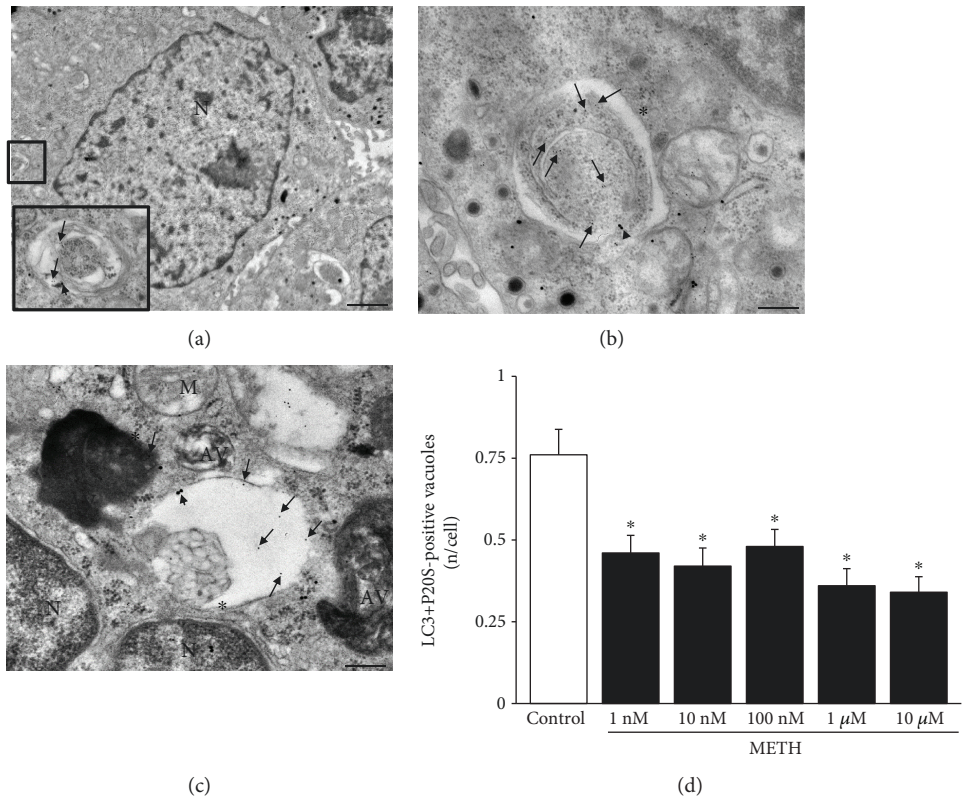

Figure 5: METH reduces the occurrence of autophagoproteasomes (APPs) dose-dependently. (a) Representative picture of a PC12 cell (low magnification) and an APP vacuole (high magnification). (b, c) Representative pictures of APP vacuoles stained for both LC3 (10 nm) and P20S (20 nm) immunogold particles. (d) Dose-dependent graph of the number of LC3 + P20S-positive vacuoles per cell from control and METH at 72 h. Values are given as the mean number of LC3 + P20S-positive vacuoles counted in 100 cells per group. Error bars represent the standard error of the mean. $^{*}p \leq 0.05$ vs. control. Arrows point to free LC3 particles (10 nm); arrowheads point to P20S particles (20 nm); asterisk (*) indicates a double membrane (b, c). N = nucleus; AV = autophagic vacuoles; M = mitochondrion. Scale bar = 220 nm.

The discrepancy between LC3 and P20S immunogold particles extends to the time course (Supplementary Figure 1). In fact, for longer time intervals following 10 μM METH, LC3 particles increase progressively (Supplementary Figure 1a), along with LC3-positive vacuoles (Supplementary Figure 1b) with a decreasing ratio between LC3 in vacuoles and LC3 in cytosol, which is time-dependent (Supplementary Figure 1c). P20S particles and vacuoles decrease slightly (Supplementary Figure 1d and Figure 1(e), respectively). The ratio between P20S in vacuoles and P20S in cytosol was similar for all time intervals (Supplementary Figure 1f). This suggests that a loss of compartmentalization for P20S is maximal already for the lowest dose of METH.

3.5. METH and Autophagoproteasome (APP). In order to document the occurrence of APP in PC12 cells and its modulation at various doses and time intervals following METH, we used confocal microscopy to document the merging between P20S and LC3 particles. As shown in representative Figure 4(a), the punctum staining for P20S and LC3 was fairly merging in baseline conditions, while only some merging could be detected also following the highest dose of METH. When we counted the amount of merging puncta detected at confocal microscopy (Figure 4(b)), these were markedly reduced following 1 μM METH at each time interval (12 h, 24 h, and 72 h). Confirming the hypothesis that a chemical binding between LC3 and P20S within vacuoles exists, we carried out Western blotting on LC3BI-II immunoprecipitates from whole cell lysates. In these experimental conditions, P20S was detected along with p62 (Figures 4(c) and 4(d)). The occurrence of p62 is the key since, as recently shown by Cohen-Kaplan et al. [86], p62 is pivotal in shuttling proteasome subunits within LC3-positive autophagosomes. In line with the key role played by both ATG and proteasome to metabolize alpha-synuclein [87, 88], we checked whether these merging organelles contain alpha-synuclein. In fact, alpha-synuclein is detected here within immunoprecipitates (Figures 4(c) and 4(d)). Incidentally, these findings indicate why, in biochemical studies, the metabolism of alpha-synuclein was attributed to ATG, UP, or both, depending on the study [89–91]. The present research paper demonstrates at the morphological level the occurrence of a single organelle hosting both UP and ATG components, which recruits alpha-synuclein (Figure 4(c)). When analyzed at ultrastuctural morphometry, these merging units between P20S and LC3 appear as vacuoles owning different shapes and structures corresponding to autophagoproteasomes (APPs, Figures 4(a), 5(b), and 5(c)). It is remarkable that,

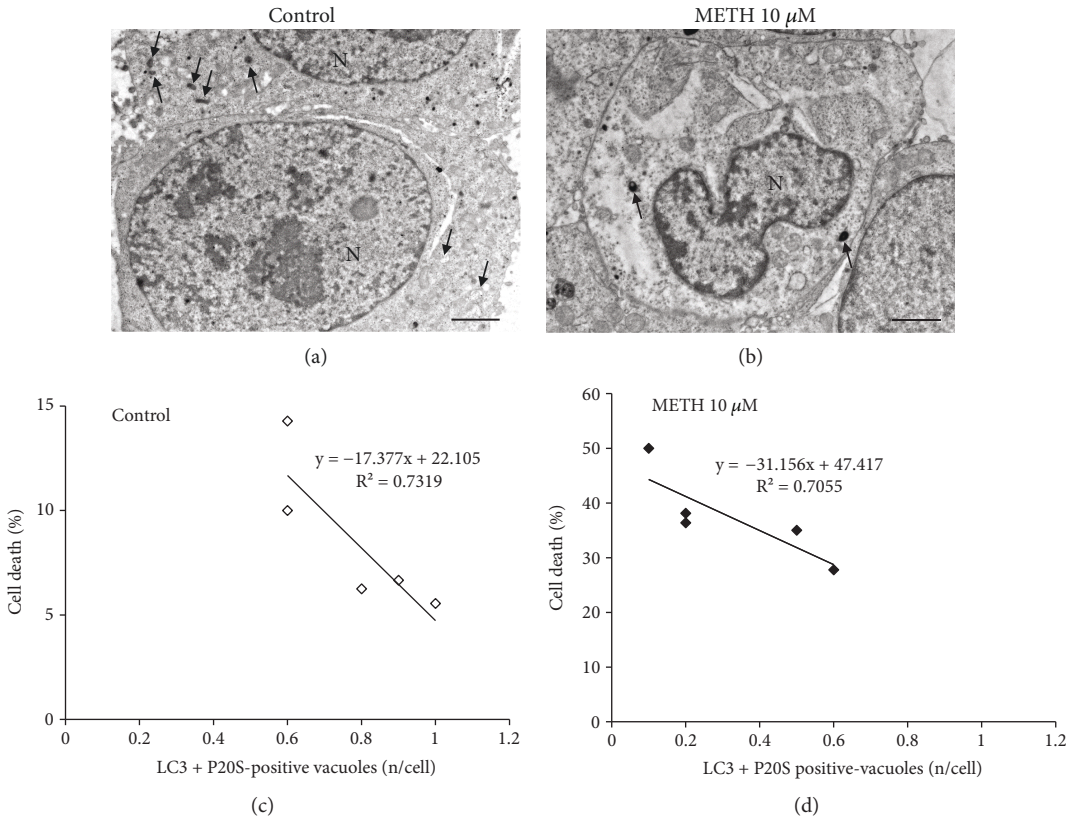

Figure 6: Inverse correlation between the occurrence of APP and METH-induced toxicity. (a) Representative micrograph from a control cell. (b) Representative micrograph from a cell following METH at 72 h. (c) Linear regression between the percentage of cell death and the number of LC3 + P20S-positive vacuoles in control. (d) Linear regression between the percentage of cell death and the number of LC3 + P20S-positive vacuoles following METH at 72 h. The puncta reported in the graphs ((c) white square and (d) black square) correspond to the number of grid ($n = 5$). Arrows point to vacuoles. N = nucleus. Scale bar = 1 μm.

according to confocal microscopy, under METH administration, a marked suppression was counted for APP for each dose of METH ranging between 1 nM and 10 μM as shown in the graph of Figure 5(d). Similarly, just like it was described for the time course detected at confocal microscopy, even at TEM, APP was similarly depressed by METH at 12, 24, and 72 h (Supplementary Figure 2). The number of APP in controls (representative Figure 6(a)) and following METH (Figure 6(b)) was plotted for a regression analysis between the amount of APPs and the number of dead cells in controls (graph of Figure 6(c)) and following METH (graph of Figure 6(d)). A negative correlation was detected between cell death and the number of APPs with a slope, which was consistent in control conditions and following METH at 10 μM. In fact, in both experimental conditions, cell death was lesser and lesser when APPs were more and more expressed. In controls, dead cells exceeded 10% in those samples owning only a few APPs/cell (roughly 0.6), while cell death was occluded down to 5% when APPs increased two-fold (graph of Figure 6(c)). As expected, the percentage of cell death reached almost 50% following the 10 μM dose of METH, when only a few APPs were produced (roughly 0.1 per cell); in contrast, cell death was toned down to 30% in those samples in which the amount of APPs was six-fold higher (roughly 0.6 per cell, graph of Figure 6(d)).

3.6. The Effects of mTOR Modulation on P20S, LC3, and Autophagoproteasome Related with METH Neurotoxicity. As previously published, mTOR activity finely tunes APP [47]. Therefore, in order to test in the present experiments the effects of specific doses of compounds, which are known to act either as mTOR inhibitors or activators, we measured the amount of the downstream product of mTOR activity (pS6). Asparagine is a well-known mTORC1 activator [92] while rapamycin is the gold standard mTORC1 inhibitor [93, 94]. The doses of these compounds were tested as reported in Figure 7. Asparagine at the dose of 50 mM activates mTOR while rapamycin at the dose of 100 nM inhibits mTOR as calculated by the amount of Western blotted pS6. Therefore, owning the right compounds at appropriated doses, we tested the effects of these compounds on cell death and amount of APPs. As shown in representative micrographs of Figure 8, we observed a variety of effects, which are in line with the key role of mTOR in METH toxicity and APP stimulation [80, 94, 95]. In fact, the dose of 10 μM METH produces roughly 35% cell death, which was totally prevented by rapamycin (100 nM). Remarkably, rapamycin alone further reduced cell death significantly below levels found in control cells. This witnesses for the presence of a baseline inherent aberrancy of mTOR regulation in this cell line, which is reminiscent of neurodegeneration [49].

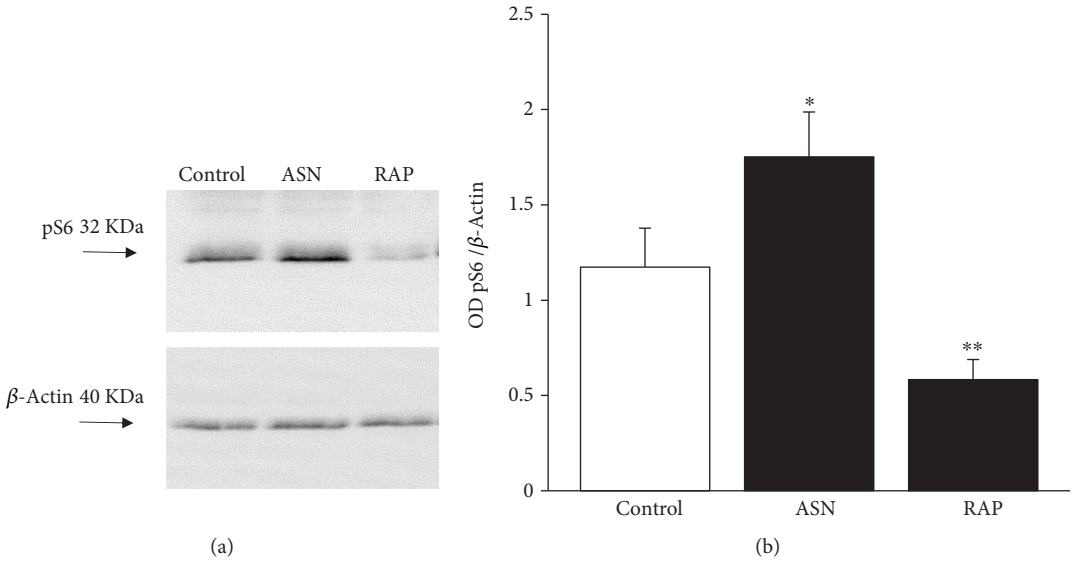

Figure 7: Modulation of pS6 levels underlie mTOR inhibition and activation by rapamycin and asparagine, respectively. (a) Representative SDS-PAGE immunoblotting of pS6 protein. (d) Densitometric analysis. Values are given as the optical density detected in six separate replicates ($n = 6$). Error bars represent the standard error of the mean. $^{*}p \leq 0.05$ vs. control; $^{**}p \leq 0.05$ vs. control and METH. ASN = asparagine; RAP = rapamycin.

Incidentally, this is the first report showing that the gold standard inhibitor of mTOR rapamycin prevents METH toxicity. This key finding provided here as side observation is in need of a dedicated experimental project. So far, only taurine and melatonin were shown to slightly prevent METH toxicity with an indirect evidence of mTOR-mediated mechanisms [94, 96], although this was interpreted using a multifaceted hypothesis. Remarkably, recent evidence, despite not addressing directly METH neurotoxicity, demonstrated that METH-induced behavioral sensitization associates with mTOR overexpression, while rapamycin reverts such an effect [97]. Again, the stimulation of DA D1 receptors, which are key in both METH-induced toxicity and behavioral sensitization [9, 98], directly promotes mTOR activation while inhibiting autophagy [99].

The present study directly relates neuroprotection with mTOR inhibition, while showing that METH impairs autophagy. This was consolidated by the deleterious effects of asparagine. In fact, in the graph of Figure 8(b), we found that asparagine alone was slightly increasing the natural cell death occurring in control cells but it did not really increase much the amount of METH-induced cell death. When all the three compounds were coadministered, the protective effects of rapamycin prevailed, with a robust suppression of cell death occurring following METH + asparagine (graph of Figure 8). These data concerning cell death were almost mirrored by each treatment in the count of APPs. In detail, METH suppressed APPs while rapamycin increased their number almost two-fold of controls. Asparagine, as expected, depressed APPs similarly to METH, while the combination METH + asparagine produced the lowest number of APPs (3-fold less than controls). It is remarkable that rapamycin rescued the loss of APPs induced following either asparagine alone or asparagine + METH (Figure 8(c)). This strengthens the significance of the present data concerning the role of mTOR in tuning METH toxicity and APPs in a reciprocal pattern.

Here, we wish to emphasize the protective effects of mTOR inhibition on natural cell death which occurs in the PC12 cell line. In fact, these cells possess an inherent aberrancy, which is useful in understanding neuronal degeneration [49]. This is partly due to an aberrancy in DA compartmentalization and vesicle polarization, where in baseline conditions most neurotransmitter is docking to the cell membrane, making this cell line highly prone to produce massive amount of self-oxidized DA metabolites [49]. It is remarkable that upgrading APPs through mTOR inhibition erases such an inborn trend to degenerate. Since UP inhibition enhances DA release, which is related to METH toxicity, it is expected that mTOR activation, by inhibiting UP activity and compartmentalization, enhances METH-induced cell death. The present research seems to uncover the molecular determinants of inherent vulnerability of the DA-PC12 cell line, by targeting specifically mTORC1 complex dysregulation.

3.7. The Effects of mTOR Modulation on Unstained Vacuoles. When these experimental conditions were applied to unstained vacuoles (representative picture of Supplementary Figure 3), data obtained were quite similar to APPs, though with some exceptions. In fact, METH increases the number of unstained vacuoles, which were further increased by rapamycin alone, way more compared with LC3-positive vacuoles (roughly 20 per cell and roughly 8 per cell, respectively). This adds further information about the previous question concerning the nature of these unstained vacuoles, which turn out to be mTOR-dependent. Unexpectedly, combined administration of METH and rapamycin instead of further increasing the number of

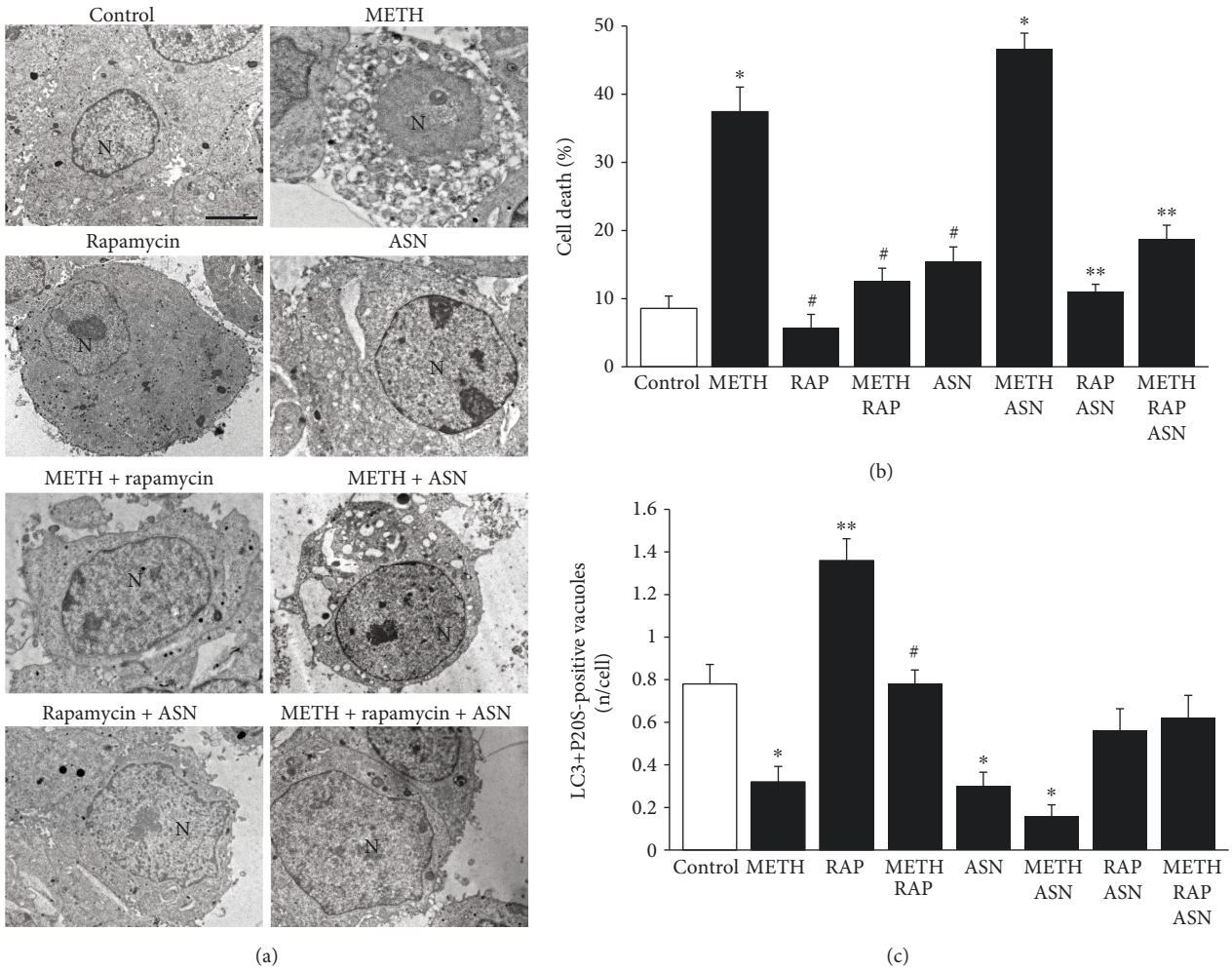

Figure 8: mTOR inhibition prevents cell death and rescues the amount of APPs induced by METH and the mTOR activator asparagine. (a) Representative micrographs of control and following METH 10 μM, rapamycin 100 nM, and asparagine 50 mM, at 72 h. (b) Graph of the percentage of cell death in control and following METH 10 μM, rapamycin 100 nM, and asparagine 50 mM, at 72 h. (c) Graph of the number of LC3 + P20S-positive vacuoles in control and following METH 10 μM, rapamycin 100 nM, and asparagine 50 mM, at 72 h. For the graph in (b), values are given as the percentage of cell counted on 5 grids. For the graph in (c), values are given as the mean number of LC3 + P20S-positive vacuoles counted in 100 cells per group. Error bars represent the standard error of the mean. $^{*}p \leq 0.05$ vs. control; $^{**}p \leq 0.05$ vs. control and METH; $^{\#}p \leq 0.05$ vs. METH. N = nucleus; ASN = asparagine; RAP = rapamycin. Scale bar = 0.5 μm.

unstained vacuoles compared with rapamycin alone produces a decrease in these vacuoles (which remain higher than controls). It is likely that, in the presence of rapamycin, there is no longer an oxidative stress, which produces an altered vesicle trafficking. In fact, mTOR inhibition stimulates both the activity and the amount of the proteasome subunit, which suppresses DA release. Thus, according to the hypothesis that unstained vacuoles are due to DA release and proteasome dysfunction mutually enhancing each other, it is expected that rapamycin occludes this component. Thus, combined METH and rapamycin administration produces a number of unstained vacuoles which is still higher than controls but lower than rapamycin alone. Asparagine alone or in combination with METH decreased unstained vacuoles, which were brought up to control the levels by adding rapamycin (Supplementary Figure 3).

These data suggest that the mechanisms by which unstained vacuoles are increased are different following rapamycin compared with METH administration, since double treatment occludes this effect instead of enhancing it. This is consistent with the opposite effects on cell death, which is induced by METH and rescued by rapamycin. In contrast, APP vacuoles despite being decreased by METH were increased by rapamycin, which witnesses for a different regulation of unstained compared with APP vacuoles.

3.8. The Effects of mTOR Modulation on LC3. Following mTOR inhibition by rapamycin, LC3 particles were never depressed below control values, even when METH and asparagine were combined. In these experimental conditions, compartmentalization of LC3 particles within vacuoles was dramatically enhanced by rapamycin. This mechanism was

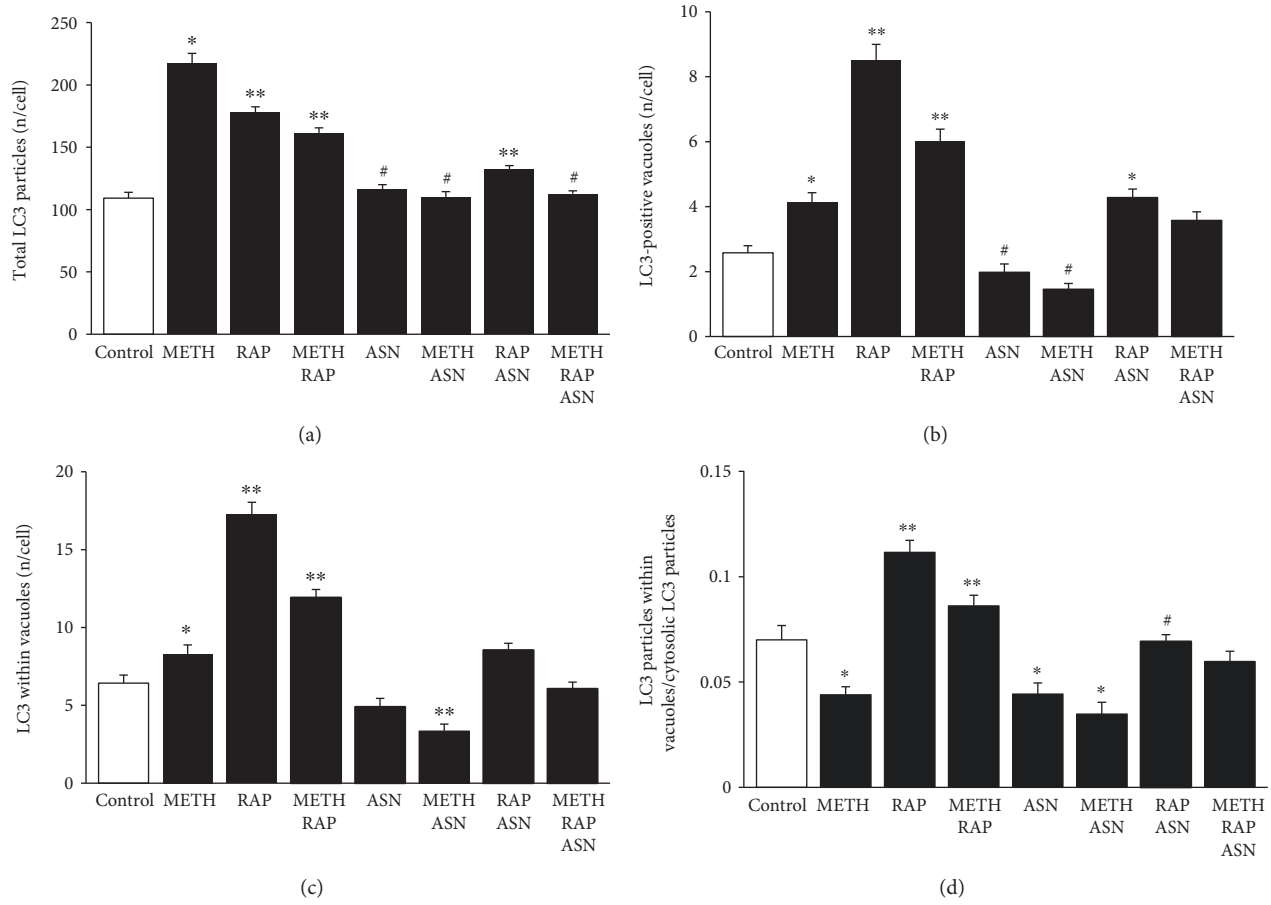

Figure 9: mTOR modulates the number and placement of LC3 particles. (a) The graph shows the number of total LC3 particles per cell in control, following METH 10 μM, rapamycin 100 nM, and asparagine 50 mM, at 72 h. (b) The graph shows the number of LC3-positive vacuoles per cell in control, following METH 10 μM, rapamycin 100 nM, and asparagine 50 mM, at 72 h. (c) The graph shows the number of LC3-positive vacuoles in control and following METH 10 μM, rapamycin 100 nM, and asparagine 50 mM, at 72 h. (d) The graph shows the ratio between the number of LC3 particles within vacuoles and cytosolic LC3 particles. Values are given as the mean number of LC3 particles and vacuoles counted in 50 cells per group. Error bars represent the standard error of the mean. $^{*}p \leq 0.05$ vs. control; $^{**}p \leq 0.05$ vs. control and METH; $^{\#}p \leq 0.05$ vs. METH.

independent from the one produced by METH; in fact, despite METH 10 μM was more effective than rapamycin 100 nM to increase total LC3 particles in the cell, rapamycin alone was much more powerful than METH alone in increasing LC3 within vacuoles (Figure 9(a)). Again, when rapamycin was combined with METH, a decrease of vacuolar LC3 was detected compared with rapamycin alone (Figure 9(b)). This indicates a strong compartmentalizing effect of rapamycin, which sharply contrasts with METH-induced LC3 dispersion (the generalized and nonspecific increase of LC3 promoted by METH, Figure 9(a)). The mTOR activator asparagine alone or in combination with METH further dispersed LC3 particles, since it decreased the placement of LC3 within vacuoles. This witnesses for a strong modulation by mTOR of LC3 compartmentalization (Figure 9(c)). This was further evidenced by counting the number of LC3 particles in the vacuoles versus LC3 particles within the cytosol (Figure 9(d)). In this case, METH decreases the ratio compared with controls, while rapamycin was increasing two-fold the ratio compared with controls and reverted the effects of METH. Asparagine alone was similar to METH and further suppressed the ratio when it was combined with METH.

3.9. The Effects of mTOR Modulation on P20S. The effects of mTOR inhibition were sharply contrasting with the effects of METH concerning the amount and placement of P20S particles. In fact, while METH depressed, rapamycin increased total P20S (Figure 10(a)). Moreover, rapamycin reverted the suppression induced by METH, while the effect of asparagine alone was less effective compared with METH. Combined administration of asparagine and METH did not alter the effects produced by METH alone. The effects of asparagine were antagonized by rapamycin. This was replicated by the number of P20S in the vacuoles (Figures 10(b) and 10(c)). When counting P20S-positive vacuoles or P20S in the vacuoles (Figures 10(b) and 10(c), respectively), although the general trend was similar to what is described in Figure 10(a), there was a remarkable difference concerning asparagine. In fact, the polarization of P20S within vacuoles was dramatically suppressed

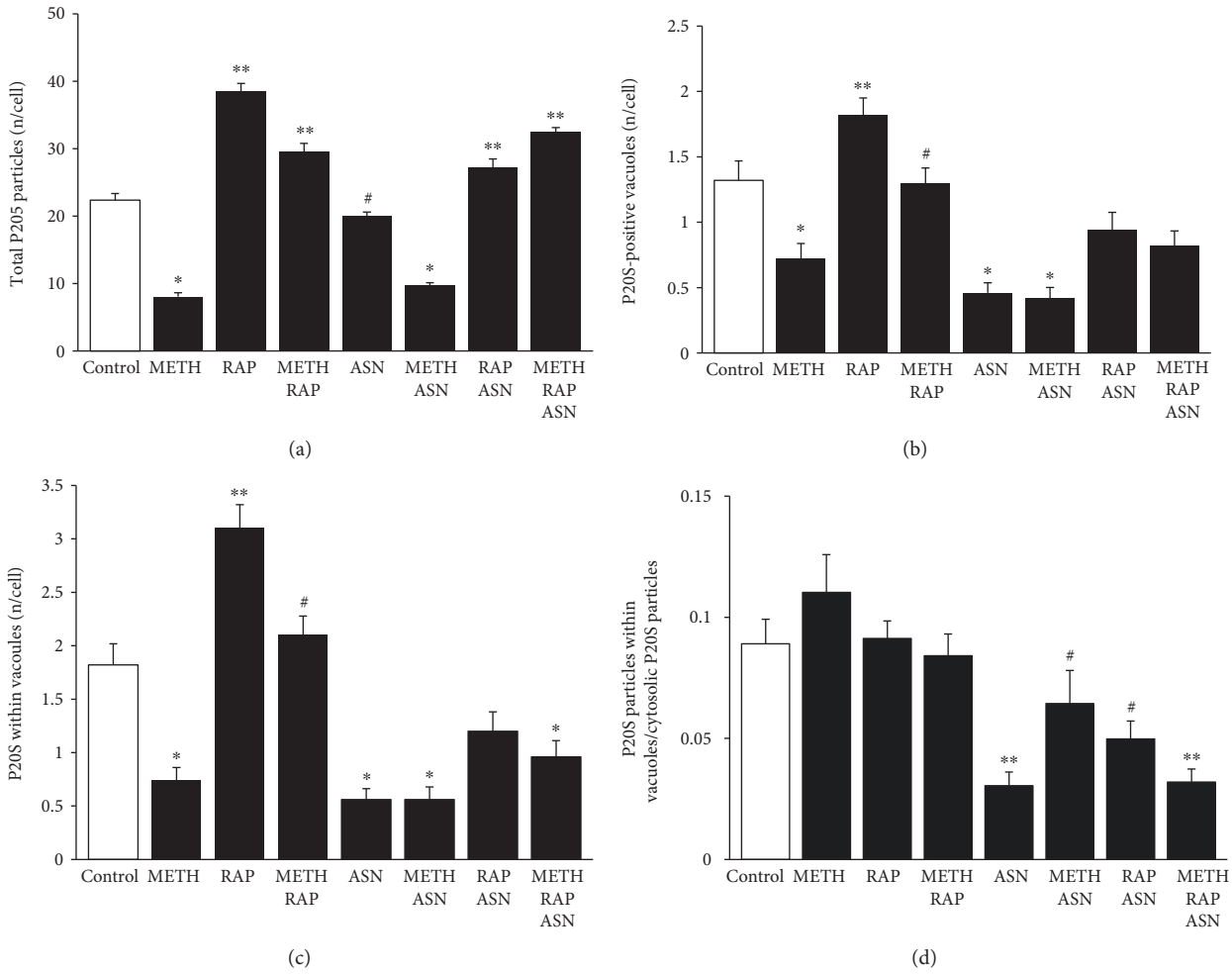

Figure 10: mTOR modulates the number and placement of P20S particles. (a) The graph shows the number of total P20S particles per cell in control, following METH 10 μM, rapamycin 100 nM, and asparagine 50 mM, at 72 h. (b) The graph shows the number of P20S-positive vacuoles per cell in control, following METH 10 μM, rapamycin 100 nM, and asparagine 50 mM, at 72 h. (c) The graph shows the number of P20S-positive vacuoles in control and following METH 10 μM, rapamycin 100 nM, and asparagine 50 mM, at 72 h. (d) The graph shows the ratio between the number of P20S particles within vacuoles and cytosolic P20S particles. Values are given as the mean number of P20S particles and vacuoles counted in 50 cells per group. Error bars represent the standard error of the mean. $^{*}p \leq 0.05$ vs. control; $^{**}p \leq 0.05$ vs. control and METH; $^{\#}p \leq 0.05$ vs. METH. ASN = asparagine; RAP = rapamycin.

by this mTOR activator even when compared with METH. Moreover, the effects of asparagine on the dispersion of P20S was so powerful that even rapamycin was not able to prevent it (Figure 10(d)).

3.10. Correlation between Autophagoproteasomes and Cell Death. The effects of all these treatments on the amount of APPs versus the occurrence of cell death were plotted in the graph of Figure 11, which remarks for various mTOR modulators and a powerful negative correlation between the number of APPs and the number of dead cells.

In conclusions, the negative correlation which was described for APP and cell death in controls and following a 10 μM dose of METH (Figure 6) was strengthened by the analysis carried out with mTOR modulators (Figure 8). This final plotting shows, at one glance, how mTOR inhibition is key for producing the merging between proteasome and autophagy to build autophagoproteasome, while it is compatible with a strong neuroprotective role exerted by such a merging organelle.

4. Concluding Remarks

METH administration is known to increase the number of ATG vacuoles within catecholamine-containing cells. This was originally published by Cubells et al. [22], and at first, it was suggested to produce ATG-mediated cell damage [22].

Nonetheless, in 2008, we demonstrated that the inhibition of ATG in METH-treated catecholamine cells instead of producing neuroprotection worsened METH neurotoxicity indicating a compensatory neuroprotection for ATG induction during METH toxicity, as confirmed by several studies [16, 37, 80, 100–102].

In line with this, in the present manuscript, we demonstrate that rapamycin administration fully rescues

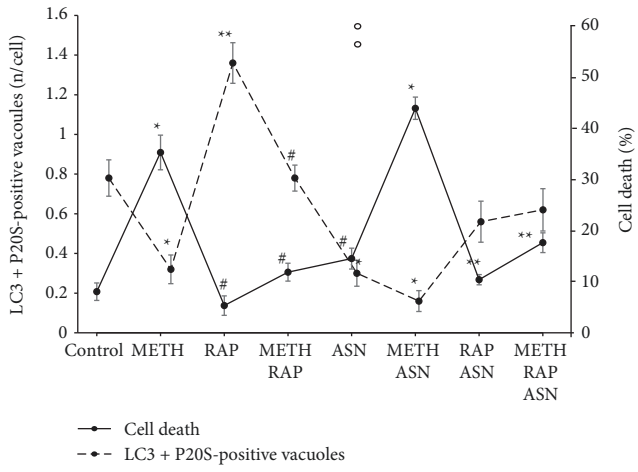

Figure 11: Inverse correlation between cell death and amount of APPs following mTOR modulation. The dashed line shows the amount of APPs while the continuous line shows the percentage of cell death. For each treatment, the values of the two lines produce a mirror image, which indicates a negative correlation. $^{*}p \leq 0.05$ vs. control; $^{**}p \leq 0.05$ vs. control and METH; $^{\#}p \leq 0.05$ vs. METH. ASN = asparagine; RAP = rapamycin.

METH-induced cell death. In the present paper, apart from strengthening the concept that mTOR inhibition and ATG protect against METH toxicity, we further detail the significance of specific ATG-related structures.

It is believed that METH-induced increase in LC3 immunofluorescence is produced by an increase in LC3-positive stagnant ATG vacuoles with an impairment of the autophagy flux [37]. However, in the present study, we demonstrate that, under METH administration, there is a loss of compartmentalization of LC3 particles within vacuoles. In fact, LC3 particles increase more in the cytosol than within vacuoles, which represents a novel insight in ATG and METH toxicity.

This leads to reconsider the significance of densely fluorescent LC3 spots detected at confocal microscopy following METH, since the greatest contribution is provided by free cytosolic LC3.

In these experimental conditions, the effects of rapamycin are demonstrated to be neuroprotective against cell death while reinstating vacuolar compartmentalization of both LC3 and P20S.

It is likely that a concomitant acceleration of activity within stagnant ATG vacuoles may concur to provide neuroprotection. In fact, asparagine, which also impairs the merge between autophagosomes and lysosomes, produces a dramatic effect.

In these experimental conditions, the occurrence of ATG vacuoles is further dissected for the concomitant presence of the P20S proteasome component. It is now well established that these LC3 + P20S vacuoles contain both ATG and proteasome markers and are named "autophagoproteasomes" (APPs) [48].

In the present study, we demonstrate that LC3 + P20S-positive vacuoles (APP) represents a clearing compartment which behaves distinctly and sometimes opposite to classic ATG (LC3-positive) compartment. This specific compartment correlates with cell survival. In line with this, alpha-synuclein, which is known to buffer oxidative species [103, 104], is involved in METH toxicity, since in alpha-synuclein knockout mice, a potentiation of METH-induced nigrostriatal damage occurs [105]. The coimmunoprecipitation of alpha-synuclein within APPs found here corroborates such a neuroprotective effect. This novel organelle may counteract also impaired mitophagy during METH administration. In fact, few key steps in mitochondrial removal are carried out by proteasome components acting during early autophagosome formation [39, 106, 107].

As a proof of principle, we cannot be satisfied yet, since one might argue that a defect in ATG progression may lead ATG vacuoles not to be able to take up the proteasome component due to a failure in the p62-driven uptake of ubiquitinated proteasomes. When such an alternative explanation is consistent, then an increased amount of P20S should be measured in the cytosol. However, the number of P20S in the cytosol was decreased by METH administration, and it was further suppressed by the concomitant administration of asparagine.

Again, if the decreased amount of UP within ATG vacuoles were related to a decrease of ATG progression (impaired shuttling of P20S within ATG vacuoles), the ratio between cytosolic *vs.* vacuolar P20S should be modified by METH, while this ratio stays steady.

Data Availability

The data used to support the findings of this study are available from the corresponding author upon request.

Conflicts of Interest

The authors declare that there is no conflict of interest regarding the publication of this paper.

Authors' Contributions

Gloria Lazzeri and Francesca Biagioni equally contributed to the present manuscript.

Acknowledgments

We are grateful to Dr. Marina Flaibani for the precious technical support. This work was supported by Ricerca Corrente 2018 (Ministero della Salute).

Supplementary Materials

Supplementary Figures 1, 2, and 3: further evidence about various METH-induced ultrastructural alterations. In all these graphs, the dose of METH was kept constant 10 μM. Supplementary Figure 1: the time dependency of METH-induced variations in LC3 and P20S particles (12 h, 24 h, and 72 h). Counts refer to whole cytosol or selectively within vacuoles. Moreover, the ratio between compartmentalized particles within vacuoles and total cytosolic particles at these

time intervals is reported. Supplementary Figure 2: the time dependency of METH-induced suppression of APPs, which concerns selectively with the number of LC3 + P20S-positive vacuoles (autophagoproteasomes) in the whole cytosol. Supplementary Figure 3: the number of unstained vacuoles in the whole cytosol following various single and combined treatments with mTOR modulators. *(Supplementary Materials)*

References

[1] N. D. Volkow, L. Chang, G. J. Wang et al., "Association of dopamine transporter reduction with psychomotor impairment in methamphetamine abusers," *American Journal of Psychiatry*, vol. 158, no. 3, pp. 377–382, 2001.

[2] D. E. Rusyniak, "Neurologic manifestations of chronic methamphetamine abuse," *Neurologic Clinics*, vol. 29, no. 3, pp. 641–655, 2011.

[3] G. C. Wagner, G. A. Ricaurte, L. S. Seiden, C. R. Schuster, R. J. Miller, and J. Westley, "Long-lasting depletions of striatal dopamine and loss of dopamine uptake sites following repeated administration of methamphetamine," *Brain Research*, vol. 181, no. 1, pp. 151–160, 1980.

[4] G. A. Ricaurte, R. W. Guillery, and L. S. Seiden, "Dopamine nerve terminal degeneration produced by high doses of methylamphetamine in the rat brain," *Brain Research*, vol. 235, no. 1, pp. 93–103, 1982.

[5] J. M. Wilson, K. S. Kalasinsky, A. I. Levey et al., "Striatal dopamine nerve terminal markers in human, chronic methamphetamine users," *Nature Medicine*, vol. 2, no. 6, pp. 699–703, 1996.

[6] F. Fornai, P. Lenzi, M. Gesi et al., "Methamphetamine produces neuronal inclusions in the nigrostriatal system and in PC12 cells," *Journal of Neurochemistry*, vol. 88, no. 1, pp. 114–123, 2004.

[7] B. Liu and D. E. Dluzen, "Effect of estrogen upon methamphetamine-induced neurotoxicity within the impaired nigrostriatal dopaminergic system," *Synapse*, vol. 60, no. 5, pp. 354–361, 2006.

[8] S. Ares-Santos, N. Granado, I. Espadas, R. Martinez-Murillo, and R. Moratalla, "Methamphetamine causes degeneration of dopamine cell bodies and terminals of the nigrostriatal pathway evidenced by silver staining," *Neuropsychopharmacology*, vol. 39, no. 5, pp. 1066–1080, 2014.

[9] S. Ares-Santos, N. Granado, I. Oliva et al., "Dopamine D(1) receptor deletion strongly reduces neurotoxic effects of methamphetamine," *Neurobiology of Disease*, vol. 45, no. 2, pp. 810–820, 2012.

[10] N. Granado, S. Ares-Santos, E. O'Shea, C. Vicario-Abejón, M. I. Colado, and R. Moratalla, "Selective vulnerability in striosomes and in the nigrostriatal dopaminergic pathway after methamphetamine administration: early loss of TH in striosomes after methamphetamine," *Neurotoxicity Research*, vol. 18, no. 1, pp. 48–58, 2010.

[11] N. Granado, S. Ares-Santos, and R. Moratalla, "D1 but not D4 dopamine receptors are critical for MDMA-induced neurotoxicity in mice," *Neurotoxicity Research*, vol. 25, no. 1, pp. 100–109, 2014.

[12] N. Granado, S. Ares-Santos, Y. Tizabi, and R. Moratalla, "Striatal reinnervation process after acute methamphetamine-induced dopaminergic degeneration in mice," *Neurotoxicity Research*, vol. 34, no. 3, pp. 627–639, 2018.

[13] F. Fornai, P. Lenzi, M. Gesi et al., "Similarities between methamphetamine toxicity and proteasome inhibition," *Annals of the New York Academy of Sciences*, vol. 1025, no. 1, pp. 162–170, 2004.

[14] F. Fornai, G. Lazzeri, A. Bandettini Di Poggio et al., "Convergent roles of α-synuclein, DA metabolism, and the ubiquitin-proteasome system in nigrostriatal toxicity," *Annals of the New York Academy of Sciences*, vol. 1074, no. 1, pp. 84–89, 2006.

[15] G. Lazzeri, P. Lenzi, C. L. Busceti et al., "Mechanisms involved in the formation of dopamine-induced intracellular bodies within striatal neurons," *Journal of Neurochemistry*, vol. 101, no. 5, pp. 1414–1427, 2007.

[16] M. Lin, P. Chandramani-Shivalingappa, H. Jin et al., "Methamphetamine-induced neurotoxicity linked to ubiquitin-proteasome system dysfunction and autophagy-related changes that can be modulated by protein kinase C delta in dopaminergic neuronal cells," *Neuroscience*, vol. 210, pp. 308–332, 2012.

[17] L. Quan, T. Ishikawa, T. Michiue et al., "Ubiquitin-immunoreactive structures in the midbrain of methamphetamine abusers," *Legal Medicine*, vol. 7, no. 3, pp. 144–150, 2005.

[18] P. K. Sonsalla, J. W. Gibb, and G. R. Hanson, "Roles of D1 and D2 dopamine receptor subtypes in mediating the methamphetamine-induced changes in monoamine systems," *Journal of Pharmacology and Experimental Therapeutics*, vol. 238, no. 3, pp. 932–937, 1986.

[19] J. W. Gibb, M. Johnson, and G. R. Hanson, "Neurochemical basis of neurotoxicity," *Neurotoxicology*, vol. 11, no. 2, pp. 317–321, 1990.

[20] D. Sulzer and S. Rayport, "Amphetamine and other psychostimulants reduce pH gradients in midbrain dopaminergic neurons and chromaffin granules: a mechanism of action," *Neuron*, vol. 5, no. 6, pp. 797–808, 1990.

[21] D. Sulzer, E. Pothos, H. M. Sung, N. T. Maidment, B. G. Hoebel, and S. Rayport, "Weak base model of amphetamine action," *Annals of the New York Academy of Sciences*, vol. 654, no. 1, pp. 525–528, 1992.

[22] J. F. Cubells, S. Rayport, G. Rajendran, and D. Sulzer, "Methamphetamine neurotoxicity involves vacuolation of endocytic organelles and dopamine-dependent intracellular oxidative stress," *Journal of Neuroscience*, vol. 14, no. 4, pp. 2260–2271, 1994.

[23] O. Suzuki, H. Hattori, M. Asano, M. Oya, and Y. Katsumata, "Inhibition of monoamine oxidase by *d*-methamphetamine," *Biochemical Pharmacolgy*, vol. 29, no. 14, pp. 2071–2073, 1980.

[24] F. Fornai, K. Chen, F. S. Giorgi, M. Gesi, M. G. Alessandri, and J. C. Shih, "Striatal dopamine metabolism in monoamine oxidase B-deficient mice: a brain dialysis study," *Journal of Neurochemistry*, vol. 73, no. 6, pp. 2434–2440, 1999.

[25] C. J. Schmidt and J. W. Gibb, "Role of the dopamine uptake carrier in the neurochemical response to methamphetamine: effects of amfonelic acid," *European Journal of Pharmacology*, vol. 109, no. 1, pp. 73–80, 1985.

[26] R. Moratalla, A. Khairnar, N. Simola et al., "Amphetamine-related drugs neurotoxicity in humans and in experimental animals: main mechanisms," *Progress in Neurobiology*, vol. 155, pp. 149–170, 2017.

[27] J. L. Cadet, S. Ali, and C. Epstein, "Involvement of oxygen-based radicals in methamphetamine-induced neurotoxicity:

evidence from the use of CuZnSOD transgenic mice," *Annals of the New York Academy of Sciences*, vol. 738, no. 1, pp. 388–391, 2006.

[28] J. P. Spencer, M. Whiteman, P. Jenner, and B. Halliwell, "5-s-Cysteinyl-conjugates of catecholamines induce cell damage, extensive DNA base modification and increases in caspase-3 activity in neurons," *Journal of Neurochemistry*, vol. 81, no. 1, pp. 122–129, 2002.

[29] N. Granado, I. Lastres-Becker, S. Ares-Santos et al., "Nrf2 deficiency potentiates methamphetamine-induced dopaminergic axonal damage and gliosis in the striatum," *Glia*, vol. 59, no. 12, pp. 1850–1863, 2011.

[30] L. Mendieta, N. Granado, J. Aguilera, Y. Tizabi, and R. Moratalla, "Fragment C domain of tetanus toxin mitigates methamphetamine neurotoxicity and its motor consequences in mice," *International Journal of Neuropsychopharmacology*, vol. 19, no. 8, article pyw021, 2016.

[31] M. J. LaVoie and T. G. Hastings, "Dopamine quinone formation and protein modification associated with the striatal neurotoxicity of methamphetamine: evidence against a role for extracellular dopamine," *The Journal of Neuroscience*, vol. 19, no. 4, pp. 1484–1491, 1999.

[32] F. Fornai, P. Longone, M. Ferrucci et al., "Autophagy and amyotrophic lateral sclerosis: the multiple roles of lithium," *Autophagy*, vol. 4, no. 4, pp. 527–530, 2008.

[33] M. Ferrucci, L. Ryskalin, F. Biagioni et al., "Methamphetamine increases prion protein and induces dopamine-dependent expression of protease resistant PrPsc," *Archives Italiennes de Biologie*, vol. 155, no. 1-2, pp. 81–97, 2017.

[34] A. Moszczynska and B. K. Yamamoto, "Methamphetamine oxidatively damages parkin and decreases the activity of 26S proteasome in vivo," *Journal of Neurochemistry*, vol. 116, no. 6, pp. 1005–1017, 2011.

[35] J. M. Brown, M. S. Quinton, and B. K. Yamamoto, "Methamphetamine-induced inhibition of mitochondrial complex II: roles of glutamate and peroxynitrite," *Journal of Neurochemistry*, vol. 95, no. 2, pp. 429–436, 2005.

[36] D. J. Barbosa, J. P. Capela, R. Feio-Azevedo, A. Teixeira-Gomes, M. L. Bastos, and F. Carvalho, "Mitochondria: key players in the neurotoxic effects of amphetamines," *Archives of Toxicology*, vol. 89, no. 10, pp. 1695–1725, 2015.

[37] R. Castino, G. Lazzeri, P. Lenzi et al., "Suppression of autophagy precipitates neuronal cell death following low doses of methamphetamine," *Journal of Neurochemistry*, vol. 106, no. 3, pp. 1426–1439, 2008.

[38] G. Beauvais, K. Atwell, S. Jayanthi, B. Ladenheim, and J. L. Cadet, "Involvement of dopamine receptors in binge methamphetamine-induced activation of endoplasmic reticulum and mitochondrial stress pathways," *PLoS One*, vol. 6, no. 12, article e28946, 2011.

[39] P. Lenzi, R. Marongiu, A. Falleni et al., "A subcellular analysis of genetic modulation of PINK1 on mitochondrial alterations, autophagy and cell death," *Archives Italiennes de Biologie*, vol. 150, no. 2-3, pp. 194–217, 2012.

[40] B. K. Yamamoto and W. Zhu, "The effects of methamphetamine on the production of free radicals and oxidative stress," *The Journal of Pharmacology and Experimental Therapy*, vol. 287, no. 1, pp. 107–114, 1998.

[41] P. S. Fitzmaurice, J. Tong, M. Yazdanpanah, P. P. Liu, K. S. Kalasinsky, and S. J. Kish, "Levels of 4-hydroxynonenal and malondialdehyde are increased in brain of human chronic users of methamphetamine," *The Journal of Pharmacology and Experimental Therapy*, vol. 319, no. 2, pp. 703–709, 2006.

[42] F. Fornai, P. Lenzi, M. Gesi et al., "Fine structure and biochemical mechanisms underlying nigrostriatal inclusions and cell death after proteasome inhibition," *Journal of Neuroscience*, vol. 23, no. 26, pp. 8955–8966, 2003.

[43] G. Lazzeri, P. Lenzi, M. Gesi et al., "In PC12 cells neurotoxicity induced by methamphetamine is related to proteasome inhibition," *Annals of the New York Academy of Sciences*, vol. 1074, no. 1, pp. 174–177, 2006.

[44] K. E. Larsen, E. A. Fon, T. G. Hastings, R. H. Edwards, and D. Sulzer, "Methamphetamine-induced degeneration of dopaminergic neurons involves autophagy and upregulation of dopamine synthesis," *Journal of Neurochemistry*, vol. 22, no. 20, pp. 8951–8960, 2002.

[45] D. Weinshenker, M. Ferrucci, C. L. Busceti et al., "Genetic or pharmacological blockade of noradrenaline synthesis enhances the neurochemical, behavioral, and neurotoxic effects of methamphetamine," *Journal of Neurochemistry*, vol. 105, no. 2, pp. 471–483, 2008.

[46] X. L. Xie, J. T. He, Z. T. Wang et al., "Lactulose attenuates METH-induced neurotoxicity by alleviating the impaired autophagy, stabilizing the perturbed antioxidant system and suppressing apoptosis in rat striatum," *Toxicology Letters*, vol. 289, pp. 107–113, 2018.

[47] P. Lenzi, G. Lazzeri, F. Biagioni et al., "The autophagoproteasome a novel cell clearing organelle in baseline and stimulated conditions," *Frontiers in Neuroanatomy*, vol. 10, p. 78, 2016.

[48] D. J. Klionsky, K. Abdelmohsen, A. Abe et al., "Guidelines for the use and interpretation of assays for monitoring autophagy (3rd edition)," *Autophagy*, vol. 12, no. 1, pp. 1–222, 2016.

[49] F. Fornai, P. Lenzi, G. Lazzeri et al., "Fine ultrastructure and biochemistry of PC12 cells: a comparative approach to understand neurotoxicity," *Brain Research*, vol. 1129, no. 1, pp. 174–190, 2007.

[50] W. P. Melega, A. K. Cho, D. Harvey, and G. Laćan, "Methamphetamine blood concentrations in human abusers: application to pharmacokinetic modelling," *Synapse*, vol. 61, no. 4, pp. 216–220, 2007.

[51] Z. Wang, X. Shi, Y. Li et al., "Blocking autophagy enhanced cytotoxicity induced by recombinant human arginase in triple-negative breast cancer cells," *Cell Death & Disease*, vol. 5, no. 12, article e1563, 2014.

[52] Y. Chen, L. Hong, Y. Zeng, Y. Shen, and Q. Zeng, "Power frequency magnetic fields induced reactive oxygen species-related autophagy in mouse embryonic fibroblasts," *The International Journal of Biochemistry & Cell Biology*, vol. 57, pp. 108–114, 2014.

[53] A. Pla, M. Pascual, J. Renau-Piqueras, and C. Guerri, "TLR4 mediates the impairment of ubiquitin-proteasome and autophagy-lysosome pathways induced by ethanol treatment in brain," *Cell Death & Disease*, vol. 5, no. 2, article e1066, 2014.

[54] K. Porter, J. Nallathambi, Y. Lin, and P. B. Liton, "Lysosomal basification and decreased autophagic flux in oxidatively stressed trabecular meshwork cells: implications for glaucoma pathogenesis," *Autophagy*, vol. 9, no. 4, pp. 581–594, 2013.

[55] D. J. Klionsky and S. D. Emr, "Autophagy as a regulated pathway of cellular degradation," *Science*, vol. 290, no. 5497, pp. 1717–1721, 2000.

[56] A. Kuma, M. Hatano, M. Matsui et al., "The role of autophagy during the early neonatal starvation period," *Nature*, vol. 432, no. 7020, pp. 1032–1036, 2004.

[57] D. J. Klionsky, J. M. Cregg, W. A. Dunn Jr. et al., "A unified nomenclature for yeast autophagy-related genes," *Developmental Cell*, vol. 5, no. 4, pp. 539–545, 2003.

[58] G. J. Stout, E. C. Stigter, P. B. Essers et al., "Insulin/IGF-1-mediated longevity is marked by reduced protein metabolism," *Molecular Systems Biology, vo.*, vol. 9, no. 1, p. 679, 2013.

[59] D. Vilchez, I. Morantte, Z. Liu et al., "RPN-6 determines *C. elegans* longevity under proteotoxic stress conditions," *Nature*, vol. 489, no. 7415, pp. 263–268, 2012.

[60] K. B. Hendil, P. Kristensen, and W. Uerkvitz, "Human proteasomes analysed with monoclonal antibodies," *Biochemical Journal*, vol. 305, no. 1, pp. 245–252, 1995.

[61] M. Kovarik, T. Muthny, L. Sispera, and M. Holecek, "Effects of β-hydroxy-β-methylbutyrate treatment in different types of skeletal muscle of intact and septic rats," *Journal of Physiology and Biochemistry*, vol. 66, no. 4, pp. 311–319, 2010.

[62] E. Jo, J. McLaurin, C. M. Yip, P. St. George-Hyslop, and P. E. Fraser, "α-Synuclein membrane interactions and lipid specificity," *Journal of Biological Chemistry*, vol. 275, no. 44, pp. 34328–34334, 2000.

[63] Y. Liu, L. Fallon, H. A. Lashuel, Z. Liu, and P. T. Lansbury Jr, "The UCH-L1 gene encodes two opposing enzymatic activities that affect alpha-synuclein degradation and Parkinson's disease susceptibility," *Cell*, vol. 111, no. 2, pp. 209–218, 2002.

[64] L. Maroteaux, J. T. Campanelli, and R. H. Scheller, "Synuclein: a neuron-specific protein localized to the nucleus and presynaptic nerve terminal," *Journal of Neuroscience*, vol. 8, no. 8, pp. 2804–2815, 1988.

[65] N. Ostrerova-Golts, L. Petrucelli, J. Hardy, J. M. Lee, M. Farer, and B. Wolozin, "The A53T alpha-synuclein mutation increases iron-dependent aggregation and toxicity," *Journal of Neuroscience*, vol. 20, no. 16, pp. 6048–6054, 2000.

[66] H. van der Putten, K. H. Wiederhold, A. Probst et al., "Neuropathology in mice expressing human alpha-synuclein," *Journal of Neuroscience*, vol. 20, no. 16, pp. 6021–6029, 2000.

[67] F. Bartolome, M. de la Cueva, C. Pascual et al., "Amyloid β-induced impairments on mitochondrial dynamics, hippocampal neurogenesis, and memory are restored by phosphodiesterase 7 inhibition," *Alzheimer's Research and Therapy*, vol. 10, no. 1, p. 24, 2018.

[68] R. Flores-Costa, J. Alcaraz-Quiles, E. Titos et al., "The soluble guanylate cyclase stimulator IW-1973 prevents inflammation and fibrosis in experimental non-alcoholic steatohepatitis," *British Journal of Pharmacology*, vol. 175, no. 6, pp. 953–967, 2018.

[69] P. Wang, L. Jiang, N. Zhou et al., "Resveratrol ameliorates autophagic flux to promote functional recovery in rats after spinal cord injury," *Oncotarget*, vol. 9, no. 9, pp. 8427–8440, 2018.

[70] D. Sun, W. Wang, X. Wang et al., "bFGF plays a neuroprotective role by suppressing excessive autophagy and apoptosis after transient global cerebral ischemia in rats," *Cell Death & Disease*, vol. 9, no. 2, p. 172, 2018.

[71] A. Du, S. Huang, X. Zhao et al., "Suppression of CHRN endocytosis by carbonic anhydrase CAR3 in the pathogenesis of myasthenia gravis," *Autophagy*, vol. 13, no. 11, pp. 1981–1994, 2017.

[72] N. Pullen and G. Thomas, "The modular phosphorylation and activation of p70s6k," *FEBS Letters*, vol. 410, no. 1, pp. 78–82, 1997.

[73] D. R. Alessi, M. T. Kozlowski, Q. P. Weng, N. Morrice, and J. Avruch, "3-Phosphoinositide-dependent protein kinase 1 (PDK1) phosphorylates and activates the p70 S6 kinase in vivo and in vitro," *Current Biology*, vol. 8, no. 2, pp. 69–81, 1998.

[74] R. D. Polakiewicz, S. M. Schieferl, A. C. Gingras, N. Sonenberg, and M. J. Comb, "μ-Opioid receptor activates signaling pathways implicated in cell survival and translational control," *Journal of Biological Chemistry*, vol. 273, no. 36, pp. 23534–23541, 1998.

[75] D. C. Finger, S. Salama, C. Tsou, E. Harlow, and J. Blenis, "Mammalian cell size is controlled by mTOR and its downstream targets S6K1 and 4EBP1/eIF4E," *Genes & Development*, vol. 16, no. 12, pp. 1472–1487, 2002.

[76] M. Saitoh, N. Pullen, P. Brennan, D. Cantrell, P. B. Dennis, and G. Thomas, "Regulation of an activated S6 kinase 1 variant reveals a novel mammalian target of rapamycin phosphorylation site," *Journal of Biological Chemistry*, vol. 277, no. 22, pp. 20104–20112, 2002.

[77] M. Bendayan and M. Zollinger, "Ultrastructural localization of antigenic sites on osmium-fixed tissues applying the protein A-gold technique," *The Journal of Histochemistry & Cytochemistry*, vol. 31, no. 1, pp. 101–109, 1983.

[78] D. D'Alessandro, L. Mattii, S. Moscato et al., "Immunohistochemical demonstration of the small GTPase RhoAA on epoxy-resin embedded sections," *Micron*, vol. 35, no. 4, pp. 287–296, 2004.

[79] J. M. Lucocq, A. Habermann, S. Watt, J. M. Backer, T. M. Mayhew, and G. Griffiths, "A rapid method for assessing the distribution of gold labeling on thin sections," *Journal of Histochemistry & Cytochemistry*, vol. 52, no. 8, pp. 991–1000, 2004.

[80] J. Ma, J. Wan, J. Meng, S. Banerjee, S. Ramakrishnan, and S. Roy, "Methamphetamine induces autophagy as a pro-survival response against apoptotic endothelial cell death through the Kappa opioid receptor," *Cell Death & Disease*, vol. 5, no. 3, article e1099, 2014.

[81] G. V. Rinetti and F. E. Schweizer, "Ubiquitination acutely regulates presynaptic neurotransmitter release in mammalian neurons," *Journal of Neuroscience*, vol. 30, no. 9, pp. 3157–3166, 2010.

[82] C. Wentzel, I. Delvendahl, S. Sydlik, O. Georgiev, and M. Müller, "Dysbindin links presynaptic proteasome function to homeostatic recruitment of low release probability vesicles," *Nature Communications*, vol. 9, no. 1, p. 267, 2018.

[83] J. Konieczny, T. Lenda, and A. Czarnecka, "Early increase in dopamine release in the ipsilateral striatum after unilateral intranigral administration of lactacystin produces spontaneous contralateral rotations in rats," *Neuroscience*, vol. 324, pp. 92–106, 2016.

[84] P. Barroso-Chinea, M. L. Thiolat, S. Bido et al., "D1 dopamine receptor stimulation impairs striatal proteasome activity in parkinsonism through 26S proteasome disassembly," *Neurobiology of Disease*, vol. 78, pp. 77–87, 2015.

[85] N. Ueda, T. Tomita, K. Yanagisawa, and N. Kimura, "Retromer and Rab2-dependent trafficking mediate PS1 degradation by proteasomes in endocytic disturbance," *Journal of Neurochemistry*, vol. 137, no. 4, pp. 647–658, 2016.

[86] V. Cohen-Kaplan, A. Ciechanover, and I. Livneh, "p62 at the crossroad of the ubiquitin-proteasome system and autophagy," *Oncotarget*, vol. 7, no. 51, pp. 83833-83834, 2016.

[87] S. Engelender, "α-Synuclein fate: proteasome or autophagy?," *Autophagy*, vol. 8, no. 3, pp. 418–420, 2012.

[88] M. Xilouri, O. R. Brekk, and L. Stefanis, "α-Synuclein and protein degradation systems: a reciprocal relationship," *Molecular Neurobiology*, vol. 47, no. 2, pp. 537–551, 2013.

[89] J. L. Webb, B. Ravikumar, J. Atkins, J. N. Skepper, and D. C. Rubinsztein, "Alpha-synuclein is degraded by both autophagy and the proteasome," *Journal of Biological Chemistry*, vol. 278, no. 27, pp. 25009–25013, 2003.

[90] M. Ferrucci, L. Pasquali, S. Ruggieri, A. Paparelli, and F. Fornai, "Alpha-synuclein and autophagy as common steps in neurodegeneration," *Parkinsonism & Related Disorders*, vol. 14, Supplement 2, pp. S180–S184, 2008.

[91] F. Yang, Y. P. Yang, C. J. Mao et al., "Crosstalk between the proteasome system and autophagy in the clearance of α-synuclein," *Acta Pharmacologica Sinica*, vol. 34, no. 5, pp. 674–680, 2013.

[92] A. S. Krall, S. Xu, T. G. Graeber, D. Braas, and H. R. Christofk, "Asparagine promotes cancer cell proliferation through use as an amino acid exchange factor," *Nature Communications*, vol. 7, article 11457, 2016.

[93] R. Loewith, E. Jacinto, S. Wullschleger et al., "Two TOR complexes, only one of which is rapamycin sensitive, have distinct roles in cell growth control," *Molecular Cell*, vol. 10, no. 3, article 10.1016/s1097-2765(02)00636-6, pp. 457–468, 2002.

[94] Y. Li, Z. Hu, B. Chen et al., "Taurine attenuates methamphetamine-induced autophagy and apoptosis in PC12 cells through mTOR signaling pathway," *Toxicology Letters*, vol. 215, no. 1, pp. 1–7, 2012.

[95] J. Wu, D. Zhu, J. Zhang, G. Li, Z. Liu, and J. Sun, "Lithium protects against methamphetamine-induced neurotoxicity in PC12 cells via Akt/GSK3β/mTOR pathway," *Biochemical and Biophysical Research Communication*, vol. 465, no. 3, pp. 368–373, 2015.

[96] P. Kongsuphol, S. Mukda, C. Nopparat, A. Villarroel, and P. Govitrapong, "Melatonin attenuates methamphetamine-induced deactivation of the mammalian target of rapamycin signaling to induce autophagy in SK-N-SH cells," *Journal of Pineal Research*, vol. 46, no. 2, pp. 199–206, 2008.

[97] S. H. Huang, W. R. Wu, L. M. Lee, P. R. Huang, and J. C. Chen, "mTOR signaling in the nucleus accumbens mediates behavioral sensitization to methamphetamine," *Progress in Neuro-Psychopharmacology & Biological Psychiatry*, vol. 86, pp. 331–339, 2018.

[98] F. Fornai, P. Lenzi, L. Capobianco et al., "Involvement of dopamine receptors and beta-arrestin in metamphetamine-induced inclusions formation in PC12 cells," *Journal of Neurochemistry*, vol. 105, no. 5, pp. 1939–1947, 2008.

[99] D. Wang, X. Ji, J. Liu, Z. Li, and X. Zhang, "Dopamine receptor subtypes differentially regulate autophagy," *International Journal of Molecular Sciences*, vol. 19, no. 5, p. 1540, 2018.

[100] R. Pitaksalee, Y. Sanvarida, T. Sinchai et al., "Autophagy inhibition by caffeine increases toxicity of methamphetamine in SH-SY5Y neuroblastoma cell line," *Neurotoxicity Research*, vol. 27, no. 4, pp. 421–429, 2015.

[101] L. Cao, M. Fu, S. Kumar, and A. Kumar, "Methamphetamine potentiates HIV-1 gp120-mediated autophagy via Beclin-1 and Atg5/7 as a pro-survival response in astrocytes," *Cell Death & Disease*, vol. 7, no. 10, article e2425, 2016.

[102] C. Zhao, Y. Mei, X. Chen et al., "Autophagy plays a pro-survival role against methamphetamine-induced apoptosis in H9C2 cells," *Toxicology Letters*, vol. 294, pp. 156–165, 2018.

[103] S. Chandra, G. Gallardo, R. Fernández-Chacón, O. M. Schlüter, and T. C. Südhof, "α-synuclein cooperates with CSPα in preventing neurodegeneration," *Cell*, vol. 123, no. 3, pp. 383–396, 2005.

[104] Y. Machida, T. Chiba, A. Takayanagi et al., "Common anti-apoptotic roles of parkin and α-synuclein in human dopaminergic cells," *Biochemical and Biophysical Research Communications*, vol. 332, no. 1, pp. 233–240, 2005.

[105] O. M. Schlüter, F. Fornai, M. G. Alessandrí et al., "Role of alpha-synuclein in 1-methyl-4-phenyl-1,2,3,6-tetrahydropyridine-induced parkinsonism in mice," *Neuroscience*, vol. 118, no. 4, pp. 985–1002, 2003.

[106] W. H. Song, Y. J. Yia, M. Sutovskya, S. Meyers, and P. Sutovsky, "Autophagy and ubiquitin–proteasome system contribute to sperm mitophagy after mammalian fertilization," *Proceedings of the National Academy of Sciences of the United States of America*, vol. 113, no. 36, pp. E5261–E5270, 2016.

[107] S. Akabane, K. Matsuzaki, S. Yamashita et al., "Constitutive activation of PINK1 protein leads to proteasome-mediated and non-apoptotic cell death independently of mitochondrial autophagy," *The Journal of Biological Chemistry*, vol. 291, no. 31, pp. 16162–16174, 2016.

Hindawi
Oxidative Medicine and Cellular Longevity
Volume 2018, Article ID 3467531, 14 pages
https://doi.org/10.1155/2018/3467531

Research Article

Repeated Cycles of Binge-Like Ethanol Intake in Adolescent Female Rats Induce Motor Function Impairment and Oxidative Damage in Motor Cortex and Liver, but Not in Blood

Luanna Melo Pereira Fernandes,[1] Klaylton Sousa Lopes,[1] Luana Nazaré Silva Santana,[1] Enéas Andrade Fontes-Júnior,[1] Carolina Heitmann Mares Azevedo Ribeiro,[2] Márcia Cristina Freitas Silva,[3] Ricardo Sousa de Oliveira Paraense,[4] Maria Elena Crespo-López,[4] Antônio Rafael Quadros Gomes,[5] Rafael Rodrigues Lima,[6] Marta Chagas Monteiro,[5] and Cristiane Socorro Ferraz Maia[1]

[1]*Laboratory of Pharmacology of Inflammation and Behavior, Faculty of Pharmacy, Institute of Health Science, Federal University of Pará, Belém, PA, Brazil*
[2]*Laboratory of Immunology, Pharmacy Faculty, Institute of Health Science, Federal University of Pará, Belém, PA, Brazil*
[3]*Laboratory of Ecotoxicology, Nucleus of Tropical Medicine, Federal University of Pará, Belém, PA, Brazil*
[4]*Laboratory of Molecular Pharmacology, Institute of Biological Sciences, Federal University of Pará, Belém PA, Brazil*
[5]*Laboratory of Microbiology and Immunology of Teaching and Research, Pharmacy Faculty, Institute of Health Science, Federal University of Pará, Belém PA, Brazil*
[6]*Laboratory of Functional and Structural Biology, Institute of Biological Sciences, Federal University of Pará, Belém, PA, Brazil*

Correspondence should be addressed to Cristiane Socorro Ferraz Maia; crismaia@ufpa.br

Received 28 April 2018; Revised 25 July 2018; Accepted 7 August 2018; Published 19 September 2018

Academic Editor: Stefania Schiavone

Moderate ethanol consumption (MEC) is increasing among women. Alcohol exposure usually starts in adolescence and tends to continue until adulthood. We aimed to investigate MEC impacts during adolescence until young adulthood of female rats. Adolescent female Wistar rats received distilled water or ethanol (3 g/kg/day), in a 3 days on-4 days off paradigm (binge drinking) for 1 and 4 consecutive weeks. We evaluate liver and brain oxidative damage, peripheral oxidative parameters by SOD, catalase, thiol contents, and MDA, and behavioral motor function by open-field, pole, beam-walking, and rotarod tests. Our results revealed that repeated episodes of binge drinking during adolescence displayed lipid peroxidation in the liver and brain. Surprisingly, such oxidative damage was not detectable on blood. Besides, harmful histological effects were observed in the liver, associated to steatosis and loss of parenchymal architecture. In addition, ethanol intake elicited motor incoordination, bradykinesia, and reduced spontaneous exploratory behavior in female rats.

1. Introduction

Ethanol is one of the oldest psychoactive substances and remains the most intoxicating drug widely used by individuals [1]. In addition to having a cultural background and being accepted in almost all organized societies [1, 2], its consumption is favored by its low cost, wide availability, and easy access [2, 3]. However, the abuse of ethanol intake is considered a public health problem with repercussions on the social environment and it causes several clinical complications [4]

that range from behavioral alterations and maladaptive long-term consequences to systemic metabolic disruption and liver failure [5].

Actually, our group has been focusing on alcohol versus adolescence versus female gender, through a heavy-drinking protocol [6–10] or a binge-drinking paradigm [11–14]. In this regard, we showed that heavy chronic EtOH intoxication (6.5 g/kg/day during 55 days) during adolescence induced neuronal loss and an expressive reduction in astrocytes in the cerebral cortex of rats [15]. In addition, the chronic EtOH administration may also potentiate the motor impairments and motor cortex damage induced by focal ischemia in female rats [8, 10].

In view of the binge-drinking paradigm, the intermittent ethanol consumption—when high ethanol dose is consumed in a short period of time followed by a period of withdrawal—is the dominant manner of alcohol misuse in adolescents and young adults [16–18]. The National Institute on Alcohol Abuse and Alcoholism (NIAAA) has recommended that this consumption pattern promotes a blood alcohol concentration level of 0.08 g/dL. Such plasmatic blood levels usually occur after the consumption of four or more drinks for women or five or more drinks for men, for a two-hour period [19]. Besides, the frequency of ethanol consumption in a binge manner among adolescents, mainly of university students, occurs 3 days a week [20]. Additionally, this ethanol consumption pattern has increased among the female gender in Brazil, especially with the younger ones [21], indicating that females have become one group that presents higher risks related to the deleterious effects of ethanol; even so, the harmful effects of ethanol among females have been poorly investigated.

In fact, there are sex differences in metabolism and response to binge-like ethanol. Some studies have reported that females display greater susceptibility to acute and long-term alterations of mood and memory after ethanol-intermittent treatment [22–24]. In addition, higher anatomical and histological alterations have been reportedly elicited by binge-drinking consumption in females than in males, which suggest that vulnerability to ethanol damage is gender dependent [25, 26]. Beyond that, oxidative balance also seems to be different between males and females. In an interesting study, Jung and Metzger [27] found an innate difference related to oxidative status displayed by ethanol exposure protocol between males and females, in which hormonal factors may contribute to the possible neuroprotector effect. However, such steroidal protection against oxidative damage was unlikely in the brain.

After ingestion, alcohol is metabolized by three pathways in the liver, that is, alcohol dehydrogenase (ADH), the microsomal ethanol oxidation system (MEOS) by induction of cytochrome P-4502E1 (CYP2E1), and catalase enzymes. These processes result in toxic and highly reactive products such as acetaldehyde and reactive oxygen species (ROS), which makes organs, such as the liver, more susceptible to alcohol-induced damage by different mechanisms that are not clear enough [28, 29]. In the brain, alcohol metabolism also shares all the mechanisms related above, generating acetaldehyde and an excess of H_2O_2, which displays oxidative damage as one of the main mechanisms of tissue injury [30, 31].

Actually, alcoholic liver disease (ALD) is among the leading causes of morbidity and mortality worldwide. Their pathophysiology includes a broad spectrum of diseases ranging from simple steatosis to more severe forms of liver injury, such as steatohepatitis, cirrhosis, and hepatocellular carcinoma [32, 33]. Of interest, among the risk factors for ALD, the pattern of alcohol consumption and female display a double risk. In women, the risk is higher due to the deficit of gastric ADH, a higher proportion of body fat, and the presence of estrogen [33].

Allied to metabolic damage, ethanol intake during adolescence has been reported as a neurotoxic drug. The main hazardous effects detected are related to its neurobehavioral alteration, in which motor function is deeply impacted [34]. However, it is still unclear if the exposure of females to ethanol in a binge-like manner causes cumulative effects on motor function from middle to late adolescence, if these effects involve oxidative stress, and how this mechanism reverberates on the motor cortex, liver, and blood. Thus, we now investigated the systemic oxidative stress effects of the binge-like ethanol paradigm and its repercussions on motor function in adolescent female rats.

2. Materials and Methods

2.1. Animals. Adolescent female *Wistar* rats ($n = 48$; $72.83 \pm 0.36\ g$) were obtained from the Animal Facility of the Federal University of Pará (UFPA) and kept in collective cages (four animals per cage). Animals were maintained in a climate-controlled room on a 12:12-h light/dark cycle (lights on 7:00 AM), with food and water *ad libitum.* All procedures were approved by the Ethics Committee on Experimental Animals of the Federal University of Pará under license number BIO-196-14 and followed the guidelines suggested by the National Institutes of Health (NIH) Guide for the Care and Use of Laboratory Animals (2011). Adolescent female rats were used because previous investigations reported that this sex appears to be more resistant to oxidative brain damage ([27], but the ethanol-induced brain injury is more evident in female than in male rodents [25]. Moreover, human female adolescents are more vulnerable than males to the adverse neurodevelopmental effects (i.e., neurotoxic effects in cerebral cortex) of heavy alcohol binge drinking [26].

2.2. Experimental Groups and Treatment. In this study, one episode of binge-like ethanol treatment was considered equivalent to a single daily intragastric administration of ethanol (3.0 g/kg/day, 20% w/v ethanol) for three consecutive days [35] to mimic the pattern occurring in human adolescents [20]. On postnatal day (PND) 35, all rats were randomly assigned to either (i) ethanol or (ii) water control groups at two different periods. One group of animals (PND 35–37) received 1 cycle of binge-like treatment (acute binge ethanol-treated adolescent rats). Other animals received 4 weeks of treatment (4 binge-like ethanol cycles), from PND 35–58, which mimics from middle to late

adolescence (for review see [36]). See Figure 1 for the timeline of the experimental design.

All animals received a single daily intragastric administration of ethanol (dose of 3.0 g/kg/day, 20% w/v ethanol) on 3 consecutive days on schedule—always between 7:00 AM and 8:00 AM [35]—and 4 consecutive days off schedule. Control subjects received comparable volumes of distilled water, according to the procedure previously described [37]. The animals' weight gain was measured prior the beginning of ethanol treatment and weekly. Moreover, the survival rate of animals was assessed throughout the entire experimental protocol period and no death was observed within repeated intermittent ethanol administration.

2.3. Behavioral Tasks. Seven and a half hours after the period of binge-like ethanol treatment, animals were conducted to the test room for acclimatization and habituation to the test environment for one hour. The behavioral tests (open-field, pole, beam-walking, and rotarod tests) were employed between 11:00 AM and 6:00 PM in a sound-attenuated room under low-intensity light (12 lux).

2.3.1. Open Field. We used an open-field apparatus to evaluate spontaneous exploratory activity to assess locomotion [38]. The rats were placed individually at the center of the open-field arena ($100 \times 100 \times 40$ cm) and were permitted to allow spontaneous locomotor activity in the apparatus for 5 min. To evaluate the horizontal and vertical locomotor activities, the total distance traveled and number of rearings were measured, as previously described [39]. The rat's activity was video monitored by a camera positioned above the arena to be analyzed off-line with the ANY-maze™ (Stoelting, USA) software by two observers blind to the treatments. The rearing parameter was manually counted.

2.3.2. Pole Test. The pole test, initially described by Ogawa et al. [40], is an experiment used to evaluate movement disorders, especially bradykinesia, characterized by an increase in latency for the execution of movements [41]. In the test, the animal is confronted with the situation of turning the body and descending from a vertical beam [38]. The equipment comprises a rough vertical beam (2×50 cm) supported on a circular platform (1 cm height; $r = 25\,cm$). The task consists of the subject's ability to turn haed down and descend to the safe platform. Briefly, animals were placed head upward on the top of the beam to perform the task in five attempts, at intervals of 60 s, in which escape latency was registered (cutoff 120 s), according to da Silva et al.'s [6] protocol. The three best scores were considered for each rat. Animals unable to conclude the task were assigned the maximum time.

2.3.3. Beam-Walking Test. The beam-walking test is used to assess motor strength and balance [42]. In fact, Carter et al. [43] suggested that this test is useful tool to motor coordination and refinement analysis. The wood apparatus consists of suspended beams (1 m) elevated 50 cm from the floor [43]. The serial beams presented 2 types of cross sections: square (28, 12, and 5 mm) and circular (28, 17, and 11 mm), both of which are linked to a secure box [38]. Initially, animals were habituated on the squared 28 mm beam for 120 s. After that, animals were submitted to each beam (from square to round) in a decreased cross-sectional area for 60 s with an interval of 60 s. Motor coordination and balance in spontaneous activity were assessed through the number of slips during the test section of each beam (adapted from [44]).

2.3.4. Rotarod. The rotarod test is widely used to assess motor coordination, balance, and ataxia [38]. Usually, it is used as a motor performance evaluation test on a rotarod apparatus (Insight®, Brazil) because it is based on measuring the ability of rodents to maintain balance on a rotating cylinder driven by a motor. The apparatus consists of a grooved metal roller (8 cm in diameter), separated into 9 cm-wide compartments elevated 16 cm. In the test training, the animals were placed on the spin axis for a period of 120 seconds at 8 rpm. After the training, the test was performed in three successive exposures of 120 seconds at 8 rpm with an intertrial interval of 60 s [6, 15]. The parameter evaluated was the latency to first fall.

2.4. Biochemical Assays

2.4.1. Samples. After behavioral assays, animals were euthanized by cervical dislocation for biochemical evaluations and histopathological note. The blood content was obtained by heart puncture and collected in tubes; concomitantly, livers and brains were removed and cooled on dry ice. Then, the motor cortex tissue was dissected from the brain and both of the tissues were frozen in liquid nitrogen. For analysis, tissue samples were thawed and resuspended in 20 mM Tris-hydrochloride (Tris-HCl) buffer, pH 7.4, at 4°C for sonic disintegration. Results were expressed as percentages of control groups. The blood, liver, and motor cortex were stored at −80°C for determination of the biochemical markers of damage. The serum was obtained by centrifugation for 10 min at 1400 ×g and stored at −80°C.

2.4.2. Biochemistry Parameter Analysis. Serum activities of aspartate and alanine aminotransferase (AST and ALT, respectively) were measured by the veterinary laboratory device Reflotron Plus (Roche Diagnostics).

2.4.3. Oxidative Biochemistry in Blood

(1) Determination of Malondialdehyde (MDA). Determination of malondialdehyde (MDA) is a method that evaluates lipid peroxidation and acts as an indicator of oxidative stress. The method is based on the reaction of MDA, among other substances, with the reaction of thiobarbituric acid reactive substances (TBARS) performed according to a previously [45] proposed method [46]. Onto each test tube, 10 nM of TBA (Sigma-Aldrich T5500) and 0.5 mL of the sample serum were added. Then, the tubes were placed in a water bath at pH 2.5 and at a high temperature (94°C × 60 min) to form the pink-coloured MDA-TBA complex. After this procedure, the samples were cooled in running water and then butyl alcohol was added to each sample to obtain the maximum extraction of MDA into the organic phase. Finally, the tubes were centrifuged at 2500 rpm for 10 minutes and

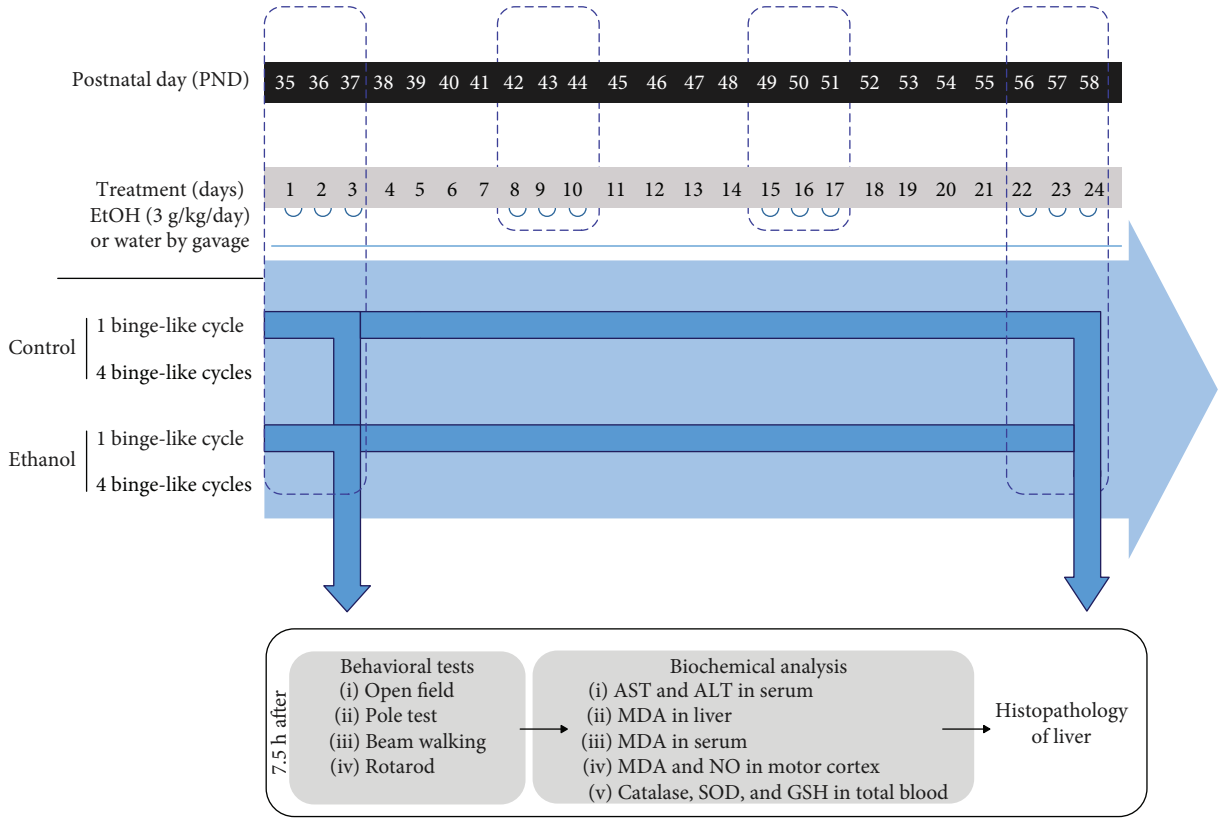

Figure 1: Experimental schedule of binge-like ethanol treatment in adolescent rats. Each cycle of binge-like ethanol administration consisted of a daily gavage administration of ethanol (3 g/kg/day) (or water to control group) for 3 consecutive days weekly. Initially, the immediate postadministration effects of either a single or repeated binge-like ethanol episodes in adolescence were assessed. Female rats underwent one cycle of binge-like ethanol treatment at postnatal day 35 (PND35) or 4 cycles of binge-like episodes (PND35–58). After motor behavioral analysis, rats were sacrificed for markers of biochemical analysis and hepatic histopathology.

the supernatant was collected and read by the spectrophotometric method (wavelength of 535 nm). Results were expressed as percentages of control groups.

(2) Superoxide Dismutase (SOD) Activity. Determination of superoxide dismutase (SOD) activity was performed according to the procedure recommended by McCord and Fridovich [47]. For this, blood samples were haemolysed into ice water (1 : 3) and then diluted in a Tris-based buffer (Tris 1 M/EDTA 5 mM, pH 8.0). This method evaluated the ability of SOD to catalyse the conversion of O^{2-} to H_2O_2 and O_2. SOD activity was measured using UV spectrophotometry at a wavelength of 550 nm.

(3) Catalase Activity. Catalase activity was determined by measuring the rate of enzymatic decomposition of H_2O_2 (10 mM) to H_2O and O_2. Blood samples were haemolysed into ice water (1 : 3) and then diluted in a Tris-based buffer (Tris 1 M/EDTA 5 mM, pH 8.0). The decay of H_2O_2 was measured using ultraviolet spectrophotometry at 240 nm, and enzyme activity was expressed in CAT units, where one unit is the amount of enzyme needed to hydrolyze 1 μmol of H_2O_2/min/mg protein.

(4) Content of Thiol Groups. The content of thiol groups was based on the ability to reduce 5,5-dithiobis-2-nitrobenzoic acid (DTNB) for nitrobenzoic acid (TNB), wherein haemolysed blood samples (20 μL) were solubilized with distilled water plus PBS/EDTA (4 mL) and mixed by vortexing according to Belém-Filho et al.'s [11] protocol. After this, 3 mL of samples was quantitated by spectrophotometry at 412 nm and the content of the thiol groups were expressed in μg/mL, as described by Riddles et al. [48].

2.4.4. Oxidative Biochemistry in Tissue Samples

(1) Lipid Peroxidation Levels in Liver and Motor Cortex. Levels of lipid peroxidation in the liver and motor cortex samples was evaluated by a method based on the reaction between MDA and N-methyl-2-phenylindole [49], expressed as moles of MDA per milligram of protein. An aliquot of homogenate was centrifuged at 2500 ×g for 30 min at 4°C, and the supernatant was used for the reaction with N-methyl-phenyl indole (NMFI) and methane sulfonic acid at 45°C, during 40 min, yielding a stable chromophore measured at 570 nm wavelength and compared with the standard curve of MDA and corrected with the protein concentration of each sample [8, 12].

(2) Determination of Nitrate/Nitrite (NOx). According to Griess method [50], NOx was measured. In short, an aliquot of cerebral cortex homogenate was centrifuged at 21,000 rpm

for 10 minutes at 4°C, and the supernatant was used to analyze nitrite levels. After this, fifty microliters of the supernatant sample or standard sodium nitrite solution was mixed with another 50 μL of the Griess reagent (0.1% N-(1-naphthyl) ethylenediamine dihydrochloride; and 1% sulfanilamide in 5% phosphoric acid; 1 : 1) and maintained at room temperature for 20 minutes. Subsequently, the tissue samples were analyzed on a spectrophotometer by absorbance at 550 nm and compared to that of standard solutions of sodium nitrite. The standard curve was elaborated by sodium nitrate ($NaNO_2$) which reflected NOx concentration and data were corrected with the protein concentration of each sample.

All results above were expressed as percentages of the control groups [8].

(3) Determination of Protein Content. Total protein content in the supernatants was assayed using the Bradford [51] methodology. Hepatic and cortical protein oxidation was measured wherein an aliquot of homogenate was incubated with the Bradford reagent (5% ethanol; 8.5% phosphoric acid; 0.25% Coomassie Brilliant Blue G-250) for 5 min at room temperature. The absorbance was measured at 570 nm and compared to standard solutions of bovine serum albumin. Results were used for the correction of MDA and nitrite concentrations [8, 12].

2.5. Histopathology of the Liver. After removing the liver, liver tissues were fixed in 10% buffered formalin, embedded in paraffin, sectioned (5 μm thick), and stained with hematoxylin and eosin (HE). All sections were stained and surveyed on a light microscope (Nikon Eclipse E200). Illustrative images from all experimental groups were obtained using a digital camera attached to the microscope (Nikon Eclipse 50i), using the software Moticam 2500 for qualitative analysis.

2.6. Statistical Analysis. Values are expressed as mean ± S.E.M. of $n = 9 – 12$ animals per group for motor behavior and $n = 3 – 6$ per group for biochemical analysis. Statistical comparison was performed by two-way ANOVA for treatment (water *vs*. ethanol) and after different binge-like ethanol cycles (after 1 cycle *vs*. after 4 cycles) as variables; multiple post hoc comparisons were performed using the Fisher-LSD test and $P < 0.05$. Rotarod and beam-walking tests were analyzed by two-way ANOVA with repeated measures (successive sessions) followed by the Fisher-LSD post hoc test.

3. Results

3.1. Impact of Repeated Cycles of Binge-Like Ethanol Exposure Causes Worse Motor Impairment in Female Adolescent Rats. The spontaneous locomotor activity, assessed by horizontal and vertical exploration (total distance traveled and number of rearing parameters, respectively) on the open-field test, is demonstrated in Figure 2(a). Two-way ANOVA (ethanol-treatment *vs.* repeated cycles) of motor behavior, assessed by horizontal and vertical exploration, revealed a significant difference only for effects of binge-like ethanol treatment ($F(1, 44) = 33.485$; $P = 0.001$ and $F(1, 37) = 11.826$; $P = 0.001$, respectively). Fisher-LSD post hoc comparisons showed that binge-like ethanol treatment induces reduction of the horizontal and vertical exploratory activity of adolescent female rats after 1 ($P < 0.001$; $P = 0.017$, respectively) and 4 binge cycles ($P = 0.007$; $P = 0.023$, respectively) of ethanol treatment.

In the pole test (Figure 2(b)), two-way ANOVA of the descent time from the vertical beam to the platform base showed a significant difference for the effect of binge-ethanol treatment ($F(1, 39) = 6.225$; $P = 0.017$). Fisher-LSD post hoc comparisons revealed that after 4 repeated cycles of binge-ethanol exposure, adolescent rats displayed an increased latency to descend from the beam to the platform in the pole test ($P = 0.028$).

To evaluate the repercussions of repeated cycles of binge-like ethanol on motor learning, coordination, and balance in adolescent rats, we subjected the animals to three consecutive sessions (8 rpm) on the rotarod apparatus (Figure 2(c)). Two-way ANOVA with repeated measures revealed a significant difference at latency to first fall of the cylinder of the rotarod apparatus for effects of binge-like ethanol treatment ($F(3, 47) = 10.858$; $P = 0.001$). Fisher-LSD post hoc comparisons revealed that a single binge-like cycle in adolescence provokes impairment on motor coordination and balance in female rats at first presentation to the rotarod apparatus ($P = 0.001$) that was recovered on the subsequent sections of the test. However, repeated binge-ethanol cycles during adolescence reduced the animal's dwell time on the rotarod's scrollbar in all successive sessions (first, second, and third) when compared to their counterparts ($P = 0.0001$, $P = 0.033$, and $P = 0.047$, respectively).

Figure 2(d) represents the performance of ethanol-treated adolescent female rats on the square and round beams of the beam-walking test. Two-way ANOVA with repeated measures revealed a significant difference at the number of slips to cross the suspended square beam by binge-like ethanol treatment ($F(3, 52) = 3.261$; $P = 0.03$), as well as related to the thickness of the cross-sectional area beams ($F(2, 52) = 26.942$; $P = 0.0001$). Fisher-LSD post hoc comparisons revealed that a single binge-like exposure generates an increase in the number of slips on the squared thinner beam (5 mm; $P = 0.044$). Indeed, repeated cycles of adolescent binge-like ethanol significantly increased the number of slips during this section of the beam, except for the larger beam (28 mm; intermediary: $P = 0.012$; and thinner cross-sectional area: $P = 0.0001$, respectively).

In order to make the task more complex, as well as to evaluate motor learning, following square beam sessions, animals were submitted to the round beams (Figure 2(d)). Two-way ANOVA with repeated measures revealed a significant difference in the number of slips to cross the suspended round beam of binge-like ethanol treatment ($F(3, 61) = 48.444$; $P = 0.0001$), as well as the thickness of the cross-sectional area beams ($F(2, 61) = 48.955$; $P = 0.0001$). Fisher-LSD post hoc comparisons revealed that a single binge-like exposure increased the number of slips on the thinner beam (11 mm; $P = 0.009$). However, the number of slips per session was significantly increased after repeated cycles of adolescent

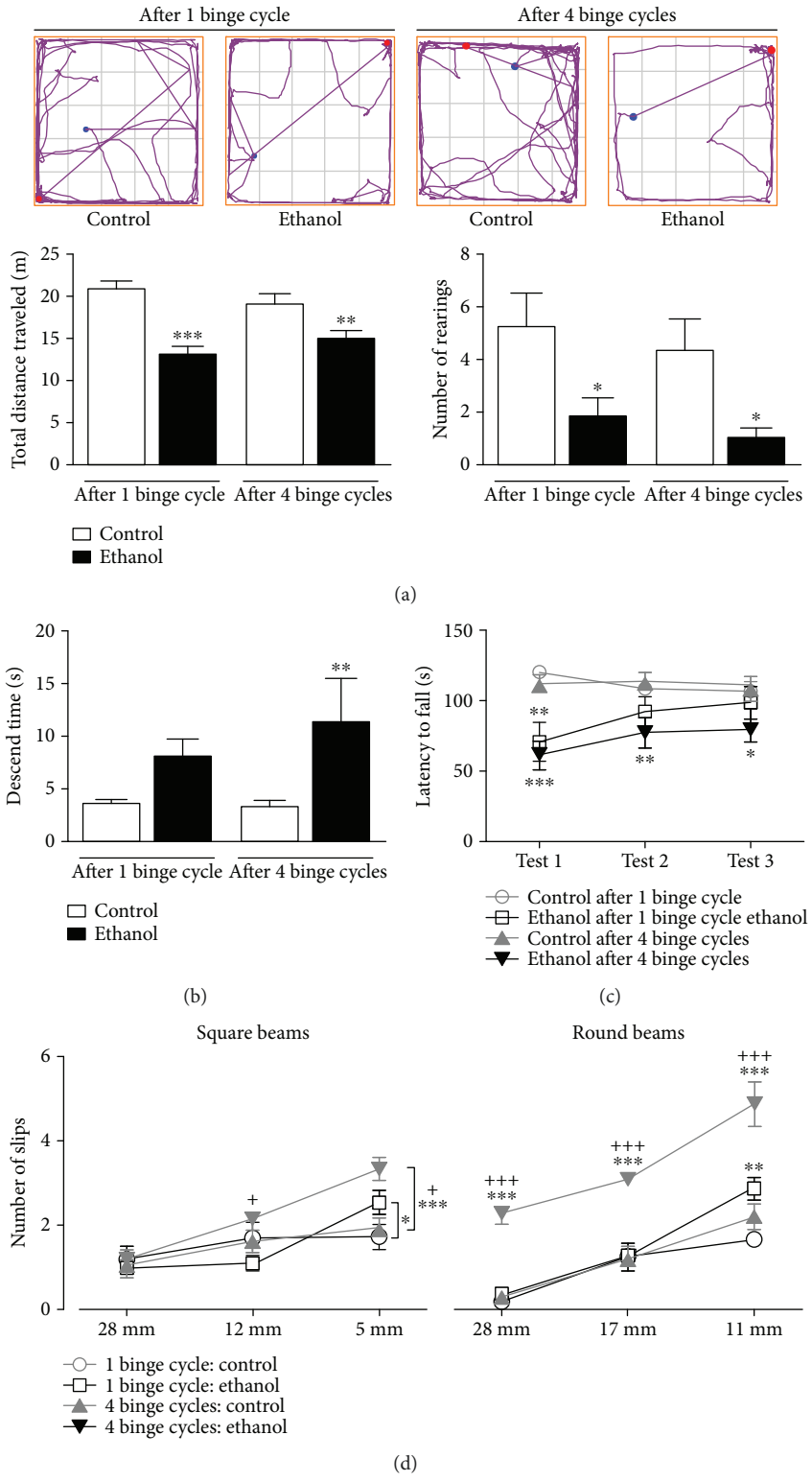

FIGURE 2: Impact of adolescent binge-ethanol exposure on motor behavior of female rats. The analysis of the total distance traveled accessed the horizontal locomotor activity, whereas the number of rearing informed the vertical locomotor activity, both measures being derived from the track plots in the open-field arena (a). (b) The descent time from vertical beam to the platform base at the pole test is shown as a measure of the kinetics of movement. (c) The latency to first fall on the cylinder of the rotarod apparatus is illustrated as a measure of the motor coordination and balance by forced locomotor activity in the rotarod test. (d) The number of slips to cross the series of graduated beams (square and round) is shown to access the motor learning, coordination, and balance by spontaneous locomotor activity in the beam-walking test. Data are mean ± SEM of $n = 9 - 12$ rats per group. $^{*}P < 0.05$, $^{**}P < 0.001$, and $^{***}P < 0.0001$ *vs.* age-matched control; $^{+}P < 0.05$ and $^{+++}P < 0.001$ *vs.* ethanol-treated after 1 binge-like cycle, all assessed using a Fisher-LSD test after two-way ANOVA.

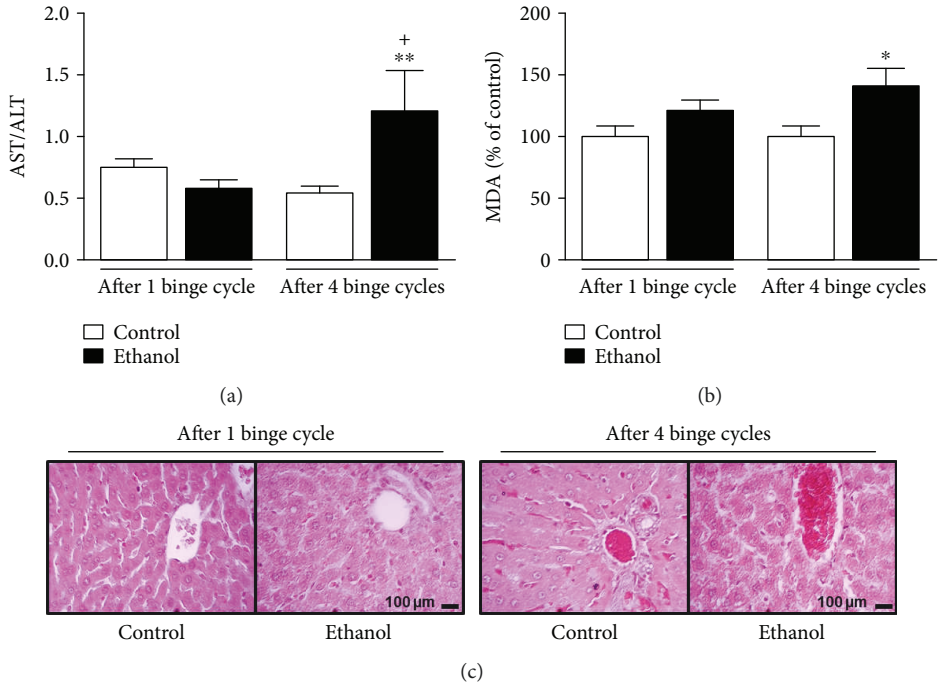

Figure 3: Postconsumption effects of repeated binge-like ethanol treatment on hepatic function of adolescent female rats. The analysis of the ratio of serum activities of aspartate aminotransferase (AST) on alanine aminotransferase (ALT) (a) and percental of malondialdehyde (MDA) levels in hepatic tissue (b). (c) The histopathology of hepatic tissue analyzed by hematoxylin/eosin (HE) staining as morphological qualitative evaluation is shown. Data are mean ± SEM of $n = 3 - 6$ animals per group. $^{*}P < 0.05$ and $^{**}P < 0.001$ *vs.* age-matched control; $^{+}P < 0.05$ *vs.* ethanol-treated after 1 binge-like cycle, all assessed using a Fisher-LSD test after two-way ANOVA. Scale = 100 μm.

binge-like ethanol in all diameters evaluated ($P = 0.0001$ for all thickness of beams).

3.2. Repeated Cycles of Binge-Like Ethanol Treatment Elicit Accumulative Effects on Hepatic Damage in Adolescent Rats. Two-way ANOVA (ethanol-treatment *vs.* repeated cycles) of liver damage, assessed by the ratio of serum activity of hepatic transaminases (AST/ALT) and tissue malondialdehyde (MDA) levels (Figures 3(a) and 3(b)), revealed a significant difference for the interaction between effects of binge-like ethanol treatment and repeated cycles ($F(1, 16) = 5.807$; $P = 0.028$) for the ratio AST/ALT, but not for MDA levels that showed only significance for effects of binge-like ethanol treatment ($F(1, 12) = 5.671$; $P = 0.035$). Fisher-LSD post hoc comparisons confirmed hepatocyte oxidative damage by high levels of MDA ($P = 0.045$) (Figure 3(b)) and hepatic transaminases ($P = 0.016$) (Figure 3(a)) in adolescent female rats after 4 cycles of binge-like ethanol treatment.

The histopathological study revealed that control group animals presented normal aspects of the cellular, extracellular, and vascular components of the liver in both periods studied in this experiment. In the ethanol-treated groups, in the acute period corresponding to the 1 binge-like ethanol cycle, the following was observed: intense microsteidosis, alteration in the morphology of the hepatocytes, and tissue parenchyma on the centrilobular region that extended to the mid-zonal region, being more scarce or having more focal segments in the peripheral and superficial segments. In the group submitted to 4 binge-like ethanol cycles, an intense microsteidosis associated to vascular congestion and visible loss of the structural cohesion of the parenchyma were observed (Figure 3(c)).

3.3. Adolescent Binge-Like Ethanol Treatment Induces Accumulative Effects on Oxidative Damage in Motor Cortex, Not Detectable Peripherally. Two-way ANOVA (ethanol-treatment *vs.* repeated cycles) of motor cortex damage, assessed by the tissue malondialdehyde (MDA) levels (Figure 4(a)), revealed significant effects of repeated cycles ($F(1, 12) = 9.159$; $P = 0.011$) and their interaction with the effects of binge-like ethanol treatment ($F(1, 12) = 9.159$; $P = 0.011$). Fisher-LSD post hoc comparisons confirmed oxidative damage in the motor cortex by high levels of MDA ($P = 0.022$) in adolescent female rats after 4 cycles of binge-like ethanol treatment. In addition, our results showed an increase of NO production in the 4 binge-like ethanol cycle animals compared to control subjects ($P < 0.0001$; Figure 4(b)). In contrast, the levels of the lipid peroxidation marker in the serum did not indicate peripheral oxidative imbalance, even after 4 cycles of ethanol treatment (Figure 4(c)).

3.4. Repeated Cycles of Binge-Like Ethanol Administration during Adolescence Cause Change in Enzymatic and Nonenzymatic Oxidative Response in Adolescent Female Rats. Two-way ANOVA (ethanol-treatment *vs.* repeated cycles) of peripheral antioxidant balance was assessed by the levels of enzymatic and nonenzymatic antioxidant agents (Figures 5(a) and 5(c)). Effects of binge-like ethanol treatment revealed a significant effect for catalase (CAT) ($F(1, 10) = 6.446$; $P = 0.029$). In addition, the repeated cycles

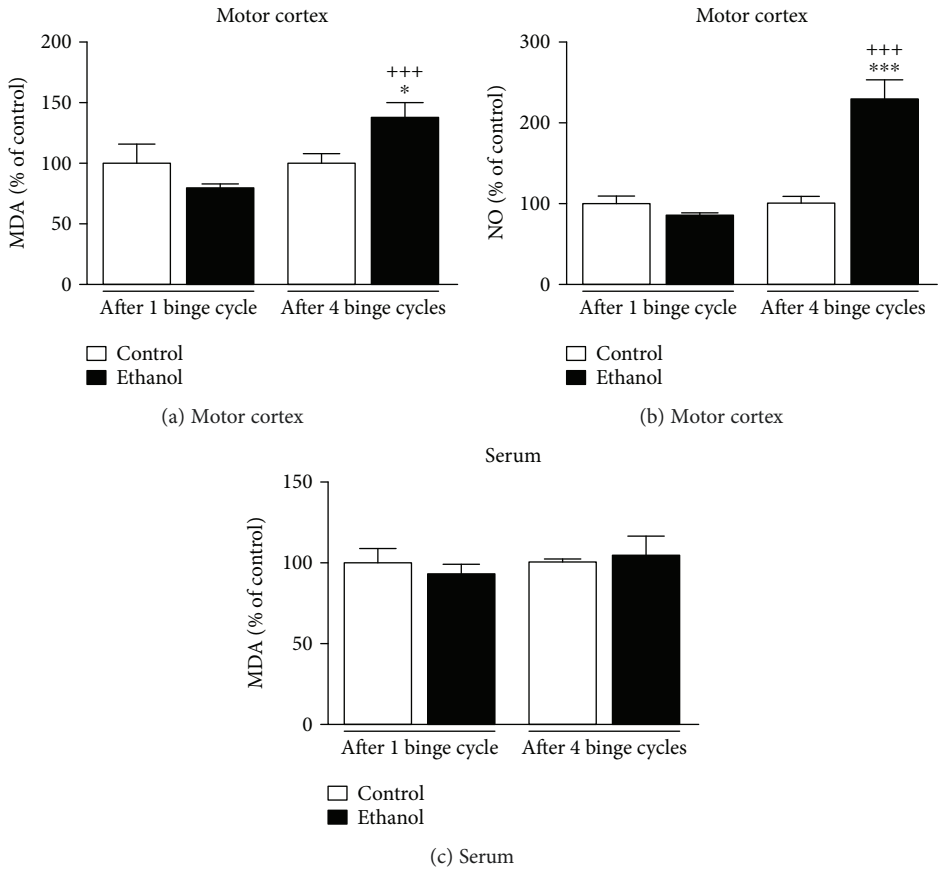

Figure 4: Binge-like ethanol administration on the marker of oxidative damage in the motor cortex and serum of adolescent female rats. The percental of malondialdehyde (MDA) levels in the motor cortex (a) and serum (c) of female rats. The percental of nitrite (NO) levels in the motor cortex (b). The results are mean ± SEM of $n = 3 – 6$ animals per group. $^{*}P < 0.05$ and $^{***}P < 0.0001$ *vs.* age-matched control; $^{+++}P < 0.001$ *vs.* ethanol-treated after 1 binge-like cycle, all assessed using a Fisher-LSD test after two-way ANOVA.

significantly influenced CAT ($F(1, 10) = 26.397$; $P = 0.001$) and SOD ($F(1, 14) = 17.286$; $P = 0.001$). On the other hand, CAT ($F(1, 10) = 26.397$; $P = 0.001$), SOD ($F(1, 14) = 17.286$; $P = 0.001$), and content of thiol ($F(1, 15) = 5.195$; $P = 0.038$) were significantly induced by the interaction of these factors. Fisher-LSD post hoc comparisons showed a significant increase in CAT ($P < 0.001$) and SOD ($P = 0.006$) levels in adolescent female rats after 1 cycle, with successive depletion of these enzymes on the 4th cycle of binge-like ethanol treatment as well as reduction in the formation of thiol groups ($P = 0.045$).

4. Discussion

The present study evidenced that the binge-like pattern of ethanol intake during adolescence in female rats induces marked liver and motor cortex oxidative stress related to repercussions on motor function. More importantly, such alterations were not reflected on the peripheral oxidative damage.

Lipid peroxidation (LPO) is a natural degenerative process in which there are interactions involving ROS and polyunsaturated fatty acids of biological membranes, jeopardizing the integrity of organelles and the cell itself [52, 53]. Alcohol consumption intensifies such a process due to ROS production during its metabolism and selectively alters mitochondrial function of the liver and other tissues [54–56]. Our data revealed that binge drinking during adolescence altered hepatic health. In fact, a single acute dose of ethanol was not sufficient to display liver alteration. However, after 4 cycles of ethanol exposure, the AST/ALT as well as the MDA levels were increased compared to its counterparts, showing liver injury caused by the ingestion of ethanol. In addition, the first episode of binge drinking resulted in microvesicular and macrovesicular steatosis in zone 3 (perivenular) that constitutes the first response of the liver to alcohol abuse. Such initial hepatic alteration was intensified by the subsequent ethanol exposure that aggravated the initial damage and reached other tissue components, thus causing vascular congestion and loss of the structural cohesion of the parenchyma. In fact, there is a consensus that alcohol is a hepatotoxic drug that also disrupts lipid metabolism. Alcohol inhibits the mitochondrial β-oxidation of fatty acids of hepatocytes and induces increased mobilization of fatty acids from adipose tissue to the liver, increasing fat accumulation [57]. However, it is the first time that it was demonstrated that a single binge-drinking episode during adolescence alters the hepatic tissue in females. In addition, we showed that the consumption of ethanol, even followed by withdrawal periods (4 days off), from adolescence until young

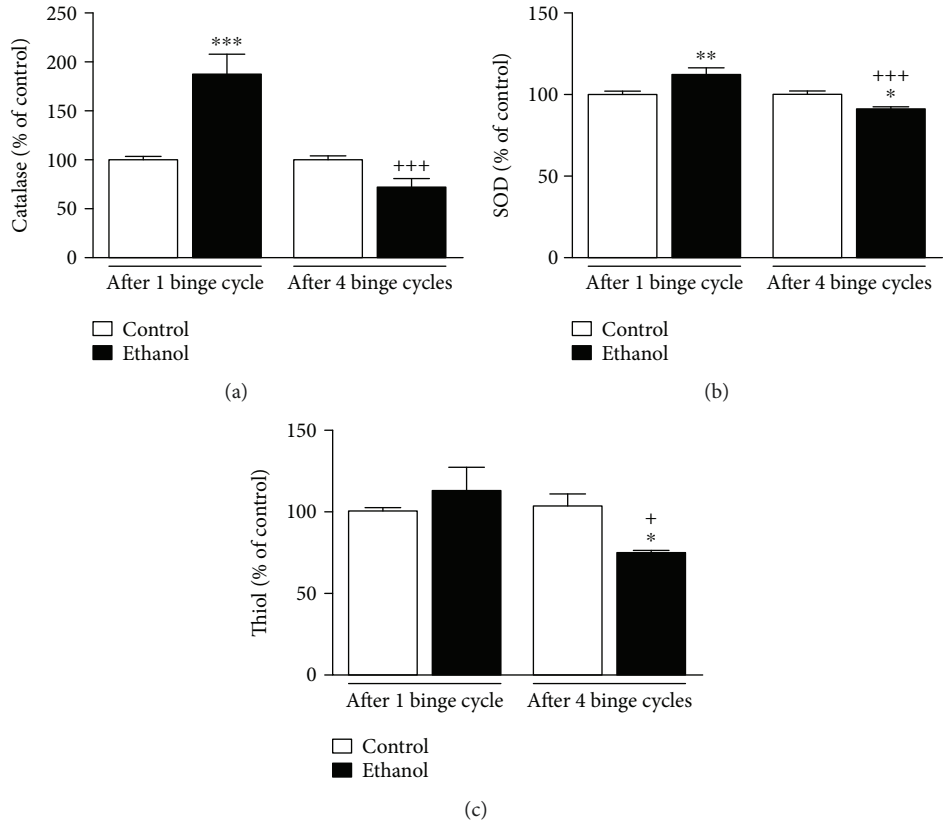

Figure 5: Effects of adolescent binge-ethanol paradigm on the oxidative enzymatic (catalase and superoxide dismutase (SOD)) and nonenzymatic (thiol groups) activities in blood of female rats. Oxidative biochemical of catalase (a) and SOD activities (b) after binge-like ethanol administration, both illustrated as % of control. (c) The content of thiol (% of control) after binge-like ethanol administration in adolescent female rats is shown. Results are mean ± SEM of $n = 4 - 5$ rats per group. $^{*}P < 0.05$, $^{**}P < 0.001$, and $^{***}P < 0.0001$ *vs.* age-matched control; $^{++}P < 0.01$ and $^{+++}P < 0.001$ *vs.* ethanol-treated after 1 binge-like cycle, all assessed using a Fisher-LSD test after two-way ANOVA.

adulthood aggravated the previous damage. Recently, Choi et al. [58] showed that chronic binge exposure led to ROS level overproduction and elevated amounts of the microsomal ethanol-oxidizing enzyme (i.e., CYP2E1 and NADPH oxidase), but not of iNOS, and decreased cell antioxidant defense (i.e., GSH and mitochondrial ALDH2 activity) in the liver.

Allied to the liver, our data also showed that after consumption of chronic binge drinking (after 4 binge cycles) in early adolescence, the antioxidant enzyme system of both CAT and SOD activities were downregulated. The reduced defense against oxidative damage may particularly affect the organs more susceptible to this type of damage (i.e., the liver and brain), becoming a major molecular contribution for the deleterious consequences observed in behavioral alterations. After this initial approach for the evaluation of the oxidative status carried in our work with CAT and SOD and based on our data, a detailed study of the detoxification enzyme systems, including glutathione peroxidase, iNOS, and NADPH oxidase, could contribute to a better understanding of the molecular processes involved in the early consequences of ethanol consumption.

Brain cells are more vulnerable to oxidative damage related to reduced levels of antioxidant enzymes and a high level of oxidant metabolism [59]. In this regard, our previous studies had already shown that the chronic EtOH exposure during adolescence reduced the astrocyte population and the number of neurons and glia cells with an increase in both nitric oxide and lipid peroxidation in the cerebral cortex [15].

EtOH is known to induce oxidative imbalance by increasing the ROS products generated by its metabolism, causing the reduction of enzymatic antioxidants, and increasing the biomarkers of macromolecules [28, 60, 61]. The main route of the alcohol metabolism is performed by the hepatic enzyme system; however, other routes can be used, such as the oxidation by the CAT antioxidant enzyme, which acts as a limited-step pathway [62]. Thus, increased systemic oxidative stress and MDA levels, as well as activation of neuroapoptotic and neuroinflammatory pathways, have also been previously associated with alcohol abuse [63, 64]. Thus, this enhanced oxidative stress may systemically contribute to cellular damage, as well as damage in the brain, leading to neurodegeneration, development of cognitive impairment, anxiety, depressive like behavior, and other psychiatric disorders [65, 66]. These reactions also promoted a reduction in CAT and SOD activity and thiol (-SH) group levels peripherally (Figures 5(a)–5(c)), possibly reflecting on the motor cortex, leading to an increase in NO and MDA levels in the motor cortex (Figures 4(a) and 4(b)). In this sense, functional motor impairment appears as a result, since such area plays a central role in both motor skill learning and execution [67].

In fact, the relationship between motor function and oxidative disturbance has been reported by other studies (for a review, see [30, 31]).

Although motor function impairment also depends on the period and time of consumption of ethanol, it is known that adolescents are less vulnerable to motor damage compared to adults because younger people are more resistant to the drug's sedative effects [68, 69]. This characteristic of adolescence can lead to increased consumption of large amounts of alcohol without generating the perception of toxicological effects.

The exploratory tendency of the animal in a new environment in the open-field test can be translated as spontaneous locomotor activity, using the parameters of total distance traveled in the arena as a measure of horizontal exploration and frequency of rearings resulting from vertical exploration [38, 39]. This study demonstrated that horizontal and vertical exploratory activities were impaired after administration of ethanol in the binge pattern. Pascual et al. [70] evaluated the effect of chronic voluntary consumption of EtOH (mean 10 g/kg) initiated at the end of the periadolescence (42–49 PND) of rodents during 5 months of intoxication. These authors found a reduction in the spontaneous locomotor activity of the animals within 8 hours after the removal of the EtOH solution, but this loss did not last for a prolonged period (15 days). In contrast, our study demonstrates that the intermittent and episodic administration of ethanol (3 g/kg) from adolescence to adulthood reduces the exploratory locomotor activity of the animals in the early withdrawal. These findings indicate the greatest harmful effect of alcohol consumption on the usual binge-drinking model among adolescents.

In order to cover the study on the various aspects of motor function, the behavioral tests of the pole test, beam-walking, and rotarod assays were used. The first one was developed to measure bradykinesia and reduction of muscle tone, evaluating the animal's ability to invert its axis and descend to the platform [38, 71]. On the other hand, the latter two evaluated coordination and motor balance [38, 42]. The development of bradykinesia is measured by the prolongation of the turnaround and descent time of the animal at the platform base [72]. This symptom is associated with abnormal functioning of the intrinsic circuitry of the basal nuclei through the selective hypoactivity of the supplemental motor area and the cortical areas, which are frontal association areas that receive subcortical entry mainly from the basal ganglia [73, 74].

Accordingly, the EtOH-intoxicated groups presented higher scores to perform the test, indicating that the EtOH intoxication, in the way of binge drinking, generated a kinetics loss of the motor activity of the animals. Thus, our findings indicate impairment in subcortical and/or subcortical connection with cortical motor areas in adolescents after repeated binge-like cycles in adolescence.

The rotarod test measures forced gait disturbances and gross motor coordination by an animal's ability to remain on a rotating rod [38]. In the present study, the administration of ethanol in the binge pattern elicited poor coordination on the first section of the test. However, the individual rats increased their skills for remaining on the rotating rod in the subsequent sections, except for animals exposed to ethanol during the adolescence until adulthood (4 cycles of ethanol). In addition to the rotarod apparatus, we employed the beam-walking paradigm to detect fine coordination through a spontaneous motor task [75]. According to the beam-walking test, motor impairment related to ataxic and dystonic characteristics can be assessed through the animal's difficulty in crossing beams of different shapes and cross-sectional areas [38]. Our study demonstrated that the administration of ethanol in the binge-drinking model elicited poor performance on the test, increasing the number of slips, mainly after 4 binge cycles. Such impairment was intensified proportionally to the difficulty of the test sections.

In this sense, for movement to occur correctly, motor areas related to the organization and control of movement (e.g., primary motor cortex, supplemental motor area, premotor, and cingulate motor) influence descending pathways and medullary interneurons through their connections with the brainstem, basal nuclei, and cerebellum [76, 77]. Thus, ataxias result from disorders of the cerebellum and/or its connections, as well as the circuitry that integrates the motor cortex and striatum [78]. Motor incoordination is often used as an index of intoxication produced by drugs that depress the central nervous system [79]. It has been observed that EtOH in the abstinence period can downregulate gabaergic neurons associated with exacerbation of the glutamatergic pathway in most areas of the brain, promoting behavioral effects typical of this period as altered motor control, learning, and memory [31, 80, 81]. Thus, the results obtained in this study reveal that repeated episodes of binge drinking increased the number of slips on the beam-walking test, as well as reduced rotarod latency probably due to these molecular events that may occur in the abstinence period. Thus, we propose that despite the intermittent periods of ethanol withdrawal, the binge-drinking pattern displays liver and motor cortex oxidative damage, which reflects on motor function in female rats. Surprisingly, such tissue damage was not detectable in blood.

Due to the deleterious effects of alcohol abuse and alcoholism, clinical studies aim at characterizing the early events leading to alcoholic diseases (i.e., motor impairment and liver damage) in order to define biomarkers, which may help clinicians establish preventive measures [82]. However, few studies have been proposed to evaluate biomarkers of early detection that might be present in individuals known as "social drinkers" or binge drinkers [83]. Muñiz-Hernández et al. [83] highlighted in their review that biomarkers that reflect oxidative damage—mainly MDA—could be used to identify damages in the earlier stages of ethanol consumption. However, for the first time, our experimental data contradict such hypothesis and reveal that MDA levels are not well indicated for early damage during the adolescent period. Particularly, we suggest that in clinical practice, blood MDA levels could not be used as a peripheral marker for ethanol misuse, since such biomarker in blood is nonspecific. Actually, we highlight that 4 binges do not cause significant lipid peroxidation in the blood despite the presence of high

levels of MDA in hepatic and motor cortex tissues associated to motor impairment and hepatic steatosis.

5. Conclusions

It is noteworthy that the binge-drinking exposure during adolescence in females may impact liver homeostasis. Besides, the liver and motor cortex seem to be more vulnerable to oxidative damage, even when systemic oxidative damage was not observed. Besides, our results show that motor alteration was altered by a binge-like ethanol paradigm, even after only one exposure. However, bradykinesia, poor coordination, and balance were impaired by subsequent administration of ethanol during adolescence until early adulthood. Would lipid peroxidation be an adequate biomarker for the hazardous effects of ethanol misuse?

Data Availability

The behavioral and oxidative data used to support the findings of this study are available from the corresponding author upon request.

Conflicts of Interest

The authors declare that there is no actual or potential conflict of interest in relation to this article.

Authors' Contributions

Luanna Melo Pereira Fernandes and Klaylton Sousa Lopes contributed equally to this work.

Acknowledgments

The authors thank the Evandro Chagas Institute for providing animals. The authors also thank Professor Luís Assunção Pereira from the Laboratory of Veterinary Pathology, Institute of Animal Health and Production, Federal Rural University of Amazônia (Pará, Brazil) for histopathological data. This work was supported by Coordenação de Aperfeiçoamento de Pessoal de Nível Superior (CAPES) and Programa Integrado de Bolsas de Iniciação Científica (PIBIC) of the Universidade Federal do Pará (UFPA) from the Governo Brasil. Carvalho received research support from CAPES. MC Monteiro is grateful for the fellowship from CNPq.

References

[1] N. Boutros, S. Semenova, and A. Markou, "Adolescent intermittent ethanol exposure diminishes anhedonia during ethanol withdrawal in adulthood," *European Neuropsychopharmacology*, vol. 24, no. 6, pp. 856–864, 2014.

[2] World Health Organization-WHO, *Global Status Report on Alcohol and Health*, World Health Organization, Geneva, Switzerland, 2014.

[3] L. D. Johnston, P. M. O'malley, J. G. Bachman, and J. E. Schulenberg, "Monitoring the future national results on adolescent drug use: overview of key findings, 2008," in *Abuse*, p. 9, National Institute on Drug Abuse. NIH Publication, Bethesda, MD, USA, 2009.

[4] K. M. Lisdahl, R. Thayler, L. M. Squeglia, and S. F. Taper, "Recent binge drinking predicts smaller cerebellar volumes in adolescents," *Psychiatry Research: Neuroimaging*, vol. 211, no. 1, pp. 17–23, 2013.

[5] V. Preedy and R. R. Watson, *Comprehensive Handbook of Ethanol Related Pathology*, Academic Press, 1st edition, 2004.

[6] F. B. R. da Silva, P. A. Cunha, P. C. Ribera et al., "Heavy chronic ethanol exposure from adolescence to adulthood induces cerebellar neuronal loss and motor function damage in female rats," *Frontiers in Behavioral Neuroscience*, vol. 12, p. 88, 2018.

[7] L. M. Fernandes, F. B. Teixeira, S. M. Alves-Junior, J. J. Pinheiro, C. S. F. Maia, and R. R. Lima, "Immunohistochemical changes and atrophy after chronic ethanol intoxication in rat salivary glands," *Histology and Histopathology*, vol. 30, no. 9, pp. 1069–1078, 2015.

[8] E. A. Fontes-Júnior, C. S. F. Maia, L. M. P. Fernandes et al., "Chronic alcohol intoxication and cortical ischemia: study of their comorbidity and the protective effects of minocycline," *Oxidative Medicine and Cellular Longevity*, vol. 2016, Article ID 1341453, 10 pages, 2016.

[9] A. C. Oliveira, M. C. Pereira, L. N. Santana et al., "Chronic ethanol exposure during adolescence through early adulthood in female rats induces emotional and memory deficits associated with morphological and molecular alterations in hippocampus," *Journal of Psychopharmacology*, vol. 29, no. 6, pp. 712–724, 2015.

[10] G. B. Oliveira, E. A. Fontes-Júnior, S. de Carvalho et al., "Minocycline mitigates motor impairments and cortical neuronal loss induced by focal ischemia in rats chronically exposed to ethanol during adolescence," *Brain Research*, vol. 1561, pp. 23–34, 2014.

[11] I. J. A. Belém-Filho, P. C. Ribera, A. L. Nascimento et al., "Low doses of methylmercury intoxication solely or associated to ethanol binge drinking induce psychiatric-like disorders in adolescent female rats," *Environmental Toxicology and Pharmacology*, vol. 60, pp. 184–194, 2018.

[12] N. C. F. Fagundes, L. M. P. Fernandes, R. S. O. Paraense et al., "Binge drinking of ethanol during adolescence induces oxidative damage and morphological changes in salivary glands of female rats," *Oxidative Medicine and Cellular Longevity*, vol. 2016, Article ID 7323627, 11 pages, 2016.

[13] L. M. P. Fernandes, S. C. Cartágenes, M. A. Barros et al., "Repeated cycles of binge-like ethanol exposure induce immediate and delayed neurobehavioral changes and hippocampal dysfunction in adolescent female rats," *Behavioural Brain Research*, vol. 350, pp. 99–108, 2018.

[14] A. N. Oliveira, A. M. Pinheiro, I. J. A. Belém-Filho et al., "Unravelling motor behaviour hallmarks in intoxicated adolescents: methylmercury subtoxic-dose exposure and binge ethanol intake paradigm in rats," *Environmental Science and Pollution Research International*, vol. 25, no. 22, pp. 21937–21948, 2018.

[15] F. B. Teixeira, L. N. Santana, F. R. Bezerra et al., "Chronic ethanol exposure during adolescence in rats induces motor impairments and cerebral cortex damage associated with oxidative stress," *PLoS One*, vol. 9, no. 6, article e101074, 2014.

[16] A. Crego, S. Rodriguez-Holguín, M. Parada, N. Mota, M. Corral, and F. Cadaveira, "Reduced anterior prefrontal cortex activation in young binge drinkers during a visual

working memory task," *Drug and Alcohol Dependence*, vol. 109, no. 1-3, pp. 45–56, 2010.

[17] J. Jacobus and S. F. Tapert, "Neurotoxic effects of alcohol in adolescence," *Annual Review of Clinical Psychology*, vol. 9, no. 1, pp. 703–721, 2013.

[18] G. Petit, C. Kornreich, P. Verbanck, A. Cimochowska, and S. Campanella, "Why is adolescence a key period of alcohol initiation and who is prone to develop long-term problem use? A review of current available data," *Socioaffective Neuroscience & Psychology*, vol. 3, no. 1, article 21890, 2013.

[19] National Institute On Alcohol Abuse And Alcoholism (NIAAA), "National Institute of Alcohol Abuse and Alcoholism Council approves definition of binge drinking," 2004, http://pubs.niaaa.nih.gov/publications.

[20] A. Pilatti, P. Etkin, E. U. Parra, and R. M. Pautassi, "Association between attendance to pregaming events and alcohol-related consequences in argentinean youth," *Health and Addictions*, vol. 18, pp. 5–16, 2018.

[21] INPAD–Instituto Nacional De Ciência E Tecnologia Para Políticas Publicas Do Álcool e Outras Drogas, "II levantamento nacional de álcool e drogas," http://www.inpad.org.br/lenad.

[22] D. E. Hartley, S. Elsabagh, and S. E. File, "Binge-like drinking and sex: effects on mood and cognitive function in healthy young volunteers," *Pharmacology, Biochemistry, and Behavior*, vol. 78, no. 3, pp. 611–619, 2004.

[23] M. Pascual, J. Montesinos, M. Marcos et al., "Gender differences in the inflammatory cytokine and chemokine profiles induced by binge ethanol drinking in adolescence," *Addiction Biology*, vol. 22, no. 6, pp. 1829–1841, 2017.

[24] L. M. Squeglia, A. D. Schweinsburg, C. Pulido, and S. F. Tapert, "Adolescent binge drinking linked to abnormal spatial working memory brain activation: differential gender effects," *Alcoholism: Clinical & Experimental Research*, vol. 35, no. 10, pp. 1831–1841, 2011.

[25] S. Alfonso-Loeches, M. Pascual, and C. Guerri, "Gender differences in alcohol-induced neurotoxicity and brain damage," *Toxicology*, vol. 311, no. 1-2, pp. 27–34, 2013.

[26] L. M. Squeglia, S. F. Sorg, A. D. Schweinsburg, R. R. Whethrill, C. Pulido, and S. F. Tapert, "Binge drinking differentially affects adolescent male and female brain morphometry," *Psychopharmacology*, vol. 220, no. 3, pp. 529–539, 2012.

[27] M. E. Jung and D. B. Metzger, "A sex difference in oxidative stress and behavioral suppression induced by ethanol withdrawal in rats," *Behavioural Brain Research*, vol. 314, pp. 199–214, 2016.

[28] J. Ostrowska, W. Łuczaj, I. Kasacka, A. Rozanaski, and E. Skrzydlewska, "Green tea protects against ethanol-induced lipid peroxidation in rat organs," *Alcohol*, vol. 32, no. 1, pp. 25–32, 2004.

[29] S. Zakhari and T.-K. Li, "Determinants of alcohol use and abuse: impact of quantity and frequency patterns on liver disease," *Hepatology*, vol. 46, no. 6, pp. 2032–2039, 2007.

[30] J. A. Hernández, R. C. López-Sánchez, and A. Rendón-Ramírez, "Lipids and oxidative stress associated with ethanol-induced neurological damage," *Oxidative Medicine and Cellular Longevity*, vol. 2016, Article ID 1543809, 15 pages, 2016.

[31] M. E. Jung and D. B. Metzger, "Alcohol withdrawal and brain injuries: beyond classical mechanisms," *Molecules*, vol. 15, no. 7, pp. 4984–5011, 2010.

[32] J. I. Beier, G. E. Arteel, and C. J. McClain, "Advances in alcoholic liver disease," *Current Gastroenterology Reports*, vol. 13, no. 1, pp. 56–64, 2011.

[33] B. Gao and R. Bataller, "Alcoholic liver disease: pathogenesis and new therapeutic targets," *Gastroenterology*, vol. 141, no. 5, pp. 1572–1585, 2011.

[34] R. M. Pautassi, J. C. Godoy, and J. C. Molina, "Adolescent rats are resistant to the development of ethanol-induced chronic tolerance and ethanol-induced conditioned aversion," *Pharmacology Biochemistry and Behavior*, vol. 138, pp. 58–69, 2015.

[35] C. Lindtner, T. Scherer, E. Zielinski et al., "Binge drinking induces whole-body insulin resistance by impairing hypothalamic insulin action," *Science Translational Medicine*, vol. 5, no. 170, article 170ra14, 2013.

[36] A. M. Maldonado-Devincci, K. K. Alipour, L. A. Michael, and C. L. Kirstein, "Repeated binge ethanol administration during adolescence enhances voluntary sweetened ethanol intake in young adulthood in male and female rats," *Pharmacology, Biochemistry, and Behavior*, vol. 96, no. 4, pp. 476–487, 2010.

[37] K. Lauing, R. Himes, M. Rachwalski, P. Strotman, and J. J. Callaci, "Binge alcohol treatment of adolescent rats followed by alcohol abstinence is associated with site-specific differences in bone loss and incomplete recovery of bone mass and strength," *Alcohol*, vol. 42, no. 8, pp. 649–656, 2008.

[38] T. Karl, R. Pabst, and S. Vonhörsten, "Behavioral phenotyping of mice in pharmacological and toxicological research," *Experimental and Toxicologic Pathology*, vol. 55, no. 1, pp. 69–83, 2003.

[39] J. C. Brenes, M. Padilla, and J. Fornaguera, "A detailed analysis of open-field habituation and behavioral and neurochemical antidepressant-like effects in postweaning enriched rats," *Behavioural Brain Research*, vol. 197, no. 1, pp. 125–137, 2009.

[40] N. Ogawa, Y. Hirose, S. Ohara, T. Ono, and Y. Watanabe, "A simple quantitative bradykinesia test in MPTP-treated mice," *Research Communications in Chemical Pathology and Pharmacology*, vol. 50, no. 3, pp. 435–441, 1985.

[41] E. Antzoulatos, M. W. Jakowec, G. M. Petzinger, and R. I. Wood, "Sex differences in motor behavior in the MPTP mouse model of Parkinson's disease," *Pharmacology Biochemistry and Behavior*, vol. 95, no. 4, pp. 466–472, 2010.

[42] J. L. Stanley, R. J. Lincoln, T. A. Brown, L. M. McDonald, G. R. Dawson, and D. S. Reynolds, "The mouse beam walking assay offers improved sensitivity over the mouse rotarod in determining motor coordination deficits induced by benzodiazepines," *Journal of Psychopharmacology*, vol. 19, no. 3, pp. 221–227, 2005.

[43] R. J. Carter, L. A. Lione, T. Humby et al., "Characterization of progressive motor deficits in mice transgenic for the human Huntington's disease mutation," *The Journal of Neuroscience*, vol. 19, no. 8, pp. 3248–3257, 1999.

[44] R. J. Carter, J. Morton, and S. B. Dunnett, "Motor coordination and balance in rodentsChapter 8," *Current Protocols in Neuroscience*, vol. 8, pp. 8.12.1–8.12.14, 2001.

[45] C. C. da Silveira, L. M. Fernandes, M. L. Silva et al., "Neurobehavioral and Antioxidant Effects of Ethanolic Extract of Yellow Propolis," *Oxidative Medicine and Cellular Longevity*, vol. 2016, Article ID 2906953, 14 pages, 2016.

[46] H. I. Kohn and M. Liversedge, "On a new aerobic metabolite whose production by brain is inhibited by apomorphine, emetine, ergotamine, epinephrine, and menadione," *The Journal of*

Pharmacology and Experimental Therapeutics, vol. 82, no. 1994, pp. 292–300, 1994.

[47] J. M. McCord and I. Fridovich, "Superoxide dismutase an enzymic function for erythrocuprein (hemocuprein)," *Journal of Biological Chemistry*, vol. 244, no. 22, pp. 6049–6055, 1969.

[48] P. W. Riddles, R. K. Andrews, R. L. Blakeley, and B. Zerner, "Jack bean urease VI. Determination of thiol and disulfide content: reversible inactivation of the enzyme by the blocking of the unique cysteine residue," *Biochimica et Biophysica Acta (BBA) - Protein Structure and Molecular Enzymology*, vol. 743, no. 1, pp. 115–120, 1983.

[49] H. Esterbauer and K. H. Cheeseman, "Determination of aldehydic lipid peroxidation products: malonaldehyde and 4-hydroxynonenal," *Methods in Enzymology*, vol. 186, pp. 407–421, 1990.

[50] L. C. Green, D. A. Wagner, J. Glogowski, P. L. Skipper, J. S. Wishnok, and S. R. Tannenbaum, "Analysis of nitrate, nitrite, and (^{15}N) nitrate in biological fluids," *Analytical Biochemistry*, vol. 126, no. 1, pp. 131–138, 1982.

[51] M. M. Bradford, "A rapid and sensitive method for the quantitation of microgram quantities of protein utilizing the principle of protein-dye binding," *Analytical Biochemistry*, vol. 72, no. 1-2, pp. 248–254, 1976.

[52] H. Kühn and A. Borchert, "Regulation of enzymatic lipid peroxidation: the interplay of peroxidizing and peroxide reducing enzymes," *Free Radical Biology and Medicine*, vol. 33, no. 2, pp. 154–172, 2002.

[53] S. T. Paolinelli, R. Reen, and T. Moraes-Santos, "Curcuma longa ingestion protects in vitro hepatocyte membrane peroxidation," *Revista Brasileira de Ciências Farmacêuticas*, vol. 42, no. 3, pp. 429–435, 2006.

[54] H. Ishii, F. Okuno, Y. Shigeta, and M. Tsuchiya, "Enhanced serum glutamic oxaloacetic transaminase activity of mitochondrial origin in chronic alcoholics," *Currents in Alcoholism*, vol. 5, pp. 101–108, 1979.

[55] A. Mansouri, C. Demeilliers, S. Amsellem, D. Pessayre, and B. Fromenty, "Acute ethanol administration oxidatively damages and depletes mitochondrial DNA in mouse liver, brain, heart, and skeletal muscles: protective effects of antioxidants," *The Journal of Pharmacology and Experimental Therapeutics*, vol. 298, no. 2, pp. 737–743, 2001.

[56] J. B. Miñana, L. Gómez-Cambronero, A. Lloret et al., "Mitochondrial oxidative stress and CD95 ligand: a dual mechanism for hepatocyte apoptosis in chronic alcoholism," *Hepatology*, vol. 35, no. 5, pp. 1205–1214, 2002.

[57] E. Baraona and C. S. Lieber, "Effects of ethanol on lipid metabolism," *Journal of Lipid Research*, vol. 20, no. 3, pp. 289–315, 1979.

[58] Y. Choi, M. A. Abdelmegeed, and B. J. Song, "Preventive effects of indole-3-carbinol against alcohol-induced liver injury in mice via antioxidant, anti-inflammatory, and anti-apoptotic mechanisms: role of gut-liver-adipose tissue axis," *The Journal of Nutritional Biochemistry*, vol. 55, pp. 12–25, 2018.

[59] I. Olmez and H. Ozyurt, "Reactive oxygen species and ischemic cerebrovascular disease," *Neurochemistry International*, vol. 60, no. 2, pp. 208–212, 2012.

[60] H. Lacaille, D. Duterte-Boucher, D. Liot, H. Vaudry, M. Naassila, and D. Vaudry, "Comparison of the deleterious effects of binge drinking-like alcohol exposure in adolescent and adult mice," *Journal of Neurochemistry*, vol. 132, no. 6, pp. 629–641, 2015.

[61] F. Nogales, R. M. Rua, M. L. Ojeda, M. L. Murillo, and O. Carreras, "Oral or intraperitoneal binge drinking and oxidative balance in adolescent rats," *Chemical Research in Toxicology*, vol. 27, no. 11, pp. 1926–1933, 2014.

[62] A. I. Cederbaum, "Alcohol metabolism," *Clinics in liver Disease*, vol. 16, no. 4, pp. 667–685, 2012.

[63] F. T. Crews and K. Nixon, "Mechanisms of neurodegeneration and regeneration in alcoholism," *Alcohol and Alcoholism*, vol. 44, no. 2, pp. 115–127, 2009.

[64] J. Haorah, S. H. Ramirez, N. Floreani, S. Gorantla, B. Morsey, and Y. Persidsky, "Mechanism of alcohol-induce oxidative stress and neuronal injury," *Free Radical Biology and Medicine*, vol. 45, no. 11, pp. 1542–1550, 2008.

[65] D. Filipovic, N. Todorovic, R. E. Bernardi, and P. Gass, "Oxidative and nitrosative stress pathways in the brain of socially isolated adult male rats demonstrating depressive- and anxiety-like symptoms," *Brain Structure and Function*, vol. 222, no. 1, pp. 1–20, 2016.

[66] S. Zakhari, "Overview: how is alcohol metabolized by the body?," *Alcohol research and health*, vol. 29, no. 4, pp. 245–254, 2006.

[67] E. R. Kandel, J. H. Schwartz, T. M. Jessell, S. A. Siegelbaum, A. J. Hudspeth, and A. J. Hudspeth, *Principles of Neural Science*, McGraw Hill Medical, eBook Kindle, 5th edition, 2013.

[68] M. B. Acevedo, R. M. Pautassi, N. E. Spear, and L. P. Spear, "Age-dependent effects of stress on ethanol-induced motor activity in rats," *Psychopharmacology*, vol. 230, no. 3, pp. 389–398, 2013.

[69] C. E. Van Skike, P. Botta, V. S. Chin et al., "Behavioral effects of ethanol in cerebellum are age dependent: potential system and molecular mechanisms," *Alcoholism, Clinical & Experimental Research*, vol. 34, no. 12, pp. 2070–2080, 2010.

[70] M. Pascual, P. Baliño, S. Alfonso-Loeches, C. M. Aragón, and C. Guerri, "Impact of TLR4 on behavioral and cognitive dysfunctions associated with alcohol-induced neuroinflammatory damage," *Brain, Behavior, and Immunity*, vol. 25, Supplement 1, pp. S80–S91, 2011.

[71] K. Matsuura, H. Kabuto, H. Makino, and N. Ogawa, "Pole test is a useful method for evaluating the mouse movement disorder caused by striatal dopamine depletion," *Journal of Neuroscience Methods*, vol. 73, no. 1, pp. 45–48, 1997.

[72] T. Matsuwaki, K. Yamanouchi, and M. Nishihara, "The effect of glucocorticoids on bradykinesia induced by immobilization stress," *Hormones and Behavior*, vol. 54, no. 1, pp. 41–46, 2008.

[73] D. J. Brooks, "Functional imaging of Parkinson's disease: is it possible to detect brain areas for specific symptoms?," in *Diagnosis and Treatment of Parkinson's Disease — State of the Art*, H. Przuntek and T. Müller, Eds., vol. 56 of Journal of Neural Transmission. Supplementum, pp. 139–153, Springer, Vienna, 1999.

[74] S. T. Grafton, "Contributions of functional imaging to understanding parkinsonian symptoms," *Current Opinion in Neurobiology*, vol. 14, no. 6, pp. 715–719, 2004.

[75] P. Curzon, M. Zhang, R. J. Radek, and G. B. Fox, "Chapter 8. The behavioral assessment of sensorimotor processes in the mouse: acoustic startle, sensory gating, locomotor activity, rotarod, and beam walking," in *Methods of behavior analysis in neuroscience*, J. J. Buccafusco, Ed., CRC Press/Taylor & Francis, Boca Raton, FL, USA, 2nd edition, 2009.

[76] K. Kurata, "Information processing for motor control in primate premotor cortex," *Behavioural Brain Research*, vol. 61, no. 2, pp. 135–142, 1994.

[77] D. G. Nair, K. L. Purcott, A. Fuchs, F. Steinberg, and J. A. Kelso, "Cortical and cerebellar activity of the human brain during imagined and executed unimanual and bimanual action sequences: a functional MRI study," *Cognitive Brain Research*, vol. 15, no. 3, pp. 250–260, 2003.

[78] T. L. Chuck, P. J. McLaughlin, M. N. Arizzi-Lafrance, J. D. Salamone, and M. Correa, "Comparison between multiple behavioral effects of peripheral ethanol administration in rats: sedation, ataxia, and bradykinesia," *Life Sciences*, vol. 79, no. 2, pp. 154–161, 2006.

[79] J. C. Crabbe, P. Metten, C. H. Yu, J. P. Schlumbohm, A. J. Cameron, and D. Wahlsten, "Genotypic differences in ethanol sensitivity in two tests of motor incoordination," *Journal of Applied Physiology*, vol. 95, no. 4, pp. 1338–1351, 2003.

[80] T. Möykkynen and E. R. Korpi, "Acute effects of ethanol on glutamate receptors," *Basic & Clinical Pharmacology & Toxicology*, vol. 111, pp. 4–13, 2012.

[81] V. Vengeline, A. Bilbao, A. Molander, and R. Spanagel, "Neuropharmacology of alcohol addiction," *British Journal of Pharmacology*, vol. 154, no. 2, pp. 299–315, 2008.

[82] S. Hartwig, V. Auwärter, and F. Pragst, "Fatty acid ethyl esters in scalp, pubic, axillary, beard and body hair as markers for alcohol misuse," *Alcohol and Alcoholism*, vol. 38, pp. 163–167, 2003.

[83] S. Muñiz-Hernández, J. B. Velázquez-Fernández, J. Díaz-Chávez, R. C. López-Sánchez, J. A. Hernández, and A. Rendón-Ramírez, "Alcoholism: common and oxidative damage biomarkers," *Journal of Clinical Toxicology*, vol. S7, no. 1, p. 6, 2014.

Hindawi
Oxidative Medicine and Cellular Longevity
Volume 2018, Article ID 4982453, 28 pages
https://doi.org/10.1155/2018/4982453

Review Article

Epigenetic Effects Induced by Methamphetamine and Methamphetamine-Dependent Oxidative Stress

Fiona Limanaqi,[1] **Stefano Gambardella**,[2] **Francesca Biagioni**,[2] **Carla L. Busceti**,[2] **and Francesco Fornai**[1,2]

[1]*Human Anatomy, Department of Translational Research and New Technologies in Medicine and Surgery, University of Pisa, Via Roma 55, Pisa, Italy*
[2]*IRCCS Neuromed, Via Atinense, Pozzilli, Italy*

Correspondence should be addressed to Francesco Fornai; francesco.fornai@med.unipi.it

Received 19 April 2018; Accepted 10 June 2018; Published 22 July 2018

Academic Editor: Margherita Neri

Methamphetamine is a widely abused drug, which possesses neurotoxic activity and powerful addictive effects. Understanding methamphetamine toxicity is key beyond the field of drug abuse since it allows getting an insight into the molecular mechanisms which operate in a variety of neuropsychiatric disorders. In fact, key alterations produced by methamphetamine involve dopamine neurotransmission in a way, which is reminiscent of spontaneous neurodegeneration and psychiatric schizophrenia. Thus, understanding the molecular mechanisms operated by methamphetamine represents a wide window to understand both the addicted brain and a variety of neuropsychiatric disorders. This overlapping, which is already present when looking at the molecular and cellular events promoted immediately after methamphetamine intake, becomes impressive when plastic changes induced in the brain of methamphetamine-addicted patients are considered. Thus, the present manuscript is an attempt to encompass all the molecular events starting at the presynaptic dopamine terminals to reach the nucleus of postsynaptic neurons to explain how specific neurotransmitters and signaling cascades produce persistent genetic modifications, which shift neuronal phenotype and induce behavioral alterations. A special emphasis is posed on disclosing those early and delayed molecular events, which translate an altered neurotransmitter function into epigenetic events, which are derived from the translation of postsynaptic noncanonical signaling into altered gene regulation. All epigenetic effects are considered in light of their persistent changes induced in the postsynaptic neurons including sensitization and desensitization, priming, and shift of neuronal phenotype.

1. Introduction

1.1. Molecular Mechanisms of Methamphetamine. Methamphetamine (METH) is a widely abused psychostimulant with powerful addictive and neurotoxic properties. This compound rapidly enters and persists within the central nervous system (CNS) [1, 2]. In fact, METH has a long half-life, which ranges from 10 to 12 hours [3]. METH kinetics within the ventral striatum parallel the time course of being "high" felt by METH users, who in fact, experience euphoria along with motor stimulation, excitation, increased energy, active waking state, sleeplessness, and alertness [4–6]. Such acute behavioral effects are due to early neurochemical events produced by METH, which consist in a rapid release of monoamines, mainly dopamine (DA), from nerve terminals. This occurs mostly within the striatum, where DA terminals are mostly abundant, though specific limbic regions and isocortical areas are involved as well [7–11]. The cellular effects induced by METH may be roughly summarized by its interaction with three molecular targets: (1) the synaptic vesicles and vesicular monoamine transporter type-2 (VMAT-2) (Figure 1). VMAT-2 belongs to the VMAT class of vesicular membrane proteins, which exist in two distinct forms, namely, VMAT1 and VMAT2. Both isoforms are responsible for the selective recognition and transport of cytosolic monoamines DA, norepinephrine (NE), and serotonin (5-hydroxytryptamine (5-HT)) within synaptic vesicles [12]. VMAT-2 and VMAT-1 are expressed in both

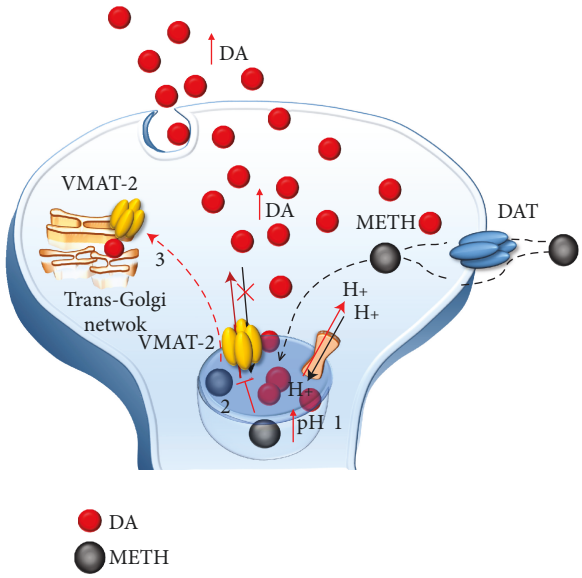

Figure 1: The effects of METH on DA-storing vesicles. METH enters into DA terminals either through the plasma membrane DAT or via passive diffusion. Within the axoplasm, it targets DA-storing vesicles to (1) disrupt their proton gradient, (2) inhibit and revert VMAT-2, and (3) displace VMAT-2 elsewhere (i.e., trans-Golgi network). These effects disrupt the physiological storage of DA, which diffuses from vesicles to the axoplasm and from the axoplasm to the extracellular space.

neuronal and nonneuronal cells such as the chromaffin cells of the adrenal medulla. However, VMAT-2 prevails in the brain where it has a higher affinity for DA and NE compared with VMAT-1 [12]. VMAT-2 plays a key role in cytosolic DA homeostasis and release, since it guarantees the vesicular packaging and storage of both newly synthesized and synapse-recycled DA; (2) the plasma membrane DA transporter (DAT) (Figure 2), which selectively takes up extracellular DA within DA terminals; and (3) the monoamine oxidase (MAO) enzyme (Figure 3), which is the main intracellular enzyme responsible for the oxidative deamination of DA, NE, and 5-HT. MAOs exist as two different isoforms, MAO-A and MAO-B, which are placed at the level of the outer mitochondrial membrane of distinct vcell populations in the CNS [13]. In fact, MAO-A are present within catecholamine-containing neurons (DA, NE, and Epinephrine neurons), whereas MAO-B occur mainly in 5-HT cells and glia. Thus, the presence of MAO-A within DA terminals is crucial for the oxidative metabolism of intracellular DA, which together with VMAT-2 and DAT mediating DA uptake within the nerve terminals and within synaptic vesicles, respectively, represent the most powerful system to surveil DA activity. The activities of all these proteins are impaired by METH, once it enters the DA terminals via either passive diffusion or DAT.

In detail, at the level of synaptic vesicles, METH produces a variety of effects, which before affecting VMAT-2, are key in releasing DA (Figure 1). These effects are summarized as follows: (1) disruption of the proton gradient through the DA-storing vesicles due to the high pKa (pKa = 10.1) of METH, which rises the acidic compartment towards basic values, thus making nonpolar DA freely diffusible out of the vesicles [14–16]; (2) direct inhibition of VMAT-2 [17, 18], which prevents DA from reentering the vesicles; and (3) redistribution of VMAT-2 molecular complex from vesicle membranes to noncanonical membrane compartments such as those of the trans-Golgi network [19, 20], where DA may be inappropriately, though poorly, stored. The loss of physiological DA storage generates massive DA extravesicular levels within DA axons [21, 22] (Figure 1). It is noteworthy that a combined effect of METH as a weak base to tone down the pH gradient needs to be accompanied by a selective effect on VMAT-2 since alkalinization per se may be nonsufficient to fully produce the typical redistribution of vesicular DA [16]. This is confirmed by administering bafilomycin, which acts as a proton pump inhibitor only, with no effects on VMAT-2. Despite decreasing the pH ratio vesicle/cytoplasm 2-fold more than METH, bafilomycin redistributes only half of METH-induced DA levels in the extracellular compartment [23]. Once in the cytosol, METH also acts at the level of mitochondria (Figure 3) where two targets are affected: (4) METH inhibits complex II at the mitochondrial respiratory chain [24] and (5) METH inhibits MAO-A placed on the outer mitochondrial membrane [13]. This latter effect occurs as a competitive inhibition of METH upon MAO-A with a 10-fold higher affinity compared with MAO-B [13]. In both mice and humans, MAO-A are quite selectively placed within DA terminals. This is key since within DA terminals, MAO-A are coupled with aldehyde dehydrogenase (AD), which converts the highly reactive by-product of DA oxidation (3,4-dihydroxyphenylacetaldehyde (DOPALD)) into the quite inert 3,4-dihydroxyphenylacetic acid (DOPAC). The impairment of MAO-A may also include uncoupling between MAO-A and AD [25] (Figure 4).

In the absence of such a compartmentalized physiological oxidative deamination, DA autooxidation produces a high amount of reactive aldehyde DOPALD, which owns a

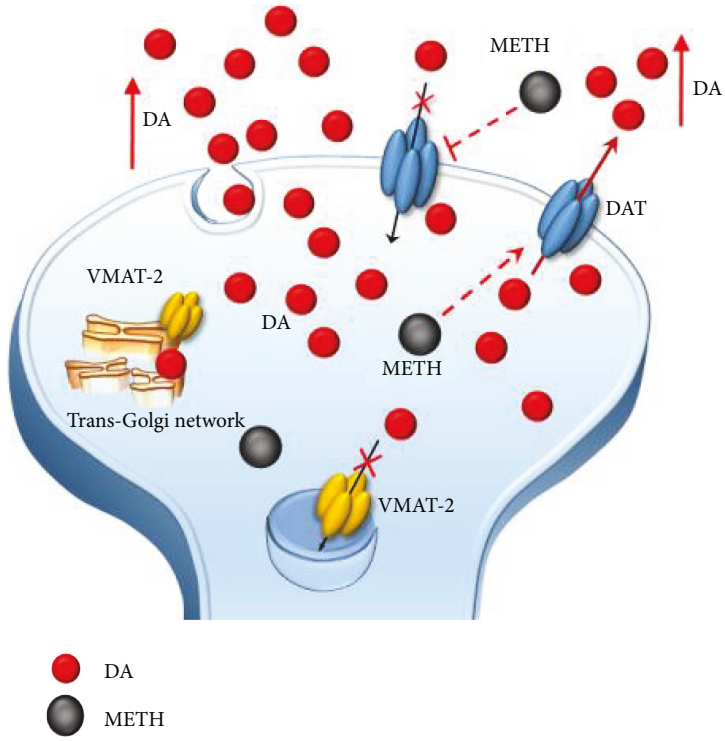

Figure 2: The effects of METH on DAT. METH impairs DAT activity either via direct inhibition or via reverting its direction. Such an effect potentiates the accumulation of freely diffusible DA in the extracellular space and prevents the main mechanisms of DA removal (reuptake within DA terminals).

dramatic oxidative potential and quickly interacts with surrounding proteins, by targeting oxidation-prone domains [25, 26]. Autooxidative DA metabolism leads to the generation of toxic quinones and highly reactive chemical species such as hydrogen peroxide (H_2O_2) and superoxide radicals, which in turn react with sulfhydryl groups and promote structural modifications of proteins, lipids, and nucleic acids within the DA axon terminals and surrounding compartments (Figure 5) [15, 27–39].

On the one hand, these effects drive a powerful oxidative stress for presynaptic DA terminals, which is key in producing nigrostriatal toxicity [27–31, 34, 40–43]. On the other hand, elevated cytosolic presynaptic DA diffuses in the extracellular space either by passive diffusion or via the reverted direction of DAT, another molecular effect which is promoted by METH (Figures 1–5) [14, 16, 33, 44]. All these effects also cause peaks of extracellular DA concentration, which produce synaptic effects at short distance. At striatal level, this paracrine environment encompasses medium-sized spiny neurons (MSNs). Nonetheless, due to the propensity of extracellular DA to diffuse at considerable distance from the DA terminals according to a volume transmission [45–47], other extrasynaptic sites may be affected as well. Such a paracrine spreading of extracellular DA is magnified during METH administration, since METH reverts DA uptake [33], thus preventing the main mechanisms of DA removal. This produces unusually high extracellular (and mostly striatal) DA levels which reach out nonneuronal targets including the neurovascular unit, which is also affected by METH administration [48, 49]. Intriguingly, the role of MAO-B enzymes in extracellular DA metabolism remains to be clearly established. In fact, although they occur outside DA cells, mainly within glia (Figures 3–5), they do not influence much the amount of extracellular DA [25, 50–53]. It is worth of noting that pulsatile METH intake/administration produces considerable oscillations of extracellular DA, which ranges from high peaks (exceeding 10-fold baseline levels) to severe deficiency (no detectable extracellular levels in brain dialysis techniques) within just a few hours [38, 54–56]. This pulsatile pattern of extracellular DA concentrations magnifies the slight variations produced by physiological release, such that, METH produces an abnormal stimulation (all and none) of postsynaptic neurons. For instance, pulsatile activation of postsynaptic DA receptors triggers noncanonical transduction pathways, which, along with the diffusion of abnormal reactive oxygen (ROS) and nitrogen (RNS) species, alter the response of postsynaptic neurons as mainly studied at the level of GABA MSNs [57–59] (Figure 6).

The impact of such a nonphysiological (in time, amount, and place) DA release is largely to blame when considering both the behavioral syndrome occurring immediately after METH intake and long-term behavioral changes including addiction, craving, relapse, and psychotic episodes, which reflect mainly the persistent alterations in postsynaptic DA brain regions following chronic METH exposure. As we shall see, overstimulation of postsynaptic DA receptors alternating with a lack of stimulation within an abnormal redox context drives most epigenetic effects. After mentioning the presynaptic effects of METH (to understand the role of redox species in causing the loss of integrity of DA axon terminals),

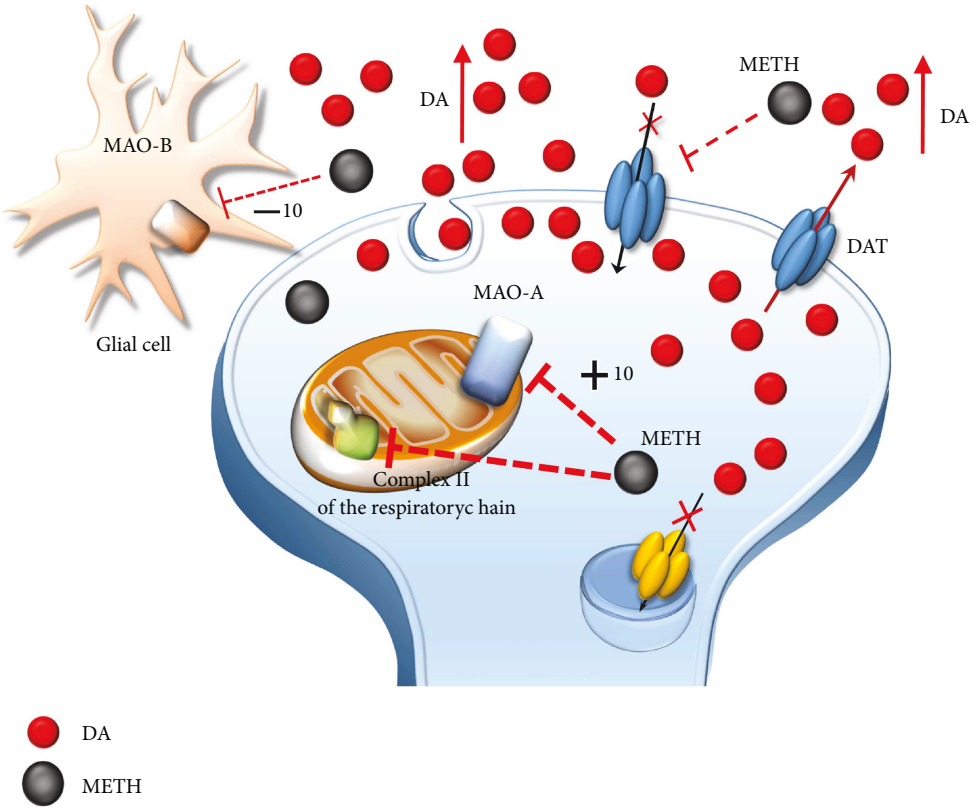

Figure 3: The effects of METH on mitochondria. METH impairs the activity of complex II of the mitochondrial respiratory chain and directly inhibits MAO-A placed on the outer mitochondrial membrane within DA terminals. METH also inhibits MAO-B placed extracellularly at the level of glia. However, the affinity of METH for MAO-B is tenfold less when compared with MAO-A. Thus, MAO-B inhibition does not influence that much the amount of extracellular DA.

the present review discusses the postsynaptic changes in relationship with epigenetics, DNA alterations, and persistent phenotypic changes produced by METH.

2. Presynaptic Effects of METH

In the present section, we wish to mention that METH produces presynaptic toxicity within DA terminals. As thoroughly revised by Moratalla et al. [34], the neurotoxic effects of high doses of METH, which occur both in a variety of experimental models and human abusers, are due to an excess of intracellular mostly DA-related, oxidative cascade (Figure 5). At first, such a toxicity was considered to be relevant only for DA axon terminals. Such neurotoxicity is documented by the following markers: (i) a steady decrease in striatal DA levels and striatal DA uptake sites [54, 60–63], (ii) loss of tyrosine hydroxylase (TH)-activity, TH immunoblotting and TH immunohistochemistry [64–71], and most directly, (iii) the occurrence of silver-stained (Fink-Heimer method) [61, 62] or amino-cupric silver-stained (de Olmos procedure) degenerating nerve fibers within the striatum [72]. Some studies also indicate the occurrence of METH-induced toxicity at the level of neuronal cell bodies in the substantia nigra pars compacta (SNpc). This was firstly reported by Sonsalla et al. [63], although this study was based on TH immunohistochemistry (which does not necessarily reflect an actual cell loss) and Nissl staining (with neither stereological counts nor positive evidence for a damage of the cell body). Further studies confirmed a loss of mesencephalic DA neurons even within the ventral tegmental area [67], but again, no stereological count was carried out. Other studies provided indirect evidence of cell death (TH immunohistochemistry, TUNEL assay, Fluoro-Jade B, or Nissl staining) [69–71, 73]. In a recent manuscript by Ares-Santos et al. [72], neuronal cell death of TH-positive neurons was visualized directly by using cupric silver staining (modified according to Beltramino and de Olmos). To our experience, a certain amount of cell loss is detectable only when very high doses of METH are administered, which corresponds to a loss of nigrostriatal DA terminals ranging over 80%, as demonstrated in the original article by Ares-Santos et al. [72]. Altogether, these findings are consistent with an increased risk to develop Parkinson's disease (PD), which is now quite well established in METH abusers [74–77]. Similarly to PD, METH produces neuronal inclusions in DA-containing PC12 cells and within SNpc neurons of mice [38, 78–84] as well as in humans [85]. These inclusions start as multilamellar whorls, which further develop as cytoplasmic inclusions reminiscent of PD-like Lewy bodies. In fact, these inclusions contain a high amount of ubiquitin and other proteins such as alpha-synuclein (α-syn), parkin, UchL1, and HSP70, which are typical markers of PD. Remarkably, most of these

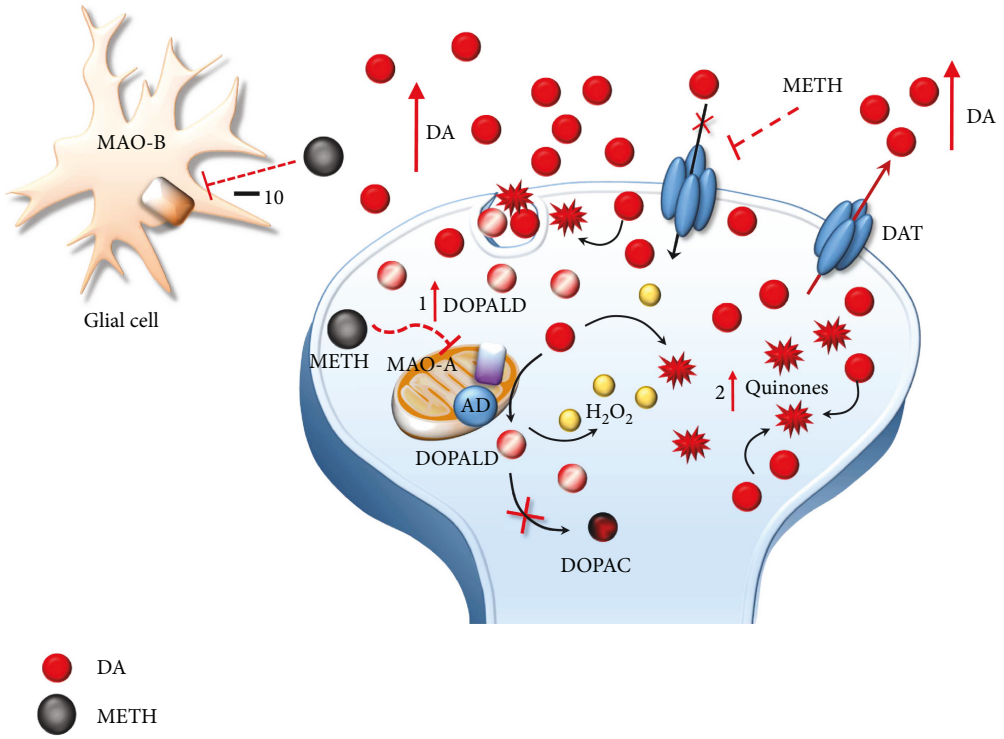

Figure 4: The effects of METH-induced MAO-A inhibition on DA metabolism. The loss of physiological DA deamination following MAO-A inhibition and its uncoupling with AD lead to the generation of highly reactive species including DOPALD (1), hydrogen peroxide (H_2O_2), and DA quinones (2).

proteins are substrates of ubiquitin proteasome- (UP-) and autophagy- (ATG-) clearing systems, which are markedly affected during METH toxicity (Figure 5) [38, 79–81, 83, 86].

3. Postsynaptic Effects of METH

METH effects on postsynaptic compartment are multifaceted. Even neurotoxicity may extend to postsynaptic neuronal cell bodies throughout the striatum, hippocampus, and frontal cortex [72, 73, 87–94]. A pioneer manuscript by Jakel and Maragos [95] discussed very well how activation of DA receptors on striatal neurons as well as DA-derived oxidative species and oxyradicals might all converge to accelerate striatal neuronal cell loss in a specific striatal neurodegenerative disorder such as Huntington disease (HD). In fact, DA itself, DA-derived free radicals, and glutamate- (GLUT-) induced excitotoxicity may synergize to produce detrimental metabolic and oxidative effects on postsynaptic non-DA neurons (Figure 6). As we shall see, the interaction between DA and GLUT, as well as the convergence of signaling cascades placed downstream plasma membrane receptors, may be enhanced under chronic METH intake. In fact, striatal postsynaptic neurons increase their responsivity to both DA and GLUT following specific patterns of chronic METH administration. Along with diffusion of free radicals, which fuel oxidative damage, the striatal compartment challenged by METH is filled with DA acting on its receptors. It is well known that overstimulation of D1-like DA receptors (mainly D1 DA receptors (DRD1)) leads to a switch in the transduction pathway towards noncanonical signaling, which, in turn, generates a number of adaptive biochemical events [96–101]. This is evident when considering that an altered DRD1 signaling produced by METH enhances corticostriatal excitation by activating GLUT receptors and potentiating GLUT release. In extreme conditions, this may produce excitotoxicity within striatal GABA neurons [102–107]. In fact, increased extracellular GLUT and activation of its N-methyl-d-aspartate (NMDA) receptors promote calcium (Ca2+) entry within neurons as well as activation of nitric oxide synthase (NOS), which trigger an enzymatic cascade further increasing reactive oxygen species (ROS) and nitrogen species (RNS) [108–111]. Thus, following METH administration, GLUT synergizes with DA to produce oxidative stress, mitochondrial dysfunction, and inflammatory reactions, which synergistically interact to promote neuronal damage (Figure 6) [34, 42, 43, 109]. In line with this, cell inclusions filled with oxidized substrates are also detectable in the cytoplasm and within the nuclei of striatal GABAergic MSNs due to an overstimulation of DRD1 under METH administration [38]. This suggests that DA, acting on DRD1 joined with DA-derived free radicals, altogether may alter even nuclear signaling within GABA cells (Figure 6) [99]. Such an effect is expected to significantly alter DNA stability [29, 110–116].

Even the occurrence of striatal cytoplasmic inclusions within MSNs is likely to be due to combined mechanisms. In fact, it is well known that oxidative stress alters cell clearing systems, which is a seminal step in the generation of inclusion bodies containing oxidized/aggregated proteins [95, 117, 118]. At the same time, administration of DRD1

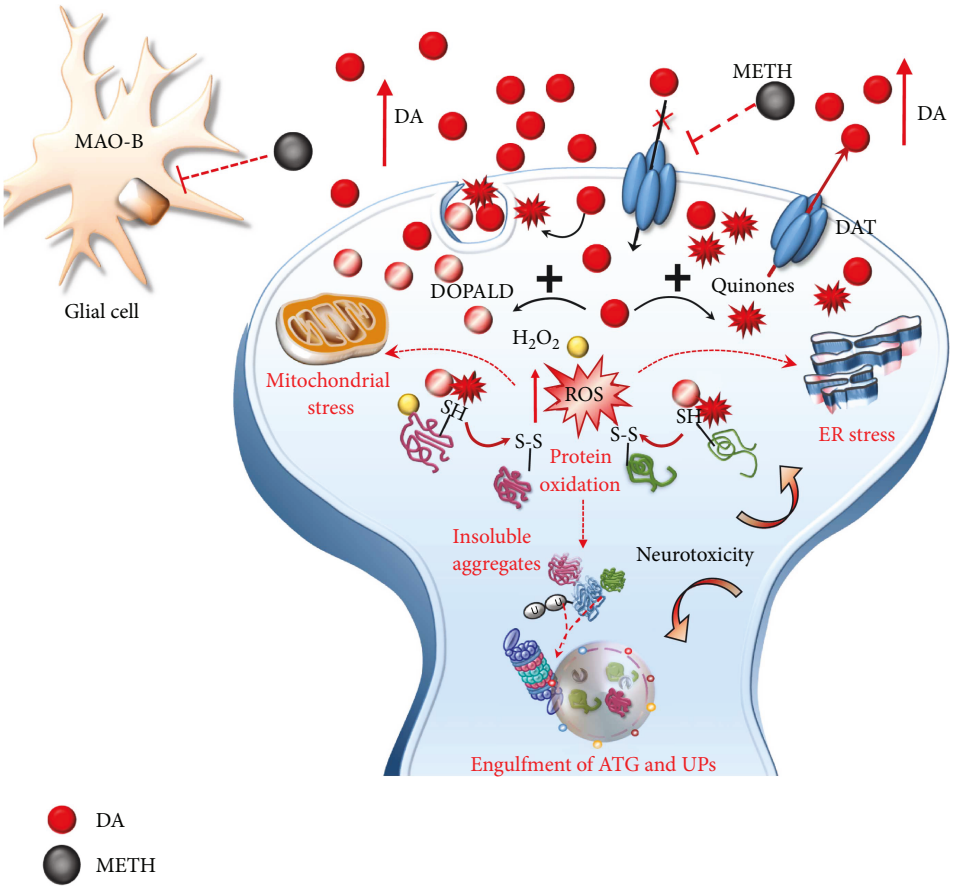

Figure 5: METH induces oxidative stress within DA terminals. Toxic DA by-products (quinones and DOPALD) together with highly reactive species such as H_2O_2 and reactive oxygen species (ROS) react with sulfhydryl groups and promote structural modifications of proteins within the DA axon terminals. The enhanced redox imbalance also disrupts the homeostasis of endoplasmic reticulum (ER) and mitochondria, which further accelerates the production of ROS. Thus, an excessive amount of misfolded/insoluble proteins and damaged organelles occurs, which leads to an engulfment of autophagy (ATG) and ubiquitin proteasome (UP) cell-clearing systems. These events converge in producing neurotoxicity within DA terminals, which may either extend to DA cell bodies.

agonists reproduces neuronal inclusions within MSNs [38], which are prevented by DRD1 antagonists [38, 82]. Nonetheless, both DRD1 antagonists/deletion of the DRD1 gene and antioxidant compounds can protect from METH-induced oxidative stress and cell injury and retard/counteract behavioral sensitization in experimental models [34, 71, 96, 97, 119–125]. In summary, the various effects of DRD1 receptor overstimulation and prooxidative processes produced by excessive DA release are likely to assemble and cooperate to produce long-lasting neurochemical changes following METH.

4. Transcriptional and Epigenetic Effects of METH

A number of papers explored the mechanisms operating at postsynaptic level to modify neuronal phenotype, in an effort to unravel potential strategies to counteract addiction. To such an aim, in the last decades, a number of studies focused on specific transduction pathways and genes activated by METH. Remarkably, studies of the last decade indicated a key role for epigenetic mechanisms in modulating the transcription of a number of genes, which underlie long-lasting behavioral alterations and biochemical events induced by METH abuse. A gap still exists concerning the signaling cascades through which METH may induce epigenetic changes via mechanisms going beyond a mere effect of DA-related oxidative stress. In the present section, studies focused on METH-induced epigenetic changes in both experimental models and human abusers are discussed. In Sections 4.1 and 4.2, we focus on the effects of METH on the abnormal DRD1-mediated biochemical cascade, subsequent recruitment of specific second messengers and redox-sensitive transcription factors (TFs), and altered expression of immediate early genes (IEGs). At last, in Section 4.3, we touch on the evidence about how epigenetic remodeling may alter gene transcription thereby producing persistent behavioral changes, which define METH addiction.

4.1. DA D1-Like Receptor-Mediated Biochemical Events Induced by METH. DA canonical signaling in the brain is mediated by five (DRD1–DRD5) G-protein-coupled receptors, which are grouped into two classes depending on which G-protein they are coupled to. D1-like receptors include DRD1 and DRD5 and they stimulate G_s and G_{olf} proteins,

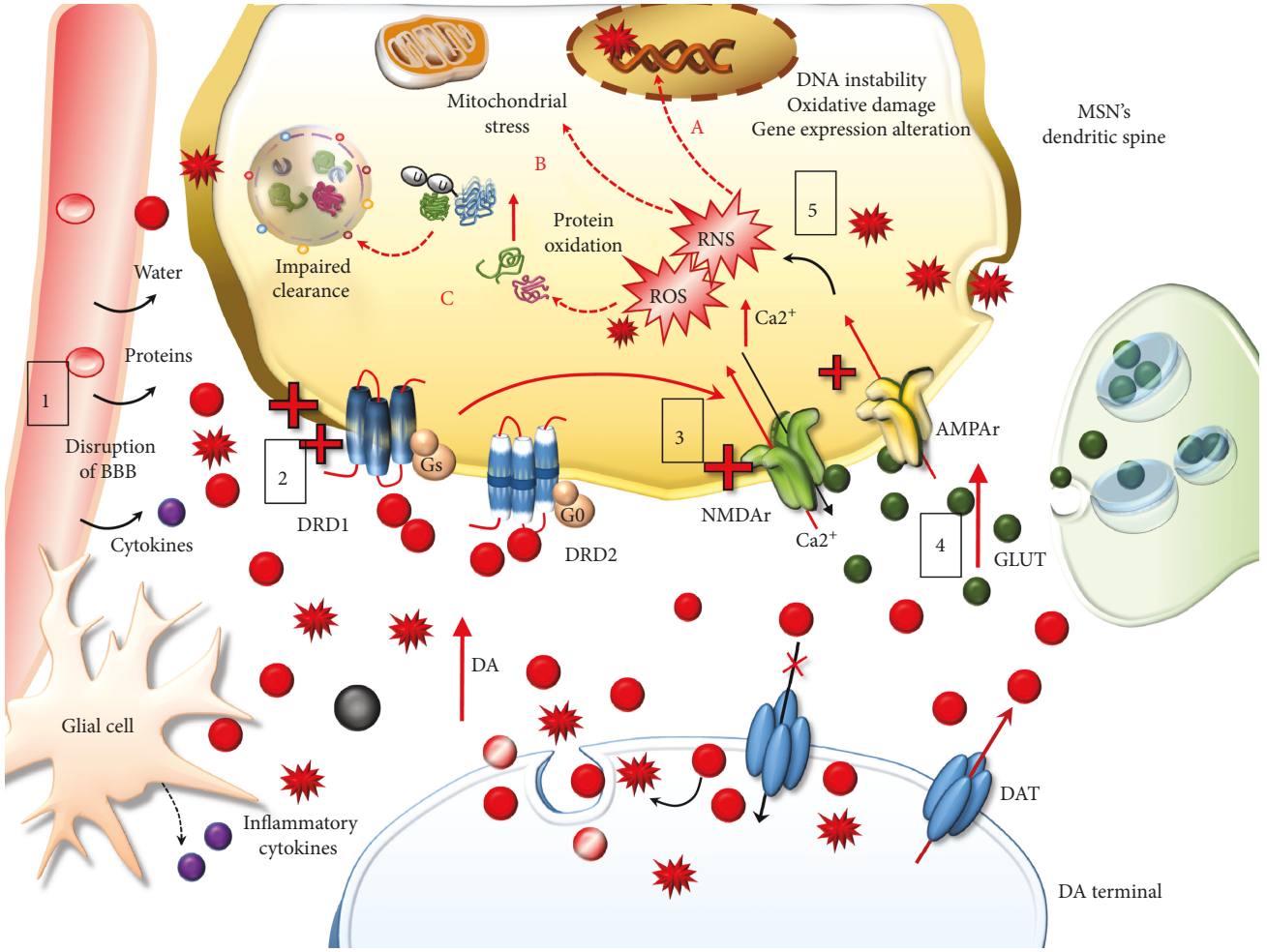

Figure 6: The effects of extracellular DA released following METH. Extracellular DA and DA-derived reactive species diffuse at considerable distance towards nonneuronal targets including the neurovascular unit (blood-brain barrier (BBB) and Glia), which is affected by METH (1). At short distance, METH produces an abnormal stimulation of postsynaptic neurons, mainly striatal MSNs. The pulsatile pattern of DA stimulation produces an abnormal pulsatile activation of postsynaptic DA D1 receptors (DRD1) (2). This leads to a series of noncanonical metabolic changes, which translate into activation of glutamate (GLUT) receptors N-methyl-d-aspartate and α-amino-3-hydroxy-5-methyl-4-isoxazolepropionic acid (NMDAr and AMPAr, resp.) (3) potentiation of GLUT release and Ca2+ entry within postsynaptic neurons (4). This event triggers an enzymatic cascade further increasing reactive oxygen species (ROS) and nitrogen species (RNS) (5). Freely diffusible DA-derived free radicals together with GLUT-derived radical species synergize to produce detrimental effects on postsynaptic non-DA neurons. These consist in DNA instability, due to oxidative damage (fragmentation and/strand breaks) and alterations in gene expression (A), mitochondrial stress (B), and oxidation of organic substrates, mainly proteins, which are prone to misfold and produce insoluble aggregates leading to an impairment of cell-clearing systems (C).

which activate adenylate cyclase (AC), thus elevating intracellular levels of cyclic adenosine monophosphate (cAMP) to increase protein kinase A (PKA) [126]. On the other hand, D2-like receptors (DRD2, DRD3, and DRD4) stimulate $G_{o/i}$ proteins [126] and they act by inhibiting AC [127]. Again, these receptors target voltage-dependent ion channels through a mechanism, which operates at the level of plasma membrane and phospholipase C (PLC) [128]. All five DA receptors are expressed in the striatum, but DRD1 and DRD2 are the most abundant, with the former being placed specifically within postsynaptic neurons and the latter being placed both presynaptically and postsynaptically (Figure 7).

For such a reason, DRD1 and DRD2 represent a cue investigation topic in the context of behavioral effects underlying drug addiction. However, the disruption of canonical DRD1 signaling is more important [57, 99, 129]. In fact, peaks and drops of DA stimulation generate the switch from canonical to noncanonical DRD1 signaling. This occurs during METH abuse in a way that is reminiscent of DA replacement therapy in advanced PD [57, 99, 130–139]. This kind of perturbation of DRD1 is the authentic drive to switch the DRD1 transduction pathway [59, 99, 131, 137]. Thus, in the presence of abnormal stimulation, DRD1 moves towards noncanonical signaling which makes MSNs supersensitive to DA stimulation despite that the number of DA receptors is not increased [99]. In fact, a chain of events follows DRD1 overstimulation, which involves metabolic transduction and transcriptional pathways, eventually switching

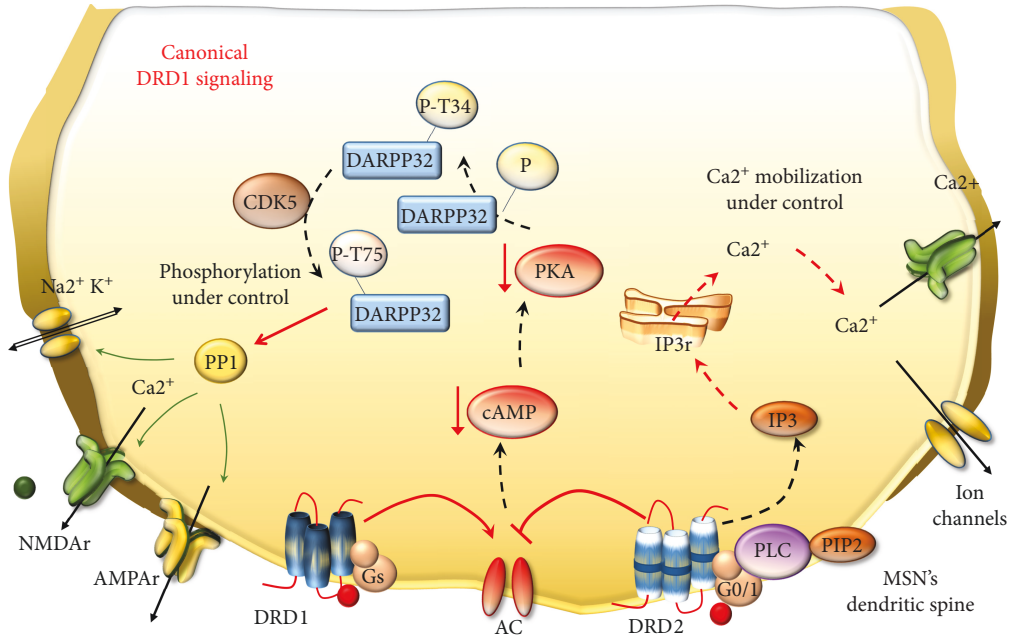

Figure 7: An overview of canonical DA receptor signaling. During physiologic DA stimulation, AC activity is balanced by the excitatory and inhibitory effects of DRD1 and DRD2, respectively. Thus, there is a physiologic downregulation of cAMP and PKA activation. PKA has a broad array of targets such as the DA- and cAMP-regulated phosphoprotein (DARPP-32), voltage-gated ion channels, and GLUT receptors. PKA phosphorylates DARPP-32 at Thr34 (P-T34), but other proteins, such as cyclin-dependent kinase 5 (CDK5), counterbalance such an effect by phosphorylating DARPP-32 at a different site (P-T75). Thus, DARPP-32 can activate phosphatase protein 1 (PP1), which can surveil phosphorylation levels of all PKA targets. Likewise, canonical stimulation of DRD2, which are coupled with PLC, generates normal levels of inositol 1,4,5 trisphosphate (IP3) which induces Ca2+ release from the endoplasmic reticulum. Since ion channels and GLUT receptors are properly functioning, intracellular Ca2+ can be efficiently mobilized.

gene expression and neuronal phenotype underlying addictive behavior in PD and METH [57, 59, 96–99, 119, 121, 132, 140–144]. Although precise signaling changes and substrates underlying this shift remain to be fully elucidated, a prominent role for AC [145] and PKA [146, 147] is well established (Figure 8). In fact, in its canonical pattern, PKA phosphorylates cellular targets, including voltage-dependent ion channels, GLUT receptors, TFs, and epigenetic enzymes involved in physiological synaptic plasticity and synaptic strength as naturally occurring in a normal striatum. When the noncanonical DRD1 transduction pathway is activated, PKA recruits mitogen-activated protein kinases (MAPKs) and extracellular signal-regulated kinases 1/2 (ERK1/2) [132, 148–153]. ERK1/2 proteins may translocate into the nucleus to phosphorylate and activate several TFs, such as the cAMP response element-binding protein (CREB), Elk-1, nuclear receptors, and H3 histones, which all regulate gene expression [152, 154–156]. A key substrate of DRD1/PKA signaling in the striatum is the DA- and cAMP-regulated phosphoprotein (DARPP-32). Following persistent METH-induced pulsatile DRD1 overstimulation, DARPP-32 is chronically enriched and abnormally phosphorylated in MSNs, where it serves neuroplastic changes and behavioral sensitization [155, 157–161]. In fact, DRD1-activated PKA directly phosphorylates DARPP-32 at threonine 34 (Thr34), which accumulates in the nucleus, where it may promote directly histone phosphorylation [162–164]. Moreover, phosphorylation at Thr34 induced by PKA converts DARPP-32 into a powerful inhibitor of protein phosphatase1 (PP1) [163], leading to abnormal PKA-mediated phosphorylation [129]. This eventually alters the very same substrates known to be affected by METH including (i) ion and voltage-gated channels and pumps, such as Ca2+ channels, Na^+ channels, Na^+, and K^+ ATPases [58, 59, 165]; (ii) GLUT receptors including α-amino-3-hydroxy-5-methyl-4-isoxazolepropionic acid (AMPA) and NMDA and their subunits GluR1 and NR1, respectively [166–173]; (iii) GLUT transporters VGLUT-1 and EAAT3 [174, 175]; (iv) GABA receptor subunits [176]; and (v) TFs, such as CREB [168] (Figure 8).

TFs, in turn, may either induce or suppress a number of downstream target genes. Noteworthy, noncanonical DRD1 stimulation initiates a vicious circle of reciprocal enhancement between DRD1 and GLUT receptor activities, since once activated, NMDA and AMPA receptors promote themselves a noncanonical phosphorylation of DARPP-32 and CREB in the striatum [168, 177]. These findings are in line with evidence showing that, following amphetamines, NMDAr and DRD1 synergistically activate ERK signaling within MSNs of the dorsal striatum and nucleus accumbens (NAc) [155]. Remarkably, regulation by DARPP-32 occurs both upstream of ERK and at the level of the downstream-activated striatal-enriched tyrosine phosphatase (STEP), which demonstrates its cyclic functional relevance [155]. In summary, ERK plays a primary role in mediating long-lasting effects of psychostimulants within the striatum (especially dorsal striatum and NAc). In fact, blockade of the ERK pathway or mutation of DARPP-32 alters locomotor

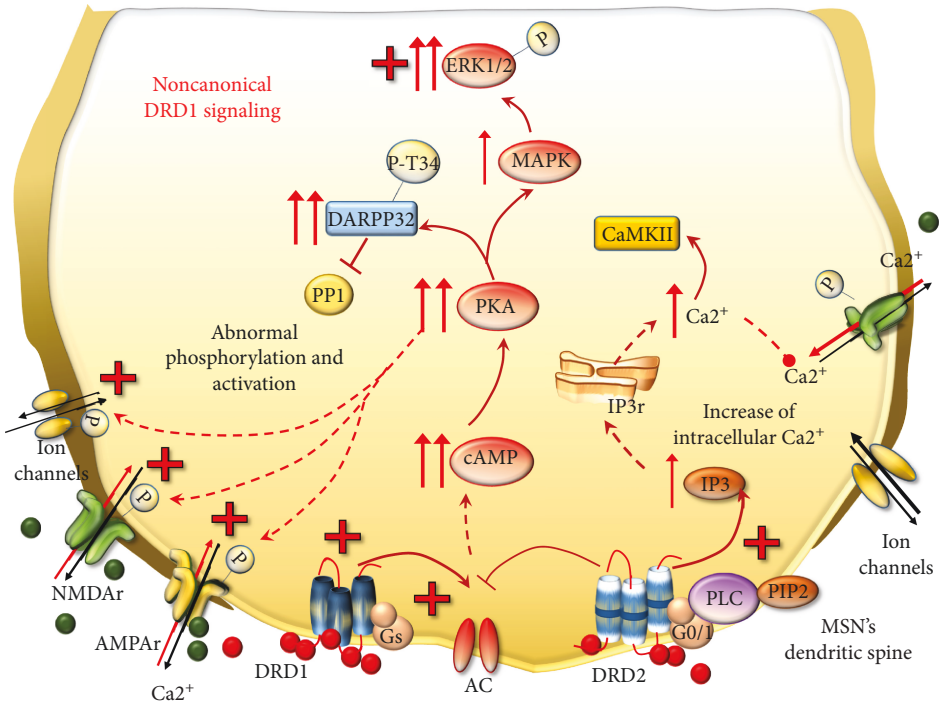

Figure 8: METH-induced noncanonical DRD1 signaling. Following METH, MSNs become supersensitive to pulsatile DA stimulation despite that the number of DA receptors is not increased. As a result, DRD1 move towards noncanonical signaling and the activity of DRD2 is enhanced. In these conditions, DRD1 overactivates AC, which enhances the production of cAMP and leads to abnormal activation of PKA. DRD1/PKA cascade turns out to increase the amount of DARPP-32 phosphorylated at Thr34, which inhibits PP1. Thus, all PKA targets, including voltage-gated ion channels and GLUT NMDAr and AMPAr, are abnormally phosphorylated and activated. In addition, DRD1/PKA leads to increased levels of MAPK and ERK1/2, which in turn phosphorylate several cytosolic and nuclear substrates. At the same time, DRD2-enhanced activity potentiates the increase of intracellular Ca2+ release, which cannot be properly mobilized, since ion channels and GLUT receptors are abnormally activated and potentiate the influx of Ca2+ within postsynaptic neurons. Such an event also promotes the activation of calmodulin-dependent kinase II (CaMKII), which can translocate into the nucleus to regulate gene expression.

sensitization induced by amphetamines [155]. Altered signaling during DRD1 overstimulation also applies to cyclin-dependent kinase 5 (CDK5), which is recruited by both DRD1 and NMDAr in the striatum [178]. In physiological conditions, CDK5 phosphorylates DARPP-32 at threonine 75 (Thr75), thus inhibiting the phosphorylation of Thr34 carried out by PKA [157, 179, 180]. The decreased phosphorylation of DARPP-32 at Thr34 could decrease PKA activity; however, in the context of noncanonical signaling, there is an activation of phosphatase protein PP2A, which in turn dephosphorylates DARPP-32 at Thr75. In this way, PKA activity turns out to inhibit CDK5-DARPP-32/Thr75 activity [163, 181]. Such a switch is typical of noncanonical DRD1 signaling triggered by DRD1/PKA pulsatile activation. Therefore, in the presence of DRD1 overstimulation, a sustained CDK5-mediated mechanism would fuel, rather than dampen, the phosphorylation of DARPP-32 at Thr34 (Figure 9).

In this way, the cyclic signaling pathway of CDK5 and DARPP-32 in the striatum represents an endogenous feedback mechanism, which is likely to enhance the phosphorylation of various substrates thus sustaining the sensitized behaviors produced by reiteration of pulsatile DRD1/PKA stimulation. In line with this, the activity of CDK5 is implicated in motor- and reward-related behaviors following drug abuse including METH [160, 178, 182, 183].

In addition to the mechanism described above, DRD1 signaling may also activate PLC to generate inositol 1,4,5 trisphosphate (IP3) which participates in Ca2+-regulated signaling pathways [184–187]. In fact, DA was reported to generate robust intracellular Ca2+ oscillations in about 40% of striatal MSNs via a DRD1-dependent mechanism involving both PKA and PLC [184]. Nonetheless, recent studies indicate the existence of DRD1-DRD2 heterodimers that require a coincident activation of both receptors for intracellular Ca2+ release. This is coupled with activation of a calmodulin-dependent kinase II (CaMKII), which translocates in the nucleus to regulate gene expression [185–187]. Taken together, these observations suggest that multiple interactions exist between PKA, PLC, and intracellular Ca^{2+} transduction mechanisms within DRD1-expressing striatal MSNs. In response to neurotransmitter receptor activation and enhanced oxidative stress, specific TFs are recruited to regulate gene transcription. These TFs are often present within large protein complexes, which bind to a specific DNA sequence corresponding to promoter or enhancer regions of target genes. In the next paragraph, we will focus on those TFs and genes recruited during METH

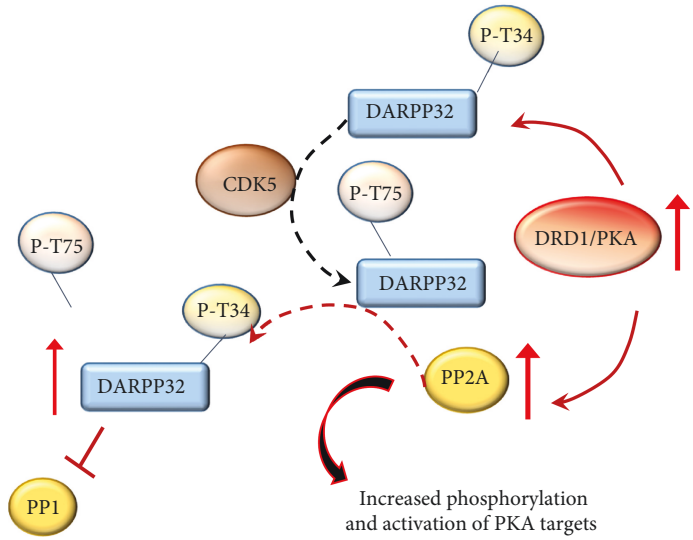

Figure 9: The effects of DRD1/PKA pathway on CDK5 and DARPP-32. In physiologic conditions, CDK5 phosphorylates DARPP-32 at Th75, thus softening the effects of PKA on DARPP-32. However, the abnormal phosphorylation of Thr34 carried out by enhanced DRD1/PKA cannot be counterbalanced by CDK5. This occurs since DRD1/PKA activates phosphatase PP2A, which inhibits the effects of CDK5 and enhances those of PKA. As a result, DARPP-32 phosphorylated at Thr34 increases and potentiates the inhibition of PP1.

administration according to the biochemical pathways we just described.

4.2. Transcription Factors and Immediate Early Genes (IEGs) Induced by METH. The cascade of biochemical events mediated by the combined effects of DA and oxidative species following METH administration activates a plethora of TF families beyond CREB, encompassing activator protein 1 (AP-1), early growth response (Egr) proteins, Elk-1, nuclear factor of activated T-cells (NFAT), nuclear factor κB (NFκB), which modulate the expression of several IEGs [98, 100, 110, 122, 123, 125, 154, 188–198]. By definition, IEGs undergo early synthesis and they can associate to form a variety of homo- and heterodimers binding to common DNA sites to regulate further gene expression. This leads to a variety of plastic effects ranging from neuronal metabolism to neuromorphology. In line with this, METH alters the expression of a multigene machinery coding for proteins involved in signal transduction, metabolic pathways, and transcriptional regulation. This alters protein expression and alters the amount of inflammatory cytokines, neuropeptides, and trophic factors (mainly brain-derived neurotrophic factor (BDNF)), as well as oxidative-, mitochondrial-, and endoplasmic reticulum stress-related events and proapoptotic cascades [91, 122, 125, 197–210]. DA-related events and oxidative mechanisms converge to alter TF expression following METH (Figure 10).

On the one hand, DA per se and its metabolites provide a powerful source of radical species, which in turn interact with DNA and TFs to modulate gene expression [110, 115, 211]. In fact, ROS can alter the DNA-binding activity of diverse TFs, by oxidizing DNA bases or specific amino acidic domains (mainly cysteine and lysine residues) of histones and/or TFs. ROS also act as signaling molecules and second messengers by activating intracellular cascades such as MAPKs. These effects converge in recruiting TFs such as AP-1 and NFκB [110, 115, 211], which govern the expression of specific IEG coding for proteins involved in neuronal functions such as death and survival control, cellular defense mechanisms, and immunological and inflammatory responses, which in turn are a powerful source of ROS. On the other hand, several studies have shown that genetic or pharmacological repression of DRD1 can revert METH-induced activation of redox-sensitive TFs, including AP-1, NFκB, CREB, Egr, and NFAT by producing a normalization of the levels of IEGs [122, 123, 212–215].

For instance, CREB, which during baseline DA stimulation is slightly recruited, becomes overactive in the presence of pulsatile DA levels, which lead to a DRD1/PKA-mediated aberrant phosphorylation cascade driven by oxidative stress and/or DRD1 overstimulation [129, 168, 216]. CREB activates genes through the binding to cAMP-responsive element (CRE). Phosphorylation of CREB by PKA at serine119 is required for its interaction with DNA, while phosphorylation at serine-133 allows CREB to interact with CREB-binding protein (CBP) in the nucleus. Members of the CREB gene family include activating transcription factors 1–4 (ATF 1–4), CREB-1, and CREB-2, and each of the ATF/CREB proteins can bind to CRE motifs as either homodimers or heterodimers. In fact, METH administration increases both phosphorylated CREB (pCREB) and members belonging to the CREB family, which then bind to CRE motif of several genes to increase their expression [91, 122, 190, 197, 205, 209, 210, 215, 217–220]. In addition, ATF/CREB dimers also bind to Fos/Jun members belonging to the AP-1 family, thus forming cross-family heterodimers [221]. AP-1 is mainly known for its role in cell proliferation, while it plays a compensatory effect on redox stress and DNA damage [222]. AP-1 DNA-binding complex is in fact a dimer composed of IEGs, which are

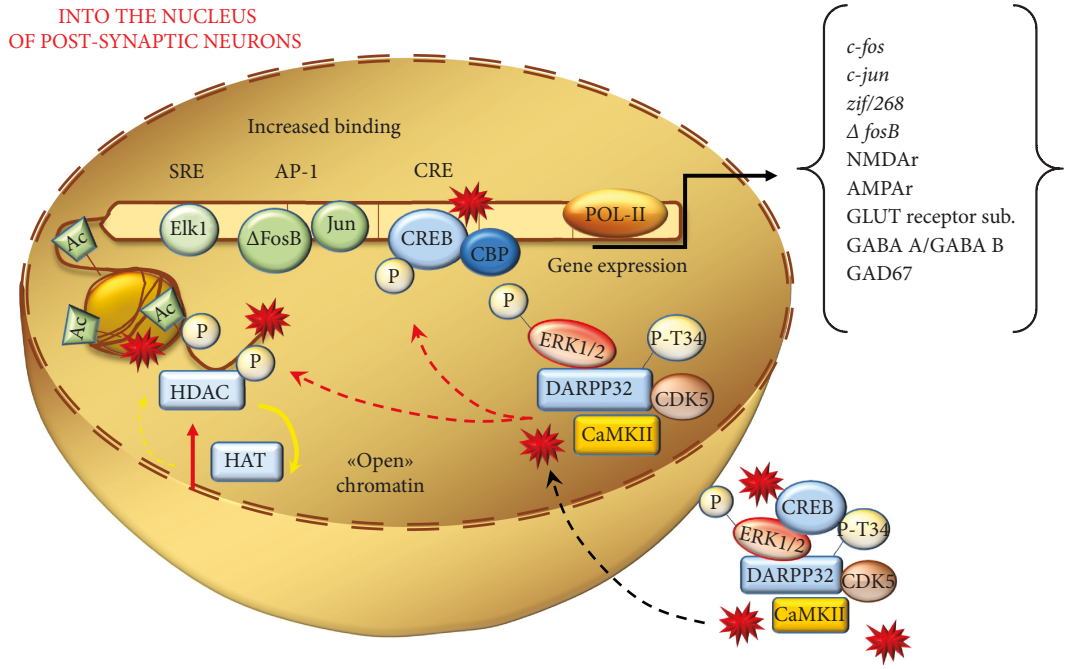

Figure 10: The nuclear effects of DRD1/PKA pathway and reactive species on postsynaptic neurons. The noncanonical DRD1 activation induced by METH produces an overactivation of several kinases, such as ERK1/2, DARPP-32-pT34, CREB, CDK5, and CaMKII. The latter, together with DA- and GLUT-derived reactive species, is shuttled into the nuclear compartment where they carry posttranslational modifications of histones and TFs. These events promote both a relaxation of chromatin structure (yielded by an increase of histone acetyltransferases (HAT)/decrease of histone deacetylases (HDAC)) and increased binding of TFs (such as Elk-1, AP-1, and CREB) at the level of their target gene sequences. These metabolic events eventually translate into an increase expression of IEGs.

members of Jun (c-Jun, Jun B, and Jun D) and Fos (c-Fos, Fos B, Fra-1, and Fra-2) TF families [222]. Several studies demonstrate that METH causes an early increase in IEG expression belonging to Jun and Fos families [91, 123, 197–199, 205–207, 209, 212, 218, 219, 223–227]. Among these genes, a special emphasis is given to ΔFosB, which consists of a stable splice variant of FosB. In fact, differently from other Fos/Jun family proteins featuring a transient induction by acute drug exposure, the increase in ΔFosB (mRNA and/or protein) persists for longer time intervals within the striatum [228, 229]. In line with this, ΔFosB may play a key role in triggering addiction [209, 218, 228, 230–232]. This posed ΔFosB as a master regulator of persistent nuclear effects induced by METH, which are the core of METH-related epigenetics. Thus, reaching out ΔFosB is considered as a key point to trigger persistent epigenetic changes through persistent alterations of transcriptional regulatory proteins (including CDK5 and epigenetic enzymes), which all influence the phenotype of MSNs [229].

ΔFosB-related epigenetic changes occurring in various nuclear sites mainly consist in acetylation/deacetylation and methylation/demethylation at the level of histones or DNA (Figure 11).

Those simple phenomena occurring in specific sites and critical time windows generate the remarkable diversity and specificity in the epigenetics of METH. In fact, the transcriptome/exome alterations generated by METH-induced epigenetics create the specific structural plasticity that we appreciate within MSNs. This is achieved by diverse effects

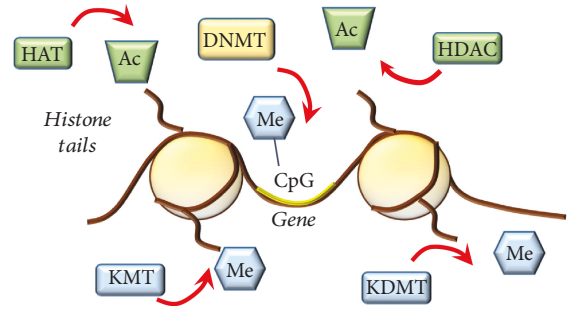

Figure 11: Summarizing main epigenetic mechanisms. This cartoon roughly reports the main epigenetic enzymes carrying structural modifications of lysine (K) residues of histone tails and DNA promoter sequences at the level of CpG islands. HATs act by adding acetyl groups (Ac) which associates with increased gene expression; HDACs repress gene expression by removing Ac from K histone residues; KMT transfer methyl (Me) groups and KDMT remove Me groups from K histone residues; the effects of KMTs and KDMT on gene transcription depend on the specific histone K that is modified; DNMTs mediate increased methylation of cytosine (C) residues in CpG islands of gene promoters, which associates with repressed gene expression.

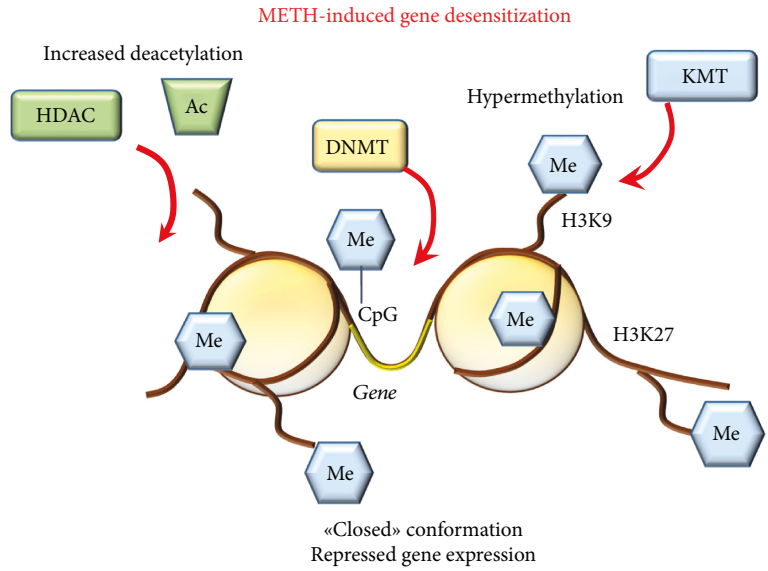

Figure 12: METH-induced gene desensitization. Exposure to chronic METH produces epigenetic effects, which repress further gene expression. This occurs mainly through increased activity of deacetylation enzymes (HDAC), increased methylation of lysine 9 and 27 (K9/K27) residues of histones (i.e., H3K9/27) by methyltransferases (KMTs) and hypermethylation of gene promoters by DNA methyltransferases (DNMTs), which produce a "closed chromatin" conformation. Me: methyl groups; Ac: acetyl groups.

on a number of genes. A critical site concerns genes involved in building the architecture of dendritic spines, such as GLUT NMDAr [108] and AMPAr [233] subunits, GABA-A [176] and GABA-B [233] receptor subunits, and the GABA-synthesizing enzyme GAD-67 [176] (Figure 10).

Beyond ΔFosB, the Egr family represents another subclass of zinc finger structural motifs involved in eukaryotic protein-nucleic acid interaction. Members of Egr include IEGs such as Egr1 (Krox-1, NGF1A, and Zif268), Egr2 (Krox20, NGF1B), Egr3 (Pilot), and Egr4 (NGF1C), which are regulated by posttranslational changes such as phosphorylation and redox state [234]. In line with this, METH activates and overexpresses several members of the Egr family, especially Egr1 and Egr2 [91, 123, 188, 198, 212, 225, 235–237].

Again, METH causes substantial increases in the expression of nuclear TF families including nuclear receptor 4a (Nr4a), nuclear factor erythroid 2- (NFE2-) related factor 2 (Nrf2), and NFAT, which regulate genes involved in metabolism, development, and axonal growth within the mammalian brain [91, 225, 226, 237]. In detail, METH produces a shuttling of NFATc3 and NFATc4 from the cytosol to the nucleus [91, 195]. Similar findings were reported for the DNA-binding protein NFκB, which, following METH, redistributes to the nucleus of striatal neurons [197, 204, 208, 209, 242]. NFκB is rapidly activated and overexpressed by METH. In detail, once in the nucleus, NFκB promotes a vicious cycle of oxidative events, which include an increased expression of inducible nitric oxide synthase (iNOS) and cyclooxygenase-2 (COX-2) to generate nitric oxide (NO), prostaglandins, and inflammatory cytokines as well as activation of the apoptosis-promoting factor p53 [200, 201, 238].

A critical point to decipher the effects of METH upon the activity of all these TFs is the pattern of drug administration. Again, early time intervals compared with late time intervals from METH exposure (i.e., withdrawal time) make a substantial difference. In most cases, acute METH induces an early activation of TFs, which is followed by upregulation of most IEGs. This early effect is short lived, which makes it unlikely to produce behavioral sensitization. This is confirmed by the fact that chronic METH administration produces opposite changes mainly featuring a downregulation of IEGs. Remarkably, chronic METH also blunts the effects of an acute single METH injection on several striatal IEG expression [237] which is more reminiscent of a "gene desensitization" (Figure 12).

Conversely, a single exposure to a subthreshold dose of METH may suffice per se to induce a persistent increased response to further administration [239], a phenomenon which mirrors the "gene priming" (Figure 13). In fact, the effects of a single dose of METH on specific genes are markedly different depending on the existence of a previous METH exposure [240, 241]. These differences appear to be related to the occurrence of a previous epigenetic switch [229, 242].

4.3. METH as a Brain Epigenetic Modifier. Epigenetics in the CNS is currently accepted as the set of mitotic changes in gene transcription and/or phenotypic alterations that occur in the absence of modifications to DNA sequence itself [243]. Dynamic epigenetic remodeling allows perpetual alterations in gene readout within cells, and within the CNS, it may have a crucial impact on neuronal function. Posttranslational modifications of histone proteins, changes in the binding of TFs at gene promoters, and covalent modifications of DNA bases represent the main mechanisms through which gene expression is regulated. Over the past decade, studies investigating the regulation of transcription, through

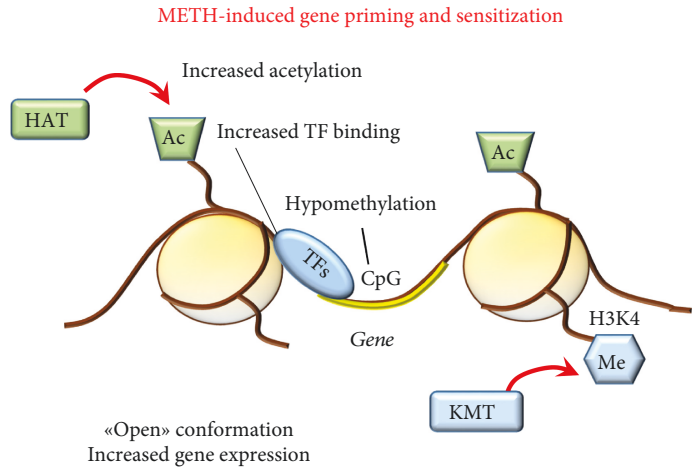

Figure 13: METH-induced gene priming and sensitization. A single dose of METH may be sufficient to induce an epigenetic switch consisting in increased gene expression. Such an effect may also occur during chronic METH resulting in long-term sensitization. This occurs through increased histone acetylation and methylation at specific K residues (i.e., H3K4) joined with poor activity of DNMTs (hypomethylation of CpGs), which altogether produce an "open" chromatin conformation and allow the binding of TFs at the level of gene promoters.

modifications of DNA (hypo-/hyper-/hydroxymethylation of cytosine residues) and chromatin structure (acetylation and methylation of histones) (Figure 11), have exploded in addiction research [244–246]. In recent years, METH was shown to induce epigenetic modifications, which underlie persistent changes in gene expression and long-lasting behavioral responses to the drug [198, 210, 228, 237, 247–251].

4.3.1. METH and Histone Acetylation. Histone acetylation and deacetylation are a dynamic process balanced by histone acetyltransferase (HAT) and histone deacetylase (HDAC), a subset of enzymes, which carry out reversible histone modifications by adding or removing acetyl groups. In general, by adding acetyl groups to histones, HATs promote gene expression by creating an "open" chromatin conformation, while HDACs produce a "closed" conformation and represses transcription by removing acetyl groups [252]. These enzymes physically interact with sequence-specific TFs and target-specific promoters, to modify acetylation patterns of core histones, thus manipulating the functional state of chromatin and orchestrating the transcriptional machinery [252]. The HAT families include CREB-binding protein (CBP)/p300, while HDACs can be classified into four families according to sequence similarities [253]. These include class I (HDAC1, HDAC2, HDAC3, and HDAC8), class II (HDAC4, HDAC5, HDAC6, HDAC7, HDAC9, and HDAC10), class III (sirtuins, SIRTs 1–7), and class IV (HDAC11) HDACs. HDACs are widely implicated in synaptic plasticity and long-term memory, which is key in drug addiction [254].

(1) Histone Acetylation and Increased Gene Expression. Acetylation-Related Transcriptional Effects of Acute METH. Several studies documented that METH at short-time intervals increases H4 acetylation (H4K5ac and H4K8ac) in the rat NAc and striatum [225, 228, 255, 256]. This associates with increased gene expression detected at early time intervals following METH [225, 255]. In detail, such an increase (mainly concerning IEGs such as Egr1, Egr2, c-Fos, JunB, Nr4a3, and corticotrophin releasing factor (Crf)) correlates with increased binding of H4K5ac to the promoters of these very same genes [225, 228, 255]. METH-induced H4 acetylation may follow either decrease in HDAC1 expression or increase in CBP expression in the Nac [255]. In fact, acute METH also induces an increase of ATF2, a member of the ATF/CREB family [255], which behaves as a HAT by acetylating histone H4 [257].

Acetylation-Related Transcriptional Effects of Chronic METH. In 2013, Krasnova et al. [210] used an experimental model of chronic METH self-administration in order to decipher large-scale epigenetic and transcriptional changes occurring specifically within the NAc and dorsal striatum, to explain compulsive behavior characterizing drug addiction [258]. In detail, METH self-administration enriches pCREB on the promoters of genes coding for c-Fos, FosB, BDNF, and (synaptophysin) Syp. Both pCREB and gene expression followed the same expression pattern being upregulated at 2 h after drug intake and going back to normal levels at 1 month of withdrawal. This suggests that CREB is relevant as an epigenetic mediator of transcriptional changes produced by METH. In contrast to c-Fos mRNA, chronic METH self-administration does not affect c-Fos protein levels after 2 or 24 h. Remarkably, at 1 month of METH withdrawal, c-Fos protein was found to be decreased compared with controls. In contrast, no changes were observed in ΔFosB mRNA levels, while ΔFosB protein was significantly increased at 2 and 24 h after chronic METH self-administration. Similarly to c-Fos, ΔFosB decreased at 1 month of withdrawal [210], which dampens an exclusive role of ΔFosB as an irreversible switch for addiction.

(2) Histone Deacetylation and Decreased Gene Expression. Deacetylation-Related Epigenetic Effects of Acute METH. A recent study shows that in HDAC2-KO mice, METH

produces a greater increase in some IEG transcripts (FosB, Fra-2, Egr1, and Egr3) when measured at early time interval (1 h postinjection) [227]. The levels of these transcripts persist for 2 hours in HDAC2-KO mice. In contrast, in WT mice, at 2 h, these IEGs are suppressed. This demonstrates that METH recruits HDAC2 to the promoters of these IEGs thereby bringing back transcript levels to normal values. Remarkably, in HDAC2-KO mice, the persistency of IEG expression is correlated with increased enrichment of pCREB on the promoters of the very same genes. Downregulation of other genes (follistatin (Fst), inhibin beta A (InhbA), neuromedin U (Nmu), cholecystokinin (Cck), and BDNF), which occurs at delayed time intervals (8, 12, and 24 h) after METH administration, combines with increased expression of HDACs in the Nac and dorsal striatum [255]. In fact, METH decreases histone H3 acetylated at lysine 9 and 18 (H3K9Ac and H3K18Ac) on the promoters of these genes [255].

Deacetylation-Related Epigenetic Effects of Chronic METH. Renthal et al. [228] found that, at 5 days of amphetamine withdrawal, when c-Fos was maximally repressed, ΔFosB accumulated on c-Fos promoter, suggesting that ΔFosB desensitizes c-Fos expression. Conversely, the HDAC inhibitor sodium butyrate reverts METH-induced repression of c-Fos, supporting the idea that hypoacetylation on the c-Fos promoter desensitizes the gene [228]. The question of whether ΔFosB remains steady linked to specific gene promoters for longer periods of time or ΔFosB alters gene inducibility by producing long-lasting chromatin changes still remains to be elucidated.

McCoy et al. [237] showed that chronic METH reduces the expression of several TFs and IEGs (i.e., AP1, Erg1-3, and Nr4a1) way below control levels. This occurs along with decreased CREB expression. Remarkably, chronic pretreatment with METH suppresses the stimulatory effects on these IEGs when elicited by an acute challenge with the drug. This paradoxical response occurs along with a greater decrease in CREB levels compared with those measured during chronic administration [237]. Similar findings were produced by Cadet et al. [225], who reported that a challenge of METH to rats treated chronically leads to downregulation of 53 out of 71 genes. These effects were related to decrease H4K5Ac binding. In addition, chronic administration of low METH doses decreases the abundance of H4K5ac, H4K12ac, and H4K16ac on the promoters of genes coding for GluA1-2 and GluN1 subunits of AMPAr and NMDAr, respectively [259]. Accordingly, there was a decrease in the expression of GLUT receptors causing a decrease in the current generated by GLUT stimulation. These phenotype changes occurred along with increased striatal expression of HDAC1, HDAC2, SIRT1, and SIRT2. A causal relationship is strengthened by the opposite effects produced by the HDAC inhibitor valproate, which prevents METH-induced alterations at the very same receptor subunits [259]. When METH is administered in higher doses, a change in the expression of different classes of HDACs is found [260]. This confirms a dose dependency for METH-induced epigenetic alterations. In fact, depending on the dose of METH being administered, sometimes, opposite phenotypic changes occur. METH was shown to upregulate other epigenetic proteins including methyl CpG-binding protein 2 (MeCP2), repressor element-1 silencing transcription factor (REST), and corepressor-REST (Co-REST), which are members of corepressor complexes with class I HDACs [259]. Among these, the multifunctional complex MeCP2 received some attention since METH increases MeCP2 expression in the ventral and dorsal striatum [261, 262].

4.3.2. METH and Histone Methylation. Histone methylation is regulated by enzymes that add methyl groups acting as writers, namely, methyltransferases (KMTs) and enzymes that remove methyl groups, acting as erasers, namely, demethylases (KDMTs). KMTs are involved in mono-, di-, and trimethylation of histone lysine residues (K), which carry specific regulatory switches [263]. In fact, histone methylation regulates both repression and activation of gene expression, depending on the specific K being modified. For instance, methylation of histone H3 at K4 (H3K4me) is associated with increased transcriptional activity whereas methylation of H3 at K9 (H3K9me) and K27 (H3K27me) is associated with repression of gene expression [263]. Moreover, several classes of KDMTs may counteract the effects of the KMTs by erasing methyl moieties.

Several studies demonstrated the involvement of KMTs and KDMTs in METH addiction [228, 247, 248]. For instance, the study of Renthal et al. [228] demonstrated that in addition to the role of HDAC1, repression of c-Fos at 5 days after drug withdrawal was associated with amphetamine-induced increase of H3K9me2 on the promoter of c-Fos. This effect correlates with increased expression levels of KMT1A. More recently, epigenetic mechanisms contributing to METH-associated memories were explored in the NAc and dorsal striatum, given their role as a hub for drug craving. While investigating such a phenomenon, Aguilar-Valles et al. [247] provided evidence that genetic ablation of KDM5C demethylase increases H3K4me at the level of promoters of IEGs including Fos and oxytocin receptor gene (Oxtr), which associates with increased METH-associated memory. On the contrary, KO mice for MLL1 (mixed lineage leukemia, a member of the KMT family) which possess decreased H3K4me and transcript levels of Fos and Oxtr genes show reduced METH-associated memory [247]. Again, METH craving was shown to be related with epigenetic changes occurring only in Fos-expressing neurons of the dorsal striatum [248]. In these neurons, significant increase in mRNA levels of IEGs (Arc, Egr1), BDNF, and its receptor tropomyosin receptor kinase B (TrkB), as well as metabotropic GLUT receptor subunits (Gria1, Gria3, and Grm1), correlates with several epigenetic enzymes including KDMA1 [248] and HDAC5 [248, 249].

4.3.3. METH and DNA Methylation. DNA methylation refers to the classic chemical covalent modification of DNA, which results from the addition of a methyl group at the 5′ position of a cytosine base via enzymes of the DNA (cytosine-5)-methyltransferases (DNMTs) family [264]. These include DNMT3A and DNMT3B, which are de novo methyltransferases, and DNMT1, that is, a maintenance methyltransferase

[264]. This primarily occurs in DNA sequences where a cytosine (C) precedes a guanine (G) with the interposition of a phosphate group (CpG). CpG sites are unevenly distributed throughout the human genome both as interspersed CpG regions and as CpG clusters representing the so-called CpG islands. In line with the concept that promoters are the most sensitive to epigenetic changes, CpG islands occur mainly within promoter regions [265]. DNA hypermethylation of CpG within promoters represses transcription while DNA hypomethylation is often associated with increased gene expression [264]. It is worth mentioning that stability and activity of DNMTs depend on posttranslational mechanisms (phosphorylation, acetylation, and methylation) carried out by several kinases, such as CDK5 [266] and histone remodeling enzymes, especially HDACs [267]. In fact, in combination with increased HDACs, chronic METH reduces DNA methylation of the promoter region of GluA1 and GluA2 AMPAr subunit genes. This is confirmed by the finding that following chronic METH, there are decreases of $5'$-methylcytosine (5mc) and $5'$-hydroxymethylcytosine (5hmc) at the level of the promoter region of these genes [259]. At striatal level, METH-induced hypomethylation or hypermethylation may also affect corticosterone and glucocorticoid receptors' gene promoters [268, 269].

(1) DNA Methylation in Human METH Abusers: The Convergent Role of DA and Oxidative Stress on Cell-Clearing Pathways and a-syn Expression. Aspired by the vast body of evidence reporting aberrant promoter DNA methylation in psychotic disorders, a recent study investigated DNA methylation and gene expression pattern in human METH-induced psychosis [270]. RNA and DNA samples were extracted from the saliva of METH-addicted patients with and without psychosis, as well as from control subjects (each group $N = 25$). Despite carrying the inherent limit of a peripheral analysis, which may not be relevant for brain alterations, these findings demonstrate DNA hypomethylation within promoters of genes related to DA metabolism. In fact, DNA hypomethylation was present on the promoter of DRD3, DRD4, and membrane-bound catechol-O-methyltransferase (MB-COMT) genes. COMT provides a methylation of a hydroxyl group (which generates a methoxy group) of DA-forming 3-methoxytyramine (3-MT). Thus, DNA hypomethylation of MB-COMT gene promoter and increased COMT expression associate with synaptic DA degradation in the prefrontal cortex in psychotic METH abusers [270, 271]. Furthermore, DNA hypomethylation of AKT1 promoter gene was detected in METH patients with and without psychosis [270]. AKT1 gene encodes a serine/threonine kinase protein, which is expressed at high levels in the brain, and it is linked to DNA transcription, neural survival and growth, synaptic plasticity, and working memory [272, 273]. For instance, AKT regulates CREB- and NFκB-dependent gene transcription [274, 275]. In addition, it phosphorylates DNMT1, thus playing a role in the switch between methylation, phosphorylation, and UPS-dependent degradation regulating DNMT1 stability and activity [276]. Remarkably, alterations of AKT levels and downstream pathways are closely related to the activity of DA receptors [277–280]. In line with this, dysregulation of AKT is reported in PD patients [281] and in METH experimental models [278]. Two downstream targets of AKT are glycogen synthase kinase 3 beta (GSK3β) and mammalian target of rapamycin (mTOR), a serine/threonine protein kinase complex. mTOR phosphorylates AKT via a feedback mechanism, while it activates p700Sk6 and 4EBP1 TFs. Once activated, TFs translocate in the nucleus to promote cell proliferation and survival. In line with this, inhibition of mTOR by the gold standard inhibitor rapamycin blocks drug-induced sensitization [282]. In contrast, mTOR activation inhibits ATG, which worsens METH toxicity [83, 283, 284]. In fact, prolonged METH exposure engulfs ATG machinery, which is upregulated as a compensatory mechanism [83, 86, 283, 284]. However, the bulk of oxidative species overwhelms the ATG machinery, which becomes progressively impaired as witnessed by the stagnant nature of ATG vacuoles suppressing the clearance of α-syn aggregates [83]. In line with this, an epigenetically induced upregulation of the α-syn coding gene SNCA was recently detected in the SN of rats exposed to METH [285], lending substance to an increase in α-syn protein levels [79]. Such an effect is associated with hypomethylation of the SNCA promoter, as shown by a decreased occupancy of MeCP2 and DNMT1 in such a region [285]. The effects of mTOR also relate to UP, which seems to be activated by mTOR inhibition [286–288] and inhibited during METH toxicity [38, 79–81, 289]. Noteworthy, the clearance of α-syn depends also on UP activity [79] and on a recently described ATG-UP merging organelle (the "autophagoproteasome"), which is directly activated by mTOR inhibition [287].

No study so far demonstrated an epigenetic regulation of SNCA within the striatum following METH; however, epigenetic modifications of SNCA have been documented in PD patients [290–292]. In fact, significant hypomethylation of CpG sites in the promoter region of SNCA is reported within leukocytes [292] and postmortem brain samples from patients with sporadic and complicated PD [290, 291, 293, 294].

4.3.4. METH and DNA Hydroxymethylation. In recent years, DNA hydroxymethylation, generated by the oxidation of 5-methylcytosine (5mC) to 5-hydroxymethylcytosine (5hmC), became increasingly important in epigenetics [295]. It has been has suggested that 5hmC recruits DNA repair proteins and DNA demethylating machinery [295]. The formation of this modified base is mediated by ten-eleven translocation (TET) proteins and by TET-dependent generation of 5-formylcytosine and carboxyl-cytosine, which are then processed by thymine DNA glycosylase (TDG) and base excision repair (BER) mechanisms. The biological functions of 5hmC, which is highly enriched in the adult brain, appear to be crucial to promote gene expression related to quick behavioral adaptation [296]. Two recent studies demonstrated that compulsive METH intake is associated with large-scale changes in DNA hydroxymethylation in the rat NAc, which is consistent with a potential role for DNA hydroxymethylation in addiction [250, 251]. Remarkably, DNA hydroxymethylation around the transcriptional start

site (TSS) or within intragenic regions of genes coding for neuropeptides was shown to occur following chronic METH administration [251]. This is the case of corticotrophin-releasing hormone/factor (Crh/Crf), arginine vasopressin (Avp) and cocaine- and amphetamine-regulated transcript propeptides (Cartpt), which increase in the NAc of METH-treated rats [251, 297]. In detail, Crh and Avp hydroxymethylation is mediated by TET1 and TET3 enzymes, respectively. In contrast, METH-induced changes in Cartpt expression derive from the binding of pCREB at the Cartpt promoter [251]. Together, these results support the hypothesis that METH produces a variety of epigenetic changes in the neuroendocrine circuitry within the NAc. This same epigenetic mechanism was recently studied within a context of compulsive METH intake [250]. It was found that in METH-addicted animals, which develop compulsive self-administration, hydroxymethylation occurs near or within genes coding for voltage-gated Ca+ channels. This occurs in different postsynaptic sites within the NAc, dorsal striatum, and prefrontal cortex of METH-addicted animals. Interestingly, hydroxymethylation of K+ channel-coding genes was found only within the NAc of nonaddicted animals [250].

5. Concluding Remarks

The influence of epigenetics in drug abuse provides a novel and deeper insight to understand the molecular mechanisms of addiction. This is key in the case of METH abuse since this drug possesses a variety of effects, which recapitulate the molecular alteration occurring in some neuropsychiatric disorders. As novel epigenetic changes are constantly being identified, it is more and more clear how simple effects induced by transient neurotransmitter alterations may translate into persistent alterations of brain physiology. Moreover, the multiplicity of findings revised here, when joined with a better knowledge of the genetic background, may clarify the interdependence between genetics and epigenetics underlying diversity in the human genome [298]. This leads to take into account the fact that a molecular cause-effect interplay between genetic and epigenetic factors during METH addiction may exist as well. Despite being yet unexplored in the context of drug abuse, such a close relationship is likely to explain the very peculiar phenotypic alterations observed during METH abuse. Such an intriguing issue surely deserves further attention and may represent a powerful tool for identifying additional genetic and epigenetic biomarkers to develop personalized treatments.

Abbreviations

3-MT: 3-Methoxytyramine
5hmc: 5′-Hydroxymethylcytosine
5-HT: 5-Hydroxytryptamine (serotonin)
5mc: 5′-Hethylcytosine
Ac: Acetyl group
AC: Adenylate cyclase
AD: Aldehyde dehydrogenase
AKT1: Ak strain-transforming oncogene homologue serine/threonine kinase 1
AMPA: α-Amino-3-hydroxy-5-methyl-4-isoxazole-propionic acid
AMPAr: α-Amino-3-hydroxy-5-methyl-4-isoxazole-propionic acid receptor
AP-1: Activator protein 1
α-syn: Alpha-synuclein
ATF 1–4: Activating transcription factors 1–4
ATG: Autophagy
Avp: Arginine vasopressin
BBB: Blood-brain barrier
BDNF: Brain-derived neurotrophic factor
BER: Base excision repair
CaMKII: Calmodulin-dependent kinase II
cAMP: Cyclic adenosine monophosphate
Cartpt: Cocaine- and amphetamine-regulated transcript propeptides
CBP/p300: CREB-binding protein/p300 histone acetyltransferase
CBP: CREB-binding protein
Cck: Cholecystokinin
CDK5: Cyclin-dependent kinase 5
CNS: Central nervous system
COMT: Catechol-O-methyltransferase
COX-2: Cyclooxygenase-2
CpG: Dinucleotide composed of cytosine (C) preceding a guanine (G) with the interposition of a phosphate group (p)
CRE: cAMP-responsive element
CREB: cAMP response element-binding protein
Crf: Corticotrophin-releasing factor
Crh: Corticotrophin-releasing hormone
DA: Dopamine
DARPP-32: Dopamine- and cAMP-regulated phosphoprotein
DAT: Dopamine transporter
ΔFosB: Splice variant of the FBJ murine osteosarcoma viral (V-Fos) oncogene homolog protein B
DNMT: DNA (cytosine-5)-methyltransferase
DOPAC: 3,4-Dihydroxyphenylacetic acid
DOPALD: 3,4-Dihydroxyphenylacetaldehyde
DRD1–5: Dopamine receptors D1–D5
EAAT3: Excitatory amino acid transporter 3
Egr1–3: Early growth response proteins 1–3
Elk-1: Transcription factor of the E twenty-six-specific (ETS) domain family
ER: Endoplasmic reticulum
ERK1/2: Extracellular signal-regulated kinases 1/2
Fos: FBJ murine osteosarcoma viral (V-Fos) oncogene homolog transcription factor family containing cellular Fos (c-Fos), Fos proteins B and D (Fos-B and Fos-D), and Fos-related antigens 1 and 2 (Fra-1 and Fra-2)
Fst: Follistatin
GAD-67: Glutamate decarboxylase 1
GLUT: Glutamate
GluA1-2: Glutamate AMPA receptor subunits 1-2
GluN1: Glutamate NMDA receptor subunit 1

$G_{o/i}$: Adenylyl cyclase inhibitor guanine nucleotide-binding protein
G_{olf}: Olfactory guanine nucleotide-binding protein
G_s: Adenylyl cyclase stimulatory guanine nucleotide-binding protein
GSK3β: Glycogen synthase kinase 3 beta
H: Histone
H_2O_2: Hydrogen peroxide
HAT: Histone acetyltransferase
HD: Huntington disease
HDAC1-11: Histone deacetylases 1–11
HSP70: Heat shock protein 70
IEGs: Immediate early genes
InhbA: Inhibin beta A
iNOS: Inducible nitric oxide synthase
IP3: Inositol 1,4,5 trisphosphate
Jun: Avian sarcoma virus (v-Jun) oncogene homolog transcription factor family containing cellular Jun (c-Jun) and Jun proteins B and D (Jun-B and Jun-D)
K: Lysine residue
KDMT: Histone lysine demethylase
KMT: Histone lysine methyltransferase
KO: Knock out
MAO-A: Monoamine oxidase type A
MAO-B: Monoamine oxidase type B
MAPK: Mitogen-activated protein kinases
MB-COMT: Membrane-bound catechol-O-methyltransferase
Me: Methyl group
METH: Methamphetamine
MLL1: Mixed lineage leukemia member of the KMT family
MSNs: Medium-sized spiny neurons
mTOR: Mammalian target of rapamycin
NAc: Nucleus accumbens
NE: Norepinephrine
NFAT: Nuclear factor of activated T-cells
NFκB: Nuclear factor κB
NMDA: N-Methyl-d-aspartate
NMDAr: N-Methyl-d-aspartate glutamate receptor
Nmu: Neuromedin U
NO: Nitric oxide
Nr4a: Nuclear receptor 4a
Nrf2: Nuclear factor erythroid 2- (NFE2-) related factor 2
Oxtr: Oxytocin receptor
pCREB: Phosphorylated CREB
PD: Parkinson's disease
PKA: Protein kinase A
PLC: Phospholipase C
PP1: Phosphatase protein 1
PP-2A: Phosphatase protein 2A
P-T34/75: Phosphorylated threonine 34/75
REST: Repressor element-1 silencing transcription factor
RNS: Reactive nitrogen species
ROS: Reactive oxygen species
SIRT: Sirtuin family of histone deacetylases
SNCA: Alpha-synuclein coding gene
SNpc: Substantia nigra pars compacta
STEP: STriatal-enriched protein tyrosine phosphatase
Syp: Synaptophysin
TDG: Thymine DNA glycosylase
TET: Ten-eleven translocation proteins
TF: Transcription factor
TH: Tyrosine hydroxylase
Thr34/75: Threonine 34/75
TrkB: Tropomyosin receptor kinase B
TSS: Transcriptional start site
UchL1: Ubiquitin C-terminal hydrolase L1
UP: Ubiquitin proteasome
UPS: Ubiquitin proteasome system
VGLUT-1: Vesicular glutamate transporter type-1
VMAT-1/-2: Vesicular monoamine transporter type-1/-2.

Conflicts of Interest

The authors declare that there is no conflict of interests regarding the publication of this paper.

Authors' Contributions

Fiona Limanaqi and Stefano Gambardella contributed equally to this work.

References

[1] J. S. Fowler, N. D. Volkow, J. Logan et al., "Fast uptake and long-lasting binding of methamphetamine in the human brain: comparison with cocaine," *NeuroImage*, vol. 43, no. 4, pp. 756–763, 2008.

[2] N. D. Volkow, J. S. Fowler, G.-J. Wang et al., "Distribution and pharmacokinetics of methamphetamine in the human body: clinical implications," *PLoS One*, vol. 5, no. 12, article e15269, 2010.

[3] R. J. Schepers, J. M. Oyler, R. E. Joseph Jr., E. J. Cone, E. T. Moolchan, and M. A. Huestis, "Methamphetamine and amphetamine pharmacokinetics in oral fluid and plasma after controlled oral methamphetamine administration to human volunteers," *Clinical Chemistry*, vol. 49, no. 1, pp. 121–132, 2003.

[4] C. W. Meredith, C. Jaffe, K. Ang-Lee, and A. J. Saxon, "Implications of chronic methamphetamine use: a literature review," *Harvard Review of Psychiatry*, vol. 13, no. 3, pp. 141–154, 2005.

[5] B. D. Homer, T. M. Solomon, R. W. Moeller, A. Mascia, L. DeRaleau, and P. N. Halkitis, "Methamphetamine abuse and impairment of social functioning: a review of the underlying neurophysiological causes and behavioral implications," *Psychological Bulletin*, vol. 134, no. 2, pp. 301–310, 2008.

[6] J. F. Marshall and S. J. O'Dell, "Methamphetamine influences on brain and behavior: unsafe at any speed?," *Trends in Neurosciences*, vol. 35, no. 9, pp. 536–545, 2012.

[7] T. Abekawa, T. Ohmori, and T. Koyama, "Effects of repeated administration of a high dose of methamphetamine on dopamine and glutamate release in rat striatum and nucleus accumbens," *Brain Research*, vol. 643, no. 1-2, pp. 276–281, 1994.

[8] S. E. Stephans and B. K. Yamamoto, "Effect of repeated methamphetamine administrations on dopamine and glutamate efflux in rat prefrontal cortex," *Brain Research*, vol. 700, no. 1-2, pp. 99–106, 1995.

[9] K. Nishijima, A. Kashiwa, A. Hashimoto, H. Iwama, A. Umino, and T. Nishikawa, "Differential effects of phencyclidine and methamphetamine on dopamine metabolism in rat frontal cortex and striatum as revealed by in vivo dialysis," *Synapse*, vol. 22, no. 4, pp. 304–312, 1996.

[10] P. Piccini, N. Pavese, and D. J. Brooks, "Endogenous dopamine release after pharmacological challenges in Parkinson's disease," *Annals of Neurology*, vol. 53, no. 5, pp. 647–653, 2003.

[11] T. Uehara, T. Sumiyoshi, H. Itoh, and M. Kurachi, "Inhibition of dopamine synthesis with alpha-methyl-*p*-tyrosine abolishes the enhancement of methamphetamine-induced extracellular dopamine levels in the amygdala of rats with excitotoxic lesions of the entorhinal cortex," *Neuroscience Letters*, vol. 356, no. 1, pp. 21–24, 2004.

[12] J. D. Erickson, M. K. Schafer, T. I. Bonner, L. E. Eiden, and E. Weihe, "Distinct pharmacological properties and distribution in neurons and endocrine cells of two isoforms of the human vesicular monoamine transporter," *Proceedings of the National Academy of Sciences of the United States of America*, vol. 93, no. 10, pp. 5166–5171, 1996.

[13] O. Suzuki, H. Hattori, M. Asano, M. Oya, and Y. Katsumata, "Inhibition of monoamine oxidase by *d*-methamphetamine," *Biochemical Pharmacology*, vol. 29, no. 14, pp. 2071–2073, 1980.

[14] D. Sulzer and S. Rayport, "Amphetamine and other psychostimulants reduce pH gradients in midbrain dopaminergic neurons and chromaffin granules: a mechanism of action," *Neuron*, vol. 5, no. 6, pp. 797–808, 1990.

[15] J. F. Cubells, S. Rayport, G. Rajendran, and D. Sulzer, "Methamphetamine neurotoxicity involves vacuolation of endocytic organelles and dopamine-dependent intracellular oxidative stress," *Journal of Neuroscience*, vol. 14, no. 4, pp. 2260–2271, 1994.

[16] D. Sulzer, "How addictive drugs disrupt presynaptic dopamine neurotransmission," *Neuron*, vol. 69, no. 4, pp. 628–649, 2011.

[17] T. E. Ary and H. L. Komiskey, "Basis of phencyclidine's ability to decrease the synaptosomal accumulation of ^{3}H-catecholamines," *European Journal of Pharmacology*, vol. 61, no. 4, pp. 401–405, 1980.

[18] J. M. Brown, G. R. Hanson, and A. E. Fleckenstein, "Methamphetamine rapidly decreases vesicular dopamine uptake," *Journal of Neurochemistry*, vol. 74, no. 5, pp. 2221–2223, 2000.

[19] V. Sandoval, E. L. Riddle, G. R. Hanson, and A. E. Fleckenstein, "Methylphenidate redistributes vesicular monoamine transporter-2: role of dopamine receptors," *Journal of Neuroscience*, vol. 22, no. 19, pp. 8705–8710, 2002.

[20] V. Sandoval, E. L. Riddle, G. R. Hanson, and A. E. Fleckenstein, "Methylphenidate alters vesicular monoamine transport and prevents methamphetamine-induced dopaminergic deficits," *Journal of Pharmacology and Experimental Therapeutics*, vol. 304, no. 3, pp. 1181–1187, 2003.

[21] A. E. Fleckenstein, T. J. Volz, E. L. Riddle, J. W. Gibb, and G. R. Hanson, "New insights into the mechanism of action of amphetamines," *Annual Review of Pharmacology and Toxicology*, vol. 47, no. 1, pp. 681–698, 2007.

[22] T. J. Volz, A. E. Fleckenstein, and G. R. Hanson, "Methamphetamine-induced alterations in monoamine transport: implications for neurotoxicity, neuroprotection and treatment," *Addiction*, vol. 102, pp. 44–48, 2007.

[23] E. Floor and L. Meng, "Amphetamine releases dopamine from synaptic vesicles by dual mechanisms," *Neuroscience Letters*, vol. 215, no. 1, pp. 53–56, 1996.

[24] J. M. Brown, M. S. Quinton, and B. K. Yamamoto, "Methamphetamine-induced inhibition of mitochondrial complex II: roles of glutamate and peroxynitrite," *Journal of Neurochemistry*, vol. 95, no. 2, pp. 429–436, 2005.

[25] M. Gesi, A. Santinami, R. Ruffoli, G. Conti, and F. Fornai, "Novel aspects of dopamine oxidative metabolism (confounding outcomes take place of certainties)," *Journal of Pharmacology and Toxicology*, vol. 89, no. 5, pp. 217–224, 2001.

[26] M. Ferrucci, F. S. Giorgi, A. Bartalucci, C. L. Busceti, and F. Fornai, "The effects of locus coeruleus and norepinephrine in methamphetamine toxicity," *Current Neuropharmacology*, vol. 11, no. 1, pp. 80–94, 2013.

[27] J. L. Cadet, S. Ali, and C. Epstein, "Involvement of oxygen-based radicals in methamphetamine-induced neurotoxicity: evidence from the use of CuZnSOD transgenic micea," *Annals of the New York Academy of Sciences*, vol. 738, no. 1, pp. 388–391, 1994.

[28] S. Jayanthi, B. Ladenheim, and J. L. Cadet, "Methamphetamine-induced changes in antioxidant enzymes and lipid peroxidation in copper/zinc-superoxide dismutase transgenic mice," *Annals of the New York Academy of Sciences*, vol. 844, no. 1, pp. 92–102, 1998.

[29] A. Hattori, Y. Luo, H. Umegaki, J. Munoz, and G. S. Roth, "Intrastriatal injection of dopamine results in DNA damage and apoptosis in rats," *NeuroReport*, vol. 9, no. 11, pp. 2569–2572, 1998.

[30] M. J. LaVoie and T. G. Hastings, "Dopamine quinone formation and protein modification associated with the striatal neurotoxicity of methamphetamine: evidence against a role for extracellular dopamine," *Journal of Neuroscience*, vol. 19, no. 4, pp. 1484–1491, 1999.

[31] M. R. Gluck, L. Y. Moy, E. Jayatilleke, K. A. Hogan, L. Manzino, and P. K. Sonsalla, "Parallel increases in lipid and protein oxidative markers in several mouse brain regions after methamphetamine treatment," *Journal of Neurochemistry*, vol. 79, no. 1, pp. 152–160, 2001.

[32] D. Sulzer and L. Zecca, "Intraneuronal dopamine-quinone synthesis: a review," *Neurotoxicity Research*, vol. 1, no. 3, pp. 181–195, 2000.

[33] D. Sulzer, M. S. Sonders, N. W. Poulsen, and A. Galli, "Mechanisms of neurotransmitter release by amphetamines: a review," *Progress in Neurobiology*, vol. 75, no. 6, pp. 406–433, 2005.

[34] R. Moratalla, A. Khairnar, N. Simola et al., "Amphetamine-related drugs neurotoxicity in humans and in experimental animals: main mechanisms," *Progress in Neurobiology*, vol. 155, pp. 149–170, 2017.

[35] P. Wells, Y. Bhuller, C. Chen et al., "Molecular and biochemical mechanisms in teratogenesis involving reactive oxygen species," *Toxicology and Applied Pharmacology*, vol. 207, no. 2, Supplement 1, pp. 354–366, 2005.

[36] T. Iwazaki, I. S. McGregor, and I. Matsumoto, "Protein expression profile in the striatum of acute methamphetamine-treated rats," *Brain Research*, vol. 1097, no. 1, pp. 19–25, 2006.

[37] I. Miyazaki, M. Asanuma, F. J. Diaz-Corrales et al., "Methamphetamine-induced dopaminergic neurotoxicity is regulated by quinone formation-related molecules," *The FASEB Journal*, vol. 20, no. 3, pp. 571–573, 2006.

[38] G. Lazzeri, P. Lenzi, C. L. Busceti et al., "Mechanisms involved in the formation of dopamine-induced intracellular bodies within striatal neurons," *Journal of Neurochemistry*, vol. 101, no. 5, pp. 1414–1427, 2007.

[39] X. Li, H. Wang, P. Qiu, and H. Luo, "Proteomic profiling of proteins associated with methamphetamine-induced neurotoxicity in different regions of rat brain," *Neurochemistry International*, vol. 52, no. 1-2, pp. 256–264, 2008.

[40] C. Harold, T. Wallace, R. Friedman, G. Gudelsky, and B. Yamamoto, "Methamphetamine selectively alters brain glutathione," *European Journal of Pharmacology*, vol. 400, no. 1, pp. 99–102, 2000.

[41] H. M. Chen, Y. C. Lee, C. L. Huang et al., "Methamphetamine downregulates peroxiredoxins in rat pheochromocytoma cells," *Biochemical and Biophysical Research Communications*, vol. 354, no. 1, pp. 96–101, 2007.

[42] I. N. Krasnova and J. L. Cadet, "Methamphetamine toxicity and messengers of death," *Brain Research Reviews*, vol. 60, no. 2, pp. 379–407, 2009.

[43] B. K. Yamamoto, A. Moszczynska, and G. A. Gudelsky, "Amphetamine toxicities classical and emerging mechanisms," *Annals of the New York Academy of Sciences*, vol. 1187, no. 1, pp. 101–121, 2010.

[44] C. J. Schmidt and J. W. Gibb, "Role of the dopamine uptake carrier in the neurochemical response to methamphetamine: effects of amfonelic acid," *European Journal of Pharmacology*, vol. 109, no. 1, pp. 73–80, 1985.

[45] J. S. Schneider, D. S. Rothblat, and L. DiStefano, "Volume transmission of dopamine over large distances may contribute to recovery from experimental parkinsonism," *Brain Research*, vol. 643, no. 1-2, pp. 86–91, 1994.

[46] K. Fuxe, K. X. Jacobsen, M. Höistad et al., "The dopamine D1 receptor-rich main and paracapsular intercalated nerve cell groups of the rat amygdala: relationship to the dopamine innervation," *Neuroscience*, vol. 119, no. 3, pp. 733–746, 2003.

[47] K. Fuxe, A. B. Dahlström, G. Jonsson et al., "The discovery of central monoamine neurons gave volume transmission to the wired brain," *Progress in Neurobiology*, vol. 90, no. 2, pp. 82–100, 2010.

[48] N. A. Northrop and B. K. Yamamoto, "Methamphetamine effects on blood-brain barrier structure and function," *Frontiers in Neuroscience*, vol. 9, p. 69, 2015.

[49] P. Turowski and B. A. Kenny, "The blood-brain barrier and methamphetamine: open sesame?," *Frontiers in Neuroscience*, vol. 9, p. 156, 2015.

[50] Y. Agid, F. Javoy, and M. B. H. Youdim, "Monoamine oxidase and aldehyde dehydrogenase activity in the striatum of rats after 6-hydroxydopamine lesion of the nigrostriatal pathway," *British Journal of Pharmacology*, vol. 48, no. 1, pp. 175–178, 1973.

[51] F. Fornai, K. Chen, F. S. Giorgi, M. Gesi, M. G. Alessandri, and J. C. Shih, "Striatal dopamine metabolism in monoamine oxidase B-deficient mice: a brain dialysis study," *Journal of Neurochemistry*, vol. 73, no. 6, pp. 2434–2440, 1999.

[52] K. F. Tipton, S. Boyce, J. O'Sullivan, G. P. Davey, and J. Healy, "Monoamine oxidases: certainties and uncertainties," *Current Medicinal Chemistry*, vol. 11, no. 15, pp. 1965–1982, 2004.

[53] M. B. H. Youdim, D. Edmondson, and K. F. Tipton, "The therapeutic potential of monoamine oxidase inhibitors," *Nature Reviews Neuroscience*, vol. 7, no. 4, pp. 295–309, 2006.

[54] G. C. Wagner, G. A. Ricaurte, L. S. Seiden, C. R. Schuster, R. J. Miller, and J. Westley, "Long-lasting depletions of striatal dopamine and loss of dopamine uptake sites following repeated administration of methamphetamine," *Brain Research*, vol. 181, no. 1, pp. 151–160, 1980.

[55] G. Battaglia, C. L. Busceti, L. Cuomo et al., "Continuous subcutaneous infusion of apomorphine rescues nigro-striatal dopaminergic terminals following MPTP injection in mice," *Neuropharmacology*, vol. 42, no. 3, pp. 367–373, 2002.

[56] G. Battaglia, M. Gesi, P. Lenzi et al., "Morphological and biochemical evidence that apomorphine rescues striatal dopamine terminals and prevents methamphetamine toxicity," *Annals of the New York Academy of Sciences*, vol. 965, no. 1, pp. 254–266, 2002.

[57] C. R. Gerfen, "Dopamine-mediated gene regulation in models of Parkinson's disease," *Annals of Neurology*, vol. 47, no. 4, Supplement 1, pp. S42–S52, 2000.

[58] D. J. Surmeier, W. Shen, M. Day et al., "The role of dopamine in modulating the structure and function of striatal circuits," *Progress in Brain Research*, vol. 183, pp. 149–167, 2010.

[59] C. R. Gerfen and D. J. Surmeier, "Modulation of striatal projection systems by dopamine," *Annual Review of Neuroscience*, vol. 34, no. 1, pp. 441–466, 2011.

[60] L. S. Seiden, M. W. Fischman, and C. R. Schuster, "Long-term methamphetamine induced changes in brain catecholamines in tolerant rhesus monkeys," *Drug and Alcohol Dependence*, vol. 1, no. 3, pp. 215–219, 1976.

[61] G. A. Ricaurte, R. W. Guillery, L. S. Seiden, C. R. Schuster, and R. Y. Moore, "Dopamine nerve terminal degeneration produced by high doses of methylamphetamine in the rat brain," *Brain Research*, vol. 235, no. 1, pp. 93–103, 1982.

[62] G. A. Ricaurte, L. S. Seiden, and C. R. Schuster, "Further evidence that amphetamines produce long-lasting dopamine neurochemical deficits by destroying dopamine nerve fibers," *Brain Research*, vol. 303, no. 2, pp. 359–364, 1984.

[63] P. K. Sonsalla, N. D. Jochnowitz, G. D. Zeevalk, J. A. Oostveen, and E. D. Hall, "Treatment of mice with methamphetamine produces cell loss in the substantia nigra," *Brain Research*, vol. 738, no. 1, pp. 172–175, 1996.

[64] M. K. Buening and J. W. Gibb, "Influence of methamphetamine and neuroleptic drugs on tyrosine hydroxylase activity," *European Journal of Pharmacology*, vol. 26, no. 1, pp. 30–34, 1974.

[65] A. J. Hotchkiss and J. W. Gibb, "Long-term effects of multiple doses of methamphetamine on tryptophan hydroxylase and tyrosine hydroxylase activity in rat brain," *Journal of Pharmacology and Experimental Therapeutics*, vol. 214, no. 2, pp. 257–262, 1980.

[66] C. J. Schmidt, J. K. Ritter, P. K. Sonsalla, G. R. Hanson, and J. W. Gibb, "Role of dopamine in the neurotoxic effects of methamphetamine," *Journal of Pharmacology and Experimental Therapeutics*, vol. 233, no. 3, pp. 539–544, 1985.

[67] H. Hirata and J. L. Cadet, "p53-knockout mice are protected against the long-term effects of methamphetamine on

dopaminergic terminals and cell bodies," *Journal of Neurochemistry*, vol. 69, no. 2, pp. 780–790, 1997.

[68] N. Granado, S. Ares-Santos, E. O'Shea, C. Vicario-Abejón, M. I. Colado, and R. Moratalla, "Selective vulnerability in striosomes and in the nigrostriatal dopaminergic pathway after methamphetamine administration: early loss of TH in striosomes after methamphetamine," *Neurotoxicity Research*, vol. 18, no. 1, pp. 48–58, 2010.

[69] N. Granado, S. Ares-Santos, I. Oliva et al., "Dopamine D2-receptor knockout mice are protected against dopaminergic neurotoxicity induced by methamphetamine or MDMA," *Neurobiology of Disease*, vol. 42, no. 3, pp. 391–403, 2011.

[70] N. Granado, I. Lastres-Becker, S. Ares-Santos et al., "Nrf2 deficiency potentiates methamphetamine-induced dopaminergic axonal damage and gliosis in the striatum," *Glia*, vol. 59, no. 12, pp. 1850–1863, 2011.

[71] S. Ares-Santos, N. Granado, I. Oliva et al., "Dopamine D_1 receptor deletion strongly reduces neurotoxic effects of methamphetamine," *Neurobiology of Disease*, vol. 45, no. 2, pp. 810–820, 2012.

[72] S. Ares-Santos, N. Granado, I. Espadas, R. Martinez-Murillo, and R. Moratalla, "Methamphetamine causes degeneration of dopamine cell bodies and terminals of the nigrostriatal pathway evidenced by silver staining," *Neuropsychopharmacology*, vol. 39, no. 5, pp. 1066–1080, 2014.

[73] J. Zhu, W. Xu, N. Angulo, and J. Angulo, "Methamphetamine-induced striatal apoptosis in the mouse brain: comparison of a binge to an acute bolus drug administration," *NeuroToxicology*, vol. 27, no. 1, pp. 131–136, 2006.

[74] B. A. Morrow, R. H. Roth, D. E. Redmond, and J. D. Elsworth, "Impact of methamphetamine on dopamine neurons in primates is dependent on age: implications for development of Parkinson's disease," *Neuroscience*, vol. 189, pp. 277–285, 2011.

[75] R. C. Callaghan, J. K. Cunningham, J. Sykes, and S. J. Kish, "Increased risk of Parkinson's disease in individuals hospitalized with conditions related to the use of methamphetamine or other amphetamine-type drugs," *Drug and Alcohol Dependence*, vol. 120, no. 1–3, pp. 35–40, 2012.

[76] K. Curtin, A. E. Fleckenstein, R. J. Robison, M. J. Crookston, K. R. Smith, and G. R. Hanson, "Methamphetamine/amphetamine abuse and risk of Parkinson's disease in Utah: a population-based assessment," *Drug and Alcohol Dependence*, vol. 146, pp. 30–38, 2015.

[77] J. J. Rumpf, J. Albers, C. Fricke, W. Mueller, and J. Classen, "Structural abnormality of substantia nigra induced by methamphetamine abuse," *Movement Disorders*, vol. 32, no. 12, pp. 1784–1788, 2017.

[78] F. Fornai, P. Lenzi, M. Gesi et al., "Methamphetamine produces neuronal inclusions in the nigrostriatal system and in PC12 cells," *Journal of Neurochemistry*, vol. 88, no. 1, pp. 114–123, 2004.

[79] F. Fornai, P. Lenzi, M. Gesi et al., "Similarities between methamphetamine toxicity and proteasome inhibition," *Annals of the New York Academy of Sciences*, vol. 1025, no. 1, pp. 162–170, 2004.

[80] F. Fornai, G. Lazzeri, A. B. Di Poggio et al., "Convergent roles of α-synuclein, DA metabolism, and the ubiquitin-proteasome system in nigrostriatal toxicity," *Annals of the New York Academy of Sciences*, vol. 1074, no. 1, pp. 84–89, 2006.

[81] G. Lazzeri, P. Lenzi, M. Gesi et al., "In PC12 cells neurotoxicity induced by methamphetamine is related to proteasome inhibition," *Annals of the New York Academy of Sciences*, vol. 1074, no. 1, pp. 174–177, 2006.

[82] F. Fornai, P. Lenzi, L. Capobianco et al., "Involvement of dopamine receptors and β-arrestin in metamphetamine-induced inclusions formation in pc12 cells," *Journal of Neurochemistry*, vol. 105, no. 5, pp. 1939–1947, 2008.

[83] R. Castino, G. Lazzeri, P. Lenzi et al., "Suppression of autophagy precipitates neuronal cell death following low doses of methamphetamine," *Journal of Neurochemistry*, vol. 106, no. 3, pp. 1426–1439, 2008.

[84] M. Ferrucci, L. Ryskalin, F. Biagioni et al., "Methamphetamine increases prion protein and induces dopamine-dependent expression of protease resistant PrPsc," *Archives Italiennes de Biologie*, vol. 155, no. 1-2, pp. 81–97, 2017.

[85] L. Quan, T. Ishikawa, T. Michiue et al., "Ubiquitin-immunoreactive structures in the midbrain of methamphetamine abusers," *Legal Medicine*, vol. 7, no. 3, pp. 144–150, 2005.

[86] L. Pasquali, G. Lazzeri, C. Isidoro, S. Ruggieri, A. Paparelli, and F. Fornai, "Role of autophagy during methamphetamine neurotoxicity," *Annals of the New York Academy of Sciences*, vol. 1139, no. 1, pp. 191–196, 2008.

[87] S. J. O'Dell, F. B. Weihmuller, and J. F. Marshall, "Multiple methamphetamine injections induce marked increases in extracellular striatal dopamine which correlate with subsequent neurotoxicity," *Brain Research*, vol. 564, no. 2, pp. 256–260, 1991.

[88] X. Deng and J. L. Cadet, "Methamphetamine-induced apoptosis is attenuated in the striata of copper-zinc superoxide dismutase transgenic mice," *Molecular Brain Research*, vol. 83, no. 1-2, pp. 121–124, 2000.

[89] X. Deng, Y. Wang, J. Chou, and J. L. Cadet, "Methamphetamine causes widespread apoptosis in the mouse brain: evidence from using an improved TUNEL histochemical method," *Molecular Brain Research*, vol. 93, no. 1, pp. 64–69, 2001.

[90] S. Jayanthi, X. Deng, P. A. H. Noailles, B. Ladenheim, and J. L. Cadet, "Methamphetamine induces neuronal apoptosis via cross-talks between endoplasmic reticulum and mitochondria-dependent death cascades," *The FASEB Journal*, vol. 18, no. 2, pp. 238–251, 2004.

[91] S. Jayanthi, X. Deng, B. Ladenheim et al., "Calcineurin/NFAT-induced up-regulation of the Fas ligand/Fas death pathway is involved in methamphetamine-induced neuronal apoptosis," *Proceedings of the National Academy of Sciences of the United States of America*, vol. 102, no. 3, pp. 868–873, 2005.

[92] J. Yu, J. Wang, J. L. Cadet, and J. A. Angulo, "Histological evidence supporting a role for the striatal neurokinin-1 receptor in methamphetamine-induced neurotoxicity in the mouse brain," *Brain Research*, vol. 1007, no. 1-2, pp. 124–131, 2004.

[93] J. P. Q. Zhu, W. Xu, and J. A. Angulo, "Methamphetamine-induced cell death: selective vulnerability in neuronal subpopulations of the striatum in mice," *Neuroscience*, vol. 140, no. 2, pp. 607–622, 2006.

[94] I. Tulloch, L. Afanador, I. Mexhitaj, N. Ghazaryan, A. G. GarzaGongora, and J. A. Angulo, "A single high dose of methamphetamine induces apoptotic and necrotic striatal cell loss lasting up to 3 months in mice," *Neuroscience*, vol. 193, no. 193, pp. 162–169, 2011.

[95] R. J. Jakel and W. F. Maragos, "Neuronal cell death in Huntington's disease: a potential role for dopamine," *Trends in Neurosciences*, vol. 23, no. 6, pp. 239–245, 2000.

[96] H. Kuribara, "Inhibition of methamphetamine sensitization by post-methamphetamine treatment with SCH 23390 or haloperidol," *Psychopharmacology*, vol. 119, no. 1, pp. 34–38, 1995.

[97] H. Kuribara, "Dopamine D_1 receptor antagonist SCH 23390 retards methamphetamine sensitization in both combined administration and early posttreatment schedules in mice," *Pharmacology Biochemistry and Behavior*, vol. 52, no. 4, pp. 759–763, 1995.

[98] H. Yoshida, M. Ohno, and S. Watanabe, "Roles of dopamine D_1 receptors in striatal fos protein induction associated with methamphetamine behavioral sensitization in rats," *Brain Research Bulletin*, vol. 38, no. 4, pp. 393–397, 1995.

[99] C. R. Gerfen, "D1 dopamine receptor supersensitivity in the dopamine-depleted striatum animal model of Parkinson's disease," *The Neuroscientist*, vol. 9, no. 6, pp. 455–462, 2003.

[100] C. Wersinger, J. Chen, and A. Sidhu, "Bimodal induction of dopamine-mediated striatal neurotoxicity is mediated through both activation of D1 dopamine receptors and autoxidation," *Molecular and Cellular Neuroscience*, vol. 25, no. 1, pp. 124–137, 2004.

[101] J. L. Cadet, S. Jayanthi, M. T. McCoy, G. Beauvais, and N. S. Cai, "Dopamine D1 receptors, regulation of gene expression in the brain, and neurodegeneration," *CNS & Neurological Disorders - Drug Targets*, vol. 9, no. 5, pp. 526–538, 2010.

[102] J. F. Nash and B. K. Yamamoto, "Methamphetamine neurotoxicity and striatal glutamate release: comparison to 3, 4-methylenedioxymethamphetamine," *Brain Research*, vol. 581, no. 2, pp. 237–243, 1992.

[103] J. F. Marshall, S. J. O'Dell, and F. B. Weihmuller, "Dopamine-glutamate interactions in methamphetamine-induced neurotoxicity," *Journal of Neural Transmission*, vol. 91, no. 2-3, pp. 241–254, 1993.

[104] S. E. Stephans and B. K. Yamamoto, "Methamphetamine-induced neurotoxicity: roles for glutamate and dopamine efflux," *Synapse*, vol. 17, no. 3, pp. 203–209, 1994.

[105] K. A. Mark, J. J. Soghomonian, and B. K. Yamamoto, "High-dose methamphetamine acutely activates the striatonigral pathway to increase striatal glutamate and mediate long-term dopamine toxicity," *Journal of Neuroscience*, vol. 24, no. 50, pp. 11449–11456, 2004.

[106] B. K. Yamamoto and M. G. Bankson, "Amphetamine neurotoxicity: cause and consequence of oxidative stress," *Critical Reviews in Neurobiology*, vol. 17, no. 2, pp. 87–118, 2005.

[107] T. B. Rodrigues, N. Granado, O. Ortiz, S. Cerdán, and R. Moratalla, "Metabolic interactions between glutamatergic and dopaminergic neurotransmitter systems are mediated through D_1 dopamine receptors," *Journal of Neuroscience Research*, vol. 85, no. 15, pp. 3284–3293, 2007.

[108] H. Yamamoto, K. Imai, E. Kamegaya et al., "Repeated methamphetamine administration alters expression of the NMDA receptor channel $\varepsilon 2$ subunit and kinesins in the mouse brain," *Annals of the New York Academy of Sciences*, vol. 1074, no. 1, pp. 97–103, 2006.

[109] B. K. Yamamoto and J. Raudensky, "The role of oxidative stress, metabolic compromise, and inflammation in neuronal injury produced by amphetamine-related drugs of abuse," *Journal of Neuroimmune Pharmacology*, vol. 3, no. 4, pp. 203–217, 2008.

[110] Y. Luo, A. Hattori, J. Munoz, Z. H. Qin, and G. S. Roth, "Intrastriatal dopamine injection induces apoptosis through oxidation-involved activation of transcription factors AP-1 and NF-κB in rats," *Molecular Pharmacology*, vol. 56, no. 2, pp. 254–264, 1999.

[111] W. Jeng, A. W. Wong, R. Ting-A-Kee, and P. G. Wells, "Methamphetamine-enhanced embryonic oxidative DNA damage and neurodevelopmental deficits," *Free Radical Biology & Medicine*, vol. 39, no. 3, pp. 317–326, 2005.

[112] W. Jeng, A. Ramkissoon, T. Parman, and P. G. Wells, "Prostaglandin H synthase-catalyzed bioactivation of amphetamines to free radical intermediates that cause CNS regional DNA oxidation and nerve terminal degeneration," *The FASEB Journal*, vol. 20, no. 6, pp. 638–650, 2006.

[113] G. Frenzilli, M. Ferrucci, F. S. Giorgi et al., "DNA fragmentation and oxidative stress in the hippocampal formation: a bridge between 3, 4-methylenedioxymethamphetamine (ecstasy) intake and long-lasting behavioral alterations," *Behavioural Pharmacology*, vol. 18, no. 5-6, pp. 471–481, 2007.

[114] Z. Johnson, J. Venters, F. A. Guarraci, and M. Zewail-Foote, "Methamphetamine induces DNA damage in specific regions of the female rat brain," *Clinical and Experimental Pharmacology and Physiology*, vol. 42, no. 6, pp. 570–575, 2015.

[115] J. A. Potashkin and G. E. Meredith, "The role of oxidative stress in the dysregulation of gene expression and protein metabolism in neurodegenerative disease," *Antioxidants & Redox Signaling*, vol. 8, no. 1-2, pp. 144–151, 2006.

[116] S. W. Burnside and G. E. Hardingham, "Transcriptional regulators of redox balance and other homeostatic processes with the potential to alter neurodegenerative disease trajectory," *Biochemical Society Transactions*, vol. 45, no. 6, pp. 1295–1303, 2017.

[117] T. Grune, T. Jung, K. Merker, and K. J. A. Davies, "Decreased proteolysis caused by protein aggregates, inclusion bodies, plaques, lipofuscin, ceroid, and 'aggresomes' during oxidative stress, aging, and disease," *The International Journal of Biochemistry & Cell Biology*, vol. 36, no. 12, pp. 2519–2530, 2004.

[118] V. Dias, E. Junn, and M. M. Mouradian, "The role of oxidative stress in Parkinson's disease," *Journal of Parkinson's Disease*, vol. 3, no. 4, pp. 461–491, 2013.

[119] H. Ujike, T. Onoue, K. Akiyama, T. Hamamura, and S. Otsuki, "Effects of selective D-1 and D-2 dopamine antagonists on development of methamphetamine-induced behavioral sensitization," *Psychopharmacology*, vol. 98, no. 1, pp. 89–92, 1989.

[120] S. J. O'Dell, F. B. Weihmuller, and J. F. Marshall, "Methamphetamine-induced dopamine overflow and injury to striatal dopamine terminals: attenuation by dopamine D_1 or D_2 antagonists," *Journal of Neurochemistry*, vol. 60, no. 5, pp. 1792–1799, 1993.

[121] M. A. Kelly, M. J. Low, M. Rubinstein, and T. J. Phillips, "Role of dopamine D1-like receptors in methamphetamine locomotor responses of D2 receptor knockout mice," *Genes, Brain and Behavior*, vol. 7, no. 5, pp. 568–577, 2008.

[122] S. Jayanthi, M. T. McCoy, G. Beauvais et al., "Methamphetamine induces dopamine D1 receptor-dependent endoplasmic reticulum stress-related molecular events in the rat striatum," *PLoS One*, vol. 4, no. 6, article e6092, 2009.

[123] G. Beauvais, S. Jayanthi, M. T. McCoy, B. Ladenheim, and J. L. Cadet, "Differential effects of methamphetamine and SCH23390 on the expression of members of IEG families of transcription factors in the rat striatum," *Brain Research*, vol. 1318, pp. 1–10, 2010.

[124] D. M. Friend and K. A. Keefe, "A role for D1 dopamine receptors in striatal methamphetamine-induced neurotoxicity," *Neuroscience Letters*, vol. 555, pp. 243–247, 2013.

[125] S. Ares-Santos, N. Granado, and R. Moratalla, "The role of dopamine receptors in the neurotoxicity of methamphetamine," *Journal of Internal Medicine*, vol. 273, no. 5, pp. 437–453, 2013.

[126] K. A. Neve, J. K. Seamans, and H. Trantham-Davidson, "Dopamine receptor signaling," *Journal of Receptors and Signal Transduction*, vol. 24, no. 3, pp. 165–205, 2004.

[127] J. C. Stoof and J. W. Kebabian, "Two dopamine receptors: biochemistry, physiology and pharmacology," *Life Sciences*, vol. 35, no. 23, pp. 2281–2296, 1984.

[128] S. Hernández-López, T. Tkatch, E. Perez-Garci et al., "D_2 dopamine receptors in striatal medium spiny neurons reduce L-type Ca^{2+} currents and excitability via a novel PLCβ1–IP_3–calcineurin-signaling cascade," *Journal of Neuroscience*, vol. 20, no. 24, pp. 8987–8995, 2000.

[129] A. Nishi, M. Kuroiwa, and T. Shuto, "Mechanisms for the modulation of dopamine D_1 receptor signaling in striatal neurons," *Frontiers in Neuroanatomy*, vol. 5, p. 43, 2011.

[130] P. K. Sonsalla, J. W. Gibb, and G. R. Hanson, "Roles of D1 and D2 dopamine receptor subtypes in mediating the methamphetamine-induced changes in monoamine systems," *Journal of Pharmacology and Experimental Therapeutics*, vol. 238, no. 3, pp. 932–937, 1986.

[131] C. Gerfen, T. Engber, L. Mahan et al., "D1 and D2 dopamine receptor-regulated gene expression of striatonigral and striatopallidal neurons," *Science*, vol. 250, no. 4986, pp. 1429–1432, 1990.

[132] C. R. Gerfen, S. Miyachi, R. Paletzki, and P. Brown, "D1 dopamine receptor supersensitivity in the dopamine-depleted striatum results from a switch in the regulation of ERK1/2/MAP kinase," *Journal of Neuroscience*, vol. 22, no. 12, pp. 5042–5054, 2002.

[133] B. P. Bejjani, I. Arnulf, S. Demeret et al., "Levodopa-induced dyskinesias in Parkinson's disease: is sensitization reversible?," *Annals of Neurology*, vol. 47, no. 5, pp. 655–658, 2000.

[134] J. G. Nutt, "Continuous dopaminergic stimulation: is it the answer to the motor complications of Levodopa?," *Movement Disorders*, vol. 22, no. 1, pp. 1–9, 2007.

[135] J. L. Taylor, C. Bishop, and P. D. Walker, "Dopamine D_1 and D_2 receptor contributions to L-DOPA-induced dyskinesia in the dopamine-depleted rat," *Pharmacology Biochemistry and Behavior*, vol. 81, no. 4, pp. 887–893, 2005.

[136] L. Chen, J. D. Bohanick, M. Nishihara, J. K. Seamans, and C. R. Yang, "Dopamine D1/5 receptor-mediated long-term potentiation of intrinsic excitability in rat prefrontal cortical neurons: Ca^{2+}-dependent intracellular signaling," *Journal of Neurophysiology*, vol. 97, no. 3, pp. 2448–2464, 2007.

[137] F. Fornai, F. Biagioni, F. Fulceri, L. Murri, S. Ruggieri, and A. Paparelli, "Intermittent dopaminergic stimulation causes behavioral sensitization in the addicted brain and parkinsonism," *International Review of Neurobiology*, vol. 88, pp. 371–398, 2009.

[138] F. Biagioni, A. Pellegrini, S. Ruggieri, L. Murri, A. Paparelli, and F. Fornai, "Behavioural sensitisation during dopamine replacement therapy in Parkinson's disease is reminiscent of the addicted brain," *Current Topics in Medicinal Chemistry*, vol. 9, no. 10, pp. 894–902, 2009.

[139] A. Fasano and I. Petrovic, "Insights into pathophysiology of punding reveal possible treatment strategies," *Molecular Psychiatry*, vol. 15, no. 6, pp. 560–573, 2010.

[140] C. R. Gerfen, R. Paletzki, and P. Worley, "Differences between dorsal and ventral striatum in Drd1a dopamine receptor coupling of dopamine- and cAMP-regulated phosphoprotein-32 to activation of extracellular signal-regulated kinase," *Journal of Neuroscience*, vol. 28, no. 28, pp. 7113–7120, 2008.

[141] T. Hamamura, K. Akiyama, K. Akimoto et al., "Co-administration of either a selective D_1 or D_2 dopamine antagonist with methamphetamine prevents methamphetamine-induced behavioral sensitization and neurochemical change, studied by in vivo intracerebral dialysis," *Brain Research*, vol. 546, no. 1, pp. 40–46, 1991.

[142] P. Vezina, "D1 dopamine receptor activation is necessary for the induction of sensitization by amphetamine in the ventral tegmental area," *Journal of Neuroscience*, vol. 16, no. 7, pp. 2411–2420, 1996.

[143] R. Kuczenski and D. S. Segal, "Sensitization of amphetamine-induced stereotyped behaviors during the acute response," *Journal of Pharmacology and Experimental Therapeutics*, vol. 288, no. 2, pp. 699–709, 1999.

[144] P. Karper, H. De La Rosa, E. Newman et al., "Role of D_1-like receptors in amphetamine-induced behavioral sensitization: a study using D_{1A} receptor knockout mice," *Psychopharmacology*, vol. 159, no. 4, pp. 407–414, 2002.

[145] K. E. Bosse, J. L. Charlton, L. L. Susick et al., "Deficits in behavioral sensitization and dopaminergic responses to methamphetamine in adenylyl cyclase 1/8-deficient mice," *Journal of Neurochemistry*, vol. 135, no. 6, pp. 1218–1231, 2015.

[146] S. Moriguchi, S. Watanabe, H. Kita, and H. Nakanishi, "Enhancement of *N*-methyl-D-aspartate receptor-mediated excitatory postsynaptic potentials in the neostriatum after methamphetamine sensitization. An in vitro slice study," *Experimental Brain Research*, vol. 144, no. 2, pp. 238–246, 2002.

[147] M. Miyazaki, Y. Noda, A. Mouri et al., "Role of convergent activation of glutamatergic and dopaminergic systems in the nucleus accumbens in the development of methamphetamine psychosis and dependence," *International Journal of Neuropsychopharmacology*, vol. 16, no. 6, pp. 1341–1350, 2013.

[148] J. Chen, M. Rusnak, R. R. Luedtke, and A. Sidhu, "D1 dopamine receptor mediates dopamine-induced cytotoxicity via the ERK signal cascade," *Journal of Biological Chemistry*, vol. 279, no. 38, pp. 39317–39330, 2004.

[149] N. Pavon, A. B. Martin, A. Mendialdua, and R. Moratalla, "ERK phosphorylation and FosB expression are associated with L-DOPA-induced dyskinesia in hemiparkinsonian mice," *Biological Psychiatry*, vol. 59, no. 1, pp. 64–74, 2006.

[150] J. E. Westin, L. Vercammen, E. M. Strome, C. Konradi, and M. A. Cenci, "Spatiotemporal pattern of striatal ERK1/2 phosphorylation in a rat model of L-DOPA–induced dyskinesia and the role of dopamine D1 receptors," *Biological Psychiatry*, vol. 62, no. 7, pp. 800–810, 2007.

[151] E. Santini, E. Valjent, A. Usiello et al., "Critical involvement of cAMP/DARPP-32 and extracellular signal-regulated protein kinase signaling in L-DOPA-induced dyskinesia," *Journal of Neuroscience*, vol. 27, no. 26, pp. 6995–7005, 2007.

[152] J. Girault, E. Valjent, J. Caboche, and D. Herve, "ERK2: a logical AND gate critical for drug-induced plasticity?," *Current Opinion in Pharmacology*, vol. 7, no. 1, pp. 77–85, 2007.

[153] V. Pascoli, E. Cahill, F. Bellivier, J. Caboche, and P. Vanhoutte, "Extracellular signal-regulated protein kinases 1 and 2 activation by addictive drugs: a signal toward pathological adaptation," *Biological Psychiatry*, vol. 76, no. 12, pp. 917–926, 2014.

[154] H. Mizoguchi, K. Yamada, M. Mizuno et al., "Regulations of methamphetamine reward by extracellular signal-regulated kinase 1/2/ets-like gene-1 signaling pathway via the activation of dopamine receptors," *Molecular Pharmacology*, vol. 65, no. 5, pp. 1293–1301, 2004.

[155] E. Valjent, V. Pascoli, P. Svenningsson et al., "Regulation of a protein phosphatase cascade allows convergent dopamine and glutamate signals to activate ERK in the striatum," *Proceedings of the National Academy of Sciences of the United States of America*, vol. 102, no. 2, pp. 491–496, 2005.

[156] V. Pascoli, A. Besnard, D. Hervé et al., "Cyclic adenosine monophosphate–independent tyrosine phosphorylation of NR2B mediates cocaine-induced extracellular signal-regulated kinase activation," *Biological Psychiatry*, vol. 69, no. 3, pp. 218–227, 2011.

[157] P. Svenningsson, A. Nishi, G. Fisone, J. A. Girault, A. C. Nairn, and P. Greengard, "DARPP-32: an integrator of neurotransmission," *Annual Review of Pharmacology and Toxicology*, vol. 44, no. 1, pp. 269–296, 2004.

[158] P. Svenningsson, A. C. Nairn, and P. Greengard, "DARPP-32 mediates the actions of multiple drugs of abuse," *The AAPS Journal*, vol. 7, no. 2, pp. E353–E360, 2005.

[159] X. H. Lin, T. Hashimoto, N. Kitamura, N. Murakami, O. Shirakawa, and K. Maeda, "Decreased calcineurin and increased phosphothreonine-DARPP-32 in the striatum of rats behaviorally sensitized to methamphetamine," *Synapse*, vol. 44, no. 3, pp. 181–187, 2002.

[160] P.-C. Chen and J.-C. Chen, "Enhanced Cdk5 activity and p35 translocation in the ventral striatum of acute and chronic methamphetamine-treated rats," *Neuropsychopharmacology*, vol. 30, no. 3, pp. 538–549, 2005.

[161] V. Zachariou, V. Sgambato-Faure, T. Sasaki et al., "Phosphorylation of DARPP-32 at threonine-34 is required for cocaine action," *Neuropsychopharmacology*, vol. 31, no. 3, pp. 555–562, 2006.

[162] P. Greengard, P. B. Allen, and A. C. Nairn, "Beyond the dopamine receptor: the DARPP-32/protein phosphatase-1 cascade," *Neuron*, vol. 23, no. 3, pp. 435–447, 1999.

[163] P. Greengard, "The neurobiology of slow synaptic transmission," *Science*, vol. 294, no. 5544, pp. 1024–1030, 2001.

[164] A. Stipanovich, E. Valjent, M. Matamales et al., "A phosphatase cascade by which rewarding stimuli control nucleosomal response," *Nature*, vol. 453, no. 7197, pp. 879–884, 2008.

[165] M. A. Andres, I. M. Cooke, F. P. Bellinger et al., "Methamphetamine acutely inhibits voltage-gated calcium channels but chronically upregulates L-type channels," *Journal of Neurochemistry*, vol. 134, no. 1, pp. 56–65, 2015.

[166] G. L. Snyder, P. B. Allen, A. A. Fienberg et al., "Regulation of phosphorylation of the GluR1 AMPA receptor in the neostriatum by dopamine and psychostimulants in vivo," *Journal of Neuroscience*, vol. 20, no. 12, pp. 4480–4488, 2000.

[167] S. Edwards, D. L. Simmons, D. G. Galindo et al., "Antagonistic effects of dopaminergic signaling and ethanol on protein kinase A–mediated phosphorylation of DARPP-32 and the NR1 subunit of the NMDA receptor," *Alcoholism: Clinical & Experimental Research*, vol. 26, no. 2, pp. 173–180, 2002.

[168] J. T. Dudman, M. E. Eaton, A. Rajadhyaksha et al., "Dopamine D1 receptors mediate CREB phosphorylation via phosphorylation of the NMDA receptor at Ser897–NR1," *Journal of Neurochemistry*, vol. 87, no. 4, pp. 922–934, 2003.

[169] R. D. Swayze, M. F. Lise, J. N. Levinson, A. Phillips, and A. El-Husseini, "Modulation of dopamine mediated phosphorylation of AMPA receptors by PSD-95 and AKAP79/150," *Neuropharmacology*, vol. 47, no. 5, pp. 764–778, 2004.

[170] C. Gao, X. Sun, and M. E. Wolf, "Activation of D1 dopamine receptors increases surface expression of AMPA receptors and facilitates their synaptic incorporation in cultured hippocampal neurons," *Journal of Neurochemistry*, vol. 98, no. 5, pp. 1664–1677, 2006.

[171] P. F. Simões, A. P. Silva, F. C. Pereira et al., "Methamphetamine changes NMDA and AMPA glutamate receptor subunit levels in the rat striatum and frontal cortex," *Annals of the New York Academy of Sciences*, vol. 1139, no. 1, pp. 232–241, 2008.

[172] W. Kerdsan, S. Thanoi, and S. Nudmamud-Thanoi, "Changes in glutamate/NMDA receptor subunit 1 expression in rat brain after acute and subacute exposure to methamphetamine," *Journal of Biomedicine and Biotechnology*, vol. 2009, article 329631, 4 pages, 2009.

[173] X. Huang, Y.-Y. Chen, Y. Shen et al., "Methamphetamine abuse impairs motor cortical plasticity and function," *Molecular Psychiatry*, vol. 22, no. 9, pp. 1274–1281, 2017.

[174] K. A. Mark, M. S. Quinton, S. J. Russek, and B. K. Yamamoto, "Dynamic changes in vesicular glutamate transporter 1 function and expression related to methamphetamine-induced glutamate release," *Journal of Neuroscience*, vol. 27, no. 25, pp. 6823–6831, 2007.

[175] W. Kerdsan, S. Thanoi, and S. Nudmamud-Thanoi, "Changes in the neuronal glutamate transporter EAAT3 in rat brain after exposure to methamphetamine," *Basic and Clinical Pharmacology and Toxicology*, vol. 111, no. 4, pp. 275–278, 2012.

[176] X. Zhang, T. H. Lee, X. Xiong et al., "Methamphetamine induces long-term changes in $GABA_A$ receptor $\alpha 2$ subunit and GAD_{67} expression," *Biochemical and Biophysical Research Communications*, vol. 351, no. 1, pp. 300–305, 2006.

[177] A. Nishi, Y. Watanabe, H. Higashi, M. Tanaka, A. C. Nairn, and P. Greengard, "Glutamate regulation of DARPP-32 phosphorylation in neostriatal neurons involves activation of multiple signaling cascades," *Proceedings of the National Academy of Sciences of the United States of America*, vol. 102, no. 4, pp. 1199–1204, 2005.

[178] K. Chergui, P. Svenningsson, and P. Greengard, "Cyclin-dependent kinase 5 regulates dopaminergic and glutamatergic transmission in the striatum," *Proceedings of the National Academy of Sciences of the United States of America*, vol. 101, no. 7, pp. 2191–2196, 2004.

[179] J. A. Bibb, G. L. Snyder, A. Nishi et al., "Phosphorylation of DARPP-32 by Cdk5 modulates dopamine signalling in neurons," *Nature*, vol. 402, no. 6762, pp. 669–671, 1999.

[180] R. B. Maccioni, C. Otth, I. I. Concha, and J. P. Munoz, "The protein kinase Cdk5," *European Journal of Biochemistry*, vol. 268, no. 6, pp. 1518–1527, 2001.

[181] A. Nishi, J. A. Bibb, G. L. Snyder, H. Higashi, A. C. Nairn, and P. Greengard, "Amplification of dopaminergic signaling by a positive feedback loop," *Proceedings of the National Academy of Sciences of the United States of America*, vol. 97, no. 23, pp. 12840–12845, 2000.

[182] J. A. Bibb, J. Chen, J. R. Taylor et al., "Effects of chronic exposure to cocaine are regulated by the neuronal protein Cdk5," *Nature*, vol. 410, no. 6826, pp. 376–380, 2001.

[183] E. C. Mlewski, F. A. Krapacher, S. Ferreras, and G. Paglini, "Transient enhanced expression of Cdk5 activator p25 after acute and chronic *d*-amphetamine administration," *Annals of the New York Academy of Sciences*, vol. 1139, no. 1, pp. 89–102, 2008.

[184] T. S. Tang and I. Bezprozvanny, "Dopamine receptor-mediated Ca^{2+} signaling in striatal medium spiny neurons," *Journal of Biological Chemistry*, vol. 279, no. 40, pp. 42082–42094, 2004.

[185] A. J. Rashid, C. H. So, M. M. C. Kong et al., "D1–D2 dopamine receptor heterooligomers with unique pharmacology are coupled to rapid activation of G_q/11 in the striatum," *Proceedings of the National Academy of Sciences of the United States of America*, vol. 104, no. 2, pp. 654–659, 2007.

[186] A. Hasbi, T. Fan, M. Alijaniaram et al., "Calcium signaling cascade links dopamine D1–D2 receptor heteromer to striatal BDNF production and neuronal growth," *Proceedings of the National Academy of Sciences of the United States of America*, vol. 106, no. 50, pp. 21377–21382, 2009.

[187] A. Hasbi, B. F. O'Dowd, and S. R. George, "Heteromerization of dopamine D2 receptors with dopamine D1 or D5 receptors generates intracellular calcium signaling by different mechanisms," *Current Opinion in Pharmacology*, vol. 10, no. 1, pp. 93–99, 2010.

[188] R. Moratalla, H. A. Robertson, and A. M. Graybiel, "Dynamic regulation of NGFI-A (zif268, egr1) gene expression in the striatum," *Journal of Neuroscience*, vol. 12, no. 7, pp. 2609–2622, 1992.

[189] A. J. Cole, R. V. Bhat, C. Patt, P. F. Worley, and J. M. Baraban, "D_1 dopamine receptor activation of multiple transcription factor genes in rat striatum," *Journal of Neurochemistry*, vol. 58, no. 4, pp. 1420–1426, 1992.

[190] C. Konradi, R. L. Cole, S. Heckers, and S. E. Hyman, "Amphetamine regulates gene expression in rat striatum via transcription factor CREB," *Journal of Neuroscience*, vol. 14, no. 9, pp. 5623–5634, 1994.

[191] C. S. Simpson and B. J. Morris, "Induction of c-fos and zif/268 gene expression in rat striatal neurons, following stimulation of D_1-like dopamine receptors, involves protein kinase A and protein kinase C," *Neuroscience*, vol. 68, no. 1, pp. 97–106, 1995.

[192] J. D. Berke, R. F. Paletzki, G. J. Aronson, S. E. Hyman, and C. R. Gerfen, "A complex program of striatal gene expression induced by dopaminergic stimulation," *Journal of Neuroscience*, vol. 18, no. 14, pp. 5301–5310, 1998.

[193] P. Svenningsson, A. A. Fienberg, P. B. Allen et al., "Dopamine D_1 receptor-induced gene transcription is modulated by DARPP-32," *Journal of Neurochemistry*, vol. 75, no. 1, pp. 248–257, 2000.

[194] J. Chen, C. Wersinger, and A. Sidhu, "Chronic stimulation of D1 dopamine receptors in human SK-N-MC neuroblastoma cells induces nitric-oxide synthase activation and cytotoxicity," *Journal of Biological Chemistry*, vol. 278, no. 30, pp. 28089–28100, 2003.

[195] R. D. Groth, J. P. Weick, K. C. Bradley et al., "D1 dopamine receptor activation of NFAT-mediated striatal gene expression," *European Journal of Neuroscience*, vol. 27, no. 1, pp. 31–42, 2008.

[196] S. W. Park, X. Shen, L.-T. Tien, R. Roman, and T. Ma, "Methamphetamine-induced changes in the striatal dopamine pathway in μ-opioid receptor knockout mice," *Journal of Biomedical Science*, vol. 18, no. 1, p. 83, 2011.

[197] J. L. Cadet, M. T. McCoy, and B. Ladenheim, "Distinct gene expression signatures in the striata of wild-type and heterozygous c-fos knockout mice following methamphetamine administration: evidence from cDNA array analyses," *Synapse*, vol. 44, no. 4, pp. 211–226, 2002.

[198] J. L. Cadet, C. Brannock, S. Jayanthi, and I. N. Krasnova, "Transcriptional and epigenetic substrates of methamphetamine addiction and withdrawal: evidence from a long-access self-administration model in the rat," *Molecular Neurobiology*, vol. 51, no. 2, pp. 696–717, 2015.

[199] P. Sheng, X. B. Wang, B. Ladenheim, C. Epstein, and J. L. Cadet, "AP-1 DNA-binding activation by methamphetamine involves oxidative stress," *Synapse*, vol. 24, no. 3, pp. 213–217, 1996.

[200] M. Asanuma and J. L. Cadet, "Methamphetamine-induced increase in striatal NF-κB DNA-binding activity is attenuated in superoxide dismutase transgenic mice," *Molecular Brain Research*, vol. 60, no. 2, pp. 305–309, 1998.

[201] M. Asanuma, I. Miyazaki, Y. Higashi, T. Tsuji, and N. Ogawa, "Specific gene expression and possible involvement of inflammation in methamphetamine-induced neurotoxicity," *Annals of the New York Academy of Sciences*, vol. 1025, no. 1, pp. 69–75, 2004.

[202] T. Barrett, T. Xie, Y. Piao et al., "A murine dopamine neuron-specific cDNA library and microarray: increased COX1 expression during methamphetamine neurotoxicity," *Neurobiology of Disease*, vol. 8, no. 5, pp. 822–833, 2001.

[203] T. Xie, L. Tong, T. Barrett et al., "Changes in gene expression linked to methamphetamine-induced dopaminergic neurotoxicity," *Journal of Neuroscience*, vol. 22, no. 1, pp. 274–283, 2002.

[204] Y. W. Lee, B. Hennig, J. Yao, and M. Toborek, "Methamphetamine induces AP-1 and NF-κB binding and transactivation in human brain endothelial cells," *Journal of Neuroscience Research*, vol. 66, no. 4, pp. 583–591, 2001.

[205] G. Flora, Y. W. Lee, A. Nath, W. Maragos, B. Hennig, and M. Toborek, "Methamphetamine-induced TNF-α gene expression and activation of AP-1 in discrete regions of mouse brain: potential role of reactive oxygen intermediates and lipid peroxidation," *Neuromolecular Medicine*, vol. 2, no. 1, pp. 71–85, 2002.

[206] D. M. Thomas, D. M. Francescutti-Verbeem, X. Liu, and D. M. Kuhn, "Identification of differentially regulated transcripts in mouse striatum following methamphetamine treatment – an oligonucleotide microarray approach," *Journal of Neurochemistry*, vol. 88, no. 2, pp. 380–393, 2004.

[207] S. Jayanthi, M. McCoy, B. Ladenheim, and J. L. Cadet, "Methamphetamine causes coordinate regulation of SRC, Cas, Crk, and the Jun N-terminal kinase–Jun pathway," *Molecular Pharmacology*, vol. 61, no. 5, pp. 1124–1131, 2002.

[208] G. Beauvais, K. Atwell, S. Jayanthi, B. Ladenheim, and J. L. Cadet, "Involvement of dopamine receptors in binge methamphetamine-induced activation of endoplasmic reticulum and mitochondrial stress pathways," *PLoS One*, vol. 6, no. 12, article e28946, 2011.

[209] I. N. Krasnova, M. Chiflikyan, Z. Justinova et al., "CREB phosphorylation regulates striatal transcriptional responses in the self-administration model of methamphetamine addiction in the rat," *Neurobiology of Disease*, vol. 58, pp. 132–143, 2013.

[210] I. N. Krasnova, Z. Justinova, and J. L. Cadet, "Methamphetamine addiction: involvement of CREB and neuroinflammatory signaling pathways," *Psychopharmacology*, vol. 233, no. 10, pp. 1945–1962, 2016.

[211] K. T. Turpaev, "Reactive oxygen species and regulation of gene expression," *Biochemistry*, vol. 67, no. 3, pp. 281–292, 2002.

[212] J. Q. Wang, A. J. W. Smith, and J. F. McGinty, "A single injection of amphetamine or methamphetamine induces dynamic alterations in c-*fos*,*zif*/268 and preprodynorphin messenger RNA expression in rat forebrain," *Neuroscience*, vol. 68, no. 1, pp. 83–95, 1995.

[213] R. Moratalla, M. Xu, S. Tonegawa, and A. M. Graybiel, "Cellular responses to psychomotor stimulant and neuroleptic drugs are abnormal in mice lacking the D1 dopamine receptor," *Proceedings of the National Academy of Sciences of the United States of America*, vol. 93, no. 25, pp. 14928–14933, 1996.

[214] X. Shi and J. F. McGinty, "D1 and D2 dopamine receptors differentially mediate the activation of phosphoproteins in the striatum of amphetamine-sensitized rats," *Psychopharmacology*, vol. 214, no. 3, pp. 653–663, 2011.

[215] K. Uno, T. Miyazaki, K. Sodeyama, Y. Miyamoto, and A. Nitta, "Methamphetamine induces Shati/Nat8L expression in the mouse nucleus accumbens via CREB- and dopamine D1 receptor-dependent mechanism," *PLoS One*, vol. 12, no. 3, article e0174196, 2017.

[216] N. Pregi, L. M. Belluscio, B. G. Berardino, D. S. Castillo, and E. T. Cánepa, "Oxidative stress-induced CREB upregulation promotes DNA damage repair prior to neuronal cell death protection," *Molecular and Cellular Biochemistry*, vol. 425, no. 1-2, pp. 9–24, 2017.

[217] M. A. Hebert and J. P. O'Callaghan, "Protein phosphorylation cascades associated with methamphetamine-induced glial activation," *Annals of the New York Academy of Sciences*, vol. 914, no. 1, pp. 238–262, 2000.

[218] J. McDaid, M. P. Graham, and T. C. Napier, "Methamphetamine-induced sensitization differentially alters pCREB and ΔFosB throughout the limbic circuit of the mammalian brain," *Molecular Pharmacology*, vol. 70, no. 6, pp. 2064–2074, 2006.

[219] N. K. Ryu, M. H. Yang, M. S. Jung, J. O. Jeon, K. W. Kim, and J. H. Park, "Gene expression profiling of rewarding effect in methamphetamine treated Bax-deficient mouse," *Journal of Biochemistry and Molecular Biology*, vol. 40, no. 4, pp. 475–485, 2007.

[220] G. Cao, J. Zhu, Q. Zhong et al., "Distinct roles of methamphetamine in modulating spatial memory consolidation, retrieval, reconsolidation and the accompanying changes of ERK and CREB activation in hippocampus and prefrontal cortex," *Neuropharmacology*, vol. 67, pp. 144–154, 2013.

[221] T. Hai and T. Curran, "Cross-family dimerization of transcription factors Fos/Jun and ATF/CREB alters DNA binding specificity," *Proceedings of the National Academy of Sciences of the United States of America*, vol. 88, no. 9, pp. 3720–3724, 1991.

[222] E. Shaulian and M. Karin, "AP-1 as a regulator of cell life and death," *Nature Cell Biology*, vol. 4, no. 5, pp. E131–E136, 2002.

[223] D. M. Bronstein, K. R. Pennypacker, H. Lee, and J. S. Hong, "Methamphetamine-induced changes in AP-1 binding and dynorphin in the striatum: correlated, not causally related events?," *Biological Signals*, vol. 5, no. 6, pp. 317–333, 1996.

[224] K. R. Pennypacker, X. Yang, M. N. Gordon, S. Benkovic, D. Miller, and J. P. O'Callaghan, "Long-term induction of Fos-related antigen-2 after methamphetamine-, methylenedioxymethamphetamine-, 1-methyl-4-phenyl-1,2,3,6-tetrahydropyridine- and trimethyltin-induced brain injury," *Neuroscience*, vol. 101, no. 4, pp. 913–919, 2000.

[225] J. L. Cadet, S. Jayanthi, M. T. McCoy et al., "Genome-wide profiling identifies a subset of methamphetamine (METH)-induced genes associated with METH-induced increased H4K5Ac binding in the rat striatum," *BMC Genomics*, vol. 14, no. 1, p. 545, 2013.

[226] F. Saint-Preux, L. R. Bores, I. Tulloch et al., "Chronic co-administration of nicotine and methamphetamine causes differential expression of immediate early genes in the dorsal striatum and nucleus accumbens of Rats," *Neuroscience*, vol. 243, pp. 89–96, 2013.

[227] O. V. Torres, M. T. McCoy, B. Ladenheim et al., "CAMKII-conditional deletion of histone deacetylase 2 potentiates acute methamphetamine-induced expression of immediate early genes in the mouse nucleus accumbens," *Scientific Reports*, vol. 5, no. 1, article 13396, 2015.

[228] W. Renthal, T. L. Carle, I. Maze et al., "ΔFosB mediates epigenetic desensitization of the c-*fos* gene after chronic amphetamine exposure," *Journal of Neuroscience*, vol. 28, no. 29, pp. 7344–7349, 2008.

[229] A. J. Robison and E. J. Nestler, "Transcriptional and epigenetic mechanisms of addiction," *Nature Review Neuroscience*, vol. 12, no. 11, pp. 623–637, 2011.

[230] H. Ujike, "Advanced findings on the molecular mechanisms for behavioral sensitization to psychostimulants," *Nihon Yakurigaku Zasshi*, vol. 117, no. 1, pp. 5–12, 2001.

[231] C. A. Tamminga and E. J. Nestler, "Pathological gambling: focusing on the addiction, not the activity," *The American Journal of Psychiatry*, vol. 163, no. 2, pp. 180-181, 2006.

[232] J. L. Cornish, G. E. Hunt, L. Robins, and I. S. McGregor, "Regional c-Fos and FosB/ΔFosB expression associated with chronic methamphetamine self-administration and methamphetamine-seeking behavior in rats," *Neuroscience*, vol. 206, pp. 100–114, 2012.

[233] A. A. Palmer, M. Verbitsky, R. Suresh et al., "Gene expression differences in mice divergently selected for methamphetamine sensitivity," *Mammalian Genome*, vol. 16, no. 5, pp. 291–305, 2005.

[234] A. M. Beckmann and P. A. Wilce, "Egr transcription factors in the nervous system," *Neurochemistry International*, vol. 31, no. 4, pp. 477–510, 1997.

[235] H. Hirata, M. Asanuma, and J. L. Cadet, "Superoxide radicals are mediators of the effects of methamphetamine on *Zif268*

(Egr-1, NGFI-A) in the brain: evidence from using CuZn superoxide dismutase transgenic mice," *Molecular Brain Research*, vol. 58, no. 1-2, pp. 209–216, 1998.

[236] N. Thiriet, J. Zwiller, and S. F. Ali, "Induction of the immediate early genes *egr-1* and *c-fos* by methamphetamine in mouse brain," *Brain Research*, vol. 919, no. 1, pp. 31–40, 2001.

[237] M. T. McCoy, S. Jayanthi, J. A. Wulu et al., "Chronic methamphetamine exposure suppresses the striatal expression of members of multiple families of immediate early genes (IEGs) in the rat: normalization by an acute methamphetamine injection," *Psychopharmacology*, vol. 215, no. 2, pp. 353–365, 2011.

[238] M. Asanuma, T. Hayashi, S. V. Ordonez, N. Ogawa, and J. L. Cadet, "Direct interactions of methamphetamine with the nucleus," *Molecular Brain Research*, vol. 80, no. 2, pp. 237–243, 2000.

[239] P. S. Frankel, A. J. Hoonakker, J. P. Danaceau, and G. R. Hanson, "Mechanism of an exaggerated locomotor response to a low-dose challenge of methamphetamine," *Pharmacology Biochemistry and Behavior*, vol. 86, no. 3, pp. 511–515, 2007.

[240] J. L. Cadet, M. T. McCoy, N. S. Cai et al., "Methamphetamine preconditioning alters midbrain transcriptional responses to methamphetamine-induced injury in the rat striatum," *PLoS One*, vol. 4, no. 11, article e7812, 2009.

[241] J. L. Cadet, C. Brannock, B. Ladenheim et al., "Methamphetamine preconditioning causes differential changes in striatal transcriptional responses to large doses of the drug," *Dose-Response*, vol. 9, no. 2, pp. 165–181, 2011.

[242] E. J. Nestler, "Transcriptional mechanisms of addiction: role of ΔFosB," *Philosophical Transactions of the Royal Society B: Biological Sciences*, vol. 363, no. 1507, pp. 3245–3255, 2008.

[243] N. A. Youngson and E. Whitelaw, "Transgenerational epigenetic effects," *Annual Review of Genomics and Human Genetics*, vol. 9, no. 1, pp. 233–257, 2008.

[244] W. Renthal and E. J. Nestler, "Epigenetic mechanisms in drug addiction," *Trends in Molecular Medicine*, vol. 14, no. 8, pp. 341–350, 2008.

[245] D. M. Walker, H. M. Cates, E. A. Heller, and E. J. Nestler, "Regulation of chromatin states by drugs of abuse," *Current Opinion in Neurobiology*, vol. 30, pp. 112–121, 2015.

[246] J. L. Cadet, "Epigenetics of stress, addiction, and resilience: therapeutic implications," *Molecular Neurobiology*, vol. 53, no. 1, pp. 545–560, 2016.

[247] A. Aguilar-Valles, T. Vaissière, E. M. Griggs et al., "Methamphetamine-associated memory is regulated by a writer and an eraser of permissive histone methylation," *Biological Psychiatry*, vol. 76, no. 1, pp. 57–65, 2014.

[248] X. Li, F. J. Rubio, T. Zeric et al., "Incubation of methamphetamine craving is associated with selective increases in expression of *Bdnf* and *Trkb*, glutamate receptors, and epigenetic enzymes in cue-activated Fos-expressing dorsal striatal neurons," *Journal of Neuroscience*, vol. 35, no. 21, pp. 8232–8244, 2015.

[249] X. Li, M. B. Carreria, K. R. Witonsky et al., "Role of dorsal striatum histone deacetylase 5 in incubation of methamphetamine craving," *Biological Psychiatry*, 2017.

[250] J. L. Cadet, C. Brannock, I. N. Krasnova et al., "Genome-wide DNA hydroxymethylation identifies potassium channels in the nucleus accumbens as discriminators of methamphetamine addiction and abstinence," *Molecular Psychiatry*, vol. 22, no. 8, pp. 1196–1204, 2017.

[251] S. Jayanthi, B. Gonzalez, M. T. McCoy, B. Ladenheim, V. Bisagno, and J. L. Cadet, "Methamphetamine induces TET1- and TET3-dependent DNA hydroxymethylation of *Crh* and *Avp* genes in the rat nucleus accumbens," *Molecular Neurobiology*, vol. 55, no. 6, pp. 5154–5166, 2018.

[252] J. Feng, S. Fouse, and G. Fan, "Epigenetic regulation of neural gene expression and neuronal function," *Pediatric Research*, vol. 61, 5, Part 2, pp. 58R–63R, 2007.

[253] E. Seto and M. Yoshida, "Erasers of histone acetylation: the histone deacetylase enzymes," *Cold Spring Harbor Perspectives in Biology*, vol. 6, no. 4, article a018713, 2014.

[254] C. G. Vecsey, J. D. Hawk, K. M. Lattal et al., "Histone deacetylase inhibitors enhance memory and synaptic plasticity via CREB: CBP-dependent transcriptional activation," *Journal of Neuroscience*, vol. 27, no. 23, pp. 6128–6140, 2007.

[255] T. A. Martin, S. Jayanthi, M. T. McCoy et al., "Methamphetamine causes differential alterations in gene expression and patterns of histone acetylation/hypoacetylation in the rat nucleus accumbens," *PLoS One*, vol. 7, no. 3, article e34236, 2012.

[256] J. H. Harkness, R. J. Hitzemann, S. Edmunds, and T. J. Phillips, "Effects of sodium butyrate on methamphetamine-sensitized locomotor activity," *Behavioural Brain Research*, vol. 239, pp. 139–147, 2013.

[257] R. A. Henry, Y. M. Kuo, and A. J. Andrews, "Differences in specificity and selectivity between CBP and p300 acetylation of histone H3 and H3/H4," *Biochemistry*, vol. 52, no. 34, pp. 5746–5759, 2013.

[258] B. J. Everitt and T. W. Robbins, "From the ventral to the dorsal striatum: devolving views of their roles in drug addiction," *Neuroscience & Biobehavioral Reviews*, vol. 37, no. 9, pp. 1946–1954, 2013.

[259] S. Jayanthi, M. T. McCoy, B. Chen et al., "Methamphetamine downregulates striatal glutamate receptors via diverse epigenetic mechanisms," *Biological Psychiatry*, vol. 76, no. 1, pp. 47–56, 2014.

[260] O. Omonijo, P. Wongprayoon, B. Ladenheim et al., "Differential effects of binge methamphetamine injections on the mRNA expression of histone deacetylases (HDACs) in the rat striatum," *NeuroToxicology*, vol. 45, pp. 178–184, 2014.

[261] J. Feng and E. J. Nestler, "MeCP2 and drug addiction," *Nature Neuroscience*, vol. 13, no. 9, pp. 1039–1041, 2010.

[262] C. R. Lewis, K. Staudinger, L. Scheck, and M. F. Olive, "The effects of maternal separation on adult methamphetamine self-administration, extinction, reinstatement, and MeCP2 immunoreactivity in the nucleus accumbens," *Frontiers in Psychiatry*, vol. 4, no. 55, p. 55, 2013.

[263] K. Hyun, J. Jeon, K. Park, and J. Kim, "Writing, erasing and reading histone lysine methylations," *Experimental & Molecular Medicine*, vol. 49, no. 4, article e324, 2017.

[264] M. M. Suzuki and A. Bird, "DNA methylation landscapes: provocative insights from epigenomics," *Nature Reviews Genetics*, vol. 9, no. 6, pp. 465–476, 2008.

[265] A. M. Deaton and A. Bird, "CpG islands and the regulation of transcription," *Genes & Development*, vol. 25, no. 10, pp. 1010–1022, 2011.

[266] I. Kameshita, M. Sekiguchi, D. Hamasaki et al., "Cyclin-dependent kinase-like 5 binds and phosphorylates DNA methyltransferase 1," *Biochemical and Biophysical Research Communications*, vol. 377, no. 4, pp. 1162–1167, 2008.

[267] A. Scott, J. Song, R. Ewing, and Z. Wang, "Regulation of protein stability of DNA methyltransferase 1 by post-translational modifications," *Acta Biochimica et Biophysica Sinica*, vol. 46, no. 3, pp. 199–203, 2014.

[268] Y. Numachi, S. Yoshida, M. Yamashita et al., "Psychostimulant alters expression of DNA methyltransferase mRNA in the rat brain," *Annals of the New York Academy of Sciences*, vol. 1025, no. 1, pp. 102–109, 2004.

[269] Y. Numachi, H. Shen, S. Yoshida et al., "Methamphetamine alters expression of DNA methyltransferase 1 mRNA in rat brain," *Neuroscience Letters*, vol. 414, no. 3, pp. 213–217, 2007.

[270] S. Nohesara, M. Ghadirivasfi, M. Barati et al., "Methamphetamine-induced psychosis is associated with DNA hypomethylation and increased expression of *AKT1* and key dopaminergic genes," *American Journal of Medical Genetics Part B: Neuropsychiatric Genetics*, vol. 171, no. 8, pp. 1180–1189, 2016.

[271] M. Sagud, D. Mück-Seler, A. Mihaljević-Peles et al., "Catechol-O-methyl transferase and schizophrenia," *Psychiatria Danubina*, vol. 22, no. 2, pp. 270–274, 2010.

[272] P. Pregelj, "Neurobiological aspects of psychosis and gender," *Psychiatria Danubina*, vol. 21, Supplement 1, pp. 128–131, 2009.

[273] M. F. Fraga and M. Esteller, "Epigenetics and aging: the targets and the marks," *Trends in Genetics*, vol. 23, no. 8, pp. 413–418, 2007.

[274] K. Du and M. Montminy, "CREB is a regulatory target for the protein kinase Akt/PKB," *Journal of Biological Chemistry*, vol. 273, no. 49, pp. 32377–32379, 1998.

[275] O. Nidai Ozes, L. D. Mayo, J. A. Gustin, S. R. Pfeffer, L. M. Pfeffer, and D. B. Donner, "NF-κB activation by tumour necrosis factor requires the Akt serine-threonine kinase," *Nature*, vol. 401, no. 6748, pp. 82–85, 1999.

[276] P. O. Estève, Y. Chang, M. Samaranayake et al., "A methylation and phosphorylation switch between an adjacent lysine and serine determines human DNMT1 stability," *Nature Structural & Molecular Biology*, vol. 18, no. 1, pp. 42–48, 2011.

[277] K. Brami-Cherrier, E. Valjent, M. Garcia, C. Pages, R. A. Hipskind, and J. Caboche, "Dopamine induces a PI3-kinase-independent activation of Akt in striatal neurons: a new route to cAMP response element-binding protein phosphorylation," *Journal of Neuroscience*, vol. 22, no. 20, pp. 8911–8921, 2002.

[278] P. C. Chen, C. L. Lao, and J. C. Chen, "Dual alteration of limbic dopamine D_1 receptor-mediated signalling and the Akt/GSK3 pathway in dopamine D_3 receptor mutants during the development of methamphetamine sensitization," *Journal of Neurochemistry*, vol. 100, no. 1, pp. 225–241, 2007.

[279] M. Lebel, C. Patenaude, J. Allyson, G. Massicotte, and M. Cyr, "Dopamine D1 receptor activation induces tau phosphorylation via cdk5 and GSK3 signaling pathways," *Neuropharmacology*, vol. 57, no. 4, pp. 392–402, 2009.

[280] J. M. Beaulieu, T. Del'Guidice, T. D. Sotnikova, M. Lemasson, and R. R. Gainetdinov, "Beyond cAMP: the regulation of Akt and GSK3 by dopamine receptors," *Frontiers in Molecular Neuroscience*, vol. 4, p. 38, 2011.

[281] L. Yang, H. Wang, L. Liu, and A. Xie, "The role of insulin/IGF-1/PI3K/Akt/GSK3β signaling in Parkinson's disease dementia," *Frontiers in Neuroscience*, vol. 12, p. 73, 2018.

[282] J. Wu, S. E. McCallum, S. D. Glick, and Y. Huang, "Inhibition of the mammalian target of rapamycin pathway by rapamycin blocks cocaine-induced locomotor sensitization," *Neuroscience*, vol. 172, pp. 104–109, 2011.

[283] M. Lin, P. Chandramani-Shivalingappa, H. Jin et al., "Methamphetamine-induced neurotoxicity linked to ubiquitin-proteasome system dysfunction and autophagy-related changes that can be modulated by protein kinase C delta in dopaminergic neuronal cells," *Neuroscience*, vol. 210, pp. 308–332, 2012.

[284] R. Pitaksalee, Y. Sanvarinda, T. Sinchai et al., "Autophagy inhibition by caffeine increases toxicity of methamphetamine in SH-SY5Y neuroblastoma cell line," *Neurotoxicity Research*, vol. 27, no. 4, pp. 421–429, 2015.

[285] W. Jiang, J. Li, Z. Zhang, H. Wang, and Z. Wang, "Epigenetic upregulation of alpha-synuclein in the rats exposed to methamphetamine," *European Journal of Pharmacology*, vol. 745, pp. 243–248, 2014.

[286] J. Zhao, B. Zhai, S. P. Gygi, and A. L. Goldberg, "mTOR inhibition activates overall protein degradation by the ubiquitin proteasome system as well as by autophagy," *Proceedings of the National Academy of Sciences of the United States of America*, vol. 112, no. 52, pp. 15790–15797, 2015.

[287] P. Lenzi, G. Lazzeri, F. Biagioni et al., "The autophagoproteasome a novel cell clearing organelle in baseline and stimulated conditions," *Frontiers in Neuroanatomy*, vol. 10, p. 78, 2016.

[288] L. Ryskalin, F. Limanaqi, F. Biagioni et al., "The emerging role of m-TOR up-regulation in brain astrocytoma," *Histology and Histopathology*, vol. 32, no. 5, pp. 413–431, 2017.

[289] A. Moszczynska and B. K. Yamamoto, "Methamphetamine oxidatively damages parkin and decreases the activity of 26S proteasome in vivo," *Journal of Neurochemistry*, vol. 116, no. 6, pp. 1005–1017, 2011.

[290] A. Jowaed, I. Schmitt, O. Kaut, and U. Wüllner, "Methylation regulates alpha-synuclein expression and is decreased in Parkinson's disease patients' brains," *Journal of Neuroscience*, vol. 30, no. 18, pp. 6355–6359, 2010.

[291] P. Desplats, B. Spencer, E. Coffee et al., "α-Synuclein sequesters Dnmt1 from the nucleus: a novel mechanism for epigenetic alterations in Lewy body diseases," *Journal of Biological Chemistry*, vol. 286, no. 11, pp. 9031–9037, 2011.

[292] Y. Y. Tan, L. Wu, Z. B. Zhao et al., "Methylation of α-synuclein and leucine-rich repeat kinase 2 in leukocyte DNA of Parkinson's disease patients," *Parkinsonism & Related Disorders*, vol. 20, no. 3, pp. 308–313, 2014.

[293] L. Matsumoto, H. Takuma, A. Tamaoka et al., "CpG demethylation enhances alpha-synuclein expression and affects the pathogenesis of Parkinson's disease," *PLoS One*, vol. 5, no. 11, article e15522, 2010.

[294] Y. Funahashi, Y. Yoshino, K. Yamazaki et al., "DNA methylation changes at *SNCA* intron 1 in patients with dementia with Lewy bodies," *Psychiatry and Clinical Neurosciences*, vol. 71, no. 1, pp. 28–35, 2017.

[295] R. Richa and R. P. Sinha, "Hydroxymethylation of DNA: an epigenetic marker," *EXCLI Journal*, vol. 13, pp. 592–610, 2014.

[296] M. Santiago, C. Antunes, M. Guedes, N. Sousa, and C. J. Marques, "TET enzymes and DNA hydroxymethylation in neural development and function — how critical are they?," *Genomics*, vol. 104, no. 5, pp. 334–340, 2014.

[297] J. L. Cadet, C. Brannock, B. Ladenheim et al., "Enhanced upregulation of CRH mRNA expression in the nucleus accumbens of male rats after a second injection of methamphetamine given thirty days later," *PLoS One*, vol. 9, no. 1, article e84665, 2014.

[298] A. Hellman and A. Chess, "Extensive sequence-influenced DNA methylation polymorphism in the human genome," *Epigenetics & Chromatin*, vol. 3, no. 1, p. 11, 2010.